ฤทธิ์ของสารสกัดจากพืชต่อการสร้างเม็ดสีเมลานินและการแสดงออกของยีนที่เกี่ยวข้องกับการสร้าง
เม็ดสีเมลานินในเซลล์เมลาโนไซท์ชนิด B16F10

นางสาวมรกต ชาตาธิคุณ

วิทยานิพนธ์นี้เป็นส่วนหนึ่งของการศึกษาตามหลักสูตรปริญญาวิทยาศาสตรดุษฎีบัณฑิต
สาขาวิชาชีวเคมีคลินิกและอณูทางการแพทย์ ภาควิชาเคมีคลินิก
คณะสหเวชศาสตร์ จุฬาลงกรณ์มหาวิทยาลัย
ปีการศึกษา 2560

Effects of plant extracts on melanin biosynthesis and melanogenetic gene expression

in B16F10 melanoma cells

Miss Moragot Chatatikun

จุฬาลงกรณ์มหาวิทยาลัย

CHULALONGKORN UNIVERSITY

A Dissertation Submitted in Partial Fulfillment of the Requirements

for the Degree of Doctor of Philosophy Program in Clinical Biochemistry and

Molecular Medicine

Department of Clinical Chemistry

Faculty of Allied Health Sciences

Chulalongkorn University

Academic Year 2017

Thesis Title   Effects of plant extracts on melanin biosynthesis and melanogenetic gene expression in B16F10 melanoma cells

By   Miss Moragot Chatatikun

Field of Study   Clinical Biochemistry and Molecular Medicine

Thesis Advisor   Anchalee Chiabchalard, Ph.D.

Accepted by the Faculty of Allied Health Sciences, Chulalongkorn University in Partial Fulfillment of the Requirements for the Doctoral Degree

............................Dean of the Faculty of Allied Health Sciences

(Assistant Professor Palanee Ammaranond, Ph.D.)

THESIS COMMITTEE

............................Chairman

(Associate Professor Rachana Santiyanont, Ph.D.)

............................Thesis Advisor

(Anchalee Chiabchalard, Ph.D.)

............................Examiner

(Assistant Professor Tewin Tencomnao, Ph.D.)

............................Examiner

(Tewarit Sarachana, Ph.D.)

............................External Examiner

(Warunya Arunotayanun, Ph.D.)

มรกต ชาตาธิคุณ : ฤทธิ์ของสารสกัดจากพืชต่อการสร้างเม็ดสีเมลานินและการแสดงออก ของยีนที่เกี่ยวข้องกับการสร้างเม็ดสีเมลานินในเซลล์เมลาโนไซท์ชนิด B16F10 (Effects of plant extracts on melanin biosynthesis and melanogenetic gene expression in B16F10 melanoma cells) อ.ที่ปรึกษาวิทยานิพนธ์หลัก: อ. ดร. อัญชลี เฉียบฉลาด, 210 หน้า.

รังสีอัลตราไวโอเลตจากแสงแดดเป็นปัจจัยสิ่งแวดล้อมที่สำคัญในการทำลายผิวและสามารถ ทำให้เกิดการสร้างเม็ดสีเพิ่มขึ้นและปัญหาทางด้านความงาม การพัฒนาสารพฤกษเคมีใหม่จาก ผลิตภัณฑ์จากธรรมชาติได้กลายเป็นที่นิยมมากในปัจจุบัน วัตถุประสงค์ของการศึกษาครั้งนี้คือการหา สารสกัดจากพืชบางชนิดที่ช่วยลดการสังเคราะห์เมลานินและการแสดงออกของยีนที่เกี่ยวข้องกับการ สร้างเมลานินในเซลล์เมลาโนไซท์ชนิด B16F10 ที่ถูกกระตุ้นด้วยฮอร์โมนชนิด alpha-melanocyte stimulating (alpha-MSH) ในการทดสอบสารฟีนอลและฟลาโวนอยด์รวมทั้งความสามารถในการ ต้านอนุมูลอิสระและฤทธิ์ในการยับยั้งเอนไซม์ไทโรซิเนสจากเห็ด เราได้ใช้พืช 13 ชนิดซึ่งถูกสกัดด้วย ตัวทำละลายปิโตรเลียมอีเทอร์, ไดคลอโรมีเทนและเอทานอล ตามลำดับ เราพบว่าปริมาณสารฟี นอลิกของสารสกัดจากพืช 13 ชนิดถูกพบมากในสารสกัดจากเอทานอล, ไดคลอโรมีเทนและ ปิโตรเลียมอีเทอร์ตามลำดับ ในขณะที่ฟลาโวนอยด์พบได้ตามปกติในสารสกัดไดคลอโรมีเทน เรายัง พบว่าสารสกัดจากพืช 4 ชนิดที่มีฤทธิ์ในการต้านสารอนุมูลอิสระสูงคือ สารสกัดเอทานอลจาก ราม ใหญ่, มังคุด, มะยม และหนอนตายหยาก นอกจากนี้เราพบว่าสารสกัดจากเอทานอลของทองพันชั่ง, รามใหญ่, มะยม, ชุมเห็ดเทศ และลำโพงขาวมีฤทธิ์ในการลดเอนไซม์ไทโรซิเนสจากเห็ดอย่างมี นัยสำคัญ ผลการทดลองของเราแสดงให้เห็นว่าสารสกัดเอทานอลของ เปล้าใหญ่, เปล้าน้อย, มะยม และทองพันชั่ง ช่วยลดการสังเคราะห์เมลานินได้อย่างมีประสิทธิภาพผ่านการยับยั้ง phospho-CREB ซึ่งมีผลต่อการยับยั้ง MITF, tyrosinase, TRP-1 และ TRP-2 งานวิจัยของเราพบว่าสารสกัดเอทานอล จากใบของเปล้าใหญ่, เปล้าน้อย, มะยมและทองพันชั่งอาจจะเป็นประโยชน์ต่อการลดการสร้างเม ลานินในโรคฝ้าได้ และอาจเป็นสารสำคัญที่ทำให้ผิวขาว

ภาควิชา	เคมีคลินิก	ลายมือชื่อนิสิต	....
สาขาวิชา	ชีวเคมีคลินิกและอณูทางการแพทย์	ลายมือชื่อ อ.ที่ปรึกษาหลัก	....
ปีการศึกษา	2560		

5676956537 : MAJOR CLINICAL BIOCHEMISTRY AND MOLECULAR MEDICINE

KEYWORDS: ALPHA-MSH / MELANIN / TYROSINASE / B16F10 MOUSE MELANOMA CELLS / ANTI-MEALANOGENIC ACTIVITY

MORAGOT CHATATIKUN: Effects of plant extracts on melanin biosynthesis and melanogenetic gene expression in B16F10 melanoma cells. ADVISOR: ANCHALEE CHIABCHALARD, Ph.D., 210 pp.

Ultraviolet radiation from sunlight is a significant environmental factor in skin damage and can induce hyperpigmentation disorder and aesthetic problem. Development of novel whitening phytochemical compounds from natural products has been become trends recently. The purpose of this study was to find some plant extracts that reduce melanin synthesis and melanogenetic gene expression in alpha-MSH-induced B16F10 mouse melanoma cells. To screen total phenolics and flavonoids, antioxidant activity, and anti-mushroom tyrosinase activity, we used 13 plants which were extracted with petroleum ether, dichloromethane and ethanol solvents, subsequently. We found that total phenolic content of 13 plants extracts was found in the high level in ethanol, dichloromethane and petroleum ether, orderly. While, flavonoid content was normally found in dichloromethane fraction. We also found that four plants extracts, containing ethanol fractions of *Ardisia elliptica*, *Garcinia mangostana*, *Phyllanthus acidus,* and *Stemona curtisii* had the high antioxidant activity. Furthermore, we found that ethanol fractions of *Rhinnacanthus nasutus, Ardisia elliptica, Phyllanthus acidus*, and *Senna alata* significantly decreased mushroom tyrosinase activity. Our results demonstrate that ethanol extracts of *Croton roxburghii, Croton sublyratus, Phyllanthus acidus* and *Rhincanthus acidus* leaves markly decreased melanin biosynthesis through suppressing phospho-CREB by inhibiting MITF, tyrosinase, TRP-1 and TRP-2. Our finding suggests that four ethanol extracts may be useful for treating melasma and as a skin-whitening agent.

Department:	Clinical Chemistry	Student's Signature ⋯⋯⋯⋯⋯⋯
Field of Study:	Clinical Biochemistry and Molecular Medicine	Advisor's Signature ⋯⋯⋯⋯⋯⋯
Academic Year:	2017	

ACKNOWLEDGEMENTS

CONTENTS

CHAPTER I

INTRODUCTION

Background and rationale

Melanin, the endproduct of melanogenesis, is responsible for determining the color of human skin, hair and eyes. Melanins are synthesized by specialized pigment cells known as melanocytes and are deposited in melanosomes (1). In daily life, human skin is exposed to ultraviolet radiation from sunlight. The sun-exposed skin increased melanin synthesis that can cause melasma. Melasma is a chronic acquired hypermelanosis which occurs systematically on sun-exposed area of the skin. Centrofacial pattern is the most common lesion and involves in the cheek, upper lip, forehead and chin (2). In respond to ultraviolet radiation from the sunlight, skin is affected indirectly by paracrine and autocrine factors including hormones, cytokines, and growth factors, whose synthesis in the epidermal cells (3). UV induces cellular damage response in epidermal cells, especially keratinocytes. Damage signals such as p53 activation induce transcription of pro-opiomelanocortin (POMC) gene which encodes production and secretion of alpha-melanocyte stimulating hormone (alpha-MSH). UV radiation induces the melanogenesis of melanocytes through a paracrine regulation process involving keratinocytes (4). On binding to the melanocortin receptor (MC1R) on melanocytes in the epidermis layer of the skin, alpha-MSH from keratinocytes activates intracellular adenylate cyclase followed by increased intracellular cyclic AMP (cAMP) level from adenosine triphosphate (ATP) (5). Cyclic AMP further activates protein kinase A (PKA). The PKA phosphorylates and activates cAMP-response element binding protein (CREB) that binds to cAMP response element (CRE) presenting in the M promoter of the microphthalmia-associated transcription factor (MITF) gene. The increase of MITF may lead to the up-regulation of melanogenic enzymes such as tyrosinase, tyrosinase-related protein 1 (TRP-1) and

tyrosinase-related protein 2 (TRP-2) (6). In the melanin synthesis, tyrosinase catalyzes the hydroxylation of L-tyrosine into 3,4-dihidroxyphenylalanine (L-DOPA) (7). Subsequently, L-DOPA is oxidized to DOPAquinone by tyrosinase. DOPAquinone is further converted to DOPAchrome which can be converted to 5,6-dihydroxyindole (DHI) or 5,6-dihydroxyindole-2-carboxylic acid (DHICA). Indole-5,6-quinone has be formed to produce black and insoluble melanin which has high molecular weight. In the presence of TRP-2 or dopachrome tautomerase (DCT), DOPAchrome is tautomerized to 5,6-dihydroxyindole-2-carboxylic acid (DHICA). TRP-1 catalyzes the oxidation of DHICA that will be changed to indole-5,6-quinone carboxylic acid which can be formed to produce brown, poorly soluble and intermediate molecular weight melanin (8). Down regulation of tyrosinase activity has been proposed to be responsible for the decreased melanin production (9).

Melasma treatment depends on whether the pigmentation is epidermal or dermal. Only epidermal pigmentation responds well to treatment. Management of melasma consists of discontinuing hormonal contraception, the avoidance of direct sun-exposure, the use of a broad-spectrum sunscreen and the avoidance of scented cosmetics (10). Hydroquinone is the most popular depigmenting agent for melasma. In the result of hydroquinone, the melanin synthesis is reduced by inhibiting tyrosinase activity. However, The adverse effects of hydroquinone include erythema, stinging, colloid milium, irritant and allergic contact dermatitis, nail discoloration, transient hypochromia, and paradoxical postinflammatory hypermelanosis (11). Thus, the development of novel whitening phytochemical compounds from natural products has been become trends recently.

At the recent, various natural products are being increasingly used in cosmetics and melasma treatment. Herbal extracts have many active compounds such as phenol, flavonoid, gallic acid, epigallocatechin, aloesin, hydroxystillbene and ellagic acid which may benefitly used in melasma treatment (12). In the previous study, flavonoids inhibited mushroom tyrosinase enzyme by chelating copper at

active site (13). Gallic acid derivatives of flavonols from green tea were identified as strong tyrosinase inhibitor. Moreover, the major active compound in the green tea were (-)-epicatechin 3-O-gallate (ECG), (-)-gallocatechin 3-O-gallate (GCG), and (-)-epigallocatechin 3-O-gallate (EGCG) which also inhibited tyrosinase (14). Therefore, natural products may be considered as new safe and efficient depigmenting agents for melasma treatment. The first aim of this study is to determine antioxidant compounds and activities of thirteen species of Thai herbs. Mushroom tyrosinase enzymes will be used to screen the ability of thirteen species of Thai plants on tyrosinase activity. After screening with mushroom tyrosinase, we investigated the inhibitory effect of selected Thai plant extracts against melanin synthesis and their molecular mechanism in alpha-MSH induced B16F10 cells. Our results demonstrate that ethanol extracts of *Croton roxburghii, Croton sublyratus, Phyllanthus acidus* and *Rhincanthus acidus* leaves significantly decreased melanin biosynthesis through suppressing phospho-CREB by inhibiting MITF, tyrosinase, TRP-1 and TRP-2. These extracts can be used as skin whitening creams or lotions.

Review of related literatures

To support the background of this study, related articles are categorized as follows:

Skin physiology

Skin is the largest organ of the body in human. Human skin is organized into three layers which are epidermis, dermis and hypodermis layers. It serves as protective barriers against biological, chemical, thermal and physical factors (15). Dermis layer is a deeper layer of the skin which is a loose connective tissue layer. Last, hypodermis layer contains a layer of subcutaneous fat cells (16).
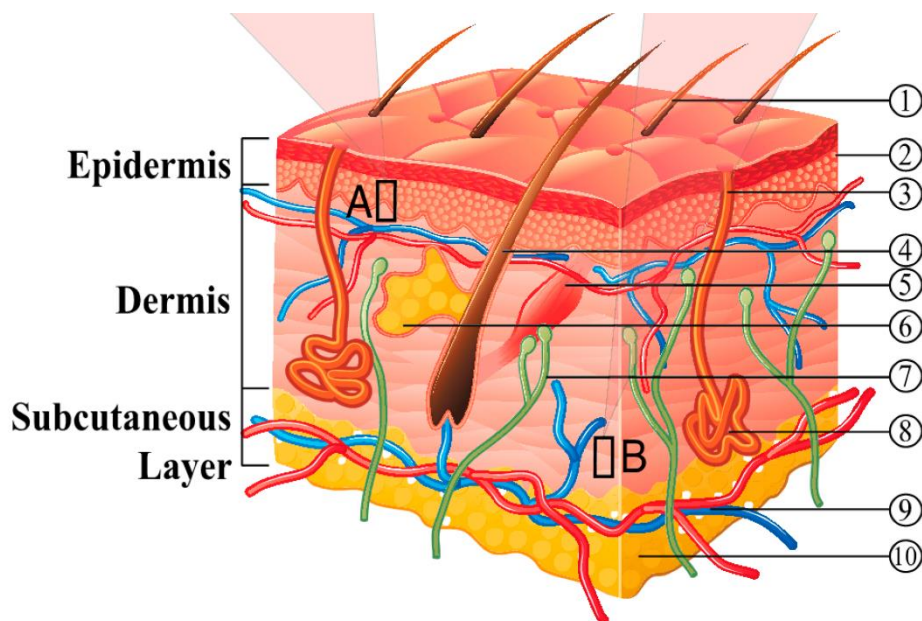
Figure 1. Skin structure. There are three layers which are epidermis, dermis and subcutaneous layers (hypodermis), containing(1) hair shaft; (2) stratum corneum; (3) sweat pore; (4) hair follicle; (5) arrector pili muscle; (6) sebaceous gland; (7) nerve; (8) eccrine sweat gland; (9) cutaneous vascular plxes; (10) adipose depot. Skin has the important roles in the control of blood circulation and body temperature (modified from Meenakshi Gaur, et al., 2017) (17).

Epidermis

Epidermis is the outermost layer of the skin which is a stratified epithelium (figure 2). The stratified epithelium contains many cells (18). Most of the keratinocytes cells are found in basal layer and formation of desmosomes and tight junctions to express as a barrier. The keratinocytes also synthesize the protein keratin. The epidermis layer is divided into four layers which is classified by keratin maturation (19). The epidermis consists of four layers: stratum basale, stratum spinosum, stratum granulosum, stratum corneum. The layers move from lower layers to surface layer (Figure 1) (20).

Stratum basale

Stratum basale layer is the innermost layer of epidermis layer (figure 2). It contains proliferating and differentiating keratinocytes, melanocytes and Merkel cells. Keratinocytes differentiate and move from bottom layer to the surface of the epidermis layer (21). Then, the keratinocytes are shed from the surface of skin as a cornified cells which act as barriers (22). The keratinocytes also attached to basement membrane of skin by hemidesmosome which is a member of cadherins (23). Melanocytes or pigment cells synthesize and transfer melanin to surrounding keratinocytes, contribute skin color and photoprotection (24). Merkel cells are also found in basal layer of the epidermis layer with large number in highly sensitive skin like finger tips and lips (25). The Merkel cells are associated with sensory nerves that they involved in mechanical transduction, secretory function, various kinds of neuropeptides and neuron-specific proteins (26). Large number of Merkel cells is found in sun-exposed area more than in normal area (27).

Stratum spinosum

Stratum spinosum is the second layer of the epidermis layer (figure 2). It locates between stratum basale and stratum granulosum. Keratinocytes from basal layer move to stratum spinosum which is called prickle cell layer. Cell shape changes from columnar to polyhedral. Then, the keratinocytes in stratum spinosum produce keratins (28). In this layer, there are Langerhans cells which are a cell type of dendritic family. The stratum spinosum have Langerhans cells which are antigen presenting cells in the immune system by migrating from epidermis to lymph nodes. They present antigens to naïve T cells and further activate innate immune response. They impact on microbial antigens, skin immunosurveillance, contact hypersensitivity and chronic inflammatory diseases of the skin (29).

Stratum granulosum

Stratum granulosum is known as a granular layer which is a thin layer of epidermis layer (as shown in figure 2). It contains 3-5 layers of flatten keratin. Keratinocytes from stratum spinosum move to this layer that they are known as granular cells. The granular cells produce two types of granules, including basophilic keratohylins and lamellar granules. The basophilic keratohylins secrete proteins like tonofilaments and filaggrin. The tonofilaments and filaggrin are keratin intermediate filaments which interact together with keratin filaments (30). In this layer, the process of keratinization is begun. The keratinocyte cells lose their nuclei and die. Moreover, there are lamellar granules in stratum granulosum. The lamellar granules are membrane-coating and also secrete lipid-rich substances. This substance assumes that the cells are connected together and also function as a waterproof barrier (31).

Stratum corneum

Stratum corneum or horny cell layer is the outermost layer of skin as shown in figure 2. This layer is composed of dead cells, packed with keratin and surrounded in extracellular space by stacked layers of lipid. Keratinocytes in stratum corneum are called corneocytes. In the normal skin, corneocytes stack 18-20 layers depending on location of the body (32). Many layers of stacked corneocytes was found in palm and sole. The corneocytes are hold together with corneodesmosomes (spot welding). Corneocytes reside in epidermal lipid matrix, containing ceramides, cholesterol and free fatty acids (FFA) (33). The epidermal lipid matrix serves as a permeability barrier or a cement (mortar) between skin cells (bricks). In addition, this barrier protects transepidermal water loss (TEWL) and keep moisture in the skin (34). So, this layer protects against infection, chemical irritants, allergens and mechanical trauma(35).

Moreover, there is another layer of the epidermis layer. It is called stratum lucidum and is between stratum granulosum and stratum corneum. Lucidum derives from lucid which means clear or transparent. This layer is a thin layer found in thick

epidermis. The stratum lucidum is only found in hairless parts of the skin, including palms of hands, soles of feet. These part is thickest skin in the body.
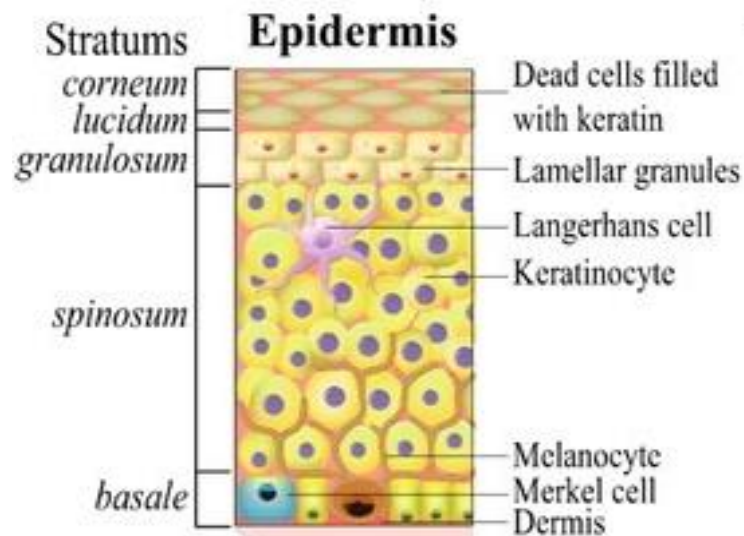

Figure 2. Structure of epidermis layer of the skin is divided into four layers which are stratum basale, spinosum, lucidum/granulosum and corneum. There are many cells in the epidermis layer, including keratinocytes, Langerhans cells, melanocytes and Merkel cells (modified from Meenakshi Gaur, et al., 2017) (17).

Dermis layer

Dermis is the second layer of skin (as shown in Figure 1). Dermis layer is located between epidermis and subcutaneous layers. The dermis layer is home of blood vessels, oil glands, sweat glands, connective tissues, nerves and other structures. The dermis is composed of two layers; thin upper layer (papillary dermis) and thicker lower layer (reticular dermis). The papillary dermis is a thin top layer which lie below epidermis layer. The papillary dermis also contains blood vessels and connective tissues. Moreover, papillary layer regulate skin temperature and nutrition supply. The reticular dermis is a thick bottom layer which has blood vessels and connective tissues for supporting skin. There are also hair follicles, oil and sweat glands, other structures in reticular dermis (36). The cells in the dermis layer are

fibroblasts, mast cells, macrophages and lymphocytes (37). Fibroblasts synthesize and degrade fibrous and non-fibrous connective tissue matrix proteins. Collagen and elastic fibers (produced by fibroblasts) are major constituents of the dermis (38). Collagen is an abundant structural protein and is the extracellular matrix component (39). Elastin is another structural protein which contributes flexibility. Decreased collagen and elastin fibers depend on the age and the damage from ultraviolet radiation which induce wrinkle skin (40). Mast cells release vasoactive and pro-inflammatory mediators for IgE mediated acute, subacute and chronic inflammation (41). Macrophages are phagocytic cells which present antigens to lymphocytes (37).

Hypodermis layer

Hypodermis layer is the deepest layer of human skin and derived from mesoderm. It is known as subcutaneous tissue. It contains a layer of subcutaneous fat cells, blood vessels and nerves. The hypodermis is responsible for regulating body temperature and protect the skin from injury (padding) (42). This layer is found in the thickest areas of the skin, including buttocks, palms, and soles of the feet. Subcutaneous fat from hypodermis is made up of adipocytes. The adipocytes organize together to from lobule separated by connective tissue. The number of adipocyte varies in different areas of the body (43).

Skin functions

Skin is the largest organ of the body. It has main four functions: protection, regulation, sensation and endocrine function.

Protection

Skin acts as a barrier which protects skin from mechanical impact, fluid, ultraviolet radiation (UVR) and infection. Skin serves as a primary defense to pressure, stress and trauma (44). The skin also acts as epidermal permeability barrier which retains body fluid and protects skin from external fluids or liquids by lipid bilayer in

stratum corneum of epidermis layer (45). Two optical properties of the skin on UV are absorption and scattering. Absorption is the loss of photon when energy is changed within the biological molecules. Scattering is the alteration of the light direction. The stratum corneum in the epidermis layer are compact, thin and light absorbing layers. Pigments in epidermis protect ultraviolet radiation by absorption. In contrast, the dermis is thick and acellular layer which serves light scattering. The stratum corneum and epidermis absorb ultraviolet-B (UVB) and ultraviolet-C (UVC) near 275 nm by tryptophan. Collagen fibers in the dermis layer functions the optical scattering (20, 46). Moreover, the skin protects against foreign substances or microorganisms (virus, bacteria and fungi) from attacking the skin. Langerhans cells are the cells in the skin that they response to microorganisms (47).

Regulation

Skin maintains body temperature through sweat glands and blood vessels in dermis layer. When ambient temperature is higher than skin temperature, the increased evaporation of the secreted sweat decrease body temperature (48). Vasodilation and vasoconstriction systems also control body temperature (49). These systems depend on thermal environment. Vasodilation refers to the relaxing of small blood vessels in the dermis layer that it induce to release some heat and decrease body temperature. While, vasoconstriction refers to the contracting of small blood vessels in the dermis (50). Moreover, fat in hypodermis layer serves as an insulation barrier which prevent heat loss and reduce the impact of cold temperature (51).

Sensation

Dermis layer contains nerves like a sensory organ. Sensations are transmitted through nerves in the skin. There are two sensory receptors in the skin, including free nerve endings and encapsulated or corpuscular receptors. Free sensory nerve ending detects touch, temperature (cold and hot), itching, pain and pressure (52). The nerve

endings are almost found in skin. While, encapsulated receptors are in the sensitive areas, including finger tips and lip. Corpuscular receptors are located in dermis layer that touch was recognized by Meissner's corpuscle. Whereas, pressure and vibration were detected by Pacinian corpuscles (53).

Endocrine function

Skin is a source of vitamin D. As shown in Figure 3, ultraviolet radiation B (UVB) from sunlight enters into epidermis layer and then photolyzes 7-dehydroxycholesterl (provitamin D_3) into previtamin D_3. The previtamin D_3 change into vitamin D_3 by isomerization. Vitamin D_3 enters the blood circulation and is hydroxylated to 25-hydroxyvitamin D (25(OH)D) by 25-hydroxylase (25-OHase). The 25(OH)D is further hydroxylated to form 1,25-dihydroxyvitamin D (1,25-[OH]$_2$-D) or calcitriol by 25-hydroxyvitaminD-1-alpha-hydroxylase (CYP27B1) in the kidney (54). 1,25-dihydroxyvitamin D in active form binds to vitamin D receptors for biological functions (55).
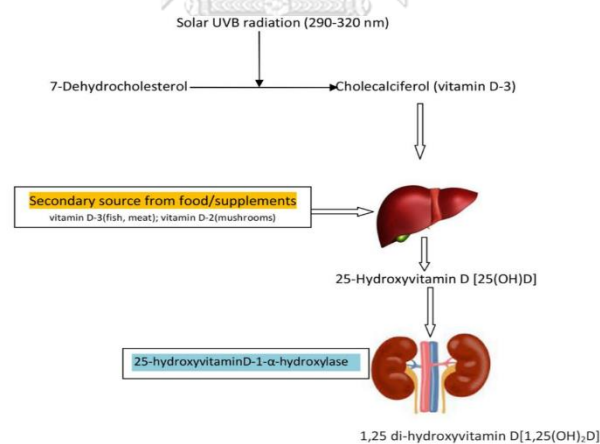
Figure 3. Vitamin D production. UVB from sunlight photolyzes 7-dehydroxycholesterol to vitamin D_3 or cholecalciferol. Then, vitamin D_3 (derived from fish, meat and skin exposure to UV) or vitamin D_2 (derived from mushrooms) is hydroxylated into 25-hydroxyvitmain D [25(OH)D] by 25-hydroxylase in liver. Then, 25(OH)D is converted to 1,25-dihydroxyvitamin D [1,25(OH)$_2$D] by 25-hydroxyvitaminD-1-alpha-hydroxylase in kidney (adapted from Weydert Joy, 2014) (56).

Melanocyte origin in the skin

Melanocytes are the most important cells in the skin pigmentary system. Melanoblast is a precursor cell of melanocyte. Melanoblasts originate from the neural crest cells. They derive from pluripotent stem cells that differentiate into many cell lineages, including neuron, glia, smooth muscle, craniofacial bone, cartilage and melanocytes. Progenitor melanoblasts migrate dorsalaterally between the mesodermal and ectodermal layers to reach their final sites in the dermis, epidermis, inner ear cochlea, choroids, ciliary body and iris (57). Melanocytes are molecularly identified by melanocyte-specific proteins as melanosomal matraix proteins (Pmel17, MART-1), microphthalmia transcription factor (MITF), tyrosinase (TYR), tyrosinase-related protein 1 and 2 (TRP 1, TRP2 or dopachrome tautomerase (DCT)) (58). Mature melanocyte are oval, long dendritic cells and smaller than keratinocytes. The number of melanocytes in the skin independently of the human race can vary at different body sites with densities between 2000 mm^{-2} in head or forearm skin to 1000 mm^{-2}. Melanocytes locate at the epidermis-dermis junction are dendritic cells with dendrite extending from the cell body. The dendritic processes of differentiated melanocytes are interspersed between neighboring keratinocytes, forming the epidermal melanin unit. Melanocytes produce melanin in melanosome before transferring the melanosomes to the surrounding keratinocytes (59). Each melanocyte contacts with about 30-40 keratinocytes in epidermal melanin units (60). In the stratum basal layer of the epidermis, the ratio of melanocytes to keratinocytes is 1:10 (figure 4). The keratinocytes control melanocyte proliferation, growth and activity via paracrine factor and cell adhesion molecules (61). Melanin granules are deposited above keratinocytes and removed with the shed epidermal cells. Melanin granules protect keratinocytes from UV radiation (62).
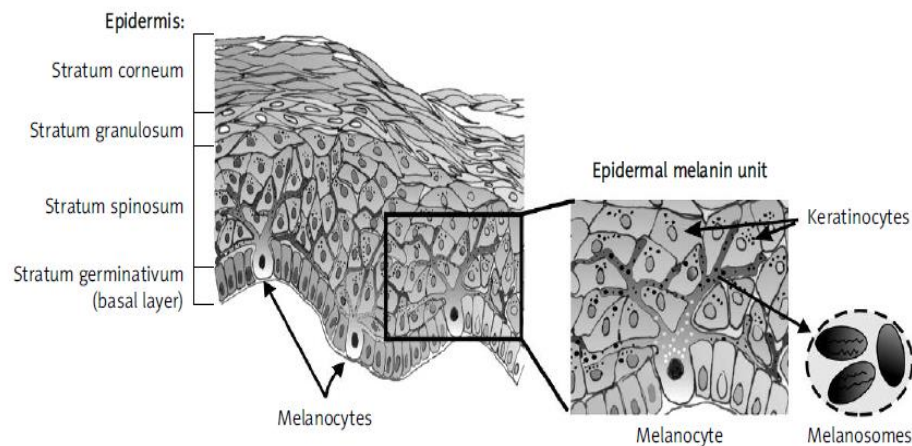
Figure 4. Scheme of the epidermis structure (adapted from Mirosława Cichorek, et al., 2013) (63). Melanocytes locate at the epidermis-dermis junction are dendritic cells with dendrite extending from the cell body. Each melanocyte contacts with about 30-40 keratinocytes in epidermal melanin units. Melanocyte produces melanin in melanosomes transported into keratinocytes to protect them from UV radiation.

Melanosome biosynthesis

Melanosome are membrane bound organelles for melanogenesis. They originate from endoplasmic reticulum (ER) of melanocytes and are synthesized on ribosome of the ER and transported to the Golgi complex where it undergoes glycosylation, which is a process essential for its normal structure and function (64). There are four maturation stages which are determined by their structure and the quantity, quality, and arrangement of the melanin (Figure 3) (65). Stage I melanosomes or premelanosomes are spherical vacuoles which lack tyrosinase activity and contain glycoprotein Pmel17 (66). Stage II eumelanosomes have elongated and structured fibrillar matrix. They contain tyrosinase enzyme and express minimal deposition of melanin. In contrast, pheomelanosomes synthesize melanin in stage II. Deposition of melanin on the internal fibrils is found in stage III. Stage IV eumelanosomes are fully melanized and their internal matrix is masked by melanin deposits (67). Melanosomes are divides into eumelanosomes and

pheomelanosomes. Eumelanosomes are large, elliptical melanosomes and contain a highly structured fibrillar glycoprotein matrix. Pheomelanosomes are smaller, spherical in shape and their disorganized glycoprotein matrix. So, the skin color is based on the size, number, shape and distribution of melanosome. Pheomelanin is the major type in red hair and also predominates in the skin type I and II. However, eumelanin is found in large amounts with dark skin and hair and is more photoprotective than pheomelanin (68).

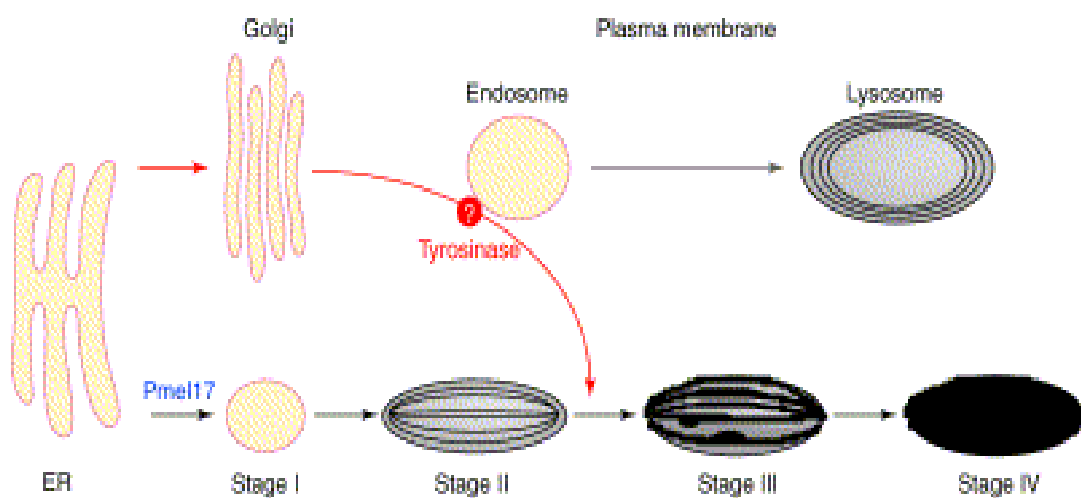Figure 5. Melanosome biogenesis (modified from Dell'Angelica, 2003) (1). Stage I premelanomsome are spherical vacuoles which lack tyrosinase activity and contain glycoprotein Pmel17. Stage II eumelanosomes have elongated and structured fibrillar matrix. Deposition of melanin on the internal fibrils is found in stage III. Stage IV eumelanosomes are fully melanized and their internal matrix is masked by melanin deposits (67).

Melanogenic proteins

The sorting of melanogenic enzymes and structural protein to melamosome is a part of melanosome maturation. Melanogenic enzymes include tyrosinase (TYR), tyrosinase-related protein 1 (TRP-1) and tyrosinase-related protein 2 (TRP-2) or DOPAchrome tautomerase (DCT) (69). Tyrosinase is a single chain type I membrane glycoprotein which catalyzes the hydroxylation of tyrosine to β-3,4-dihydroxyphenylalanine (DOPA) and the subsequent oxidation of DOPA to DOPAquinone (70). Tyrosinase is synthesized in the endoplasmic reticulum as a precursor protein. Nascent chain of tyrosinase is processed in the Golgi complex where sialic acid and sugar are added to the peptide via N- and O-glycosidase linkages through glycosylation. Glycosylation steps are required for trafficking/sorting of tyrosinase into the Golgi apparatus and ultimately into endosomes and finally into melanomes in stage II. In the melanosome, tyrosinase is found in the melanosomal outer membrane. Tyrosinase protein is divided into three domains: the inner melanosomal domain, the transmembrane domain and the cytoplasmic domain. Histidine residues in the inner melanosomal domain bind copper ions that are required to tyrosinase activity. The tyrosinase cytoplasmic domain has the sequence (glutamic-X-X-glutamine-proline-leucine-leucine, "X" represents for any amino acids) that is required in cellular trafficking of tyrosinase to melanosomes. In addition, the cytoplamic domain participates in the regulating tyrosinase via phosphorylation of serine residues (Ser) (figure 6) (12).

Figure 6. Tyrosinase protein structure. Tyrosinase protein has three domains: the inner melanosomal domain, the transmembrane domain and the cytoplasmic domain. Histidine residues in the inner melanosomal domain bind copper ions that are required to tyrosinase activity. In addition, the cytoplamic domain participates in the regulating tyrosinase via phosphorylation of serine residues (Ser) (adapted from Hee-Young Park, et al., 2001) (71).
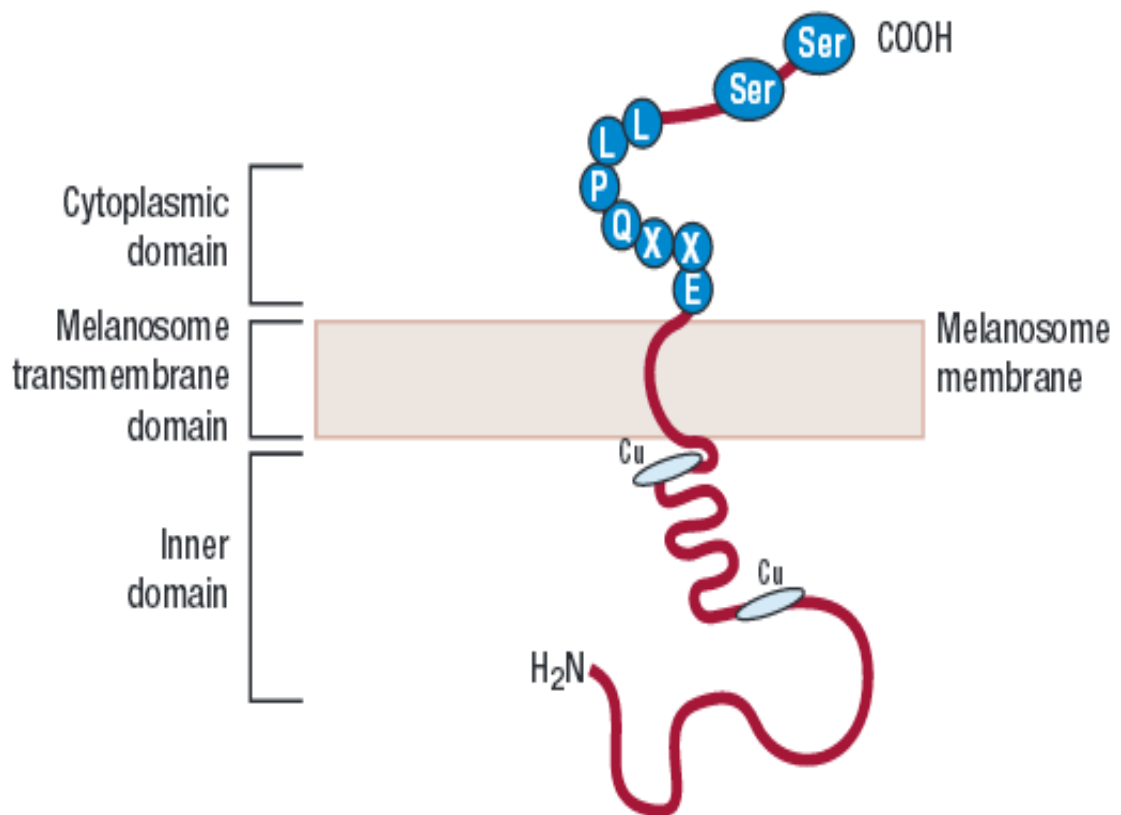
Tyrosinase-related proteins are divided into two types including tyrosinase-related protein 1 (TRP-1) and tyrosinase-related protein 2 (TRP-2). TRP-1 and TRP-2 are glycoproteins located within melanosomes. TRP-1 is synthesized in the endoplasmic reticulum and undergoes several glycosylation steps. TRP-1 forms a complex with tyrosinase. The specific melanogenic function of TRP-1 is the oxidation of 5,6-dihydroxyindole-2-carboxylic acid (DHICA) to an indole 5,6-quinone carboxylic acid. TRP-1 also plays a role in tyrosinase activation or stabilization (72). Like tyrosinase and TRP-1, TRP-2 is known as DOPAchrome tautomerase. TRP-2 is a glycoprotein which is synthesized in the endoplamic reticulum and undergoes many maturation steps in the Golgi and trans-Golgi network. TRP-2 converts DOPAchrome to carboxylated derivative DHICA. TRP-2 also requires zinc ions for its enzymatic activity (73).

Other proteins in melanogenic process are structural proteins which are fibrillar matrix proteins within the melanosomes. These proteins are required for deposition of melanin. Pmel17 and MART-1 are melanosomal structural matrix proteins. Pmel17 is a glycoprotein which forms fibril matrix in melanosomes (74). Alpha-Melanocyte stimulating hormone (α-MSH) induces Pmel17 transcription through MITF. Pmel17 is systhesized in the endoplasmic reticulum and undergoes glycosylation, and final cleavage. After its synthesis, Pmel17 is delivered to stage I melanosomes to form fibrillar structure which is the backbone of eumelanosome matrix, contributes to elliptical melanosome, and promotes melanin polymerization (75). MART1/Melan A is a membrane associated protein which is found in stage I and II melanosomes and forms a complex with Pmel17. MART1 affects the expression, stability, trafficking, and processing of Pmel17 within the melanosomes (figure 7) (76).
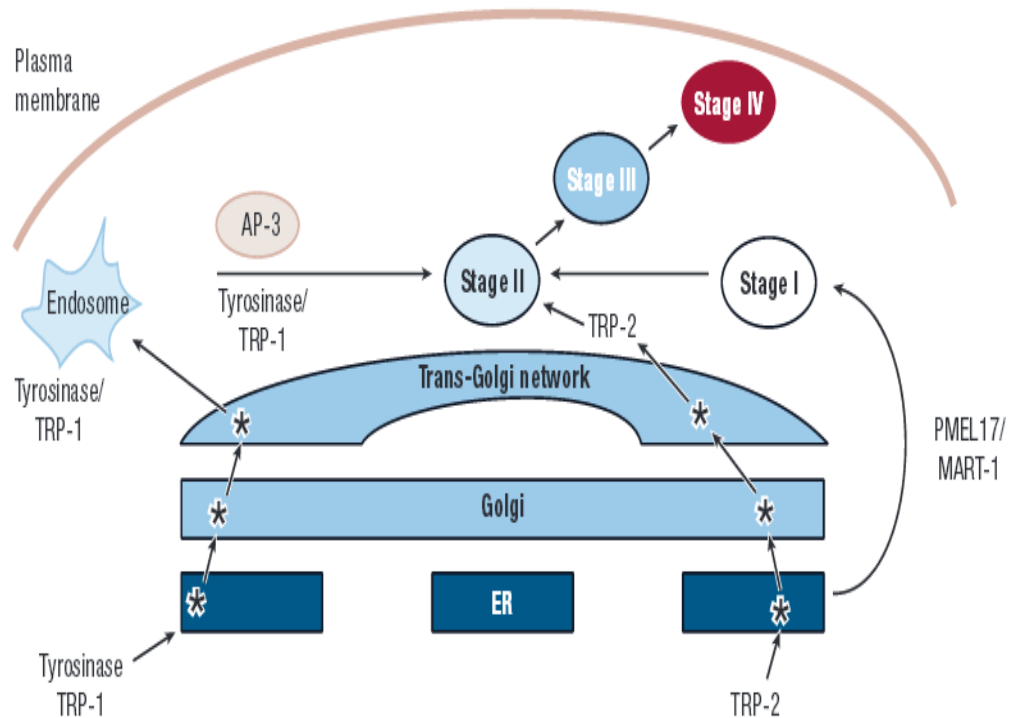
Figure 7. Sorting of melanosomal proteins into melanosomes. Tyrosinase and tyrosinase-related protein 1 (TRP-1) are synthesized in the endoplasmic reticulum (ER) and, after additional maturation steps (*) in the Golgi and Trans-Golgi network, are packaged in endosome. Maturaition steps of TRP-2 are same in tyrosinase and TRP-1. Melanosomes originate in the ER as stage I premelanosome containing PMEL17 and MART-1. Then, they mature to stage II melanosomes and fill with tyrosinase/TRP-1 in a process directed by adaptor protein 3 (AP-3). Melanosomes become progressively darker as melanin biosynthesis replace (adapted from Hee-Young Park, et al., 2001) (71).

Process of skin pigmentation

Melanin, the endproduct of melanogenesis, is responsible for determining the color of human skin, hair and eyes. Melanins are divided into two types including eumelanin and pheomelanin in melanosomes. Eumelanin is dark, brownish black and insoluble melanin. In contrast, pheomelanin is light, reddish yellow, sulfur containing and soluble melanin (77). Melanins are synthesized by specialized pigment cells known as melanocytes and are deposited in melanosomes (1).

Melanin biosynthesis requires tyrosinase, tyrosinase-related protein 1 and 2. The first step of melanin formation is mediated by tyrosinase (figure 6). This enzyme catalyzes the hydroxylation of L-tyrosine into 3,4-dihydroxyphenylalanine (L-DOPA) (7). Inhibition of this reaction blocks melanin synthesis (9). Subsequently, L-DOPA is oxidized to DOPAquinone by tyrosinase. The tyrosinase reaction results in the generation of superoxide anion (O_2^-) (78). DOPAquinone is further converted to DOPAchrome which can be converted to 5,6-dihydroxyindole (DHI) or 5,6-dihydroxyindole-2-carboxylic acid (DHICA). The 5,6-dihydroxyindole DHI is oxidized to indole-5,6-quinone which can be formed as a black , insoluble melanin and high molecular wright. The oxidation from DHI into quinone produces hydrogen peroxide (H_2O_2). Other melanogenic proteins involve the melanin synthesis. In the presence of tyrosinase-realated protein 2 (TRP-2), known as DOPAchrome tautomerase, DOPAchrome is tautomerized to 5,6-dihydroxyindole-2-carboxylic acid (DHICA). Tyrosinase-realated protein 1 (TRP-1), also known as DHICAoxidase, catalyzes the oxidation of DHICA to indole-5,6-quinone carboxylic acid which can be formed to produce brown, poorly soluble and intermediate molecular weight melanin. The oxidation from DHICA into indole-5,6-quinone carboxylic acid results in the production of O_2^- (79). A series of enzymatic reactions in eumelanin synthesis has resulted in reactive oxygen species formation such as O_2^- and H_2O_2 (80). In the absence of thiol is immediately converted to DOPA chrome and leads to eumelanin synthesis. However, the presence of sulfphydryl donor (glutathione or cysteine) can

react with DOPAquinone intermediates to form cysteinylDOPA which becomes the red/yellow, soluble, and low molecular weight pheomelanin (figure 8) (8).

In the expression phase of melanin synthesis, the melanin-filled melanosomes are transferred to the surrounding keratinocytes by the melanocyte dendrites. The protease protease-activated receptor 2 (PAR-2), which is expressed on keratinocytes but not on melanocytes, increases in melanosome transfer. Finally, the melanin becomes visible and is degraded during the keratinocytes move to the outer stratum corneum. The melanin pigments are shed with desquamation (81). An increase of melanin pigment over the epidermis layer is referred to as a facultative pigmentation. A major stimulus of facultative pigmentation in human is an ultraviolet radiation (UVR). UVR-induced skin pigmentation or tanning involves several processes. UVR increases the number of melanocytes and melanosome distribution. The expression of tyrosinase and other melanogenic enzymes is up-regulated to UVR exposure (82). These radiations trigger the development of epidermal pigmentation and occur more intensely in sun-exposed areas with melasma than the adjacent skin
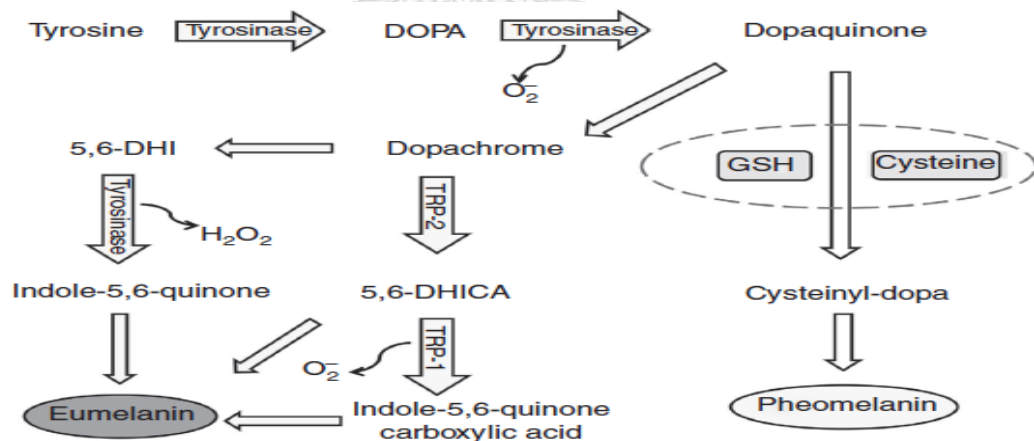
(83).

Figure 8. Generation of reactive oxygen species (ROS) in the melanin biosynthetic pathway (adapted from Denat L., et al., 2014) (84). Melanin biosynthesis starts with an amino acid tyrosine which is converted to L-DOPA (3,4 dihydroxyphenylalanine) in the rate limiting step of melanin synthesis by tyrosinase. L-DOPA is also converted to

DOPAquinone by tyrosinase enzyme. DHI (5,6-dihydroxyindole) or DHICA (5,6-dihydroxyindole-2-carboxylic acid) is subsequently formed to produce eumelanin. In other ways, the presence of glutathione or cysteine, DOPA quinone can form pheomelanin which is a red/yellow melanin (71, 85). A series of enzymatic reactions in eumelanin synthesis has resulted in reactive oxygen species formation such as O_2^- and H_2O_2 (80).

Fritzpatrick's skin type

Fritzpatrick skin type is categorized into 6 types (skin type I-VI). Skin color ranges from fair (skin type I) to very dark (skin type VI). It is based on three main factors, including genetic disposition, reaction to sun exposure and tanning habits. The skin type is determined genetically which impacts on color of eyes and hair (86). UVA and UVB exposure from sunlight also is the one of factors which involves in skin type. Minimal erythema dose (MED) is recognized as the erythemal radiant exposure which produces an erythema lesion. Moreover, the skin color depends on tanning habits which include sun bathing, artificial tanning and tanning cream (87). Fritzpatrick's skin type is shown in Table 1.

Table 1. Fritzpatrick's skin type (87).

Skin type	Skin, hair and eye color	Sunburn and tanning history	UVA MED (mJ/cm^2)	UVB MED (mJ/cm^2)
I	-Ivory white skin -Blonde hair -Blue, gray or green eyes	Burns easily, never tans	20-35	15-30
II	-White skin -Blonde or red hair -Blue eyes	Burn easily, tans minimally with difficulty	30-45	25-40
III	-White skin -Light brown hair	Burn moderately, tans moderately	40-55	30-50

	-Brown eyes	and uniformly		
IV	-Beige-olive, lightly tanned -Medium brown hair -Brown eyes	Burns minimally, tans moderately and easily	50-80	40-60
V	-Moderate brown or tanned skin -Dark hair -Brown eyes	Rarely burns, tans profusely	70-100	60-90
VI	-Dark brown or black skin -Black hair -Brown eyes	Rarely burns, tans profusely	100	90-150

MED=Minimal Erythema Dose.

Ultraviolet radiation (UVR): major factor for melasma

In daily, human skin is exposed to ultraviolet radiation from sunlight, occupational light sources and phototherapy. Ultraviolet radiation (UVR) is a component of the electromagnetic spectrum which is divided into three main parts of wavelengths: ultraviolet (5%), visible (50%) and infrared light (45%) (figure 9). UVR is the sunlight which produces three main types such as UVA (320-400 nm), UVB (290-320 nm) and UVC (100-290 nm). Three main types of the sunlight are emitted, only UVA and UVB pass to the earth's surface. All UVC and most of UVB (95%) are absorbed by the ozone layer at up to 310 nm (88). UVC has the shortest wavelengths and highest energy but UVA has the longest wavelength and least energetic photons. UVB photon is between UVA and UVC. Both UVB and UVC are absorbed by proteins and nucleic acids that they cause skin erythema. UVA is not absorbed by proteins and nucleic acids so UVA does not produce skin erythema (89). UVA penetrates deeply into dermis layer (90). UVA generates reactive oxygen species (ROS) which can damage DNA via indirect photosensitizing reactions (91). UVB is directly absorbed by

DNA which induces formation of photoproducts such as cyclobutane pyriminidine dimer and 6-4 photoproduct. The 6-4 photoproducts induce mutation in the epidermal cells and lead to the development of cancer cells (92). UVA induces skin aging, immediate and persistent pigmentation (tanning). UVB is responsible for sunburn, delayed tanning, wrinkling, photoaging and skin cancer (93).
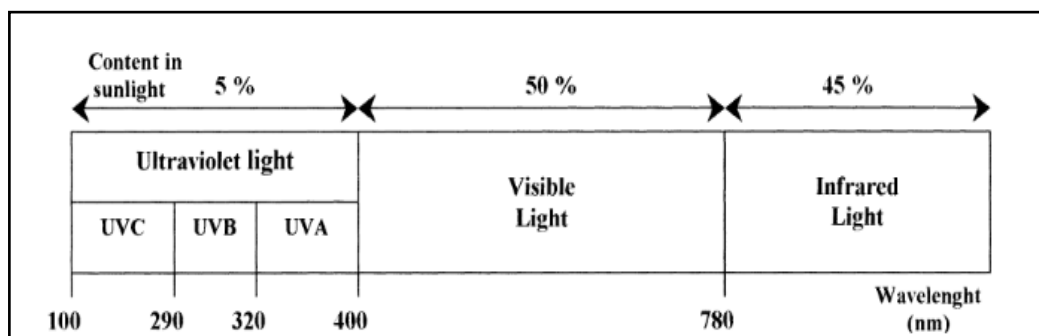
Figure 9. Solar radiation spectrum. Electromagnetic spectrum is divided into three main parts of wavelengths: ultraviolet (5%), visible (50%) and infrared light (45%). Ultraviolet radiation is subdivide into three main ultraviolet lights which contain UVA (320-400 nm), UVB (290-320) and UVC (100-290 nm) (adapted from Svobodova A, et al., 2006) (94).

α-MSH/MC1R as mediator in the skin pigmentation

Alpha-melanocyte stimulating hormone (Alpha-MSH or α-MSH) is a neuropeptide which expresses in pituitary gland. Biosynthesis of alpha-MSH depends on proteolytic cleavage of the large proopiomelanocortin (POMC) precursor (95). However, alpha-MSH and other melanocortin peptides are produced at extrapituitary sites, including skin. The alpha-MSH acts as autocrine or paracrine factor hormone in the regulation of melanocytes and skin pigmentation. Tanning is caused directly by the response of melanocytes to ultraviolet radiation (UVR), but it is affected indirectly by paracrine and autocrine factors including hormones, cytokines, and growth factors, whose synthesis in the epidermal cells or keratinocytes is influenced by UVR (3). More than 120 genes have been shown to regulate pigmentation in mammals. The major determinant of pigment phenotype is a melanocortin 1

receptor (MC1R) (96). The MC1R is expressed in a number of cells which contain endothelial cells, fibroblasts, and keratinocytes, but the highest expression is found in melanocytes. The MC1R is G-protein coupled receptor (GPCR). Its function is regulated by α-MSH and adrenocorticotropic hormone (ACTH) (97).

As shown in figure 10, UV induces cellular damage response in epidermal cells, especially keratinocytes. Damage signals such as p53 activation extremely change keratinocyte physiology, induce cell cycle arrest, activate DNA repair and promote apoptosis (98). DNA and cellular damage in keratinocytes further activate transcription of pro-opiomelanocortin (POMC) gene that encodes production and secretion of alpha-MSH, adrenocorticotropic hormone (ACTH) and β-endorphin. UV radiation induces melanogenesis of melanocytes through a paracrine regulation process involving keratinocytes (4). On binding to the melanocortin receptor (MC1R) on melanocytes in the epidermis layer of the skin, alpha-MSH activates intracellular adenyl cyclase followed by increased intracellular cyclic AMP (cAMP) level as a secondary messenger from adenosine triphosphate (ATP) (5). Cyclic AMP leads to activate protein kinase A (PKA). The PKA phosphorylates and activates the cAMP-response element binding protein (CREB) which binds to cAMP response element (CRE) presenting in the M promoter of the microphthalmia-associated transcription factor (MITF) gene. The increase of MITF may lead to the up-regulation of melanogenic enzymes such as tyrosinase, tyrosinase-related protein 1 (TRP-1) and tyrosinase-related protein 2 (TRP-2) (6). These enzymes control eumelanin synthesis in the melanocytes. The eumelanin is the most important of two melanins for skin pigment. Thus, α-MSH/MC1R signaling increases pigment synthesis by melanocytes and deposition of melanin in surrounding keratinocytes that it causes hyperpigmentation or melasma in UV-exposed skin (99).
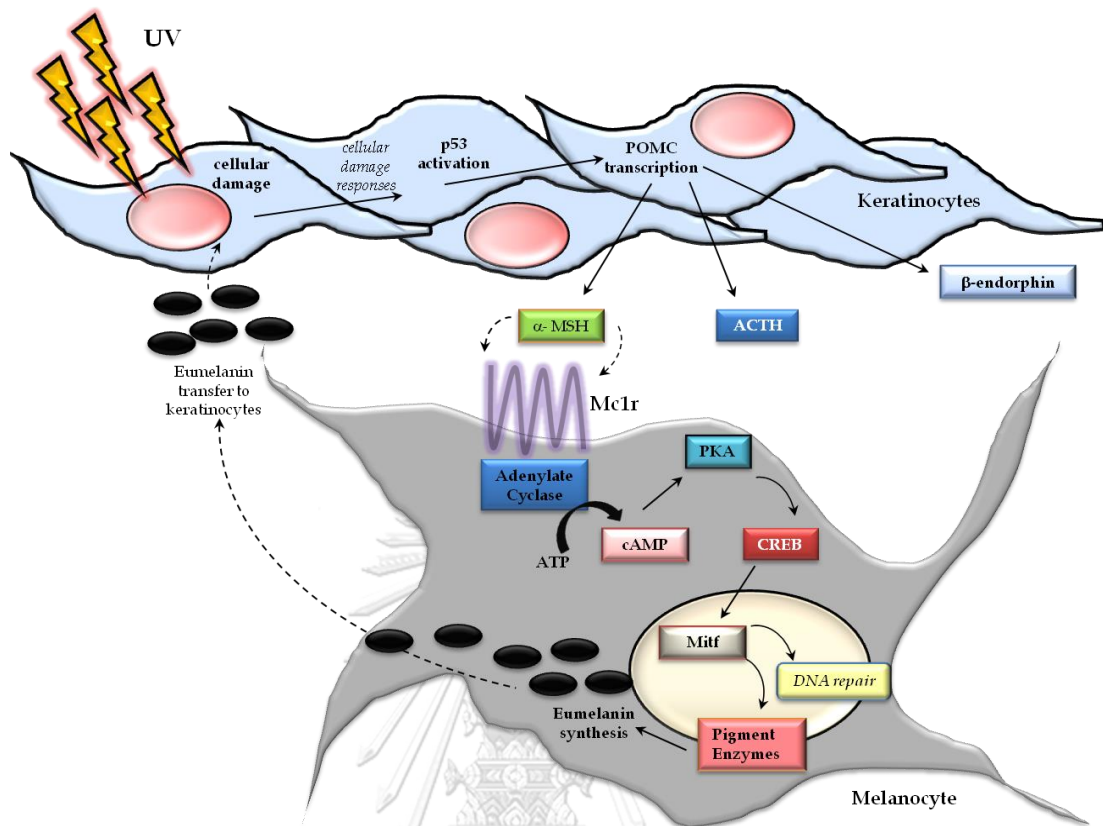
Figure 10. **α**-MSH/MC1R as mediator in skin pigmentation. UV radiation induces the melanogenesis of melanocytes through a paracrine regulation process involving keratinocytes (4). UV induces cellular damage which induces p53 activation. The p53 further activates transcription of pro-opiomelanocortin (POMC) gene that encodes production and secretion of alpha-MSH, adrenocorticotropic hormone (ACTH) and **β**-endorphin. On binding to MC1R, **α**-MSH from keratinocytes activates adenylate cyclase which upregulates cAMP level, leading to CREB activation and binding to CRE in MITF promoter to induce MITF transcription. The increased MITF may lead to up-regulate of pigment enzymes for melanin synthesis (adapted from D'Orazio J, et al., 2013) (100).

Melasma

Melasma is a chronic acquired hypermelanosis which occurs systematically on sun-exposed area of the skin. Centrofacial pattern is the most common lesion and involves in cheek, upper lip, forehead and chin. M*alar pattern* is found on the cheek and nose. *Mandibular pattern* involves ramus of the mandible. However, it can occasionally occur in other sun-exposed areas of the body. Genetic background, sun exposure, age (elderly) and female sex hormones are classical involving factors (2). Moreover, melasma may affect any races; it is much more common in the darker skin types (skin types III to V) than in the lighter skin types. It is most commonly found in the light brown skin, especially in people of East Asian, Southeast Asian, and Hispanic origin who live in the areas of high exposure to ultraviolet radiation (101). This disease has the lesion on the face, so this disease has an impact on quality of life. Melasma in females is most commonly associated with pregnancy but it is also found in woman taking oral contraceptive pills, estrogen replacement therapy and certain other medications. The mechanism of hyperpigmentation by estrogen is associated with the presence of estrogen receptors on the melanocytes which activate the cells to produce more melanin. Other factors in the epidemiology of melasma are photosensitizing and anticonvulsant medications, mild ovarian or thyroid dysfunction, and certain cosmetics. One of the most important factors in melasma is a UV exposure (102). Pathogenesis of the melasma contains the overexpression of alpha-MSH, the increase in size of melanosomes in keratinocytes and melanocytes, the high amount of melanin and the high level of tyrosinase activity (103).

Facial melasma patterns

Melasma is characterized by hyperpigmentation on the face. Melasma lesion is shown as macules (freckle-like spot) and larger brown patches. The lesions are located on both sides of face and irregular border. Facial melasma patterns are divided into to three types.

1. Centrofacial pattern

Centrofacial patten is the most common lesion of melasma. It is found on cheek, upper lip, forehead, and chin (104).

Figure 11. Centrofacial pattern of melasma (104).

2. Malar pattern

M*alar pattern* is found on cheek and nose (104).

Figure 12. Malar pattern of melasma (104).

3. Mandibular pattern

Mandibular pattern involves ramus of the mandible (105).

Figure 13. Mandibular pattern of melasma (105).

Wood's light examination

Wood's light examination is a test in which skin is expose to black light emitted by Wood lamp. Black light as UVA light is in ultraviolet spectrum that it is opaque to all radiation, except wavelength 320-400 nm (peak at 365 nm). A wood lamp is a high pressure mercury arc covered with filter (made from barium silicate with 9% nickel oxide) (106). UVA penetrates into stratum corneum and epidermis layer where melanin is located. In dark room, wood's light shine directly on the affected area and look for color change or fluorescence. Normal skin does not fluoresce under wood's light. Wood's light is used to examine the depth of melanin in skin and to classify melasma into four types; epidermal, dermal, mixed and Wood's light inapparent. This examination is also used to prognosis the treatment (107).

1. Epidermal type

   Epidermal type (skin surface) is the most common type that melanin is increased in the epidermis layer of the skin, especially stratum corneum. The epidermal melasma responds well to treatment and has dark brown color (108).
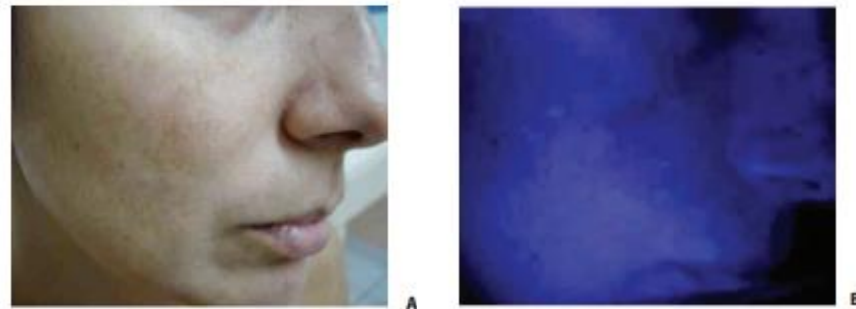

Figure 14. Epidermal type. A) Clinic; B) Examination under Wood's light (109).

2. Dermal type

   In dermal type, the pigmentation shows no enhancement of color and responds poorly to treatment. The dermal melasma has many melanophages in the dermis layer (108).
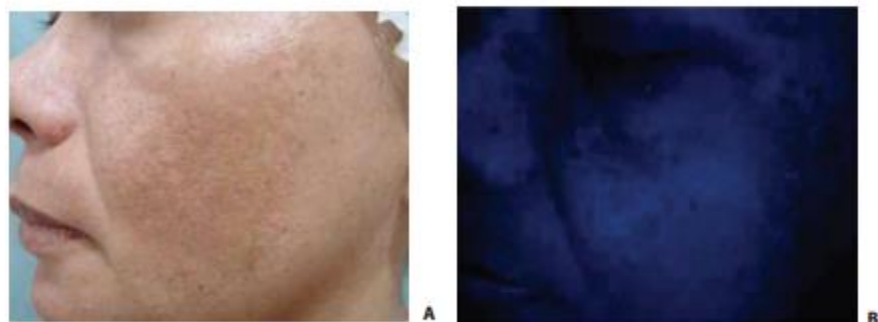
Figure 15. Dermal type. A) Clinic; B) Examination under Wood's light (109).

3. Mixed type

    In mixed type, clinical feature is combined between epidermal and dermal types. Melasma lesion can be found only few sites (108).

Figure 16. Mixed type. A) Clinic; B) Examination under Wood's light (109).

4. Wood's light inapparent type (fourth type)

    In intermediate type, the pigment is apparent in individuals with skin type V and VI (108).

    In addition, depending on the natural history of the lesions, melasma may also be divided into transient and persistent type. The transient type disappears within one year of discontinuance of hormone stimuli like pregnancy or oral contraceptive pills. The persistent type persists more than one year after withdrawal of hormone stimuli and is maintained by UV factor and other factors (110).

Etiological factors for melasma

    There are many factors which involve on the onset of melasma, including genetic factors, sun exposure, female sex hormones, other factors (111).

1. Genetic factors

    People with skin type III, IV or V and female gender are predisposition factors for melasma. Pigmentation disorders are often found in Hispanic and Asian racial groups with Fitzpatrick skin types III/V (112).A global survey of international experts of nine countries (United States of America, France, Germany, Netherlands, Mexico, Italy, Singapore, South Korea, Hong Kong) found that 48% of

324 women with melasma had a family history of melasma disease (113). However, genetic factors of melasma is still unknown.

2. Sun exposure

Sun exposure is the most important of environment factor in melasma. UV radiation from sunlight activate the production of free radicals that can stimulate melanin synthesis (114). Moreover, UV ray can induce melanocyte proliferation, migration and melanogenesis directly. Indirectly, UV stimulate the release of endothelin 1, alpha-melanocyte stimulating hormone (α-MSH) and adrenocorticotropic hormone (ACTH) from keratinocytes and basic fibroblast growth factor (bFGF) (115). As shown in figure 17, UV induces the effect of endothelin 1 through binding on endothelin receptor type B (ETB) and activating ERK1/2. ERK1/2 further phosphorylates to p90 which also phosphorylates to cAMP respond element binding protein (CREB). Activated CREB leads to activate Microphthalmia-associated transcription factor (MITF) which is a transcription factor for melanogenic enzymes (116). Moreover, UV stimulates α-MSH production and ACTH from keratinocytes. Binding of α-MSH or ACTH on melanocortin 1 receptor (MC1R), activates cyclic adenosine monophosphate (cAMP) dependent protein kinase A (PKA). PKA further activates the MAP kinases ERK1/2 for activating MITF (117). Basic FGF binds to tyrosine kinase receptor and activates protein kinase C (PKC). PKC also activates the MAP kinase ERK1/2 which leads to activate MITF (118). Both α-MSH and ET-1 activate Akt survival pathway which also contribute to activate MITF activity for inhibiting apoptosis (119).
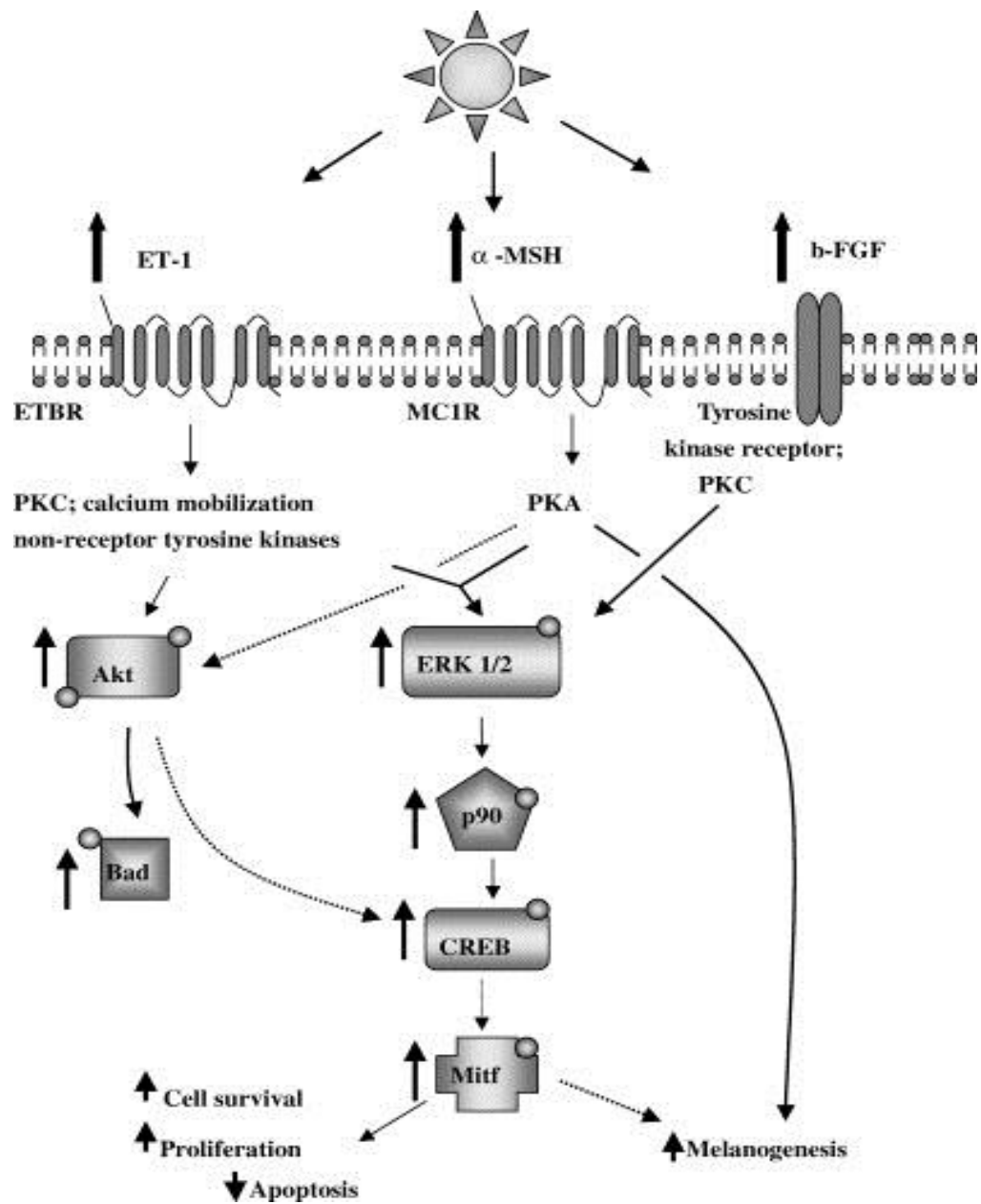
Figure 17. Effect of UV in skin keratinocytes and melanocytes. Exposure to UV, keratinocytes release various factors such as endothelin 1 (ET-1), alpha-melanocyte stimulating hormone (α-MSH) and basis fibroblast growth factor (bFGF). ET-1 and α-MSH activate the MAP kinases ERK1/2 for MITF activity. Basic FGF activates the MAP kinases ERK1/2 through PKC. Activated MITF has the effect on cell survival, proliferation and melanogenesis in melanocytes (adapted from Kadekaro AL, et al., 2003) (120).

3. Female sex hormones

Female sex hormones (during pregnancy) and oral contraceptive pills are related to melasma. Sex hormone, including estrogen, estriol and progesterone was elevated in association with melasma (121). Estrogen receptors are found on melanocytes. Estrogen receptors are divided into two types; estrogen receptor alpha (ER-α) and estrogen receptor beta (ER-β) (122). Elevated estrogens from pregnancy or oral contraceptive pills have impact on melanin synthesis. Estrogens bind to estrogen receptors in nucleus through non genomic fashion. PDZ domain containing 1 (PDZK1) protein is a downstream mechanism of estrogens in melasma which promotes transcription of tyrosinase and melanosome transfer without increasing the number of melanocytes and keratinocytes (123).

Figure 18. Effect of estrogens on nucleus receptor of melanocyte through PDZK1. PDZK1 facilitates estrogens through estrogen receptor alpha (ER-α) that this action increases the transcription of tyrosinase and melanosome transfer in the skin. CFTR = cystic fibrosis transmembrane conductance regulator; ER = estrogen receptor; NHE =

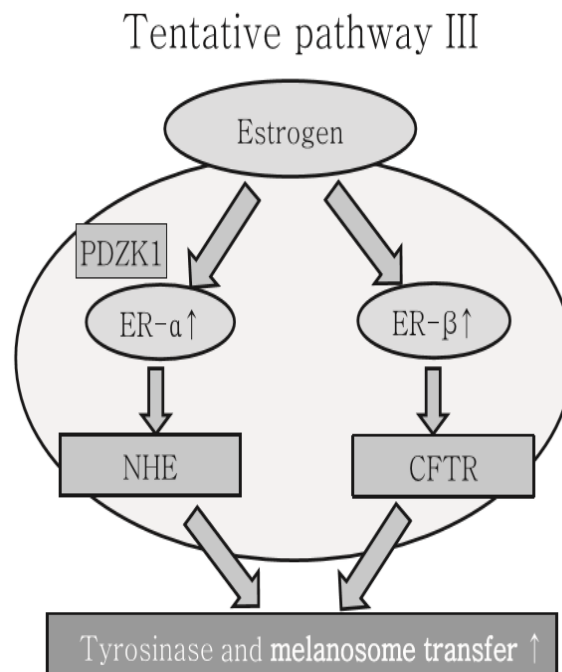sodium hydrogen exchanger; PDZK1 = PDZ domain containing 1 (adapted from Lee AY, et al., 2014) (112).

4. Other factors

Melasma can occur from drugs, containing phototoxic agents, phenothaizines and anticonvulsants (124). Moreover, other agents such as anticonvulsivants, antimalarials, tetracyclines, amiodarone, sulfonylureas, iron, copper, gold, silver, arsenic, and bismuth, also stimulate melanin synthesis. However, it is still unclear (111). Normally, cosmetics have many mixtures such as perfumes, preservatives, emulsifiers and stabilizers, lipids, and alcohols. Many chemicals in cosmetics (colophony, PPD, balsam peru, cetostearyl alcohol, lanolin, bees wax, formaldehyde, fragrances, musk mix, vanillin, rose oil, triclosan, or other antiseptics) occur to change pigmentation. Skin contact sensitivity from cosmetics is an important factor of melasma which is not related to pregnancy or contraceptive pills (125).

Melasma treatment

Melasma treatment depends on whether the pigmentation is epidermal or dermal. Only epidermal pigmentation responds well to treatment. Management of melasma consists of discontinuing hormonal contraception, the avoidance of direct sun-exposure, the use of a broad-spectrum sunscreen and the avoidance of scented cosmetics. Topical corticosteroids have been included in several clinical trials for the treatment of melasma to decrease the irritation caused by depigmenting agents (10).

1. Topical treatment

    1.1   Hydroquinone (HQ)

        Hydroquinone is the most popular depigmenting agent for melasma. It is commonly use at the concentrations of 2-4%. High concentrations of hydroquinone induce skin irritation. The hydroquinone is a phenolic compound. Its structure is similar with tyrosine, so it can bind to

tyrosinase enzymes at copper binding site. In the result of this reaction, the melanin synthesis is reduced by inhibiting tyrosinase activity. However, the hydroquinone is oxidized semi-quinone-like as free radical. This radical can damage protein and lipid (126). Moreover, the radicals can cause degradation of melanosomes and melanocytes. The adverse effects of hydroquinone include erythema, stinging, colloid milium, irritant and allergic contact dermatitis, nail discoloration, transient hypochromia, and paradoxical postinflammatory hypermelanosis (11). In addition, the prolonged usage of hydroquinone leads to ochronosis (127). Combination treatment is recommended more than single treatment. The most popular combination consists of hydroquinone, a topical steroid, and retinoic acid (128).

1.2   Kojic acid (KA)

Kojic acid (5-hydroxy-2 hydroxymethyl-4-pyrone) is a naturally occurring fungal product derived from several species of Acetobacter, Aspergillus, and Penicillium (129). It is widely used at concentrations ranging from 1 to 4%. It reduces melanin synthesis by inhibiting tyrosinase activity only (130). Side effects of kojic acid are redness, stinging and exfoliation (131).

1.3   Arbutin

Arbutin is also one of the most commonly depigmenting agents for melasma. Arbutin, a beta-D-glucopyranoside hydroquinone derived from bearberry plant (132). It inhibits tyrosinase activity and melanosome maturation in human melanocytes without affecting on mRNA transcription of tyrosinase (133). This compound is less toxic than hydroquinone. However, arbutin can cause allergic contact dermatitis (134).

1.4   Tretinoin

Tretinoin is a retinoid. It is used to combine with hydroquinone for melasma. It disperses pigment granules in keratinocytes, interfere melanosome transfer and accelerate skin turnover (135). It also inhibits tyrosinase activity (136). Concentrations of tretinoin range from 0.05% to 0.1% (137). Side effects of tretinoin contain burning, erythema, scaling and dry skin. High dose of tretinonin induces skin inflammation which cause hyperpigmentation (138).

1.5   Azelaic acid (AzA)

Azelaic acid is a nine carbon (C9) dicarboxylic acid. It is an irreversible tyrosinase inhibitor. But it has the cytotoxic and antiproliferative effects on melanocytes (139). Concentrations of azelaic are between 10% and 20%. At dose of 20% azelaic acid induces skin pruritus, buring, stinging and tingling. Other side effects of azelaic acid are erytherma, dryness, rash, irritation and dermatitis (140).

1.6   Corticosteroids

Topical corticosteriods are anti-inflammatory and anti-metabolic effect which reduce epidermal turnover (141). They contain 0.01% fluocinolone acetonide resulting in inhibition of prostaglandins and leukotrienes from epidermal cells (142). Adverse effects of corticosteroids include erythema, prustles, and papules. Moreover, topical corticosteroids can also produce allergic contact dermatitis by themselves (143).

1.7   Glycolic acid (GA)

Glycolic acid (GA) is an alpha hydroxyl acid with high polarity. It contains two carbon atoms. One carbon atom is with a carboxyl group while another carbon atom is with a hydroxyl group. Usually, it is used at concentration of 10-20% in skin whitening cream (144). It can decrease melanin by peeling stratum corneum, accelerating epidermolysis, dispersing melanin in basal layer, and increasing collagen in dermis layer (145).

1.8   Combination treatment

Combination treatment is more effective than single use. This combination is composed of hydroquinone 4%, tretinoin 0.05%, and fluocinolone acetonide 0.01%. This formula is applied in the first line treatment for melasma. When patients have sensitivity to the triple combination, dual ingredients (hydroquinone and glycolic acid) or single dose should be considered (146). Hydroquinone inhibit melanin synthesis (126). While, tretinoin helps to increase keratinocyte proliferation (135). And fluocinolone acetonide serves as a topical steroids which reduce inflammation from hypopigmenting agents (142).

2. Dermabrasion

Dermabrasion is a treatment to remove top layer of skin (epidermis layer or reticular dermis) by using a diamond fraise (147). It is a technique for chemical exfoliation, facial resurfacing and scar revision (148). After dermabrasion, there are many side effects, including postoperative erythema, pruritus, milia formation, hypertrophic scarring and infection (149). So, dermabrasion is not a standard treatment for melasma.

3. Intense pulsed light therapy (IPL)

Intense pulsed light therapy (IPL) is a device which is high intensity light source. This device uses flashlamp and bandpass filters to produce polychromatic noncoherent light in the wavelength of 400-2000 nm (150). While, light pulses was generated by bursts of electrical current passing through a xenon gas-filled chamber. Output of lamp is sent directly to the distal end of handpiece resulting in the release of energy pulse onto the skin surface via sapphire or quartz block. IPL has a cooling system (cryogen spray, contact cooling or forced refrigerated air) in which protect the epidermis layer to contact with the crystal of handpiece. The IPL has a specific wavelength, fluences, pulse durations, and pulse intervals for the treatment of a wide sprectrum of skin conditions (151). The IPL is based on the principle of photothermolysis to target at cellular or tissue levels. There are three main chromophores in the skin such as hemoglobin, water and melanin. These chromophores can absorb broad spectrum wavelength of light. The broad spectrum

wavelength released from IPL leads to stimulate the emission of green, yellow, red, and infrared wavelengths. The chromophores can be target concurrently (150). The IPL is a selective therapy for removing melanocytic lesions in epidermal or mixed types of melasma. The IPL is more effective in epidermal type of melasma (152). After treatment with IPL, there are erythema and edema within 24-48 hours that it is typical. However, IPL is less effective in melasma treatment (153).

4. Laser treatment

Lasers have been used in various skin condition, including melasma, post-inflammatory hyperpigmentation (PIH), nevus, lentigines, and tattoos. The lasers are sources of high intensity monochromatic coherent light. Laser treatment is based on the principle of selective photothermolysis. The laser treatment depends on the wavelength, pulses and fluence (154). There are three types of lasers for melasma treatment as the following:

4.1   Green light lasers: flashlamp-pumped pulsed dye laser (PDL) (510 nm), frequency doubled QS Nd:YAG (Q Switched Neodymium: Yttrium Aluminium Garnet-532 nm)

Green light lasers penetrate into epidermis layer. Oxyhaemoglobin can absorb green light laser, resulting in bruising and purpura. Then, purpura can developed into post inflammatory hyperpigmentation or PIH (155).

4.2   Red light lasers: Q-Switched (QS) Ruby (694 nm), Q-Switched Alexandrite (755 nm)

Red lasers have longer wavelengths so it can enter into deep layer, especially dermis. They can be used to treat epidermal type of melasma without brusing. Because haemoglobin cannot absorb red lasers. However, these lasers lead to photoacoustic mechanical disruption of melanin (153). Pulse duration of QS ruby is between 20 and 50 ns while QS alexandrite has pulse duration from 50 to 100 ns (154).

4.3   Near-infrared: Q-Switched neodymium: yttrium-aluminium-garnet (QS Nd:YAG) (1064 nm)

YAG laser has a pulse duration about 10 ns. This laser can be absorbed melanin less than green and red lasers but it can penetrate into deep layer. So, this laser is more useful in darker skin (156).

Herbal therapy for melasma

Chemical agents are used as depigmenting agents in dermatology and cosmetics. Especially, hydroquinone is the most popular depigmenting agents for melasma treatment but it had many side effects (11). The activity of kojic acid, also used as depigmenting agent, inhibit tyrosinase activity; however, it induced dermatitis and cytotoxicity (157). Thus, many researchers seek new agents for melasma treatment. The new agents should be safety and efficacy without side effects. Naturally occurring herbal extracts, active compounds such as phenol, flavonoid, gallic acid, epigallocatechin, aloesin, hydroxystillbene and ellagic acid (12). In the previous study, flavonoids inhibited mushroom tyrosinase enzyme by chelating copper at active site (13). Gallic acid derivatives of flavonols from green tea were identified as strong tyrosinase and inhibitor. Moreover, the major active compound in the green tea were (-)-epicatechin 3-O-gallate (ECG), (-)-gallocatechin 3-O-gallate (GCG), and (-)-epigallocatechin 3-O-gallate (EGCG) which also inhibited tyrosinase (14). In addition, aloesin from aloe plant modulated melanogenesis through tyrosinase inhibition (158). Hydroxystillbene derivatives such as oxyresveratrol and resveratrol had the high affinity to tyrosinase (159). However, some data reported that resveratrol reduced microphthalmia-associated transcription factor and tyrosinase promoter activities in melanocytes culture (160). Yoshimura and collaborators found that ellagic acid from a pomegranate extract inhibited the proliferation of melanocytes and melanin synthesis in UV-induced skin pigmentation on the back of brownish guinea pigs (161). The depigmenting agents from natural products are shown in table 2. Therefore, natural products may be considered as new, safety and efficient depigmenting agents for melasma treatment.

Table 2. Some skin-whitening agents and their effects on melanin synthesis.

Compounds	Plants	Mechanism	Reference
Aloesin	Aloe	Tyrosinase inhibition	(158)
Arbutin	Bearberry	Inhibit tysoinase and melanosome maturation	(132)
Ascorbic acid	Green tea	Tyrosinase inhibition	(14)
(-)EpiCatechin-3-O-Gallate (ECG)	Green tea	Tyrosinase inhibition	
(-)-epigallocatechin 3-O-gallate (EGCG)	Green tea	Inhibit tyroinase and decrease MITF expression	(14)
Ellagic acids	Pomegranate	Tyrosinase inhibition	(161)
Gallic acid	Green tea	Tyrosinase inhibition	(14)
Imperatorin	*Angelica dahurica*	Inhibit mRNA of tyroinase	(162)
Hydroxystillbene derivatives;oxyresveratrol, resveratrol	Grape	Tyrosinase inhibition	(159, 163)
Oxyresveratrol and trans-dihydromorin	*Cudrania tricuspidata*	Inhibit tyrosinase and decrease MITF expression	(164)

Plants

In this study, we used 13 plants for determining effects of plant extracts on melanin synthesis.

1. *Ardisia elliptica* Thunb.

Botanical description

Ardisia elliptica is evergreen tree with smooth stem and new foliage often reddish. Leaves are oblong to oval, fleshy, leathery, and alternate. Petal is pink. Fruits are rounded drupe, red returning to black when ripe (165).

Scientific classification

Family	Myrsinaceae
Genus	*Ardisia*
Species	*Ardisia elliptica*

Species information

Scientific name	*Ardisia elliptica* Thunb.
Common name	Shoebutton ardisia
Local name	Ram-Yai
Synonyms	*Ardisia polycephala* Wall., *Ardisia solanacea* Roxb., *Ardisia humilis* Vahl.
Origin	India, China, Southeast Asia

Medicinal properties

Ardisia elliptica is a medicinal plant for alleviating chest pain, fever, diarrhea, and liver poisoning. Methanol extract of A. *elliptica* leaves was found to inhibit platelet aggregation that β-amyrin is one of bioactive compounds (166). Methanol extract of leaves also showed antioxidant activity with DPPH that it contains alkaloids, carbohydrates, steroids, and tannins (167). Fruit extract of A. *elliptica* had antibacterial activity against veterinary Salmonella that there are three active compounds in fruit extract, including syringic acid, isorhamnetin and quercetin (168). Moreover, leaves and fruits extracts of A. *elliptica* almost had the same chemical constituents, as shown in table 2 and 3. One of chemical constituents is clindamycin which has antibacterial activity against Escherichia coli and Staphylococcus aureus (169). Major compounds in methanol leaf extract contain Gingerol, Aspidin,

Triangularin, and Salicyl acyl glucuronide detected by Liquid Chromatography-Mass Spectrometry (LC-MS) (170). Bauerenol is an active compound in leaf extract which was found the toxicity with teratologic manifestations (axial deformation and yolk sac edema), and inhibition of blastema cell proliferation and differentiation (171).

Table 2. Chemical constituents of methanol leave extract of *Ardisia elliptica* (169).

Chemical constituents	Leaves extract
2-methoxy-1-(2-nitroethenyl)-3-benzene	√
Chlorfenapyr	√
Clindamycin	√
Decamethyl-cyclopentasiloxane	√
1-naphthyl ester acetoxyacetic acid	√
5-hydroxymeth 2-furancarboxaldehyde	√
Methyl 3-amino-2-thiophenecarboxyldehyde	√
4-cyanophenyl 2,6-difluorobenzoic acid	√
2,4-bis(1,1-dimethylethyl)-phenol	√

Table 3. Chemical constituents of methanol fruit extract of *Ardisia elliptica* (169).

Chemical constituents	Fruits extract
2-methoxy-1-(2-nitroethenyl)-3-benzene	√
Clindamycin	√
Decamethyl-cyclopentasiloxane	√
1-naphthyl ester acetoxyacetic acid	√
5-hydroxymeth 2-furancarboxaldehyde	√
Dodecamethyl-cyclohexasiloxane	√
tetradecamethyl-cyclohexasiloxane	√
Tridec-2-ynyl 2.6-difluorobenzoic acid	√
2,4-bis(1,1-dimethylethyl)-phenol	√

2. *Croton roxburghii* N.P.Balakr

<u>Botanical description</u>

Croton roxburghii is a medium tree. It has greenish crenate or serrate leaves, grayish brown colored bark, and creamish yellow root (172).

<u>Scientific classification</u>

Family	Euphorbiceae
Genus	Croton
Species	*Croton roxburghii*

<u>Species information</u>

Scientific name	*Croton roxburghii* N.P.Balakr
Local names	Plao Luang, Plao Yai
Synonyms	*Croton oblongifolius* Roxb.,
	Oxydectes oblongifolia Kuntze,
	Oxydectes persimilis (Müll.Arg.) Kuntze
Origin	Asia

<u>Medicinal properties</u>

Aqueous and alcoholic extracts of *Croton roxburghiii* bark and leaf are responsible for antibacterial property against S*taphylococcus aureus* and *Escherichia coli* (173). In addition, petroleum ether, acetone, ethanol, methanol, and aqueous extract of C. *roxburghii* showed the inhibition of *Candida species*. There are many phytochemical compounds such as tannins, phenolics, flavonoids, carbohydrates, proteins, and amino acids in polar extracts (ethanol, methanol, and aqueous) (174). Moreover, stem, bark and leaves of C. *roxburghiii* is used as herbal treatment for ringworm, wounds, scabies, skin diseases, liver diseases, diarrhea, fever and headache (172). Croton family has a lot of alkaloids and is known as medicinal plants (175).

3. *Croton sublyratus* Kurz.

Botanical description

   Croton sublyratus is a shrub or small tree. It has obovate leaves in Thailand. Fruits are develop when staminate flowers still are in bud (176).

Scientific classification

   Family   Euphorbiceae

   Genus   Croton

   Species   *Croton sublyratus*

Species information

   Scientific name   *Croton sublyratus* Kurz.

   Local name   Plao noi

   Synonyms   *Oxydectes sublyrata* (Kurz) Kuntze

   Origin   South-East Asia

Medicinal properties

   Plaunotol from leaves of *Croton sublyratus* is an acyclic diterpenoid which showed a potential anti-angiogenic effect in human umbilical vein endothelial cells (HUVEC) (177). Plaunotol also had antibacterial activity against Staphylococcus aureus isolated from patients' skin with atopic dermatitis (178). Moreover, plaunotol from ethanol extract of C. *sublyratus* had the highly effective antigastric ulcer properties in rats (179). Admistration of a partitially purified plaunotol extract (PPE) at 1,100 mg/kg/day over 6 months induced bile duct hyperplasia in male and female rats, congestion and dilations of neuronal tubes in female rats. However, therapeutic dose (11-550 mg/kg) of PPE didn't induce pathological changes in liver and kidney cells. This crude extracts of C. *sublyratus* may be developed as a healthcare product (179).

4. *Datura metel* L.

Botanical description

        Datura metel L. is an erect shrub with spreading branches. It has simple, alternate, green, and glabrous leaves. Its flower are large, solitary, and trumpet-liked. Color of flower varies from white, yellow, light to dark purple A capsule of fruit is covered with short spines (180).

Scientific classification

Family	Solanaceae
Genus	*Datura*
Species	*Datura metel*

Species information

Scientific name	*Datura metel* L.
Common names	Devil's trumpet, metel, thorn apple
Local name	Lam Phong Kao
Synonyms	*Datura fastuosa*, *Datura chlorantha*, *Datura stramonium*
Origin	East Asia, India

Medicinal properties

        Methanol, acetone and dichloromethane extracts of *Datura metel* leaves had the inhibitory effect of mushroom tyrosinase activity (181). Dried leaves of D. *metel* contain alkaloids, flavonoids, saponins, steroids and tannins (182). D. *metel* is a medicinal herb for epilepsy, hysteria, heart diseases, cough, convulsions, diarrhea and skin diseases (183). Major compounds in D. *metel* leaves are atropine and hyoscyamine. Atropine affects in neuron and cardiovascular system. It bind competitively to peripheral and central muscarinic receptors. Hyoscyamine and scopolamine impacts on central and peripheral nervous systems by acting as an anti-muscarinic compound (184) .

5. *Garcinia mangostana* Linn.

<u>Botanical description</u>

      Garcinia mangostana Linn. (GML) is a tropical evergreen tree. It has leathery and glabrous leaves. Fruits are dark-purple or reddish with white, soft and juicy edible pulp when ripe (185).

<u>Scientific classification</u>

Family	Guttiferae
Genus	*Garcnia*
Species	*Garcinia mangostana*

<u>Species information</u>

Scientific name	*Garcinia mangostana* Linn.
Common names	mangosteen
Local name	Mung Kut
Origin	India, Myanmar, Malaysia, Sri Lanka and Thailand

<u>Medicinal properties</u>

      Ethanol extract of *Garcinia mangostana* pericarps showed the inhibitory effect of tyrosinase activity (186). G. *mangostana* also reduced TNF-alpha which is a pro-inflammatory cytokine of acne caused by *Propionibacterium acnes* (187, 188). Fruit of mangosteen is the main source of xanthones. Polyphenolic xanthones, including α-mangostin induced apoptosis and inhibited cell proliferation in cancer cells (breast and prostate cancers) (189). Pericarp of mangosteen has many active compound such as xanthones, terpenes, anthocyanins, tannins and phenols. Xanthones in pericarp are α-mangostin, β-mangostin, γ-mangostin, garcinone E, and gartanin. Pharmacoligical activites of xanthones in pericarp are antioxidant, anti-tumor, anti-allergic, anti-inflammatory, anti-bacterial, anti-fungal, and anti-viral activities (190). However, crude methanolic extract of pericarp at 1000 mg/kg had a lethal dose in female BALB/c mice and also induced acute oral toxicity. While, at dose of 100 and 200 mg/kg had the effective dose of anti-tumor activity (191).

6. *Gynura pseudochina* (L.) DC.

<u>Botanical description</u>

Gynura pseudochina (L.) DC. is a perennial herbaceous plant with semi-succulent stem. It has elliptic and coarsely dentate leaf with multicellular hairs. Flower of G. *pseudochina* is yellow to red corolla on short peduncle (192).

<u>Scientific classification</u>

Family	Asteraceae
Genus	*Gynura*
Species	*Gynura pseudochina*

<u>Species information</u>

Scientific name	*Gynura pseudochina* (L.) DC.
Local name	Warn Ma Ha Kan
Synonym	*Gynura miniata*
Origin	Africa

<u>Medicinal properties</u>

Methanol extract of *Gynura pseudochina* leaves showed the inhibition of nuclear factor-**K**B that Quercetin-rutinoside, 3, 5- dicaffeoyl quinic acid, 4, 5 dicaffeoyl quinic acid and 3-, or 5- caffeoyl quinic acid were found in the extract. In addition, leaves and rhizomes have been used traditionally for skin inflammation as well as viral infection (193). G. *pseudochina* extract also decreased psoriasis lesion in the patients, because of downregulation of nuclear factor-**K**B (194). Moreover, leaves of G. *pesudochina* contains pyrrolizidine alkaloids which have adverse effects in animal and human such as hepatotoxic, pneumotoxic, genotoxic, neurotoxic, and cytotoxic (195).

7. *Hibiscus mutabilis* L.

<u>Botanical description</u>

    Hibiscus mutabilis L. is a shrub tree. Flowers can be single or double. They open white to pink and change to deep red in the evening. Leaves are simple, bright green, hairy and deeply lobed (196).

<u>Scientific classification</u>

Family	Malvaceae
Genus	*Hibiscus*
Species	*Hibiscus mutabilis*

<u>Species information</u>

Scientific name	*Hibiscus mutabilis* L.
Common names	Confederate rose, Dixie rosemallow, cotton, rosemallow
Local name	Phud Tarn
Synonym	*Hibiscus sinensis*
Origin	China

<u>Medicinal properties</u>

    Methanol extract of *Hibiscus mutabilis* leaves showed a potential diabetic effect in alloxan-induced diabetic rat and decreased mortality rate (197). Ferulic acid and caffeic acid from methanol leave extract were identified as α-glucosidase inhibitor (198). H. *mutabilis* also has rutin and isowuercitin in leaves (199). Moreover, methanol extract of H. *mutabilis* leaves displayed tyrosinase inhibition and antibacterial activity At the concentration of 8 mg/ml of methanol extract of H. *mutabilis* leaves significantly reduced tyrosinase activity about 25%. While, methanol extract of H. *tiliaceus* at 7 mg/ml had the strongest inhibition of tyrosinase activity about 42% (200). Ethanol extract of H. *mutabilis* also decreased IL-6, NO and TNF-α levels in the inflammatory cells (201).

8. *Ipomoea pes-caprae* (L.) R.br.

Botanical description

Ipomoea pes-caprae (L.) R.br. grows above the high tide line along coastal beaches. I has thick root. Leaves of *I. pescaprae* are thick, smooth and alternate. Flowers are auxiliary funnel-shaped and pink to purple (202).

Scientific classification

Family	Convolvulaceae
Genus	*Ipomoea*
Species	*Ipomoea pes-caprae*

Species information

Scientific name	*Ipomoea pes-caprae* (L.) R.br.
Common names	Beach morning glory, railroad vine, sea morning glory, goat's feet
Local name	Pak Bung Ta le
Synonym	*Ipomoea pes-caprae* ssp. *brasiliensis*, *Ipomoea biloba*
Origin	Asia

Medicinal properties

Topical application of I. p*es-caprae* leaves reduced carrageenan-induced paw oedema and ear edema in rat (203). Petroleum extract of I. *pes-caprae* neutralized jellyfish venom, resulting in the decrease of dermatitis lesion (204). Non polar and polar extracts of I. p*es-caprae* contain tannin and saponin (205). Alkaloids, carbohydrates, glycosides, flavonoids, tannins, sterols and terpenoids are also found in leaf and stem extracts Moreover, there are many phytochemical constituents in whole plants with different solvents (as shown in table 4). Ethanol extracts of I. p*es-caprae* leaves restored markly the level of blood glucose, AST, ALT and ALP in diabetic rats (206). Moreover, topical application of I. p*es-caprae* leaf extract significantly inhibited the inflammation by reducing prostaglandin and leukotriene (207). However, high dose of I. p*es-caprae* ethanolic extract from leaves (over 2,000 mg/kg) induced acute oral toxicity (208).

Table 4. Phytochemical constituents of whole plant from *Ipomoea pes-caprae* (209).

Phytochemicals	Hexane	Benzene	Chloro-form	Ethyl acetate	Acetone	Methanol
Carbohydrates	+	-	-	+	+	+
Monosaccharides	-	-	-	++	+	+
Free reducing sugars	++	-	-	-	-	++
Combined reducing sugars	-	-	-	-	-	+
Tannins	-	+	-	+	+	-
Free anthraquinones	-	+	-	+	+	-
Steroids	-	+	+	+	+	+
Cardiac glycosides	-	+	+	+	+	-
Terpenoids	-	++	++	+	+	+
Saponins	-	-	+	++	++	-
Flavonoids	-	-	-	++	++	+
Soluble starch	-	-	-	+	+	+
Alkaloids	-	+	-	+	+	+

+ ve – present, - ve - Absent

9. *Phyllanthus acidus* (L.) Skeels

<u>Botanical description</u>

Phyllanthus acidus (L.) Skeels is ornamental shrub or tree. Tree's dense and bushy crown is composed of thickish, rough and main branches. Leaves are long, thin, and smooth on the upperside and blue-green on the underside. Flowers are small, pink and appear in clusters. Fruits are numerous, oblate, pate to yellow (210).

<u>Scientific classification</u>

Family	Euphorbiaceae
Genus	*Phyllanthus*
Species	*Phyllanthus acidus*

<u>Species information</u>

Scientific name	*Phyllanthus acidus* (L.) Skeels
Common names	Malay gooseberry, Tahitian gooseberry, Country gooseberry, Star gooseberry, West India gooseberry, simply gooseberry tree
Local name	Ma Yom
Synonym	*Cicca acida* Merr., *Cicca disticha* L. *Averrhoa acida* L.
Origin	Brazil

<u>Medicinal properties</u>

Aqueous extract of *Phyllanthus acidus* leaves had the hepatoprotective protective against acetaminophen and thioacetamide induced hepatoxicity in Wistar rats (211). Ethanol extract of P. *acidus* leaves showed hypoglycemic and hypolipidemic in streptozotocin induced diabetic rats without side effects that these results are related to antioxidant activities of P. *acidus* (212). In addition, ethanol extract of P. *acidus* leaves also had antimicrobial activity and alpha-amylase inhibition (213). Leaves of P. acidus contains many phytochemical constituents in different solvents, such as tanins, anthraquinones, flavonoids, alkaloids, terpenoids, saponins, cardiac glycosides, and glycosides,as shown in table 5 (214).

Table 5. Phytochemical constituents of *Phyllanthus acidus* leaves (214).

Phytochemicals	Distilled water	Petroleum ether	Acetone	Ethanol
Tanins	+	+	+	+
Anthraquinones	+	+	+	+
Flavonoids	+	+	+	+
Alkaloids	-	-	+	+
Terpenoids	+	+	+	+
Saponins	+	+	+	+
Cardiac glycosides	+	+	+	+
Glycosides	-	+	+	+
Reducing sugars	-	+	-	-
Phlobatanins	-	-	+	+
Steroids	+	+	+	+

+ ve – present, - ve - Absent

จุฬาลงกรณ์มหาวิทยาลัย

CHULALONGKORN UNIVERSITY

10. *Rhinacanthus nasutus* (L.) Kurz

<u>Botanical description</u>

   Rhinacanthus nasutus (L.) Kurz is a shade loving perennial shrub. Leaves are ovate to oblong, narrowed and pointed at the end. Flowers are the upper of the tip and white color (215).

<u>Scientific classification</u>

Family	Acanthaceae
Genus	*Rhinacanthus*
Species	*Rhinacanthus nasutus*

<u>Species information</u>

Scientific name	*Rhinacanthus nasutus* (L.) Kurz
Common names	Snake jasmine, dainty spurs
Local name	Thong Phan Chang
Synonym	*Justicia nasuta* Linn., *Pseuderanthemum connatum* Lindau, *Rhinacanthus communis* (Linn.) Kurz.
Origin	India and China

<u>Medicinal properties</u>

   Methanol extract of *Rhinacanthus nasutus* leaves improved the activity of oxidative enzymes such as glucose-6-phosphate dehydrogenase (G6PD), succinate dehydrogenase (SDH) and glutamate dehydrogenase (GDH) by increasing the levels in diabetic rats (216). Rhinacanthin C (Rn-C) from R. *nasutus* leaves showed a potent anti-inflammatory activity by decreasing prostaglandin synthesis. Rhinacanthin C is a one of naphthoquinones and major compound from leaf extract (217). Moreover, Rhinacanthin c inhibited osteoclast differentiation induced by receptor activator of nuclear factor-**K**B ligand (218). R. *nasutus* have many types of phytochemicals, as shown in table 6 (219). Methanol extract of R. *nasutus* leaves was orally administered at dose of 200mg/kg/day for 30 days, it did have toxic effect as well as 250 mg/kg/day in the previous study (220, 221).

Table 6. Phytochemical constituents of *Rhinacanthus nasutus* leaf.

Phytochemical constituents	Petroleum ether extract	Ethyl acetate extract	Chloroform extract	Methanol extract
Alkaloids	-	+	-	+
Anthraquinones	-	+	-	+
Carbohydrates	-	-	-	+
Cardiac glycosides	-	-	-	-
Flavonoids	-	+	-	+
Saponins	-	+	-	+
Phytosterols	+	+	+	+
Triterpenoids	+	+	+	+
Polyphenols	-	+	-	+

+ ve – present, - ve - Absent

จุฬาลงกรณ์มหาวิทยาลัย
CHULALONGKORN UNIVERSITY

11. *Senna alata* **(L.) Roxb.**

<u>Botanical description</u>

   Senna alata (L.) Roxb. is an ornamental shrub. Leaves are simple pinnate and spiral arranged. Flowers are yellow. At maturity, fruits spit open along one side with flattened (222).

<u>Scientific classification</u>

   Family   Leguminosae

   Genus   *Senna*

   Species   *Senna alata*

<u>Species information</u>

   Scientific name   *Senna alata* (L.) Roxb.

   Common names   Emperor's candlesticks, candle bush,

             Candelabra bush, Christmas candles,

             Empress candle plant, ringworm shrub, candle

             tree

   Local name   Chom Hed Test

   Synonym   *Cassia alata (L.), Cassia bracteata L.f.,*

             Cassia herpetica Jacq., Cassia rumphiana (D.C.)

             Bojer, Herpetica alata (L.) Raf.

   Origin   America

<u>Medicinal properties</u>

   Ethanol extract of *Senna alata* from 10 different locations in North, North-east, Central and South of Thailand contained anthraquinones. There were rhein and aloe-medin as major chemical constituents. It also showed the inhibition of fungi and aerobic bacteria (223). In addition, herbal soap formulated with ethanol extract of S. *alata* showed antimicrobial activity against microbial skin flora (224). Secondary metabolites of S. *alata* leaves are flavonoids, glycoside, anthraquinone (chrysoppphanol, emodin, aloe-emodin, rhein, isochrysophanol), polyphenol, and few compounds such as ellagitannin, naphthalene and xanthones (225). Alkaloid

from *S. alata* leaves at doses of 250, 500 and 1000 mg/kg/day from days 10 until day 18 post-coitum showed several potential effects on the maternal and fetal outcomes of pregnant rats, including anti-implantation, anti-gonadotropic, anti-progesteronic, selective estrogenic, embryonic resorption and fetotoxic activities. Nevertheless, it could not induce to abort in rats (226). Similarly, Swiss albino mice were orally treated at dose of 1,000, 2,000, 3,000 mg/kg in each group for 15 days. The results showed that there was no toxicity in mice treated with those concentrations (227).

12. *Stemona curtisii* Hook.f.

Botanical description

Stemona curtisii is perennial, rhizomatous and erect herb. Leaves of S. *curtisii* are simple, alternate and green color.

Scientific classification

Family	Stemonaceae
Genus	*Stemona*
Species	*Stemona curtisii*

Species information

Scientific name	*Stemona curtisii* Hook.f.
Local names	Non Tai Yak
Origin	Asia

Medicinal properties

Stemona species have been used as natural pesticides and medicinal plants for skin treatment and respiratory diseases (228). Root extract of *Stemona curtisii* have alkaloids which is composed of stemocurtisine, stemocurtisinol, oxyprostemonine, 1-hydroxyproto stemonine and stemocurtisine N-oxide (229). Stemocurtisine, stemocurtisinol and oxyprotostemonine from roots of S. *curtisii* showed mosquitocidal activity (230). However, bioinsectiside from S. *curtisii* at doses of 500, 1,000, 2,000 mg/kg induced the death in male rats about 20, 80 and 100%, orderly for 14 days. Moreover, those doses also reduced motor activity, respiratory rate and violent convulsion (231).

13. *Streblus asper* Lour.

<u>Botanical description</u>

Streblus asper Lour. is a small tree and is also rigid shrub. Its leaves are rigid, oval-shaped and irregular toothed. Fruits are in pisiform with perianth yellow (232).

<u>Scientific classification</u>

Family	Moraceae
Genus	*Streblus*
Species	*Streblus asper*

<u>Species information</u>

Scientific name	*Streblus asper* Lour.
Common names	Bar-inka, Berrikka, Rudi, Sheora, Koi, Siamese rough bush and tooth brush tree.
Local name	Koi
Origin	Southeast asia

<u>Medicinal properties</u>

Anti-bacterial activity was found in 50% ethanol extract of *Streblus asper* leaves against Streptococcus species (233). Ethanol extract of S. *asper* leaves also inhibited the adherence of *Candida albicans* to human buccal epithelial cells (234). Moreover, ethanol extract of S. *asper* leaves showed a potential anti-inflammatory agent by suppressing COX-2 and i-NOS mRNA expression in RAW264.7 macrophage cells (235). Root bark of S. *asper* is a rich source of cardiac glycosides. While, volatile oil of its leaves are composed of phytol, α-farnesene, trans-farnesyl acetate, caryophyllene and trans-trans-α-farnesene. Other chemical constituents were α-copaene, β-elemene, caryophyllene, geranyl acetone, germacrene, δ-cadinene, caryophyllene oxide and 8-heptadecene (236). Methanol and petroleum ether extracts of S. *asper* (up to 2,000 mg/kg) did not induce mortality in Swiss albino mice (237).

Conceptual framework
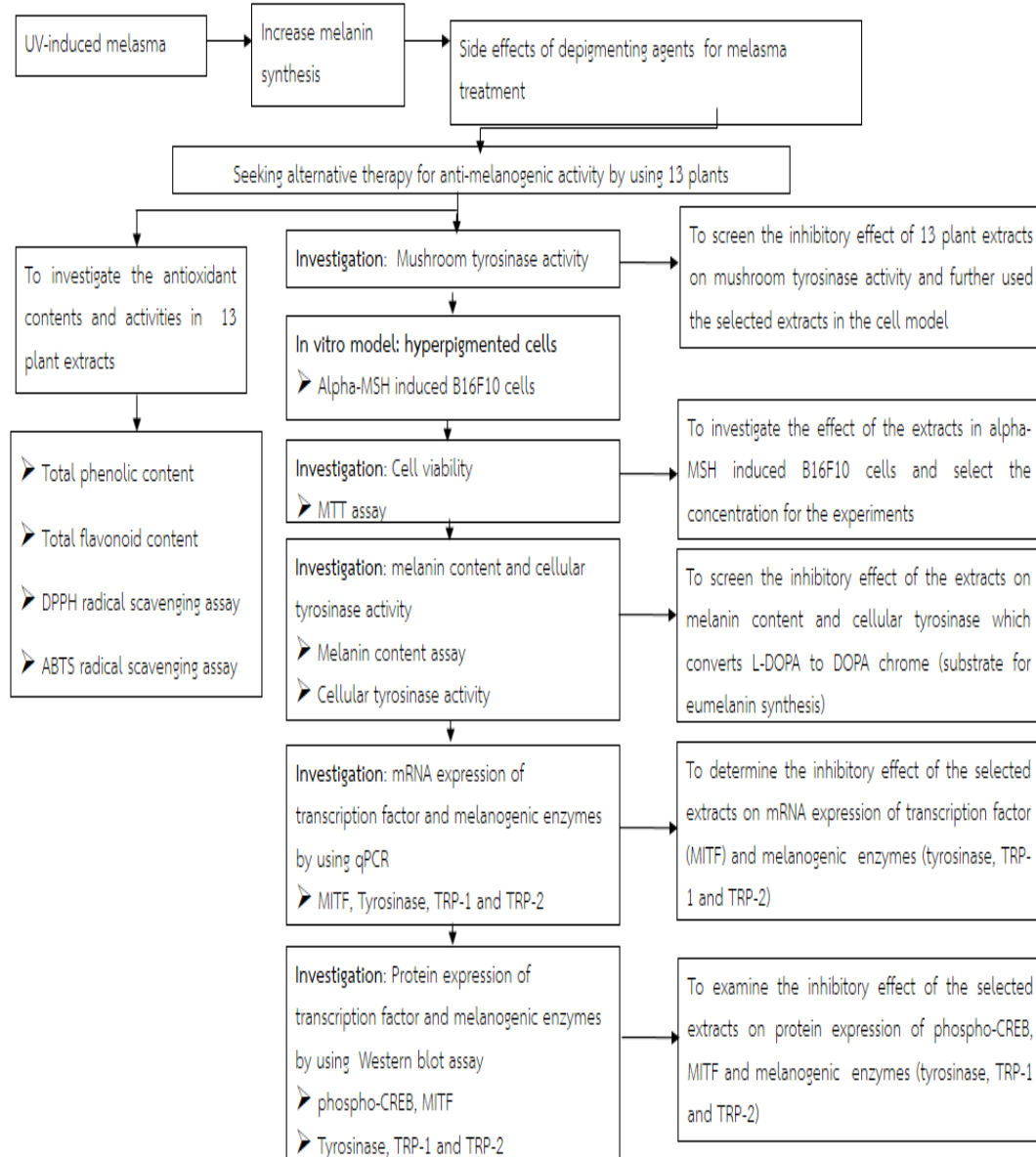
UV; ultraviolet radiation, alpha-MSH; alpha melanocyte stimulating hormone, MC1R; melanocortin-1 receptor, phospho-CREB; phosphorylated cAMP respond element binding protein, MITF; microphthalmia-associated transcription factor, TYR; tyosinase, TRP-1; tyrosinase related protein-1, TRP-2; tyrosinase relate

Experiment procedure


```
UV-induced melasma  →  Side effects of current depigmenting agents
                              Seeking for alternative therapy
Antioxidant content
and activities                13 Plants  →  Anti-melanogenic activity

Anti-mushroom                           In vitro model: hyperpigmented cells
tyrosinase activity                     Alpha-MSH induced B16F10 mouse melanoma cells
Select some plant extracts
```

Investigation: Cell viability
- MTT assay

To investigate the effect of the extracts in alpha-MSH induced B16F10 cells and choose the concentrations

Investigation: Melanin content and tyrosinase activity
- Melanin content
- Cellular tyrosinase activity

To screen the inhibitory effect of the extracts on melanin content and cellular tyrosinase activity which converts L-DOPA to DOPAchrome (as substrate for eumelanin)

Investigation: mRNA expression of transcription factor and melanogenetic enzymes by using qPCR
- MITF
- Tyrosinase, TRP-1 and TRP-2

To determine the inhibitory effect of the selected extracts on mRNA expression of transcription factor and melanogenic enzymes

Investigation: Protein expression of transcription factor and melanogenetic enzymes by using Western blot analysis
- MITF
- Tyrosinase, TRP-1 and TRP-2

To examine the inhibitory effect of the selected extracts on protein expression of transcription factor and melanogenic enzymes

Investigation: Upstream signaling molecules
- Phospho-CREB

To estimate the effect of the selected extracts on phospho-CREB which binds to CRE of MITF promoter

Data analysis

CHAPTER II

MATERIALS AND METHODS

2.1 Materials

2.1.1 Material and chemicals

Chemical	Company, Country
2,2′-Azino-bis(3-ethylbenzothiazoline-6- sulfonic acid) diammonium salt (ABTS)	Merck, Germany
3-(4, 5-dimethylthianisol-2-yl)-2, 5-diphenyl -2H-tetrazolium bromide (MTT)	Calbiochem, Germany
3,4-dihydroxy-L-phenylalanine (L-DOPA)	Sigma Aldrich, USA
30% Acrylamide/BIS Solution (37.5:1)	Bio-Rad, USA
Agarose	Vivantis, USA
Alpha-melanocyte stimulating hormone	Merck, Germany
Aluminium Chloride ($AlCl_3$)	Sigma Aldrich, USA
Ammonium persulfate	Vivantis, USA
Anti-CREB, Anti-phospho-CREB, Anti-MITF, Anti-GAPDH	Cell Signaling, USA
Anti-TRP-1, Anti-TRP-2, Anti-TYR	Abcam, UK
Arbutin	TCI, Japan
Ascorbic acid	Merck, Germany
Bovine serum albumin	GE healthcare, UK
Bradford reagent	Bio-Rad, USA
Chloroform	RCI Labscan, Thailand
Dichloromethane	Merck, Germany
Diethyl pyrocarbonate (DEPC)	Sigma Aldrich, USA
Dimethyl sulfoxide (DMSO)	RCI labscan, Thailand
DNA ladder size 100 bp	Fermantas, Germany
DPPH (2,2-Diphenyl-1-picrylhydrazyl)	Merck, Germany

Dulbecco's Modified Eagle Medium (DMEM)	Hyclone, USA
ECL Western blotting substrate	Thermoscientific, USA
EDTA-trypsin 0.25% (1X)	Gibco, Canada
Ethanol	Merck, Germany
Ethidium Bromide	Sigma Aldrich, USA
Gallic acid	Sigma Aldrich, USA
GBX Developer	Carestream, USA
GBX Fixer	Carestream, USA
Hydrochloric acid (HCl)	Merck, Germany
Fetal Bovine Serum (FBS)	Sigma Aldrich, USA
Folin Ciocalteu's Phenol Reagent	Sigma Aldrich, USA
Glycerol	Bio Basic Inc., Canada
Glycine	Vivantis, USA
Hydrochloric acid (HCl)	Merck, Germany
Isopropanol	RCI Labscan, Thailand
Kojic acid	Sigma Aldrich, USA
Melanin	Sigma Aldrich, USA
Methanol	Merck, Germany
Oligo dT_{18}	Bioneer, South Korea
Penicillin-Streptomycin solution	Hyclone, USA
Petroleum ether	Merck, Germany
Phosphate buffer saline (10X) solution	Hyclone, USA
Primer	Bioneer, South Korea
Protease inhibitor cocktail	Sigma Aldrich, USA
Protease/phosphatase inhibitor cocktail (10X)	Bio-Rad, USA
Protein marker	Bio-Rad, USA
qPCR Master mix	Bioneer, South Korea
Quercitin	Sigma Aldrich, USA
Ribozol RNA extraction reagent	Amresco, USA

RIPA lysis buffer (10X)	Merck, Germany
RT premix	Bioneer, South Korea
Secondary antibody (anti-mouse IgG, HRP-linked antibody and anti-rabbit IgG, HRP-linked antibody)	Cell Signaling, USA
Sodium carbonate	Merck, Germany
Sodium chloride (NaCl)	Merck, Germany
Sodium dodecyl sulphate (SDS)	Vivantis, USA
Sodium hydroxide (NaOH)	Merck, Germany
Sodium phosphate dibasic anhydrous (Na_2HPO_4)	Sigma Aldrich, USA
Sodium phosphate monobasic anhydrous (NaH_2PO_4)	Sigma Aldrich, USA
Tris base	Vivantis, USA
Tris HCl	Vivantis, USA
Trypan blue stain (0.4%)	Invitrogen, USA
Trypsin 0.25% (1X) solution with 0.1% EDTA	Invitrogen, USA
Tween20	Vivantis, USA
Tyrosinase from mushroom	Sigma Aldrich, USA

2.1.2 Tool and Device

Tool/Device	Company, Country
-20 °C freezer	Sanyo Electric, Japan
4°C refrigerator	Sharp, Japan
6, 96 well cell culture plate	Corning Inc., USA
-80°C deep freezer	Liofreeze, USA
96 well non-sterile plate	Corning Inc., USA
Adhesive Optical Sealing film	Bioneer, South Korea
Aluminium cryogenic vial storage	Nunc, Denmark
Analytical balance	Mettler Toledo,Switzerland
Autoclave	Hirayama, Japan

Autopipette 0.5-10 µl	Bio-Rad, USA
Autopipette 200-1000 µl	Mettler Toledo, Switzerland
Autopipette 20-200 µl	Mettler Toledo, Switzerland
Autopipette 2-20 µl	Bio-Rad, USA
Basic power supply	Bio-Rad, USA
Beaker (50, 100, 250, 500, 1000 ml)	Schott Duran, Germany
Block heater	Wealtec Corp, USA
Cell culture flask (25, 75 cm^2)	Nunc, Denmark
Centrifuge	Beckman Coulter, USA
Centrifuge tube (15, 50 ml)	Nest, China
CO_2 incubator	Thermo Scientific, USA
Conical tube rack	Nunc, Denmark
Cryovial tube 2.0 ml	Nunc, Denmark
Disposable serological pipette (5, 10 ml)	Nest, China
Disposable syringe	Nipro, Thailand
Electrophoresis power supply	Bio-Rad, USA
ELISA plate reader	BioTek, USA
Evaporator	Genevac, USA
Exicycler™ 96 Real-Time Quantitative Thermal Block	Bioneer, South Korea
Extraction thimble	Whatman, USA
Filter paper	Whatman, USA
Flask (50, 100, 250, 500, 1000 ml)	Schott Duran, Germany
Gel documentation (Gel Doc) systems	Syngene, UK
Gel Electrophoresis apparatus	Bio-Rad, USA
Glass bottles (500, 1000 ml)	Schott Duran, German
Hemocytometer	Hausser Scientific, USA
High speed grinder	Rong Tsong Precision Technology Co., China
Hot air oven	Memmert, Germany
Hypercassette	GE Healthcare, UK

Hyperfilm ECL	GE Healthcare, UK
Hypodermic needle	Nipro, Thailand
Incubator shaker	INFORS HT, Switzerland
Incubator	Memmer, Germany
Inverted microscope	Olympus, Japan
Laminar flow cabinet	Haier, China
Laminar flow clean blench	Esco, Singapore
Light microscope	Olympus, Japan
Liquid nitrogen tank	Taylor-Wharton, USA
Magnetic stirrer	Daihan LabTech, South Korea
Micro High Speed Refrigerated Centrifuge	Vision Scientific, South Korea
Microcentrifuge	Eppendorf, Germany
Microcentrifuge tube (1.5 ml)	Nest, China
Mini Protean Tetra cell	Bio-Rad, USA
Mini Transblot Electrophoretic Transfer cell	Bio-Rad, USA
Multichannel pipette (20-200 µl)	Gilson, France
Multilabel reader	Perkin Elmer Inc., Finland
PCR tube (0.2 ml)	Kirgen, China
pH meter	Mettler Toledo,Switzerland
Pipette Controller	Thermo Scientific, USA
Pipette tips (10, 1000 µl)	Jet Biofil, China
Pipette tips (20, 200 µl)	Nest, China
Plate shaker	Desaga, Germany
Polyvinyldiene fluoride (PVDF) membrane	GE Healthcare, UK
Rotary evaporator	Heidolph Instruments, Germany
Serological pipette (1, 5, 10, 25 ml)	Corning Inc., USA
Soxhlet extractor	Lab Heat, Germany
Sterile syringes filter	Corning Inc., USA
Test sieves no.16	Jayant scientific Ind., India

UV-Visible spectrophotometer for RNA	Beckman Coulter, USA
Vacuum concentrator	ThermoElectro Corperation, USA
Volumetric flask (100, 1000 ml)	Pyrex, USA
Vortex mixer	FinePCR, South Korea
Waterbath	Memmert, Germany

2.2 Plant materials

Thirteen species of plants in this study were selected based on the traditional use with the skin treatment. Twelve species of leaves were collected from HRH Princess Sirindhorn Herb Garden, Rayong province, Thailand. Mangosteens were obtained from Chanthaburi province, Thailand. These plants were authenticated and deposited at Herbarium, Department of Botany in Faculty of Science, Chulalongkorn University, Thailand.

1. *Ardisia elliptica* Thunberg

Ardisia elliptica Thunb. is in the Myrsinaceae family. Its common names are shoebutton ardisia in English and Ram Yai in Thai. Leaves of this plant were collected from HRH Princess Sirindhorn Herb Garden, Rayong province, Thailand. Herbarium voucher number was 015122 (BCU).


Figure 19. *Ardisia elliptica* Thunb.

2. *Croton roxburghii* N.P.Balakr

     Croton roxburghii N.P.Balakr is in the Euphorbiceae family. Its Thai names are Plao Yai and Plao Laung. Leaves of this plant were collected from HRH Princess Sirindhorn Herb Garden, Rayong province, Thailand. Herbarium voucher number was 015126 (BCU).

Figure 20. *Croton roxburghii* N.P.Balakr

3. *Croton sublyratus* Kurz.

     Croton sublyratus Kurz. is in the Euphorbiceae family. Its Thai names is Plao Noi. Leaves of this plant were collected from HRH Princess Sirindhorn Herb Garden, Rayong province, Thailand. Herbarium voucher number was 015127 (BCU).

Figure 21. *Croton sublyratus* Kurz.

4. *Datura metel* L.

       Datura metel L. is in the Solanaceae family. Its common names are thorn apple in English and Lam phong khao in Thai. Leaves of this plant were collected from HRH Princess Sirindhorn Herb Garden, Rayong province, Thailand. Herbarium voucher number was 015133 (BCU).


Figure 22. *Datura metel* L.

5. *Garcinia mangostana* Linn.

       Garcinia mangostana Linn. is in the family Guttiferae. Its common name is mangosteen in English. Pericarps of this plant were obtained from Chanthaburi province, Thailand. Herbarium voucher number was 015279 (BCU).

Figure 23. *Garcinia mangostana* Linn.

6. *Gynura pseudochina* (L.) DC.

    Gynura pseudochina (L.) DC. is in the family Asteraceae. Its Thai local name is Warn Ma Ha Kan. Pericarp of this plant were collected from HRH Princess Sirindhorn Herb Garden, Rayong province, Thailand. Herbarium voucher number was 015124 (BCU).

Figure 24. *Gynura pseudochina* (L.) DC.

7. *Hibiscus mutabilis* L.

    Hibiscus mutabilis L. is in the Malvaceae family. Its common names are cotton rose or confederate rose in English and Phud Tarn in Thai. Leaves of this plant were collected from HRH Princess Sirindhorn Herb Garden, Rayong province, Thailand. Herbarium voucher number was 015130 (BCU).

Figure 25. *Hibiscus mutabilis* L.

8. *Ipomoea pes-caprae* (L.) R.br.

  Ipomoea pes-caprae (L.) R.br. is in the Convolvulaceae family. Its common name are beaching morning glory in English and Pak Bung Talae in Thai. Leaves of this plants were collected from HRH Princess Sirindhorn Herb Garden, Rayong province, Thailand. Herbarium voucher number was 015250 (BCU).

Figure 26. *Ipomoea pes-caprae* (L.) R.br.

9. *Phyllanthus acidus* (L.) Skeels

  Phyllanthus acidus (L.) Skeels is in the Euphorbiaceae family. Its common name are star gooseberry in English and Ma Yom in Thai. Leaves of this plants were collected from HRH Princess Sirindhorn Herb Garden, Rayong province, Thailand. Herbarium voucher number was 015128 (BCU).
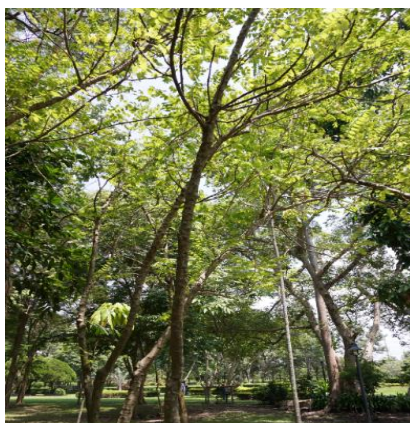
Figure 27. *Phyllanthus acidus* (L.) Skeels

10. *Rhinacanthus nasutus* (L.) Kurz

    Rhinacanthus nasutus (L.) Kurz is in the Acanthaceae family. Its common name are white crane flower in English and Thong Phan Chang in Thai. Leaves of this plants were collected from HRH Princess Sirindhorn Herb Garden, Rayong province, Thailand. Herbarium voucher number was 015129 (BCU).

Figure 28. *Rhinacanthus nasutus* (L.) Kurz

11. *Senna alata* (L.) Roxb.

    Senna alata (L.) Roxb. is in the Leguminosae family. Its common name are ringworm brush or seven golden candle-stick in English and Chom Hed Test in Thai. Leaves of this plants were collected from HRH Princess Sirindhorn Herb Garden, Rayong province, Thailand. Herbarium voucher number was 015125 (BCU).

Figure 29. *Senna alat a* (L.) Roxb.

12. *Stemona curtisii* Hook.f.

Stemona curtisii Hook.f. is in the Stemonaceae family. Its Thai local name is Non Tai Yak. Leaves of this plants were collected from HRH Princess Sirindhorn Herb Garden, Rayong province, Thailand. Herbarium voucher number was 015123 (BCU).

Figure 30. *Stemona curtisii* Hook.f.

13. *Streblus asper* Lour.

Streblus asper Lour. is in the Moraceae family. Its common names are Siamese rough bush or tooth brush tree in English and Koi in Thai. Leaves of this plants were collected from HRH Princess Sirindhorn Herb Garden, Rayong province, Thailand. Herbarium voucher number was 015131 (BCU).
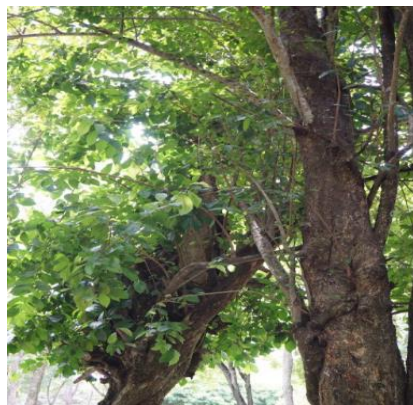
Figure 31. *Streblus asper* Lour.

2.3 Cell culture model

B16F10 mouse melanoma cells (CRL-6475) were purchased from the American Type Culture Collection (ATCC, USA). These cells were used as alpha-melanocyte stimulating hormone induced melasma. The cells were cultured in Dulbecco's Modified Eagle Medium/High glucose (DMEM/HG), supplemented with 10% fetal bovine serum (FBS) and antibiotics (100 U/mL penicillin and 100 µg/mL streptomycin) in a 5% CO_2 humidified atmosphere at 37°C. Subculturing of cells was completed to detach the cells from a culture flask by trypsin 0.25% (1X) solution with 0.1% EDTA. The cells were stained with trypan blue solution (0.4%) and counted using a hemocytometer. The B16F10 cells were seed into 6 or 96 well
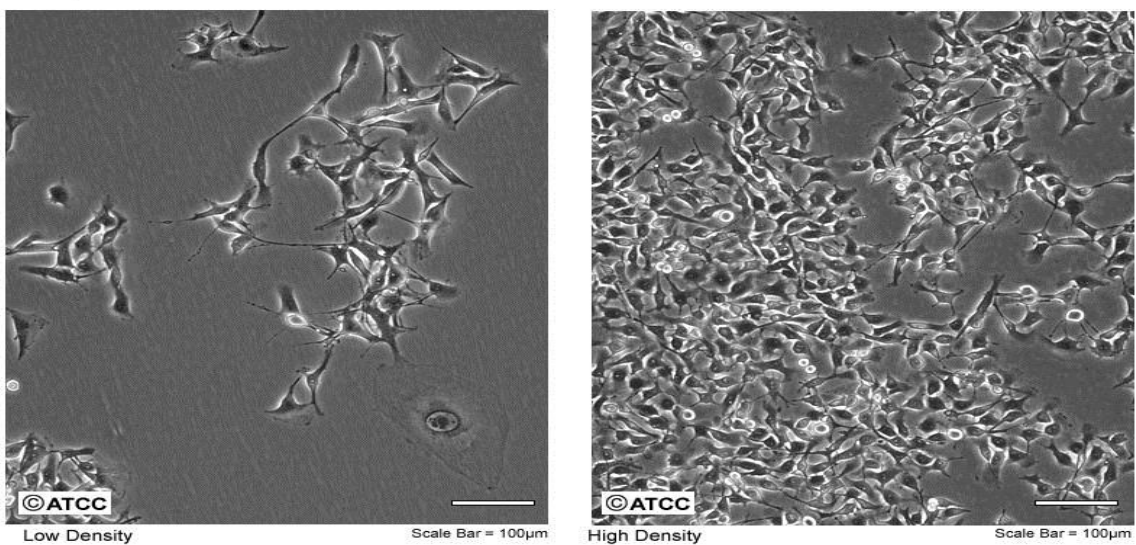
culture plate for an experiment.

Figure 32. B16F10 mouse melanoma cell line. Cell morphology of this cell line is mixed between spindle-shaped and epidermal-like cell (adapted from ATCC).

2.4 Experiment procedure

2.4.1 Preparation of plant extracts

Fresh leaves and pericarps were rinsed with water and dried in hot air oven at 45°C. The dried plants were ground into a fine powder by blender and filtered with sieve no.16. The dried powder (10 g) in thimble was extracted in organic solvents (1:40, W/V), including petroleum ether, dichloromethane and ethanol solvents, orderly by Soxhlet extractor. Principle of Soxhlet method, it is only required for the desired compound in a limited solubility in a solvent. The dried powder of the desired compound is placed in a thimble which is a filter paper. The solvent is in a flask and further heated to reflux. The solvent vapor moves up to a distillation arm and floods over the thimble in a chamber. A condenser makes the solvent cools down and then drops the solvent into the thimble. When the chamber is filled with the solvent, the solvent backs down to the flask (238). This process is repeated many times until the solvent in the chamber is clear. After extraction, the solvents were removed by using a vacuum rotary evaporator under reduced pressure. Finally, the crude extracts were concentrated by the MiVac Quattro concentrator. The concentrated samples were dissolved in dimethyl sulfoxide (DMSO) at 100 mg/ml and stored at -20°C. Yields of dry extracts were presented in as %w/w dry plant materials. Prior to use in the cells, the plant extracts were filtered through a 0.2 μm pore size filter and kept at -20°C.

2.4.2 Determination of antioxidant content in plant extracts

2.4.2.1 Total phenolic content

Total phenolic content of plant extracts was evaluated using the Folin-Ciocalteu method (239). This method is a colorimetric assay for phenolic and polyphenolic antioxidants. The Folin-Ciocalteu reagent is mixture between phosphomolybdate and phosphotungstate. This method depends on a phenolic or polyphenolic compound (reducing agent) which reduces phosphomolybdic/phosphotungstic acid complexes (yellow color) to a blue-colored complex in alkaline condition. Gallic acid was served as a standard.

Procedure

1. Prepare 10% Folin-Ciocalteu reagent by adding 2 ml of Folin-Ciocalteu reagent with 18 ml of distilled water.

2. Prepare 0.1 M Na_2CO_3 by dissolving 10.60 g of Na_2CO_3 in 100 ml of distilled water.

3. Prepare Gallic acid solution as standard at the concentration of 1.56, 3.13, 6.25, 12.5, 25, 50, 100 μg/ml in distilled water.

4. Dilute the plant extracts at 1 mg/ml in distilled water (in microcentrifuge tube).

   Add the plant extracts and reagents as shown in table 7.

   Table 7. Procedure step for total phenolic content.

Reagent	Standard blank (μl)	Standard (μl)	Sample blank (μl)	Sample (μl)
Plant extracts	-	-	50	50
Gallic acid as a standard solution	50	50	-	-
Distilled water	50	-	50	-
10% Folin-Ciocalteau reagent	-	50	-	50
1 M Na_2CO_3	50	50	50	50

5. Incubate at room temperature for 1 h in a dark condition.

6. Measure the absorbance at 750 nm using microplate reader.

7. Prepare a standard curve between the absorbance and concentration of gallic acid.

8. Calculate total phenolic content of each plant extracts expressed as mg gallic acid equivalents (GAE)/g dry plant material.

2.4.2.2 Total flavonoid content

Total flavonoid content (TFC) was determined using the aluminium chloride ($AlCl_3$) colorimetric assay (240). The principle of this method is based on the formation of stable complex between aluminium chloride and the C-3 or C-5 hydroxyl group of flavones and flavonols. Moreover, the aluminium chloride also reacts with ortho-dihydroxyl groups in A- or B- ring of flavonoids to product the acid labile complex (241). Quercitin was used as a standard.

Procedure

1. Prepare 2% $AlCl_3$ solution by dissolving 1 g of $AlCl_3$ in 50 ml of distilled water.
2. Prepare quercetin at the concentration of 1.56, 3.13, 6.25, 12.5, 25, 50, 100 µg/ml in 80% ethanol solution.
3. Dilute each plant extract at 1 mg/ml in 80% ethanol solution.
4. Mix the plant extracts with reagents as shown in table 8.

    Table 8. Procedure step for total flavonoid content.

Reagent	Standard blank (µl)	Standard (µl)	Sample blank (µl)	Sample (µl)
Plant extract	-	-	50	50
Quercitin (standard)	50	50	-	-
80% Ethanol	50	-	50	-
2% $AlCl_3$	-	50	-	50

5. Incubate at room temperature for 40 nm and protect from the light.
6. Measure the absorbance at 415 nm using microplate reader.
7. Prepare a standard curve between the absorbance and concentration of quercetin.
8. Calculate total flavonoid content expressed as mg quercitin equivalents (QE)/g dry plant material.

2.4.3 Determination of antioxidant activity in plant extracts

2.4.3.1 DPPH (2, 2-Diphenyl-1-picrylhydrazyl) scavenging activity   DPPH

scavenging activity assay were performed as described by Yamasaki et al (242).This assay is based on a hydrogen donor from antioxidant. Antioxidant activity depends on the disappearance of DPPH$^\bullet$ in the samples. Usually, DPPH$^\bullet$ has a purple color and shows a strong absorption maximum at 517 nm. When DPPH$^\bullet$ accepts a hydrogen atom from donor (plant extracts), the color changes from purple to yellow color. The equation of this principle is shown as below.

$$DPPH^\bullet + RH \longrightarrow DPPH\text{-}H + R^\bullet$$

RH = Hydrogen donor or antioxidant (plant extracts)

Procedure

1. Prepare 2.5 M DPPH solution by adding 4.95 g of DPPH dissolved in 50 ml of absolute methanol (prepare freshly before use).

2. Adjust the absorbance of DPPH solution about 0.7±0.02 at 514 nm.

3. Prepare ascorbic acid (a standard) at the concentration of 1.56, 3.13, 6.25, 12.5, 25, 50 µg/ml dissolved in absolute methanol.

4. Dilute each plant extract at 1 mg/ml in absolute methanol (final concentration at 100 µg/ml).

5. Mix each plant extract with reagents as shown in table 9.

Table 9. Procedure step for DPPH assay.

Reagent	Control (µl)	Standard blank (µl)	Standard (µl)	Sample blank (µl)	Sample (µl)
Plant extract	-	-	-	20	20
Ascorbic acid	-	20	20	-	-
DPPH solution (absorbance 0.7±0.02)	180	-	180	-	180
Absolute methanol	20	180	-	180	-

6. Incubate at room temperature for 30 min and protect from the light.

7. Measure the absorbance at 517 nm using plate reader.

8. Calculate scavenging activity (%) using the following formula

   % scavenging activity = $100 \times (Abs_{control} - (Abs_{sample} - Abs_{sample-blank}))/Abs_{control}$

9. Express as mg vitamin C equivalent antioxidant capacity (VCEAC)/g dry plant material by calculating from the standard curve between %scavenging activity of each extract and the concentration of ascorbic acid.

2.4.3.2 ABTS (2, 2'-azinobis (3-ethylbenzothiazoline-6-sulfonic acid) radical) scavenging activity

ABTS free radical scavenging activity was performed as previously described by Re et al (243). This assay is based on the ability of lipophilic and hydrophilic antioxidants to scavenge the radical cation of ABTS. ABTS (colorless) is oxidized into $ABTS^{\bullet+}$ (green color) by oxidizing agent ($KMnO_4$). The $ABTS^{\bullet+}$ has a strong absorption maximum at 734 nm (green color) and is reduced into ABTS (colorless) by antioxidant (hydrogen donor) from plant extracts. Antioxidant activity is proportional to decolorize of ABTS in the sample from the plant extracts. The equation is shown as below.

$$ABTS + \text{oxidizing reagent} \longrightarrow ABTS^{\bullet+}$$
$$ABTS^{\bullet+} \text{ (green)} + \text{antioxidant} \longrightarrow ABTS \text{ (colorless)}$$

Procedure

1. Prepare 7 mM ABTS solution by weighting 144 mg of ABTS dissolved in 40 ml of distilled water.

2. Prepare 2.45 mM $KMnO_4$ by adding 33.1 mg of $KMnO_4$ in 50 ml of distilled water.

3. Prepare $ABTS^{\bullet+}$ solution by mixing between 8 ml of 7 mM ABTS solution and 12 ml of 2.45 mM $KMnO_4$ and stand in a dark condition at $4^{\circ}C$ for 16-18 h (prepare freshly before use).

4. Prepare ascorbic acid (a standard) at the concentration of 3.13, 6.25, 12.5, 25, 50, 100 µg/ml in absolute ethanol.

5. Dilute ABTS$^{\bullet+}$ solution in absolute ethanol to give the absorbance about 0.7±0.02 at 734 nm.

6. Add each plant extract with reagents as shown in table 10.

Table 10. Procedure step of ABTS assay.

7.

Reagent	Control (µl)	Standard blank (µl)	Standard (µl)	Sample blank (µl)	Sample (µl)
Plant extract	-	-	-	20	20
Ascorbic acid (a standard)	-	20	20	-	-
ABTS$^{\bullet+}$ working reagent (absorbance 0.7±0.02)	180	-	180	-	180
Absolute ethanol	20	180	-	180	-

Incubate at room temperature for 45 min in a dark condition.

8. Measure the absorbance at 734 nm using microplate reader.

9. Calculate scavenging activity (%) using the following formula

% scavenging activity = 100× (Abs$_{control}$-(Abs$_{sample}$-Abs$_{sample-blank}$))/Abs$_{control}$

10. Express as mg vitamin C equivalent antioxidant capacity (VCEAC)/g dry plant material by calculating from the standard curve between %scavenging activity of each extract and the concentration of ascorbic acid.

2.4.4 Anti-mushroom tyrosinase activity of plant extracts

Dopachrome method was performed with slight modification (244). The principal of this method, tyrosinase enzyme catalyzes the oxidation of L-DOPA (3, 4-dihydroxy-L-phenylalanine) to o-dopaquinone. Through a series of non-enzymatic reaction, o-dopaquinones is rapidly converted into DOPAchrome as a substrate for melanin, which absorbs the wavelength at 492 nm. DOPAchrome has an orange color. This assay is used to measure the quantification of DOPAchrome which generates from tyrosinase enzyme with L-DOPA. Enzyme inhibition is propotional to the DOPAchrome development. Downregulation of tyrosinase activity has been proposed to be responsible for the decreased melanin production. Kojic acid was served as positive control. The equation of this assay is shown as below.

$$L\text{-DOPA} \xrightarrow{\text{tyrosinase}} L\text{-DOPA quinone} + H_2O \longrightarrow \text{DOPAchrome}$$

Procedure

1. Prepare 0.02 M sodium phosphate buffer at pH 6.8 by weighting 0.43 g of Na_2HPO_4 and 0.41 g of NaH_2PO_4 and dissolve in 300 ml of distilled water.

2. Prepare 2.5 mM L-DOPA by adding 2.465 mg of L-DOPA in 5 ml of sodium phosphate buffer.

3. Prepare 203.3 unit/ml murhroom tyrosinase by adding 0.5 mg of mushroom tyrosinase in 5 ml of sodium phosphate buffer pH6.8 (prepare freshly).

4. Prepare kojic acid at 1 mg/ml (final concentration at 100 µg/ml) dissolved in DMSO.

5. Dilute each plant extract at 10 mg/ml (final concentration at 1 mg/ml) dissolved in DMSO.

6. Mix each plant extract with reagents as shown in table 11.

Table 11. Procedure step for melanin content assay.

Reagent	Control blank (µl)	Control (µl)	Sample blank (µl)	Sample (µl)
Plant extract	-	-	20	20
Dimethysulfoxide (DMSO)	20	20	-	-
0.02 M Sodium	160	140	160	140

phosphate buffer pH 6.8				
203.3 unit/ml of mushroom tyrosinase	-	20	-	20
Mix and incubate at room temperature for 10 min				
2.5 mM L-DOPA	20	20	20	20
Mix and incubate at room temperature for 20 min and measure the absorbance at 492 nm				

7. Calculate the percent inhibition of tyrosinase activity (%) using following formula.

% Tyrosinase inhibition = 100 × [(ΔA_{492} of control – ΔA_{492} of sample)/ ΔA_{492} of control]

2.4.5 Effect of plant extracts on alpha-melanocyte stimulating hormone induced B16F10 cells

2.4.5.1 Culture method for cell line

B16F10 mouse melanoma cells were cultured in in Dulbecco's Modified Eagle Medium/High glucose (DMEM/HG), supplemented with 10% fetal bovine serum (FBS) and antibiotics (100 U/mL penicillin and 100 µg/mL streptomycin) in a 5% CO_2 humidified atmosphere at 37℃.

2.4.5.1.1 Subculture

Culture property of B16F10 cells is adherent. Morphology of this cell is mixed between spindle-shaped and epithelial-like cells. This cells are easily handle.

Procedure

1. Remove and discard the old culture medium.
2. Rinse the cells with 0.25% trypsin-EDTA solution to remove trypsin inhibitors in serum.
3. Add 1 ml of 0.25% trypsin-EDTA solution into 25 cm^2 flask.
4. Incubate at 37°C in 5% CO_2 incubator for 5 min.
5. Observe the cells under an inverted microscope. Ovoid to shake flask while waiting cells to detach.

6. Add 3 ml of fresh complete growth medium and mix gently by an autopipette.

7. Add the cells into new culture vessel in appropriate density for experiments.

2.4.5.2. Exposure of B16F10 cells to plant extracts or α-MSH solution

- Plant extracts: The plant extracts were dissolve in DMSO at 100 mg/ml and filtered through 0.2 μm. The stock of the plant extracts was diluted in fresh DMEM/HG with 10% FBS at the concentration of 3.125, 6.25, 12.5, 25, 50 and 100 μg/ml.

- Alpha-MSH solution (1 μM): The stock solution were diluted in phosphate buffer saline solution (PBS) and filtered through 0.2 μm. The stock of alpha-MSH solution was diluted in fresh DMEM/HG with 10% FBS at the concentration of 1 μM.

- The cells were treated with alpha-MSH solution and plant extracts for 48 h. After treatment, the cells were used to determine for other experiments.

2.4.5.3 Cell viability assay

The cell viability was carried out as described using 3-(4,5-dimethylthiazol-2-yl)-2,5-diphenyl tetrazolium bromide (MTT) (245). MTT is a colorimetric method for assessing mitrochrondial activity. The MTT (yellow tetrazole) is reduced by NAD(P)H dependent cellular oxidoreductase enzymes in viable cells to insoluble formazan (purple color) as shown in Figure 33. The insoluble purple formazan dye is quantified by measuring the absorbance at a 500-600 nm. This assay is used to measure the cytotoxic effect of plant extracts on alpha-melanocyte stimulating hormone-induced B16F10 cells.
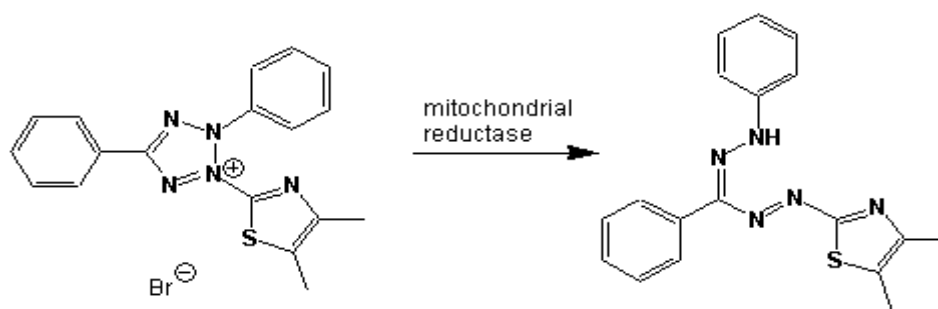
Figure 33. Reduction reaction of MTT assay.

Procedure

1. Seed B16F10 cells (5,000 cells/well) into 96 well culture plate and incubate at 37°C in 5% CO_2 incubator for 24 h.

2. Treat the cells with 1 μM alpha-MSH and plant extracts at 3.125, 6.25, 12.5, 25, 50 and 100 μg/ml and incubate at 37°C in 5% CO_2 incubator for 48 h. Total volume of each well was 200 μl.

3. Add 20 μl of MTT solution (5 mg/ml) into each well and incubate at 37°C in 5% CO_2 incubator for 4 h.

4. Remove culture medium and dissolve insoluble purple formazan by adding 200 μl of DMSO for each well.

5. Mix the plate and measure the absorbance at 550 nm.

6. Express the relative cell viability (%) by calculating the absorbance value of each experimental extract-treated group to compare with control group.

$$\% \text{ Cell viability} = 100 \times \frac{\text{Abs(treated cells)} - \text{Abs(blank of treated cells)}}{\text{Abs(control)} - \text{Abs(blank of control)}}$$

2.4.5.4 Effect of alpha-MSH and plant extracts on cellular melanin content

Melanin content in the cultured B16F10 cells was measured using a previously reported method (246). Melanin is synthesized by specialized pigment cells known as melanocytes and are deposited in melanosomes (1). Melanin biosynthesis requires tyrosinase, tyrosinase-related protein 1(TRP-1) and 2 (TRP-2). The first step of melanin formation is mediated by tyrosinase. In this assay, the cells were treated with 1 μM of alpha-MSH to increase melanin content in the cells. Inhibitory of melanin content was determined by oxidative degradation of cellular melanin in heat alkaline. Kojic acid served as positive control. The soluble melanin content was measured by spectrophotometer at 475 nm.

Procedure

1. Seed the cells (1×10^5 cells/well) into 6 well culture plate and incubate at 37°C in 5% CO_2 incubator for 24 h.

2. Stimulate the cells with 1 µM of alpha-MSH and plant extracts, and incubate for 48 h. Untreated cells served as control cells. Alpha-stimulated cells was used as an alpha-MSH group.

3. Remove culture medium and wash the cells with PBS twice.

4. Add 500 **µl** of 0.25 (% v/v) trypsin EDTA solution and incubate for 5 min.

5. Dilute trypsin EDTA solution with 700 **µl** of culture medium and transfer into microcentrifuge tube.

6. Centrifuge at 13,000 g for 10 min and discard supernatant.

7. Count the cells (500,000 cells/tube).

8. Dissolve the cellular melanin with 1 N NaOH at 80°C for 1 h.

9. Measure the absorbance of melanin content at 475 nm.

10. Determine melanin content by using a standard curve of a synthetic melanin.

11. Calculate melanin content of sample by comparing with total melanin content of control cells (100%).

$$\% \text{ Total melanin content} = 100 \times \frac{\text{Abs(treated cells)} - \text{Abs(blank of treated cells)}}{\text{Abs(control)} - \text{Abs(blank of control)}}$$

2.4.5.5 Total protein determination by Bradford assay

Protein concentration of sample (cellular tyrosinase activity and western blot assay) was determined by using Bradford protein assay. The Bradford protein assay is a dye-binding assay that a color change of dye is responsible to various concentrations of protein samples. This method is based on the absorbance shift of Coomassie brilliant blue G-250 dye when binding to protein occurs. This dye binds to primarily basic and acidic protein residues. The red form of the dye is converted into

its blue form to bind to the protein. The absorbance was measured at 595 nm. Bovine serum albumin (BSA) served as a standard (247).

Procedure

1. Prepare a dye reagent by diluting 10 ml of dye reagent in 40 ml of distilled water and filter the dye reagent through Whatman NO.1 to remove particulates.

2. Prepare five dilutions (0.03125, 0.0625, 0.125, 0.25, 0.5 mg/ml) of bovine serum albumin as a protein standard dissolved in distilled water.

3. Dilute 5 µl of sample in 70 µl of distilled water (1:15).

4. Add 10 µl of diluted sample or standard into 96 well plate.

5. Add 200 µl of diluted dye reagent into each well.

6. Mix and stand at room temperature for 5 min.

7. Measure absorbance at 595 nm.

8. Prepare a standard curve from the absorbance of bovine serum albumin.

9. Calculate protein concentration of sample from the standard curve in microgram protein (µg).

2.4.5.6 Effect of plant extracts on cellular tyrosinase activity in alpha-MSH-induced B16F10

Tyrosinase activity was determined by measuring the rate of L-DOPA oxidation by using a previously described method (248). L-DOPA as a substrate is oxidized to DOPAquinone by tyrosinase. DOPAquinone is further converted to DOPAchrome which is a substrate for eumelanin. This assay was used to determine the effect of plant extracts on cellular tyrosinase activity of alpha-MSH-treated cells. Kojic acid served as a positive control.

Procedure

1. Seed the cells (1×10^5 cells/well) into 6 well culture plate and incubate at 37°C in 5% CO_2 incubator for 24 h.

2. Treat the cells with alpha-MSH and plant extracts, and incubate for 48 h. Untreated cells served as control group. Alpha-MSH stimulated cells was used as an alpha-MSH group.

3. Remove culture medium and place the cell culture plate on ice.

4. Wash the cells with PBS twice and lyse the cells with 1% Triton X-100/PBS on ice.

5. Incubate the culture plate on ice for 5 min and scrape the adherent cells using a cold plastic cell scraper.

6. Transfer cell lysate into a pre-cooled tube and stand on ice for 10 min.

7. Centrifuge at 13,000 g for 10 min and gently move the tubes from the microcentrifuge.

8. Place on ice and transfer the supernatant into a new tube kept on ice.

9. Quantify protein using Bradford assay and dilute protein concentration at 40 µg in 1% Triton X-100/PBS.

10. Prepare 0.1 mM sodium phosphate buffer and adjust pH 6.8.

11. Prepare 5 mM L-DOPA dissolve in sodium phosphate buffer pH 6.8 (prepare freshly).

12. Add cell lysate (40 µg) and reagents as following in table 12.

Table 12. Procedure step for cellular tyrosinase activity.

Reagent	Control (µl)	Sample (µl)
Cell lysate (40 µg) in 0.1 mM sodium phosphate buffer pH 6.8	100	100
5 mM L-DOPA	100	100

13. Incubate at 37°C for 1 h and measure the absorbance at 475 nm.

14. Calculate cellular tyrosinase activity of sample by comparing with cellular tyrosinase activity of control cells (100%).

$$\text{\% Tyrosinase activity} = 100 \times \frac{\text{Abs(treated cells)} - \text{Abs(blank of treated cells)}}{\text{Abs(control)} - \text{Abs(blank of control)}}$$

2.4.5.7 Effect of plant extracts on melanogensis-related gene expression in alpha-MSH induced B16F10 cells

Effect of plant extracts on melanogenesis-related gene expression in alpha-MSH induced B16F10 cells was carried out by real-time polymerase chain reaction or quantitative PCR (qPCR). This assay is based on gene expression level in untreated group and plant extracts treated group. RNA isolation from sample was reversed into cDNA using reverse transcriptase. The cDNA was amplified with specific primers using qPCR.

Procedure

A. RNA isolation

1. Seed cells (1×10^5 cells/well) into 6 well culture plate and incubate at 37°C with 5% CO_2 for 24 h.

2. Treat the cells with 1 μM alpha-MSH and plant extracts for 48 h.

3. Remove culture medium and wash with PBS twice.

4. Add 1 ml of Ribozol reagent into each well and incubate at room temperature for 10 min.

5. Mix cell lysate using autopipette and transfer into microcentrifuge tube.

6. Add 200 μl of chloroform into each tube and mix vigorously.

7. Centrifuge at 14,000 g for 15 min.

8. After centrifugation, there are three main layers in a tube, including top layer (clear, aqueous), middle layer (white precipitated DNA) and bottom layer (pink organic phase).

9. Transfer an aqueous layer (400 μl) into a new tube using autopipette.

10. Add 400 μl of isopropanol and stand at room temperature for 10 min.

11. Centrifuge at 14,000 g for 10 min. There is a pellet in the bottom of a tube.

12. Pour off isopropanol and add 1 ml of 75% ethanol in DEPC-treated water.

13. Mix gently and wash three times by centrifuging at 14,000 g for 5 min.

14. Remove ethanol solution every time and dry pellet.

15. Add 30 µl of DEPC-treated water into tube and incubate at 65°C for 15 min.

16. Measure RNA concentration at 260 nm.

17. Express the RNA concentration as µg/ml.

B. Reverse transcription

1. Mix RNA template with oligo dT$_{18}$ (0.5 µg, 100 pmole) and incubate at 70°C for 5 min (total volume 20 µl).

2. Place the tube on ice quickly and transfer into AccuPower$^{®}$ RT Premix tube and then fill up the reaction volume with DEPC-distilled water.

3. Dissolve the lyophilized blue pellet by vortexing and briefly spin down.

4. Perform the synthesis reaction as follows:

    42°C, 60 min (cDNA synthesis)

    94°C, 5 min   (reverse transcriptase inactivation)

5. Keep cDNA sample at -20°C before use.

Table 13. Specific primers for qPCR.

Gene	Sequence	Annealing Temperature ($^{\circ}$c)	Product size
GAPDH	Forward: 5' CTTTGTCAAGCTCATTTCCTGG 3' Reverse: 5' TCTTGCTCAGTGTCCTTGC 3'	57	133 bp
MITF	Forward : 5'AGGACCTTGAAAACCGACAG 3' Reverse: 5' GGTGGATGGGATAAGGGAAAG 3'	57	116 bp
TYR	Forward: 5' CTAACTTACTCAGCCCAGCATC 3' Reverse:	58	150 bp

	5' GGGTTTTGGCTTTGTCATGG 3'		
TRP-1	Forward: 5'AGCCCCAACTCTGTCTTTTC 3' Reverse: 5' GGTCTCCCTACATTTCCAGC 3'	56	134 bp
TRP-2	Forward: 5' TCCAGAAGTTTGACAGCCC 3' Reverse: 5' GGAAGGAGTGAGCCAAGTTATG 3'	57	135 bp

C. Real time PCR using SYBR Green

Real time PCR was performed by using *Exicycler*™ 96 Quantitative Real-Time PCR System. PCR was carried out by SYBR green I. Specific primers (Bioneer, Korea) are as follows:

Set up the experiment and realtime PCR program on Exicycler™ 96 Real-Time Quantitative Thermal block.

1. Quantify cDNA by Accupower® 2X GreenStar qPCR master mix which contains SYBR Green Dye I and Hotstart top DNA polymerase.

2. Mix cDNA and reagents as shown in table 14.

   Table 14. Procedure step for Real Time PCR.

Reagents	1 Reaction (12.5 µl)
2X Greenstar master mix	6.25
PCR F-primer (10 pmole)	0.5
PCR R-primer (10 pmole)	0.5
Template (1 µg)	1
DEPC-treated water	4.25

3. Carefully seal an optical adhesive film for real-time PCR on tube.

4. Mix vigorously to resuspend the master mix and spin down.

5. Load the tubes into real-time PCR machine and start the program.

6. Calculate a fold change in mRNA level using $\Delta\Delta$ct method ($2^{-\Delta\Delta\text{ct}}$) for relative quantification between sample and control. GAPDH served as an internal control.

2.4.5.8 Effect of plant extracts on protein level of melanogenesis-related gene expression in alpha-MSH induced B16F10 cells

Effect of plant extracts on protein level (MITF, TYR, TRP-1, TRP-2, phosphor-CREB and CREB) was carried out by Western blot assay. This assay is based on protein level of gene expression in alpha-MSH group and plant extracts treated group. For these proteins, B16F10 cells were incubated with 1 μM of α-MSH and treated with the plant extracts for 48 h. After incubation, the cellular proteins were extracted from the cells. The protein concentrations were evaluated by using Bradford protein assay. The protein solutions from harvested cells were subjected to 10% SDS-PAGE and transferred to Polyvinylidene fluoride (PVDF). The blots were blocked with 5% of non-fat dry milk or bovine serum albumin. MITF, tyrosinase, TRP-1 and TRP-2 bands were detected with the appropriate primary antibodies and then further incubated with horseradish peroxidase-conjugated secondary antibody. Bound antibodies were detected using an enhanced chemiluminescence kit following the manufacturer's instructions. Loading control will be assessed using anti-GAPDH antibody (249).

Procedure

A. Protein extraction

1. Seed cells (1×10^5 cells/well) into 6 well culture plate and incubate at 37°C with 5% CO_2 for 24 h.

2. Treat the cells with 1 μM of alpha-MSH and plant extracts for 48 h.

3. Remove culture medium and wash with PBS twice on ice.

4. Add 100 μl of lysis buffer (RIPA with 1X protease inhibitor) and incubate 10 min on ice.

5. Scrape adherent cells off the well using a cold plastic cell scraper, then gently transfer the cell suspension into a pre-cooled microcentrifuge tube.

6. Maintain on ice for 10 min.

7. Centrifuge in a microcentrifuge at 13,000 g for 20 min.

8. Gently remove the tubes and plate on ice, aspirate supernatant and add into a new tube, and discard the pellet.

B. Determination of protein concentration

1. Dilute bovine serum albumin (BSA) in 96 well plate at the concentration of 0.03125, 0.0625, 0.125, 0.25, 0.50 mg/ml.

2. Dilute sample and lysis buffer in distilled water at ratio 1:15

3. Add 10 µl of sample or standard into each well.

4. Add 200 µl of Bradford reagent and incubate at room temperature at 5 min.

5. Determine the protein concentration at 595 nm.

C. Sample preparation

1. 30 µg of cell lysate dissolved in lysate buffer (15 µl).

2. Add 5 µl of 4x Laemmli sample buffer.

3. Boil each cell lysate in sample buffer at 95°C for 10 min.

D. Loading, running and transferring the gel

1. Load 30 µg of total protein from cell lysate into each well of 10%SDS-PAGE gel.

2. Run gel at 90 V for 30 min and 120 V for 90 min.

3. Active PVDF membrane in methanol for 5 min and in transfer buffer for 15 min.

4. Place the gel in transfer buffer for 15 min.

5. Assemble the transfer sandwich from cathode to anode (sponge, filter paper, gel, activated PVDF membrane, filter paper, and sponge) and make sure no bubbles are trapped in sandwich.

6. Place the cassette in the transfer tank and place ice pack in tank.

7. Transfer the gel at 150 mA for 90 min.

E. Antibody incubation

1. Block with 5% nonfat dry milk or 5% bovine serum albumin (BSA) in TBST for 1 h and wash 3 times for 10 min with TBST.

2. Incubate the primary antibody solution against target protein at $4^{\circ}C$ as following:

    -   Anti-MITF   (1:1,000)
    -   Anti-Tyrosinase   (1:1,000)
    -   Anti-TRP-1   (1:2,000)
    -   Anti-TRP-2   (1:2,000)
    -   Anti-phospho CREB   (1:1,000)
    -   Anti-CREB   (1:1,000)
    -   Anti-GAPDH   (1:10,000)

3. Rinse the blot 3 times for 10 min with TBST.

4. Incubate in the HRP-conjugated secondary antibody solution for 1 h at room temperature.

    -   Secondary antibody (1:2000) for MITF and tyrosinase, phospho-CREB, CREB
    -   Secondary antibody (1:5000) for TRP-1, TRP-1, GAPDH

5. Rinse the blot 3 times for 10 min with TBST.

6. For signal development, follow Pierce™ ECL Western Blotting Substrate (Ratio 1:1). Remove excess reagent and cover the membrane with transparent plastic wrap.

7. Detect band using X-ray film in darkroom.

2.4.5.9 Data analysis

All experiments were performed at least in three independent times. These results were expressed as the mean ± *standard error* of the *mean (S.E.M). Statistical significance of the results was analyzed using One way ANOVA* and Dunnett's testing of post-hoc analysis using the SPSS statistics with $P < 0.05$ considered to be statistically significant.

CHAPTER III

RESULTS

3.1 Determination of plant extracts

3.1.1 Extraction yields

Yields of dry extracts were presented in as % w/w dry plant material. The scientific names, plant parts and percent yields are shown in table 15 and figure 34. The percent yields of 13 Thai plants had the range from 0.73% to 31.11%. *Ardisia elliptica* had the highest yield in petroleum ether (19.89%) and ethanol extract (31.11%) whereas *Garcinia mangostana* Linn. had the highest percent yield from dichloromethane extract (11.07%). The variation of percent yield depends on the species of the plants.

Table 15. Extraction yields of 13 plant extracts.

Scientific name	%Yield (w/w dry plant material)		
	Petroleum ether	Dichloromethane	Ethanol
Ardisia elliptica Thunb.	19.89	3.25	31.11
Croton roxburghii N.P.Balakr	7.50	4.82	8.17
Croton sublyratus Kurz	7.33	4.03	3.32
Datura metel L.	6.44	4.13	14.15
Garcinia mangostana Linn.	4.94	11.07	18.64
Gynura pseudochina (L.) DC.	8.00	2.76	3.79
Hibiscus mutabilis L.	6.30	2.79	0.73
Ipomoea pes-caprae (L.) R.br.	6.38	4.50	3.98
Phyllanthus acidus (L.) Skeels	9.70	2.86	4.20
Rhinacanthus nasutus (L.) Kurz	4.43	2.86	5.35
Senna alata (L.) Roxb.	5.84	3.52	7.63
Stemona curtisii Hook.f.	7.55	4.10	6.34
Streblus asper Lour.	3.87	2.53	3.56
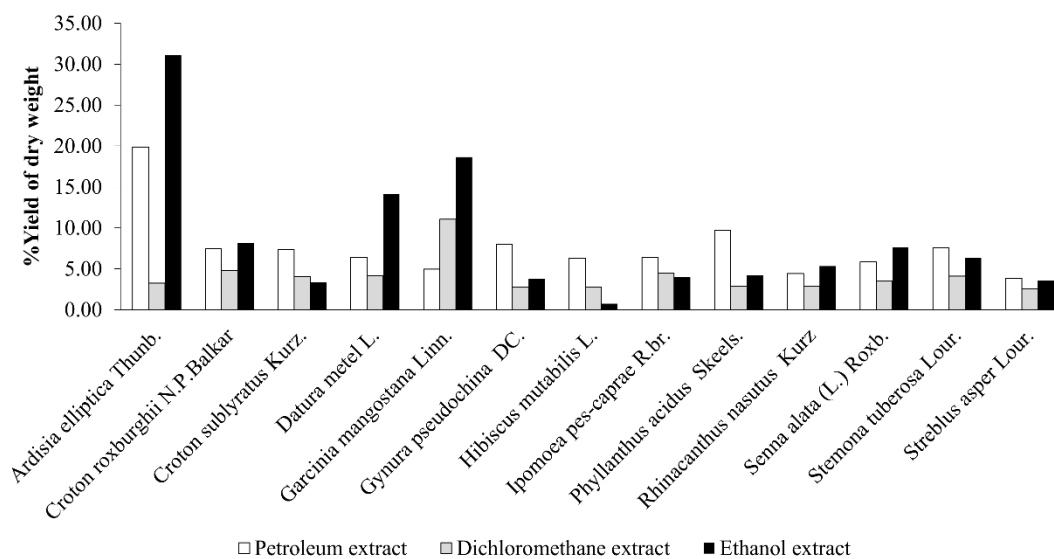
Figure 34. %Yield of 13 plant extracts.

3.1.2 Determination of antioxidant content in plant extracts

Phenolics are the largest group of phytochemicals found in plants and have various biological activities in animals and humans (250). Therefore, total phenolic content in the plants was determined by Folin-Ciocalteu method. In addition, Flavonoids are pigments in flowers, leaves, fruits and seeds. These compounds are secondary metabolites of plants and widely distributed among plant species (251). Next, flavonoid content within the Thai plants was evaluated using the Aluminium chloride colorimetric assay. Chemical agents are used as depigmenting agents in dermatology and cosmetics. Especially, hydroquinone is the most popular depigmenting agents for melasma treatment but it has many side effects (11). Thus, many researchers seek new agents for melasma treatment. The new agents should be safety and efficacy without side effects. Naturally occurring herbal extracts, active compounds such as phenol, flavonoid, gallic acid, epigallocatechin, aloesin, hydroxystillbene and ellagic acid (12). In this study, we tested the phenolic and flavonoid content in 13 plants.

3.1.2.1 Total phenolic content of 13 plant extracts

The extracts had a wide range in the quantity of phenols as shown in table 16 and figure 35, and values varied from 2.51 ± 0.22 to 84.00 ± 6.23 mg GAE/g dry plant material. *Ardisia elliptica* had the highest phenol content in all three fractions of plants, whereas the lowest phenolic content was presented in the petroleum ether extract of *Stemona curtissi*. Overall, the ethanol fractions had the richest phenolic content, followed by dichloromethane fractions, while petroleum ether fractions with low polarity had the lowest phenolic content compared with the other solvents. In previous studies, dichloromethane leaf extract of *Ardisia elliptica* had a phenolic content of 101 ± 1.3 mg GAE/g dry weight (252). Moreover, a methanol extract of ripe *Ardisia* fruit contained 5.64 ± 0.37 g GAE/100 g extract (253). Hence, leaves and fruits of *Ardisia elliptica* have a high phenolic content that can be easily extracted with methanol, dichloromethane and ethanol.

Table 16. Total phenolic contents of 13 plants obtained from different solvents.

Extract	Total phenolic content (mg GAE/g dry plant material)		
	Petroleum ether	Dichloromethane	Ethanol
Ardisia elliptica	22.26 ± 1.77	59.97 ± 2.90	84.00 ± 6.23
Croton roxburghii	3.57 ± 0.25	9.60 ± 0.46	19.41 ± 0.81
Croton sublyratus	4.73 ± 0.38	6.74 ± 0.51	16.28 ± 0.29
Datura metel	8.30 ± 0.29	11.43 ± 0.17	18.92 ± 1.50
Garcinia mangostana	19.75 ± 1.44	31.07 ± 2.30	80.79 ± 2.94
Gynura pseudochina	3.26 ± 0.11	9.18 ± 0.65	12.76 ± 0.81
Hibiscus mutabilis	3.44 ± 0.14	7.14 ± 0.48	17.05 ± 0.64
Ipomoea pes-caprae	4.72 ± 0.29	11.18 ± 0.53	37.91 ± 3.36

Phyllanthus acidus	4.65 ± 0.46	10.05 ± 0.74	50.52 ± 2.66
Rhinacanthus nasutus	5.04 ± 0.30	9.14 ± 0.39	17.09 ± 1.44
Senna alata	4.59 ± 0.21	9.48 ± 0.44	36.83 ± 2.30
Stemona curtisii	2.51 ± 0.22	7.76 ± 0.30	59.67 ± 3.28
Streblus asper	4.19 ± 0.30	8.22 ± 0.39	23.10 ± 1.84

Each value is mean ± SEM of triplicate independent analyses. GAE = Gallic Acid Equivalent.
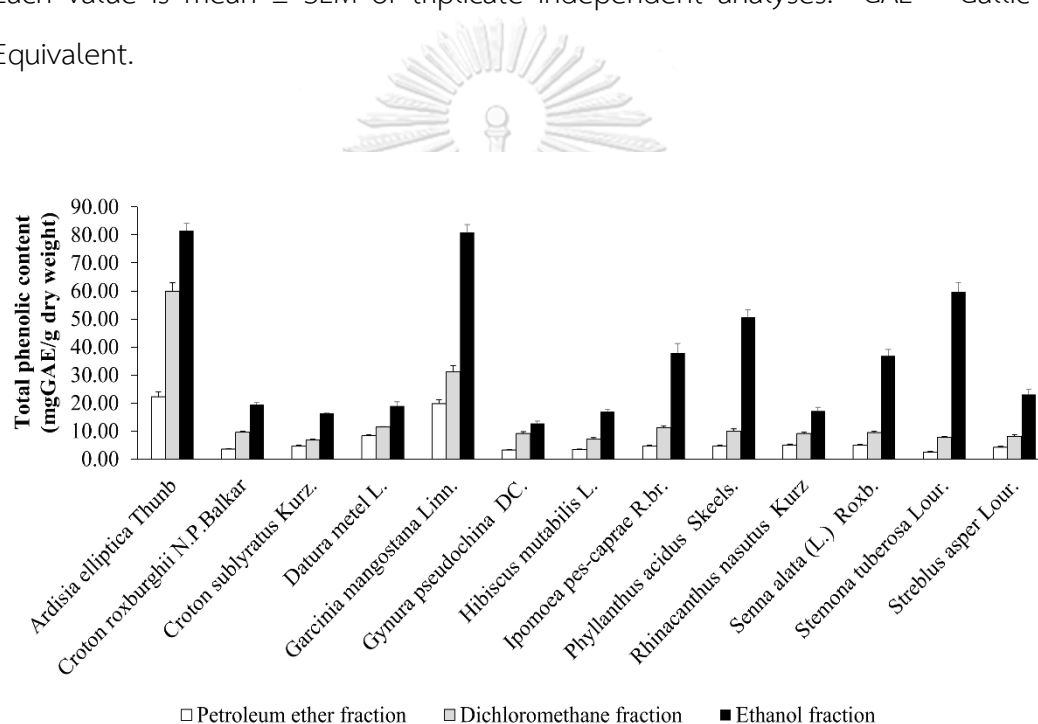
Figure 35. Total phenolic content of 13 plant extracts.

3.1.2.2 Total flavonoid content of 13 plant extracts

Total flavonoid content substantially varied among the plant species ranging from 2.04 ± 0.16 to 31.38 ± 0.81 mg QE/g dry plant material (table 17 and figure 36). In general, dichloromethane extracts yielded the highest flavonoid level compared with the other solvents. Of all extracts, the highest flavonoid quantity was found in the ethanol extract from leaves of *Senna alata* (31.38 ± 0.81 mg QE/g dry material). In a previous study, high flavonoid content was found in water (4.25 mg QE/ 100 g) and methanol fractions (3.97 mg QE/ 100 g) of *Senna alata* (254). Thus, *Senna alata* preparations have high flavonoid content when extracted with high polarity solvents including ethanol, methanol and water. On the other hand, *Ardisia elliptica* (23.14 ± 1.10 mg QE/g dry material) had the richest flavonoid content in dichloromethane fractions. Fruit of this plant also had high flavonoid content 36.91 ± 2.37 mg QE/g extract (255). Hence, fruit and leaves of *Ardisia elliptica* are rich in flavonoids. Moreover*, Ipomoea pes-caprae* (L.) had the highest flavonoid content among petroleum ether extracts (27.48 ± 2.59 mg QE/g dry material). The lowest detectable flavonoid level was in the ethanol extract from *Datura metel*. By stark contrast, flavonoids were not found in petroleum ether and dichloromethane extracts of *Stemona curtisii*, petroleum ether extracts of *Streblus asper* and *Phyllanthus acidus*. However, flavonoids have many biological activities containing UVB protection (256), anti-inflammatory (257), anti-hepatotoxicity (258) and anti-cancer (259), etc.

Table 17. Total flavonoid contents of 13 plants obtained from different solvents.

Plants	Total flavonoid content (mg QE/g dry plant material)		
	Petroleum ether	Dichloromethane	Ethanol
Ardisia elliptica	19.87 ± 1.26	23.14 ± 1.10	18.56 ± 1.45
Croton roxburghii	4.25 ± 0.35	12.34 ± 0.29	7.54 ± 0.35
Croton sublyratus	18.55 ± 0.53	20.78 ± 1.49	14.86 ± 0.95
Datura metel	17.65 ± 1.62	16.77 ± 1.30	2.04 ± 0.16
Garcinia mangostana	5.35 ± 0.10	11.13 ± 0.37	3.20 ± 0.05
Gynura pseudochina	4.87 ± 0.35	18.60 ± 1.06	3.69 ± 0.21
Hibiscus mutabilis	3.71 ± 0.24	18.79 ± 1.78	3.71 ± 0.09
Ipomoea pes-caprae	27.48 ± 2.59	18.68 ± 0.66	17.66 ± 0.29
Phyllanthus acidus	NA	15.80 ± 1.04	11.74 ± 0.74
Rhinacanthus nasutus	16.98 ± 0.40	19.88 ± 1.98	9.53 ± 0.26
Senna alata (L.) Roxb.	7.71 ± 0.36	13.97 ± 1.10	31.38 ± 0.81
Stemona curtisii	NA	NA	14.50 ± 0.86
Streblus asper	NA	18.66 ± 1.28	11.29 ± 1.04

Each value is mean ± SEM of triplicate independent analyses. QE = Quercetin equivalent; NA = Not Available.
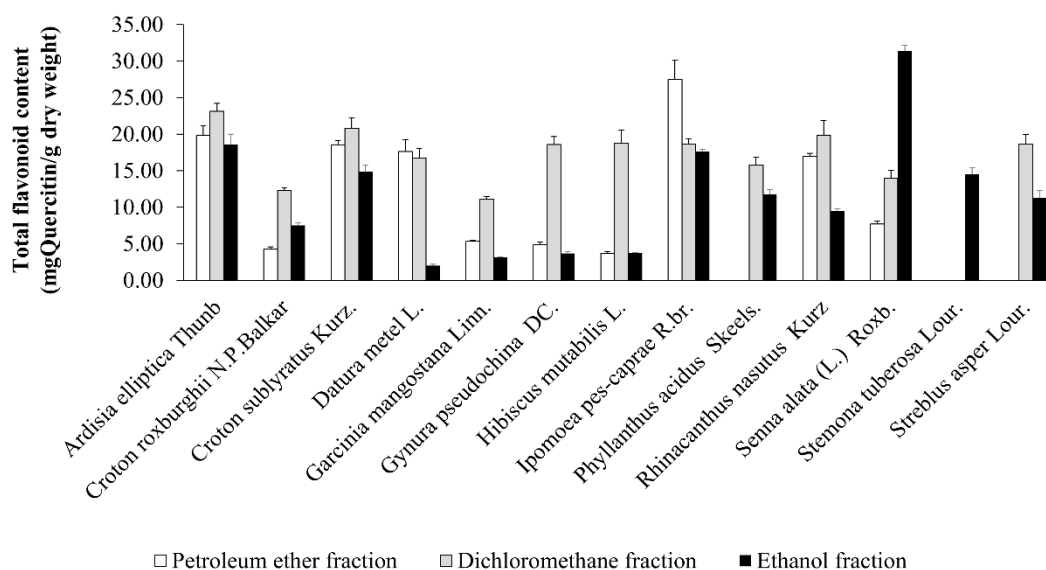
Figure 36. Total falvonoid content of 13 plant extracts.

3.1.3 Determination of antioxidant activity in plant extracts

3.1.3.1 DPPH (2, 2-Diphenyl-1-picrylhydrazyl) scavenging activity

As shown in Table 18 and figure 37, scavenging activities within the extracts greatly varied ranging from $7.11 \pm 0.59\%$ to $96.17 \pm 0.05\%$. Ethanol extracts had the highest levels of free radical scavenging activity compared with the other extracts, and all ethanol extracts were active. The ethanol of *Ardisia elliptica* extract had the highest scavenging activity at 96%. Moreover, the next strongest antioxidant activities (> 90%) were observed in ethanol fractions from *Stemona curtisii*, *Phyllanthus acidus*, and *Garcinia mangostana*. In terms of the other solvents, *Ardisia elliptica*, also had the richest scavenging activity among the petroleum ether fractions, and *Garcinia mangostana* had the highest antioxidant activity in the dichloromethane fractions. Other investigators have also reported that dichloromethane fractions of *Ardisia elliptica* leaves and stems have high levels of antioxidant activity by the DPPH assay, so this plant is very interesting to investigate further as a herbal treatment (252). The lowest scavenging ability was detected in *Croton sublyratus* from petroleum ether fractions. No scavenging activity was detected in 6 petroleum ether

extracts, and 2 dichloromethane extracts. The extracts from ethanol fractions with high polarity obviously showed better antioxidant activity than fractions with lower polarities containing dichloromethane and petroleum ether. As shown in Figure 38, Correlation of DPPH scavenging activity was compared with total phenolic content and total flavonoid content. High correlation was observed between DPPH scavenging activity and total phenolic content (R^2 = 0.8948). However, total flavonoid content did not correlate with DPPH scavenging activity (R^2 = 0.0462) (Figure 39). These results suggested that the phenolic content is the major constituent for DPPH scavenging activity in 13 plant extracts.

Table 18. Free radical scavenging activity by DPPH assay.

Extract	Percent Scavenging Activity (%)			mg VCEAC/g dry weight		
	Petroleum ether	Dichloro-methane	Ethanol	Petroleum ether	Dichloro methane	Ethanol
Ardisia elliptica	49.29 ± 1.29	71.35 ± 6.11	96.17 ± 0.05	12.09 ± 0.94	20.23 ± 0.99	24.93 ± 0.19
Croton roxburghii	8.34 ± 0.57	15.79 ± 1.21	36.89 ± 1.37	1.03 ± 0.09	2.38 ± 0.13	8.45 ± 0.84
Croton sublyratus	7.11 ± 0.59	14.34 ± 0.65	27.64 ± 0.91	0.67 ± 0.07	1.85 ± 0.06	5.29 ± 0.30
Datura metel	14.67 ± 1.10	14.85 ± 0.64	28.72 ± 0.67	2.00 ± 0.12	2.30 ± 0.06	5.83 ± 0.26
Garcinia mangostana	28.90 ± 0.99	80.87 ± 0.47	94.54 ± 0.15	6.18 ± 0.33	20.42 ± 0.20	24.28 ± 0.20
Gynura pseudochina	NA	11.90 ± 0.71	13.54 ± 0.67	NA	1.49 ± 0.03	1.82 ± 0.13
Hibiscus	NA	NA	26.28 ±	NA	NA	4.29 ±

			0.93			0.21
Ipomoea pes-caprae	NA	16.27 ± 0.14	64.06 ± 1.23	NA	2.49 ± 0.19	16.79 ± 0.41
Phyllanthus acidus	NA	17.64 ± 1.05	94.17 ± 0.61	NA	3.06 ± 0.28	23.84 ± 0.73
Rhinacanthus nasutus	7.38 ± 0.46	15.35 ± 1.27	29.63 ± 1.41	1.01 ± 0.08	2.32 ± 0.21	6.50 ± 0.16
Senna alata	11.18 ± 0.99	17.99 ± 0.61	63.74 ± 0.54	1.48 ± 0.14	3.13 ± 0.31	15.35 ± 0.13
Stemona curtisii	NA	NA	93.63 ± 0.22	NA	NA	23.55 ± 0.55
Streblus asper	NA	14.65 ± 0.92	45.14 ± 0.67	NA	1.94 ± 0.13	10.45 ± 0.30

Each value is mean ± SEM of triplicate independent analyses. Calculations of values are described in the methods section. VCEAC is Vitamin C Equivalent Antioxidant capacity, and NA denotes not available.
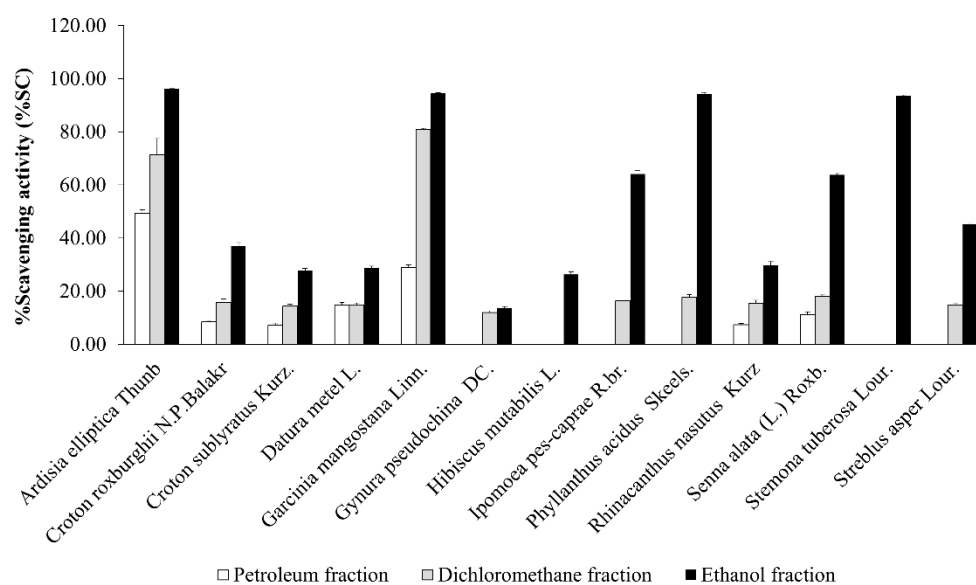
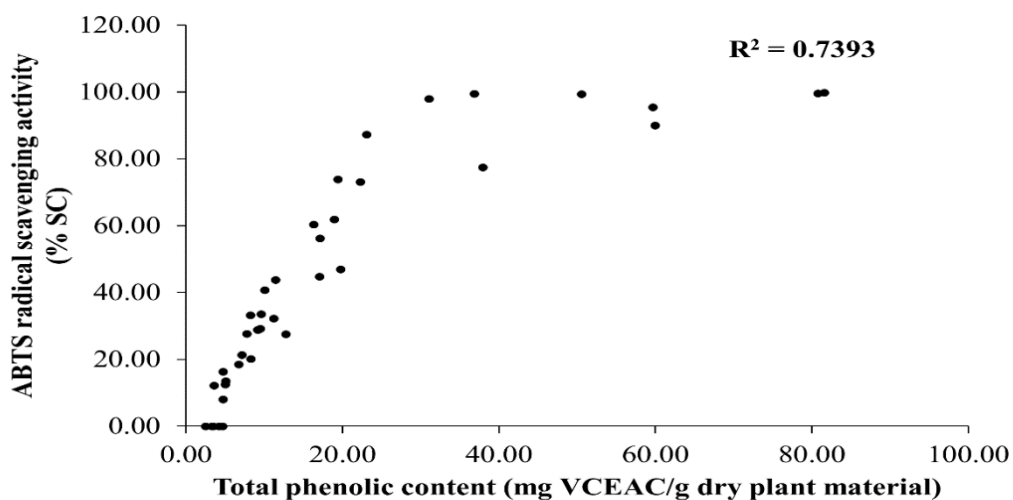Figure 37. %DPPH scavenging activity of 13 plant extracts.
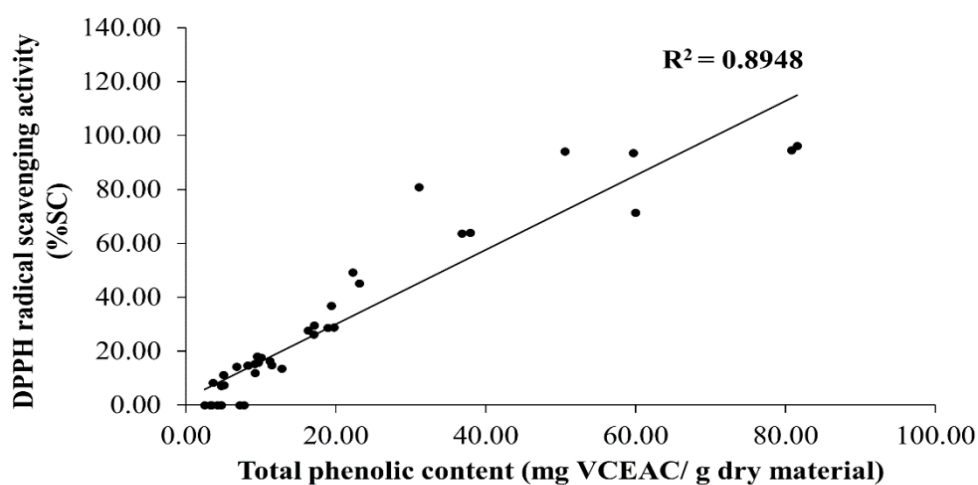
Figure 38. Correlations between DPPH scavenging activity and total phenolic content of 13 plant extracts from petroleum ether, dichloromethane and ethanol extracts (R^2 = 0.8948). Values were evaluated by linear regression analysis, and correlation coefficients expressed as R^2 are shown in the panels.
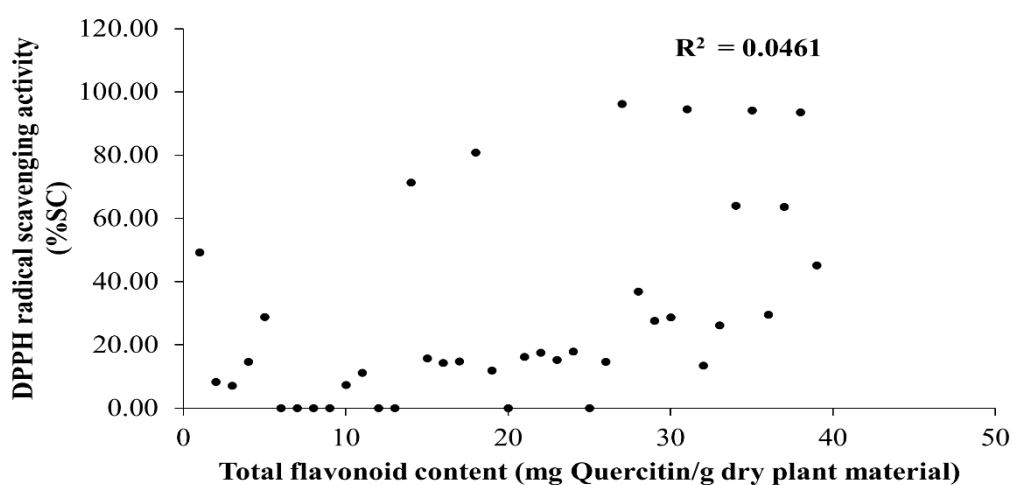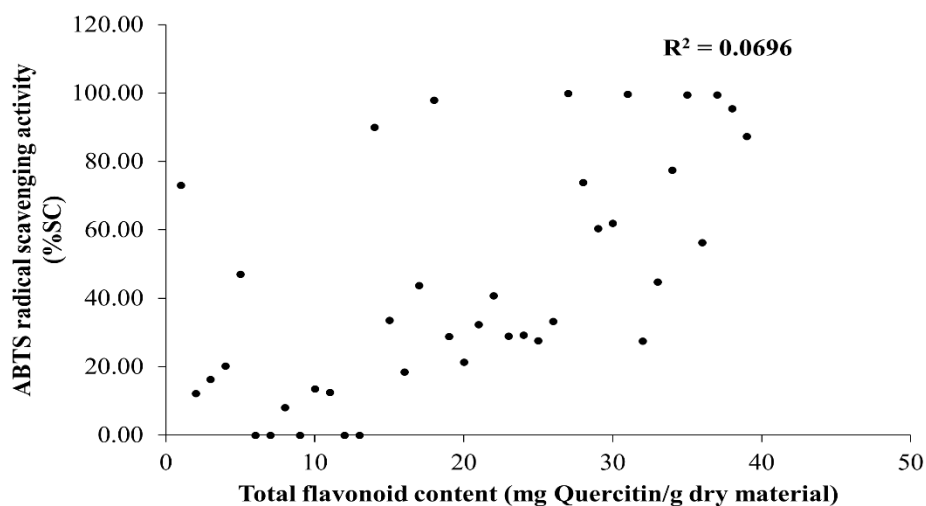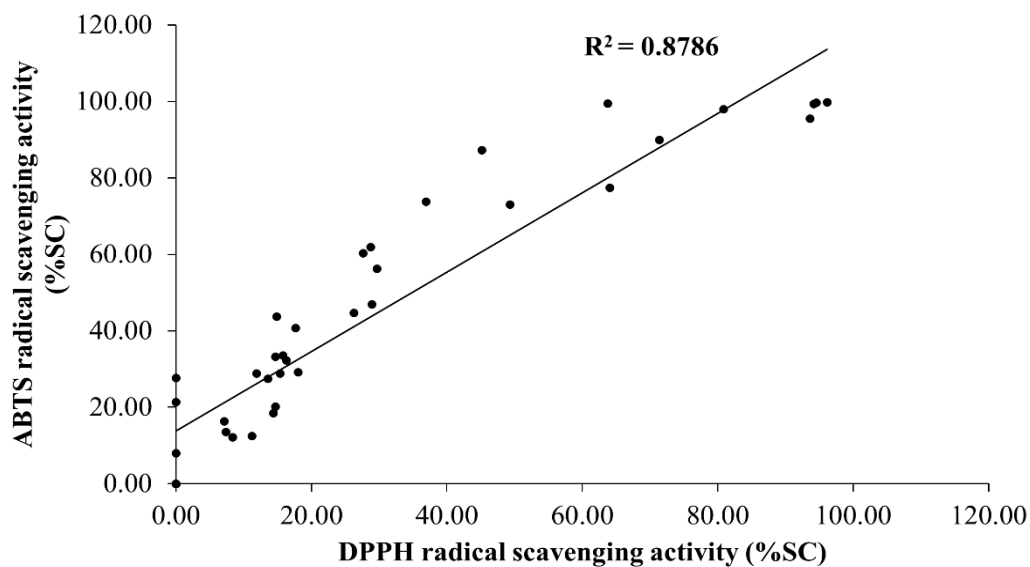
Figure 39. Correlations between DPPH scavenging activity and total flavonoid content of 13 plant extracts from petroleum ether, dichloromethane and ethanol extracts (R^2 = 0.0461). Values were evaluated by linear regression analysis, and correlation coefficients expressed as R^2 are shown in the panels.

3.1.3.2 ABTS (2, 2'-azinobis (3-ethylbenzothiazoline-6-sulfonic acid) radical) scavenging activity

Like the DPPH assay, scavenging activity in the ABTS assay greatly varied among the plant preparations with a similar broad range from 8.03 ± 0.54% to 99.84 ± 0.07% (table 19 and figure 40). In agreement with the DPPH assay, ethanol extracts contained the highest levels of scavenger activity compared with the other extracts. Again, the highest scavenging activities in ethanol, dichloromethane and petroleum ether extracts were from the same plants as revealed by the DPPH assay. Furthermore, the next strongest scavenging activities (> 90%) were observed in the same 4 ethanol fractions as detected by the DPPH assay. Moreover, no scavenging activity was found in the same 5 petroleum ether extracts. In general, the values obtained with the ABTS assay were higher than the DPPH values. Hence, the scavenging activity in the ethanol extract from *Senna alata* became >90%, and, now, scavenger activity was detected in all dichloromethane extracts, and petroleum ether extracts from *Ipomoea pes-caprae* that was not found by the DPPH assay. As shown in Figure 41, total phenolic content of plant extracts positively correlated with

ABTS radical scavenging activity (R^2 = 0.7393). Our finding found that there was no significant relationship between ABTS radical scavenging activity and total flavonoid content (R^2 = 0.0696) (Figure 42). Similar to total phenolic content, DPPH radical scavenging activity of plant extracts highly correlated with ABTS radical scavenging activity (Figure 43). These results suggested that the phenolic content in plant extracts is the major active compound for free radical scavenging activities.

Extract	%Scavenging activity (%SC)			mg VCEAC/g dry plant weight		
	Petroleum ether	Dichloro methane	Ethanol	Petroleum ether	Dichloro methane	Ethanol
Ardisia elliptica	73.08 ± 1.48	90.01 ± 0.54	99.84 ± 0.07	65.28 ± 1.86	86.34 ± 1.07	96.97 ± 0.34
Croton roxburghii	12.19 ± 0.91	33.54 ± 0.65	73.86 ± 1.22	9.14 ± 0.45	33.22 ± 0.46	69.62 ± 0.90
Croton sublyratus	16.34 ± 0.69	18.47 ± 0.73	60.36 ± 0.17	13.07 ± 1.29	17.81 ± 1.20	58.62 ± 0.68
Datura metel	20.17 ± 0.68	43.79 ± 0.89	61.94 ± 0.50	16.42 ± 0.65	42.36 ± 1.11	60.06 ± 0.16
Garcinia mangostana	47.01 ± 2.73	97.96 ± 0.85	99.66 ± 0.05	45.10 ± 2.45	95.19 ± 1.43	96.52 ± 0.34
Gynura pseudochina	NA	28.88 ± 0.45	27.52 ± 1.66	NA	28.00 ± 0.36	25.37 ± 1.99
Hibiscus mutabilis	NA	21.36 ± 0.51	44.74 ± 0.23	NA	20.34 ± 0.42	43.29 ± 1.26
Ipomoea pes-caprae	8.03 ± 0.54	32.30 ± 1.93	77.43 ± 1.74	4.53 ± 0.34	31.41 ± 2.73	75.16 ± 2.37
Phyllanthus acidus	NA	40.72 ± 1.25	99.43 ± 0.17	NA	40.06 ± 1.90	96.27 ± 0.10

Rhinacanthus nasutus	13.55 ± 0.49	28.90 ± 0.57	56.26 ± 0.90	10.60 ± 0.24	28.29 ± 1.77	53.26 ± 1.95
Senna alata	12.51 ± 0.41	29.21 ± 1.35	99.45 ± 0.11	8.79 ± 0.17	28.97 ± 0.56	96.28 ± 0.12
Stemona curtisii	NA	27.65 ± 1.30	95.49 ± 0.25	NA	27.48 ± 0.11	91.91 ± 0.63
Streblus asper	NA	33.22 ± 0.77	87.32 ± 0.39	NA	32.92 ± 1.57	83.78 ± 0.90

Table 19. Scavenging activity by ABTS assay.

Each value is mean ± SEM of triplicate independent analyses. Calculations of values are described in the methods section. VCEAC = Vitamin C Equivalent Antioxidant capacity; NA = not available
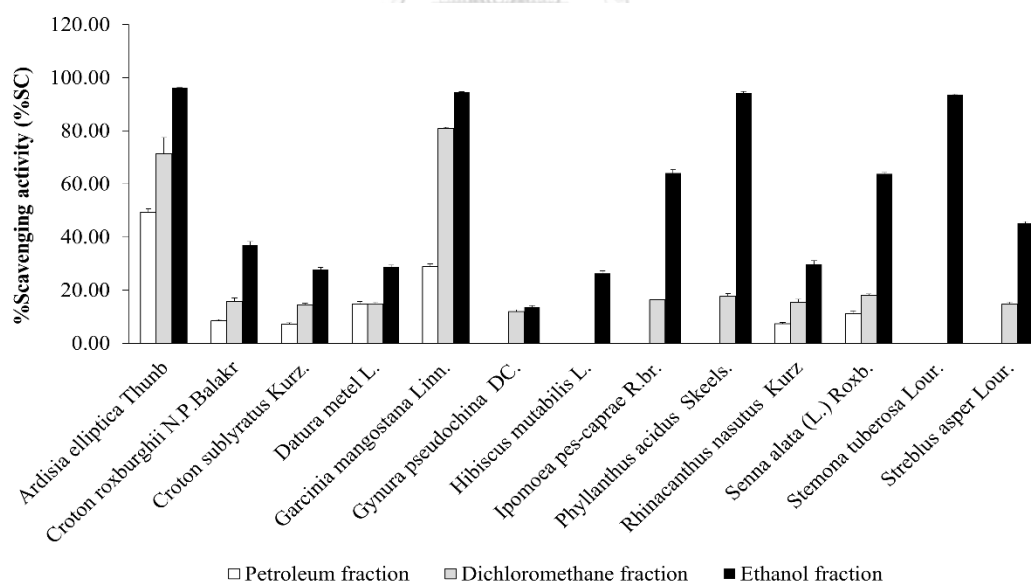
Figure 40. %ABTS scavenging activity of 13 plant extracts.

Figure 41. Correlations between ABTS scavenging activity and total phenolic content of 13 plant extracts from petroleum ether, dichloromethane and ethanol extracts (R^2 = 0.7393). Values were evaluated by linear regression analysis, and correlation coefficients expressed as R^2 are shown in the panels.

Figure 42. Correlations between ABTS scavenging activity and total flavoniod content of 13 plant extracts from petroleum ether, dichloromethane and ethanol extracts (R^2 = 0.0696). Values were evaluated by linear regression analysis, and correlation coefficients expressed as R^2 are shown in the panels.

Figure 43. Correlations between ABTS scavenging activity and DPPH scavenging activity from petroleum ether, dichloromethane and ethanol extracts (R^2 = 0.8786). Values were evaluated by linear regression analysis, and correlation coefficients expressed as R^2 are shown in the panels.

3.1.4 Anti-mushroom tyrosinase activity of plant extracts

The ability of compounds from 13 plants to inhibit mushroom tyrosinase activity was evaluated using an in vitro assay with L-DOPA as the substrate. Kojic acid served as a positive control, and caused maximal enzymatic inhibition of 93.38 ± 1.63%. As shown in Figure 44, only ethanol extracts significantly inhibited tyrosinase activity with *Ardisia elliptica* preparations being the exception. The petroleum ether and dichloromethane fractions of *Ardisia elliptica* inhibited tyrosinase activity by approximately 20%. The ethanol fraction from *Rhinacanthus nasutus* was the most potent tyrosinase inhibitor, followed by ethanol extracts from *Ardisia elliptica* and *Phyllanthus acidus*. Obviously, 6 plants had the high phenolic content, especially *Ardisia elliptica*. Moreover, ethanol extract of *Senna alata* had the richest flavonoid content which can inhibit tyrosinase activity. Active compounds from the plants such as arbutin, aloesin, gentisic acid, flavonoids, hesperidin, licorice, niacinamide,

yeast derivatives, and polyphenols, inhibit melanogenesis without cytotoxicity to melanocyte (260)
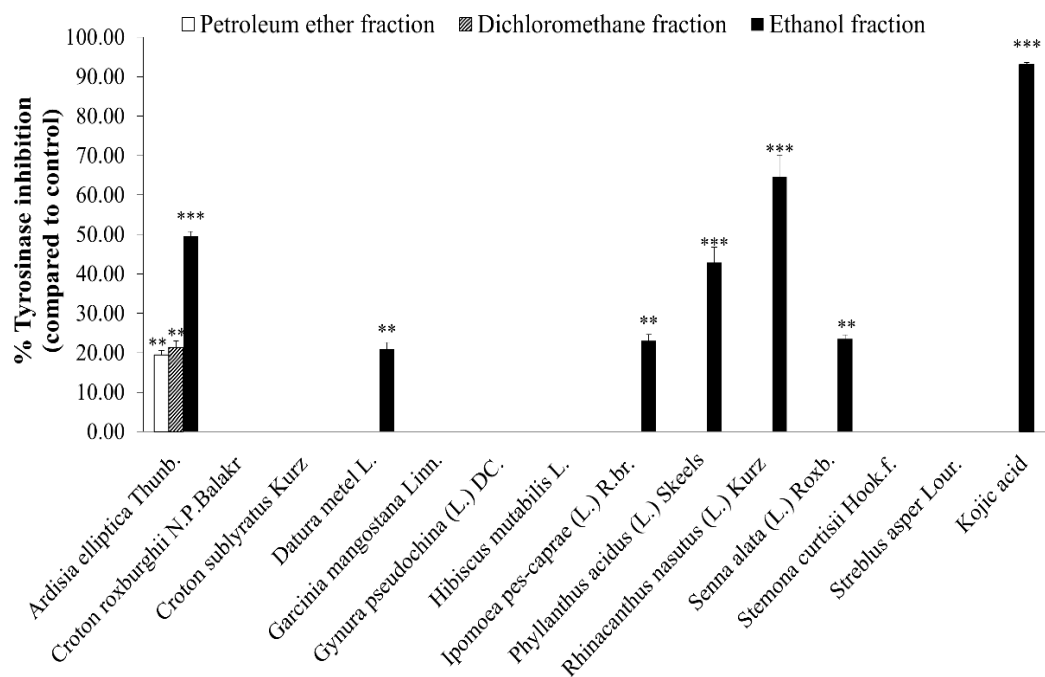
Figure 44. Anti-mushroom tyrosinase activity of 13 plant extracts by DOPAchrome reaction. The data was shown as mean ± SEM. **$P < 0.01$ and ***$P<0.001$ indicate significant differences as compared to control (untreated group).

3.1.5 Effect of plant extracts on alpha-melanocyte stimulating hormone induced B16F10 cells

3.1.5.1 Effect of ethanol fractions from 13 plants on cell viability

The cell viability was carried out as described using 3-(4, 5-dimethylthiazol-2-yl)-2,5-diphenyl tetrazolium bromide (MTT) (245). The MTT (yellow tetrazole) is reduced by NAD(P)H dependent cellular oxidoreductase enzymes in viable cells to insoluble formazan (purple color). This assay is used to measure the cytotoxic effect of plant extracts on alpha-melanocyte stimulating hormone-induced B16F10 cells. B16F10 cells were incubated with 1 μM alpha-MSH and various concentrations of each ethanol extracts for 48 h.

3.1.5.1.1 Effect of ethanol fraction from *Ardisia elliptica* on cell viability

We determined the cytotoxic effect of ethanol fractions from *Ardisia elliptica* on B16F10 treated with 1 μM of alpha-MSH and various concentrations (range, 3.125-100 μg/ml). Control cells exposed to medium only. As shown in Figure 45, ethanol extract of *Ardisia elliptica* did not show cytotoxic effect on B16F10 in concentration range 3.125-25 μg/ml) when compared with alpha-MSH group. Whereas at the dose of 50-100 μg/ml reduced viable cells significantly compared to alpha-MSH group. We selected the highest concentration (25 μg/ml) which did not reduce viable cells for melanin content and cellular tyrosinase activity assay.
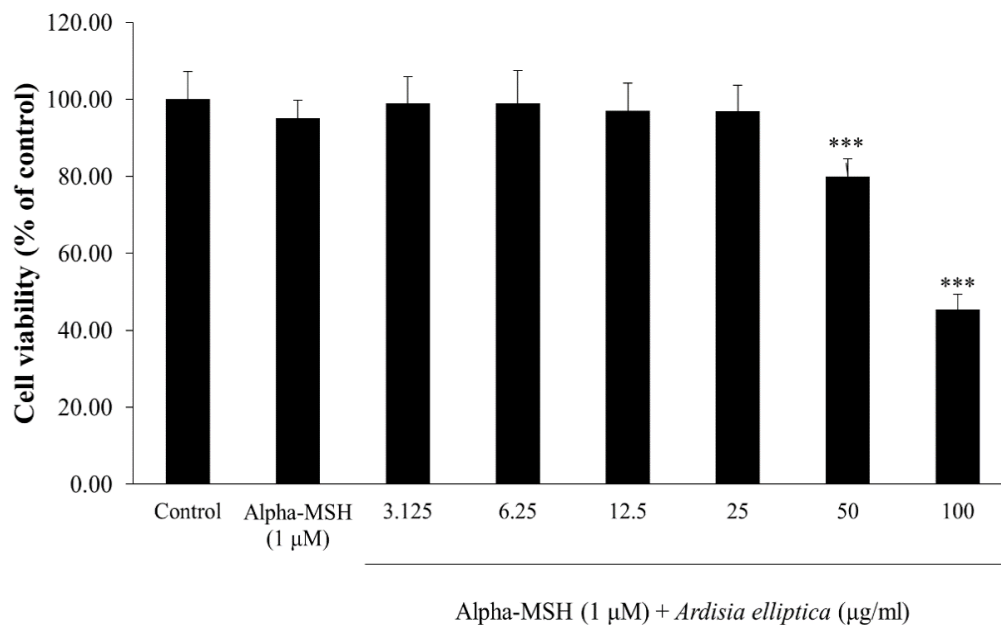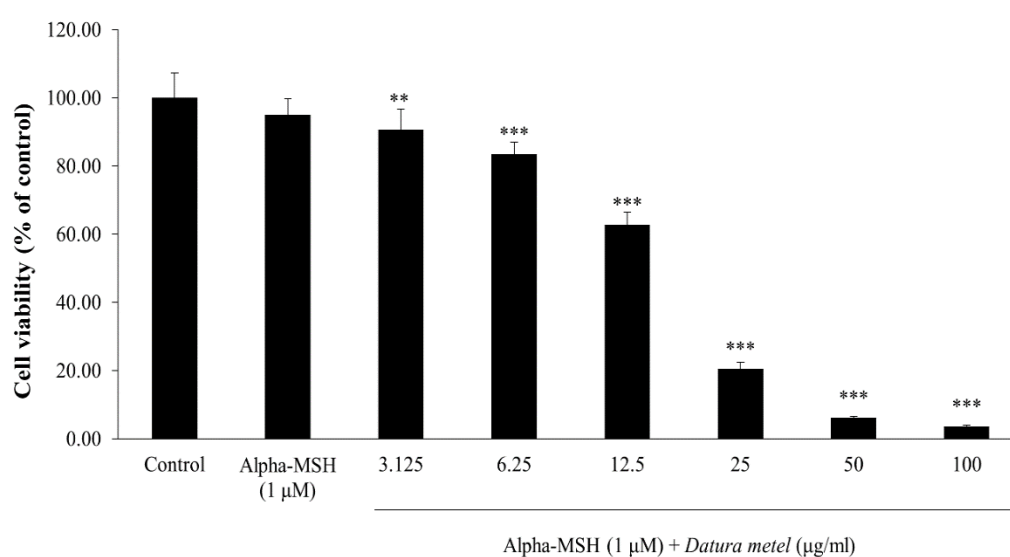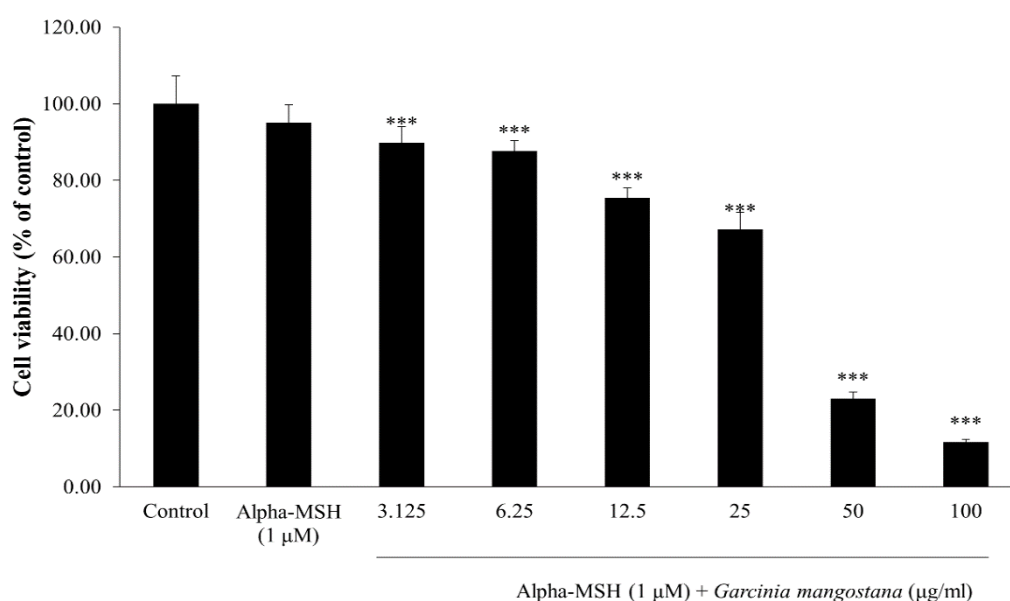
Figure 45. Effect of *Ardisia elliptica* on cell viability of B16F10 cells using MTT assay. B16F10 cells were incubated for 48 h in the presence of *Ardisia elliptica* at different concentrations. Each percentage values for treated cells is reported relative to that of control group. Data are the mean ± SEM from three independent experiments. ***P<0.001: statistically significant vs Alpha-MSH group.

3.1.5.1.2 Effect of ethanol fraction from *Croton roxburghii* on cell viability

The effect of ethanol fraction from *Croton roxburghii* is shown in Figure 46. The results showed that the ethanol crude extract of *Croton roxburghii* at the concentration of 100 µg/ml had the cytotoxic effect by reducing viable cells when compared with alpha-MSH group. There were no growth inhibition in concentration range 3.125-50 µg/ml. In further experiment, we used the highest concentration (50 µg/ml) for investigating the effect of *Croton roxburghii* on melanogenesis.
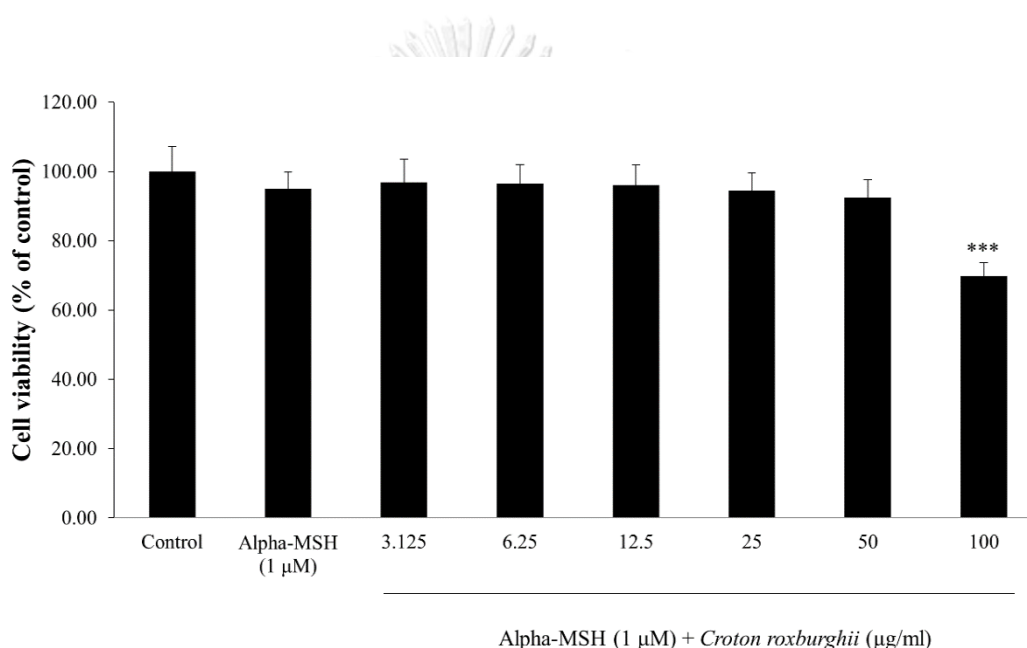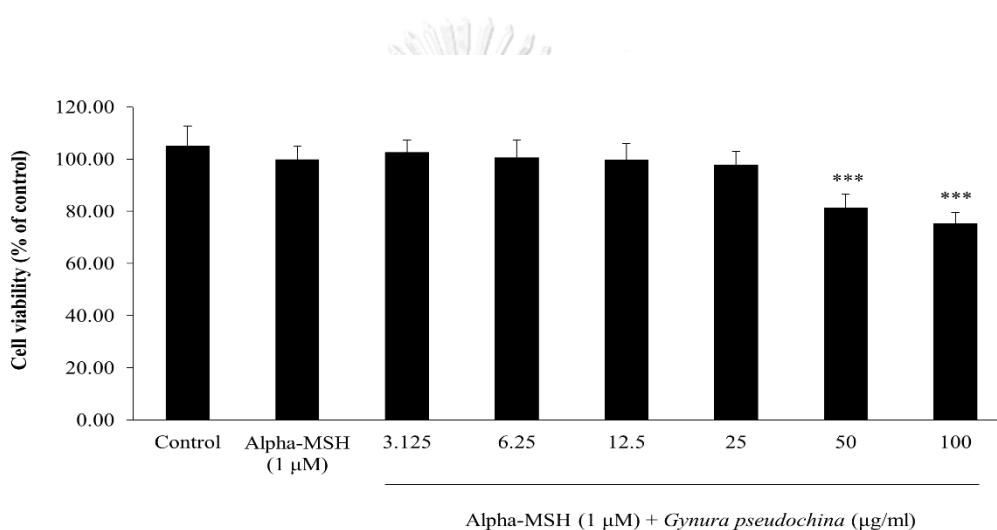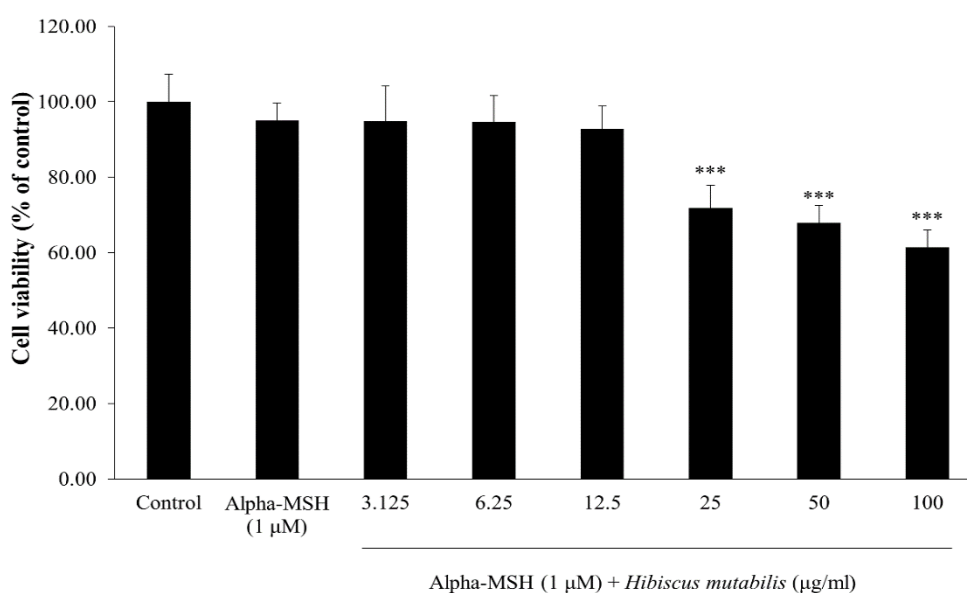

Figure 46. Effect of *Croton roxburghii* on cell viability of B16F10 cells using MTT assay. B16F10 cells were incubated for 48 h in the presence of *Croton roxburghii* at different concentrations. Each percentage values for treated cells is reported relative to that of control group. Data are the mean ± SEM from three independent experiments. ***P<0.001: statistically significant vs Alpha-MSH group.

3.1.5.1.3 Effect of ethanol fraction from *Croton sublyratus* Kurz on cell viability

        To evaluate the cytotoxic effect of ethanol extract from *Croton sublyratus* on alpha-MSH-stimulated B16F10 cells, MTT was used to investigate the effect of *Croton sublyratus* on cell viability. As shown in Figure 47, at the test concentration of 200 µg/ml reduced cell viability significantly. However, *Croton sublyratus* at the range 3.125-100 µg/ml had no cytotoxic effect on B16F10 cells. The highest concentration at 100 µg/ml were chosen for further experiment.
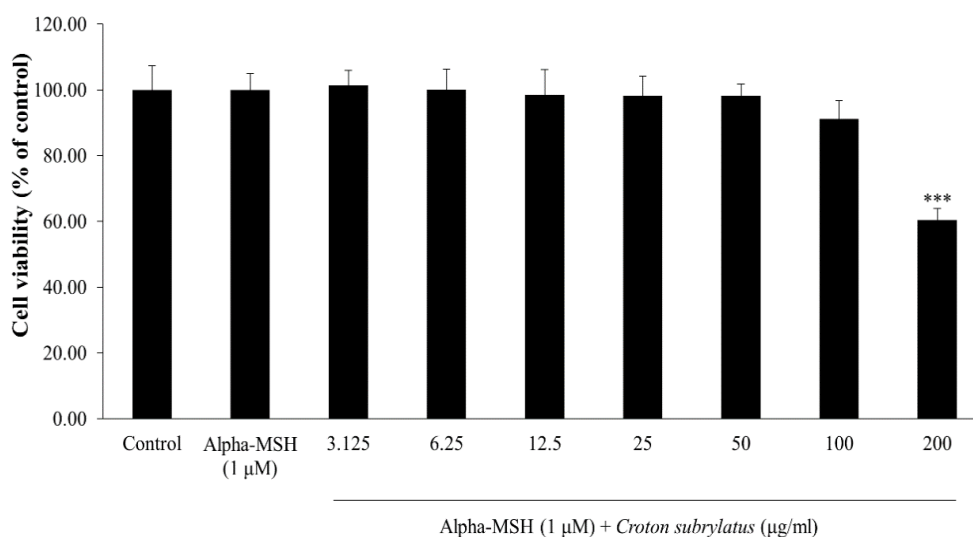
Figure 47. Effect of *Croton sublyratus* on cell viability of B16F10 cells using MTT assay. B16F10 cells were incubated for 48 h in the presence of *Croton sublyratus* at different concentrations. Each percentage values for treated cells is reported relative to that of control group. Data are the mean ± SEM from three independent experiments. ***P<0.001: statistically significant vs Alpha-MSH group.

3.1.5.1.4 Effect of ethanol fraction from *Datura metel* on cell viability

We tested the cytotoxic effect of ethanol fraction from *Datura metel* on alpha-MSH-treated B16F10 cells. As shown in Figure 48, all concentrations in range from 3.125 to 100 μg/ml reduced the cell viability significantly when compared to alpha-MSH group. These results showed that the *Datura metel* extract had the cytotoxic effect in B16F10 cells. So we did not use this extract for next experiment.

Figure 48. Effect of *Datura metel* on cell viability of B16F10 cells using MTT assay. B16F10 cells were incubated for 48 h in the presence of *Datura metel* at different concentrations. Each percentage values for treated cells is reported relative to that of control group. Data are the mean ± SEM from three independent experiments. **P<0.01, ***P<0.001: statistically significant vs Alpha-MSH group.

3.1.5.1.5 Effect of ethanol fraction from *Garcinia mangostana* on cell viability

Results of cytotoxic evaluation against B16F10 cells of *Garcinia mangostana* extract were shown in Figure 49. The ethanol extract of *Garcinia mangostana* exhibited significant activity against B16F10 cell at all concentrations (3.125-100 µg/ml) compared with alpha-MSH group. We did not use this plant for further experiment.
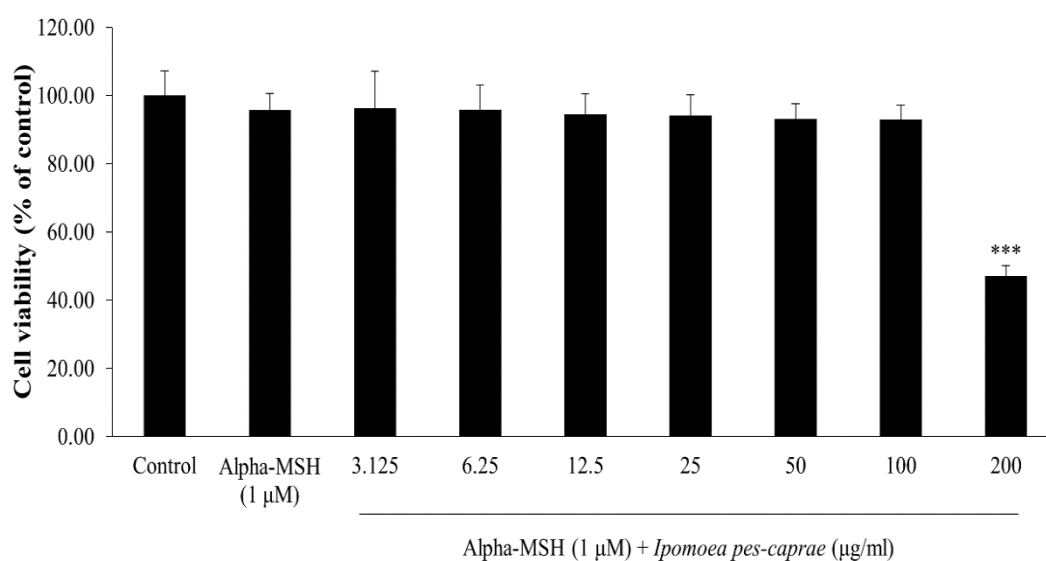

Figure 49. Effect of *Garcinia mangostana* on cell viability of B16F10 cells using MTT assay. B16F10 cells were incubated for 48 h in the presence of *Garcinia mangostana* at various concentrations. Each percentage values for treated cells is reported relative to that of control group. Data are the mean ± SEM from three independent experiments. ***P<0.001: statistically significant vs Alpha-MSH group.

3.1.5.1.6 Effect of ethanol fraction from *Gynura pseudochina* on cell viability

Cytotoxic activity of ethanol extract from *Gynura pseudochina* was carried out against B16F10 cells at different concentrations including 3.125-100 µg/ml and graphically represented in Figure 50. The results showed that *Gynura pseudochina* extract had a significant effect on B16F10 cell at the concentration of 50 and 100 µg/ml when compared with alpha-MSH group. However, at concertation range between 3.125-25 µg/ml had no growth inhibition. We selected the highest dose of *Gynura pseudochina* (25 µg/ml) for other experiments.
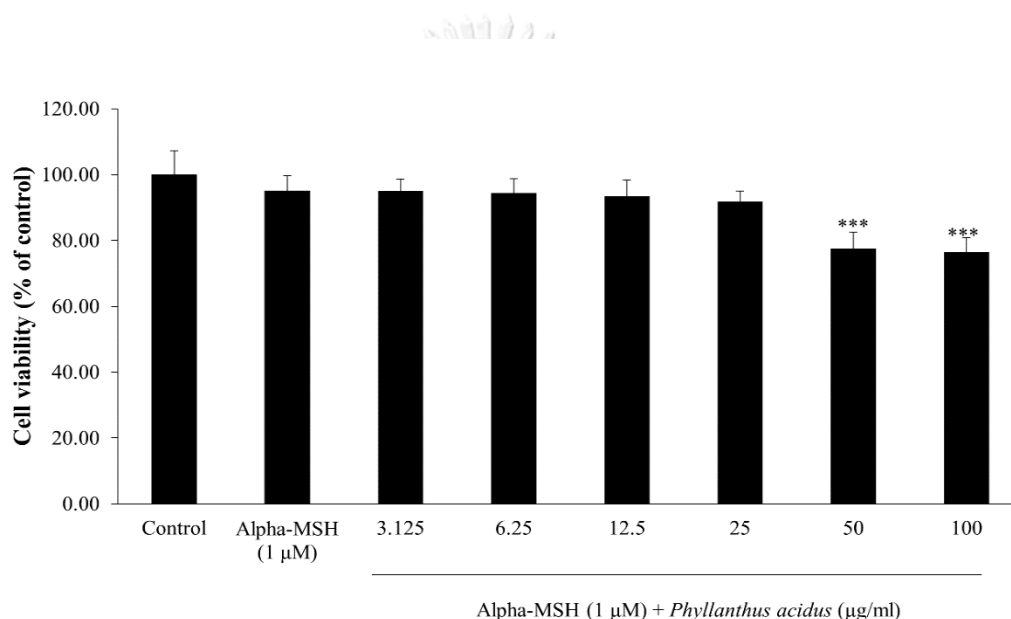

Figure 50. Effect of *Gynura pseudochina* on cell viability of B16F10 cells using MTT assay. B16F10 cells were incubated for 48 h in the presence of *Gynura pseudochina* at various concentrations. Each percentage values for treated cells is reported relative to that of control group. Data are the mean ± SEM from three independent experiments. ***$P<0.001$: statistically significant vs Alpha-MSH group.

3.1.5.1.7 Effect of ethanol fraction from *Hibiscus mutabilis* on cell viability

Cytotoxic effect of ethanol fraction from *Hibiscus mutabilis* at different concentration was determined by MTT assay. As shown in Figure 51, the results showed that at the dose of 25-100 µg/ml reduced viable cell significantly when compared with alpha-MSH group. Whereas, *Hibiscus mutabilis* in concentration range from 3.125 to 12.5 µg/ml did not show cytotoxic activity in B16F10 cells. So, I selected ethanol extract of *Hibiscus mutabilis* at 12.5 µg/ml for further experiment.
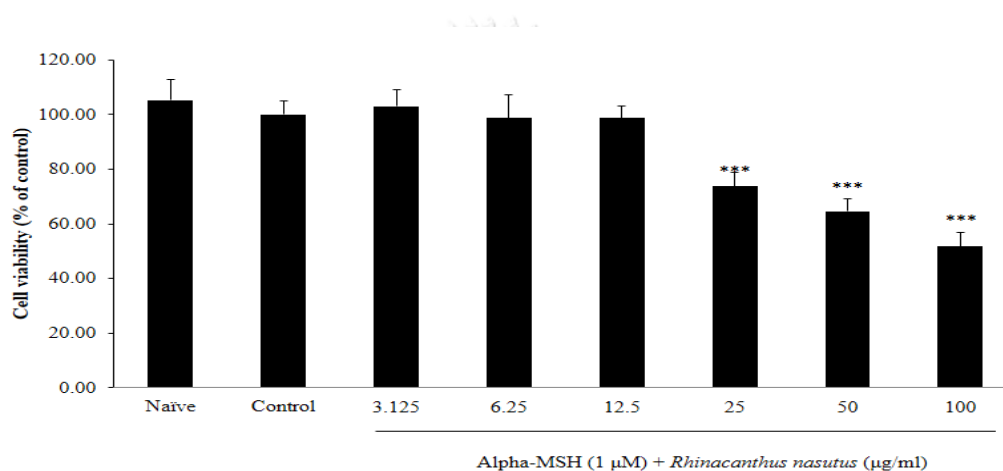

Figure 51. Effect of *Hibiscus mutabilis* on cell viability of B16F10 cells using MTT assay. B16F10 cells were incubated for 48 h in the presence of *Hibiscus mutabilis* at various concentrations. Each percentage values for treated cells is reported relative to that of control group. Data are the mean ± SEM from three independent experiments. ***P<0.001: statistically significant vs Alpha-MSH group.

3.1.5.1.8 Effect of ethanol fraction from *Ipomoea pes-caprae* on cell viability

We determined the effect of ethanol extract of *Ipomoea pes-caprae* at seven different concentrations in B16F10 cells for 48 h. This extract had toxic effect significantly in B16F10 cells at the concentration of 200 µg/ml when compared with alpha-MSH group. However, there were six concentrations (3.125-100 µg/ml) of this extract which had no cytotoxic effect in the cells (Figure 52). So, we used the concentration at 100 µg/ml of *Ipomoea pes-caprae* for further experiment.
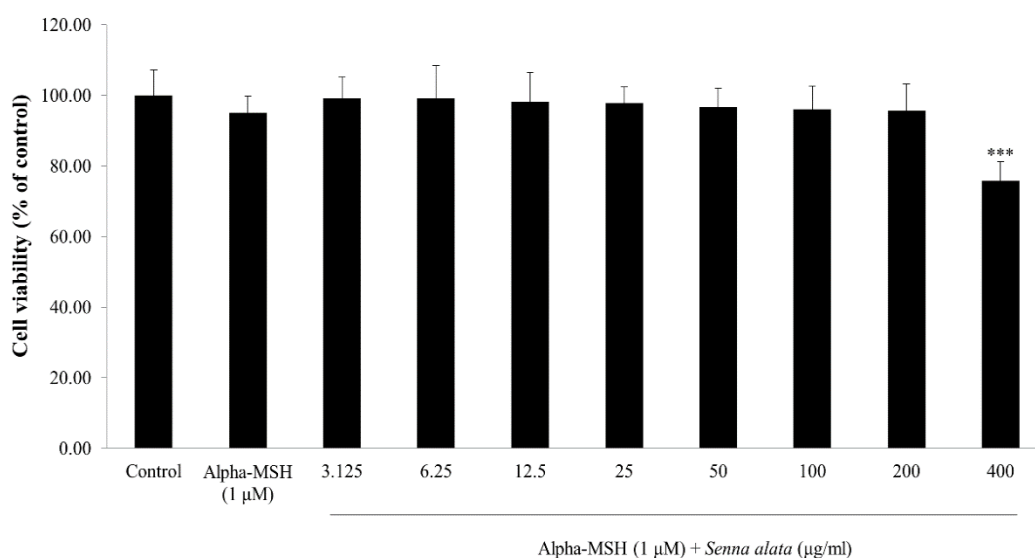

Figure 52. Effect of *Ipomoea pes-caprae* on cell viability of B16F10 cells using MTT assay. B16F10 cells were incubated for 48 h in the presence of *Ipomoea pes-caprae* at various concentrations. Each percentage values for treated cells is reported relative to that of control group. Data are the mean ± SEM from three independent experiments. ***P<0.001: statistically significant vs Alpha-MSH group.

3.1.5.1.9 Effect of ethanol fraction from *Phyllanthus acidus* on cell viability

The cytotoxic effect was carried out for ethanol extract of *Phyllanthus acidus*. This extract were screened for its cytotoxic effect in B16F10 cells. Results are represented in Figure 53. At the high concentrations of the extract (50 and 100 μg/ml) showed significantly cytotoxic effect in the cells when compared with alpha-MSH group. But the concentration of 3.125-25 μg/ml had no cytotoxic effect in the cells. So, the concentration at 25 μg/ml of *Phyllanthus acidus* was selected for melanin content and cellular tyrosinase activity assay.
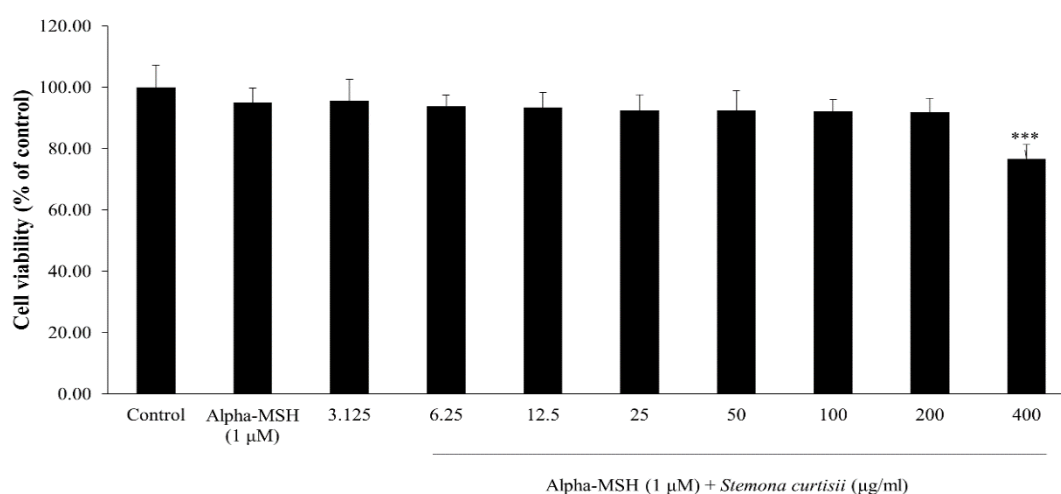

Figure 53. Effect of *Phyllanthus acidus* on cell viability of B16F10 cells using MTT assay. B16F10 cells were incubated for 48 h in the presence of *Phyllanthus acidus* at various concentrations. Each percentage values for treated cells is reported relative to that of control group. Data are the mean ± SEM from three independent experiments. ***$P<0.001$: statistically significant vs Alpha-MSH group.

3.1.5.1.10 Effect of ethanol fraction from *Rhinacanthus nasutus* on cell viability

         B16F10 were treated with different concentrations of ethanol fraction from *Rhinacanthus nasutus* for 48 h. As shown in Figure 54, the results exhibited the cytotoxic effect of this extract in concentration range of 25-100 µg/ml. Three concentrations of *Rhinacanthus nasutus* (3.125, 6.25 and 12.5 µg/ml) did not show toxic effect in B16F10 cellls when compared with alpha-MSH group. We used the concentration at 25 µg/ml of *Rhinacanthus nasutus* extract for further experiments.
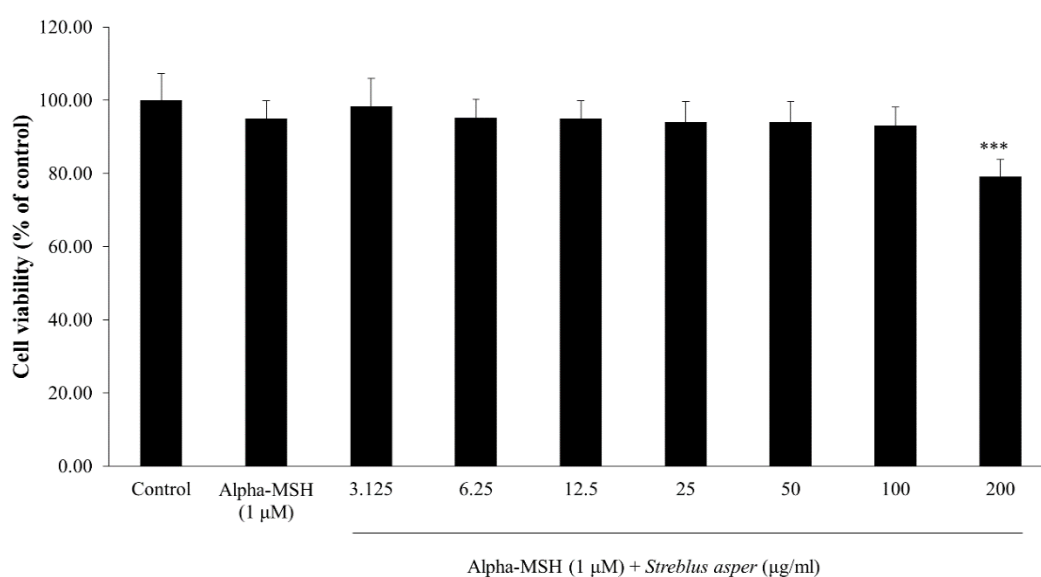

Figure 54. Effect of *Rhinacanthus nasutus* on cell viability of B16F10 cells using MTT assay. B16F10 cells were incubated for 48 h in the presence of *Rhinacanthus nasutus* at various concentrations. Each percentage values for treated cells is reported relative to that of control group. Data are the mean ± SEM from three independent experiments. ***$P<0.001$: statistically significant vs Alpha-MSH group.

3.1.5.1.11 Effect of ethanol fraction from *Senna alata* on cell viability

Toxic effect of ethanol fraction from *Senna alata* was tested by MTT assay. B16F10 cells were treated with eight concentrations of *Senna alata* for 48 h. The results showed that only one concentration (400 µg/ml) decreased viable cells significantly as compared with alpha-MSH group. While, other concentrations (3.125 to 200 µg/ml) had no cytotoxic effect in B16F10 cells. So, we selected at dose of 400 µg/ml for next experiment (Figure 55).

Figure 55. Effect of *Senna alata* on cell viability of B16F10 cells using MTT assay. B16F10 cells were incubated for 48 h in the presence of *Senna alata* at various concentrations. Each percentage values for treated cells is reported relative to that of control group. Data are the mean ± SEM from three independent experiments. ***P<0.001: statistically significant vs Alpha-MSH group.

3.1.5.1.12 Effect of ethanol fraction from *Stemona curtisii* on cell viability

MTT assay was used to determine the concentration which had no toxic effect in B16F10 cells. As shown in Figure 56, we tested different concentrations of *Stemona curtisii* including 3.125, 6.25, 12.5, 25, 50, 100, 200 and 400 µg/ml in alpha-MSH induced B16F10 cells. The highest dose (400 µg/ml) reduced cell viability significantly as compared with alpha-MSH group. So, the concentrations of 200 µg/ml was chosen for subsequent procedures.

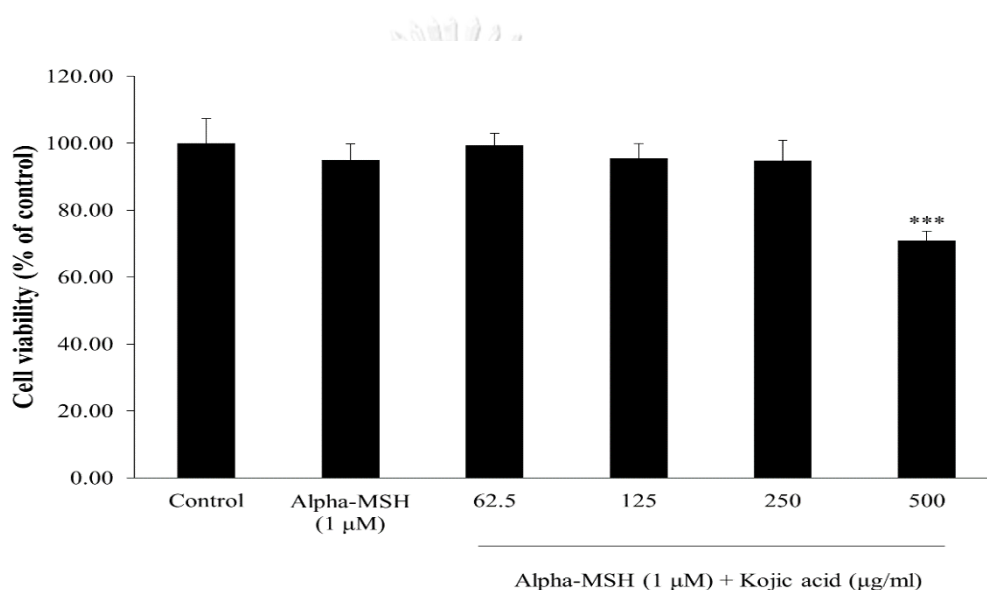Figure 56. Effect of *Stemona curtisii* on cell viability of B16F10 cells using MTT assay. B16F10 cells were incubated for 48 h in the presence of *Stemona curtisii* at various concentrations. Each percentage values for treated cells is reported relative to that of control group. Data are the mean ± SEM from three independent experiments. ***P<0.001: statistically significant vs Alpha-MSH group.

3.1.5.1.13 Effect of ethanol fraction from *Streblus asper* on cell viability

We examined the ethanol fraction from *Streblus asper* for toxicity in B16F10 cells by MTT assay with different concentrations. As shown in Figure 57, *Streblus asper* was significantly cytotoxic to B16F10 cells at concentration of 200 µg/ml when compared to alpha-MSH group. However, other concentrations (3.125-100 µg/ml) was not toxic in the cells. So, we used 100 µg/ml of *Streblus asper* extract for other experiments.

Figure 57. Effect of *Streblus asper* on cell viability of B16F10 cells using MTT assay. B16F10 cells were incubated for 48 h in the presence of *Streblus asper* at various concentrations. Each percentage values for treated cells is reported relative to that of control group. Data are the mean ± SEM from three independent experiments. ***$P < 0.001$: statistically significant vs Alpha-MSH group.

3.1.5.1.14 Effect of kojic acid on cell viability

Kojic acid is known as whitening agent or melasma treatment. We used kojic acid as a positive control. Four concentration of kojic acid was determined by MTT assay. As shown in Figure 58, there was a significant reduction in cell viability after treatment with kojic acid at 500 µg/ml when compared to alpha-MSH group. But other concentrations (62.5, 125, 250 µg/ml) did not show cytotoxic effect in B16F10 cells. We used kojic acid at the dose of 250 µg/ml for melanin content and cellular tyrosinase activity assay.

Figure 58. Effect of kojic acid on cell viability of B16F10 cells using MTT assay. B16F10 cells were incubated for 48 h in the presence of kojic acid at various concentrations. Each percentage values for treated cells is reported relative to that of control group. Data are the mean ± SEM from three independent experiments. ***P<0.001: statistically significant vs Alpha-MSH group.

3.1.5.2 Effect of alpha-MSH and plant extracts on cellular melanin content

We used the highest concentration of ethanol extracts which was not toxic to B16F10 cells by MTT assay. To determine the ability of selected plant extracts on alpha-MSH mediated melanogenesis, examined the quantity of melanin content in the presence of alpha-MSH. In this assay, the cells were stimulated with alpha-MSH at 1 µM and incubated with each plant extract for 48 h. Kojic acid served as positive control for inhibiting melanin content in the cells. While control cells were not treated with alpha-MSH or plant extracts. We calculated the melanin content from standard curve of synthetic melanin and compared against alpha-MSH-treated cells. As shown in figure 59, alpha-MSH group have melanin content more than the control cells about 2.5 fold of control cells. Kojic acid at 250 µg/ml markly decreased melanin content when compared with alpha-MSH group. Whereas, four plant extracts including *Croton roxburghii*, *Croton sublyratus*, *Phylllanthus acidus,* and *Rhinacanthus nasutus*, significantly reduced melanin production by 118.28%, 147.98%, 150.21% and 144.21%, respectively. In addition, *Hibiscus mutabilis* and *Stemona curtisii* also significantly inhibited alpha-MSH-stimulated melanin content (P<0.05, P<0.01, respectively). However, melanin content was significantly increased in the cells treated with *Ardisia elliptica*, *Senna alata* and *Streblus asper.* Moreover, *Gynura pseudochina* and *Ipomoea pes-caprae* did not reduce alpha-MSH-induced melanin synthesis. All of these results, we diluted the concentrations of *Croton roxburghii*, *Croton sublyratus*, *Phylllanthus acidus* and *Rhinacanthus nasutus* for determining the effect of different concentrations on alpha-MSH stimulated melanin content. After that, we selected the two concentrations of four plants for next experiment.
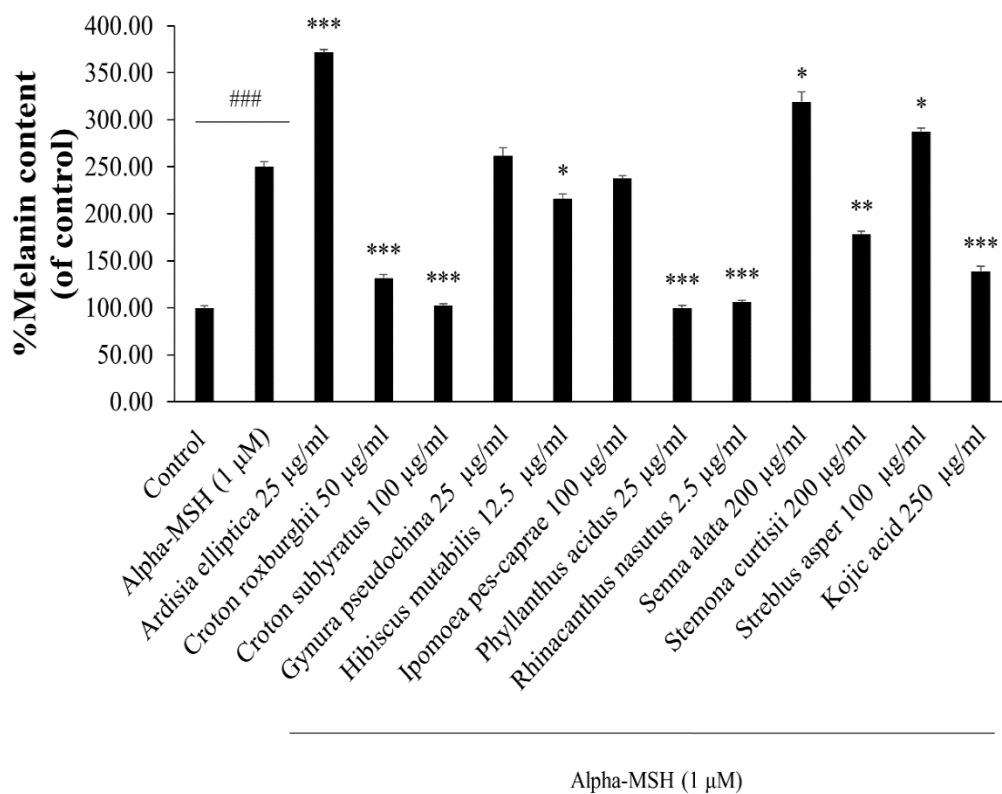
Figure 59. Effect of alpha-MSH and plant extracts on cellular melanin content. B16F10 cells were treated with plant extracts in the presence of 1 µM of alpha-MSH. Kojic acid served as positive control. Each percentage values for treated cells is reported relative to that of control group. Data are the mean ± SEM from three independent experiments. [###]P<0.001: statistically significant vs Control group. *P<0.05, **P<0.01, ***P<0.001: statistically significant vs Alpha-MSH group.

3.1.5.2.1 Effect of *Croton roxburghii* on cellular melanin content

We used *Croton roxburghii* at 6.25, 12.5, 25 and 50 µg/ml in alpha-MSH stimulated B16F10 for 48 h. As show in Figure 60, *Croton roxburghii* at the concentration of 12.5, 25 and 50 µg/ml, significantly inhibited alpha-MSH stimulated melanin production in a dose dependent manner by 30.56%, 65.88% and 118.28%, respectively. However, *Croton roxburghii* at 6.25 µg/ml did not reduce melanin content when compared with alpha-MSH group. So, we chose two concentrations (25 and 50 µg/ml) for the melanogenic proteins by qPCR and Western blot assay.
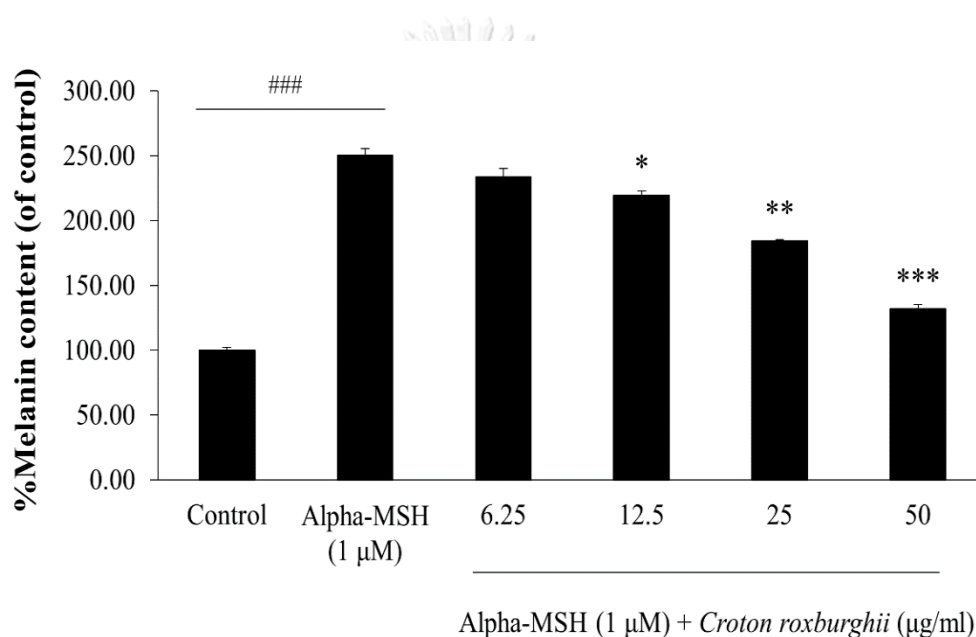
Figure 60. Effect of *Croton roxburghii* on cellular melanin content. B16F10 cells were treated with *Croton roxburghii* in the presence of alpha-MSH (1 µM) for 48 h. Each percentage values for treated cells is reported relative to that of control group. Data are the mean ± SEM from three independent experiments. $^{###}$P<0.001: statistically significant vs Control group. *P<0.05, **P<0.01, ***P<0.001: statistically significant vs Alpha-MSH group.

3.1.5.2.2 Effect of *Croton sublyratus* on cellular melanin content

To determine the effect of *Croton sublyratus* on melanin synthesis, B16F10 cells were exposed to alpha-MSH (1 μM) for 48 h in the presence of *Croton sublyratus* at 12.5, 25, 50 and 100 μg/ml. As shown in Figure 61, the amount of melanin content was significantly decreased in a dose dependent manner when compared to alpha-MSH treated cells. Ethanol extract of *Croton sublyratus* at 50 and 100 μg/ml markly reduced melanin production by 117.35% and 168.45%, respectively. Whereas, at 12.5 and 50 μg/ml of *Croton sublyratus* extract did not suppress melanin production. Therefore, we used 50 and 100 μg/ml for further experiment.
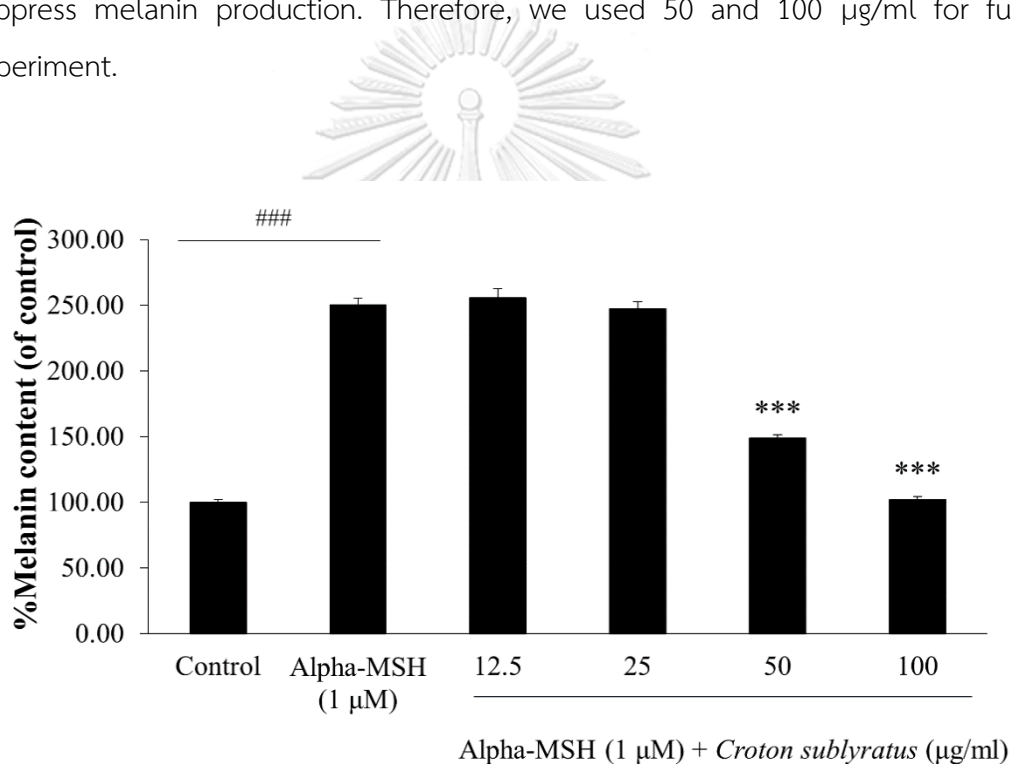
Figure 61. Effect of *Croton sublyratus* on cellular melanin content. B16F10 cells were treated with *Croton sublyratus* in the presence of alpha-MSH (1 μM) for 48 h. Each percentage values for treated cells is reported relative to that of control group. Data are the mean ± SEM from three independent experiments. [###]$P<0.001$: statistically significant vs Control group. ***$P<0.001$: statistically significant vs Alpha-MSH group.

3.1.5.2.3 Effect of *Phyllanthus acidus* on cellular melanin content

To determine the inhibitory effect of *Phyllanthus acidus* on melanin production, B16F10 cells were exposed to alpha-MSH in the presence of different concentration of ethanol extract from *Phyllanthus acidus* leaves. The results indicated that the melanin content was suppressed by two concentrations of *Phyllanthus acidus* when compared with control cells. The residual melanin production was 52.24% and 173.24% of control for 12.5 and 25 µg/ml of *Phyllanthus acidus* extract (Figure 62). Thus, we used these concentration for estimating the effect of *Phyllanthus acidus* on melanogenic proteins.
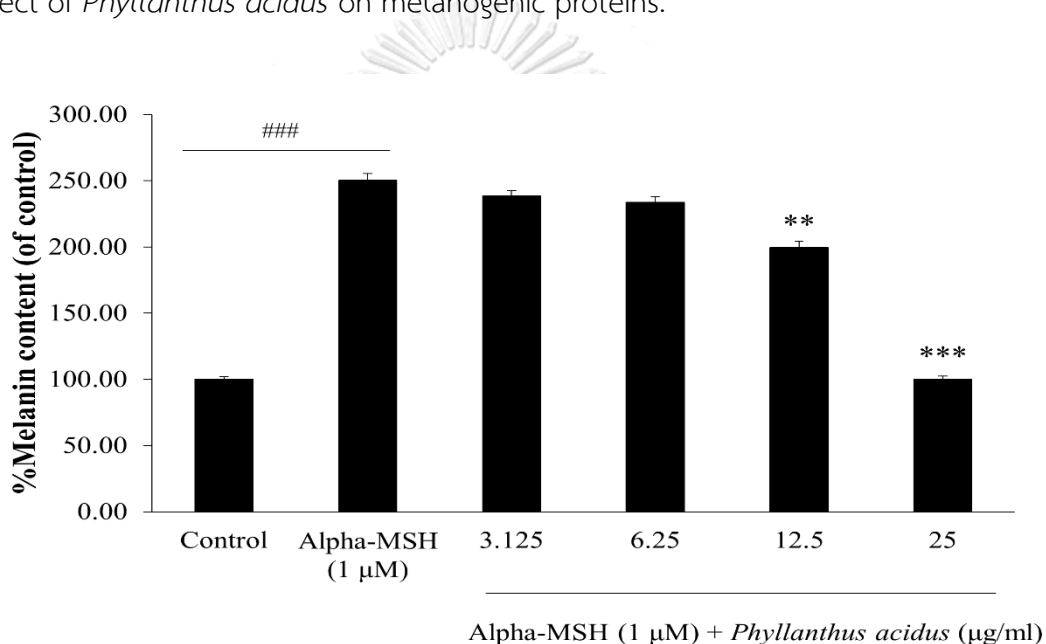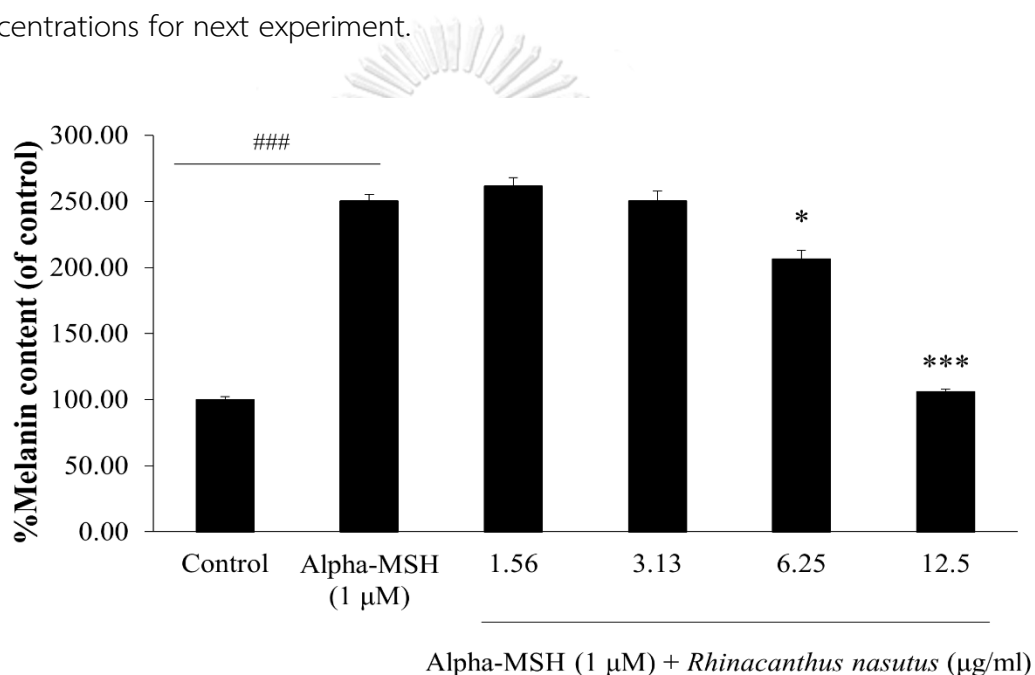

Figure 62. Effect of *Phyllanthus acidus* on cellular melanin content. B16F10 cells were treated with *Phyllanthus acidus* in the presence of alpha-MSH (1 µM) for 48 h. Each percentage values for treated cells is reported relative to that of control group. Data are the mean ± SEM from three independent experiments. $^{###}$P<0.001: statistically significant vs Control group. **P<0.01, ***P<0.001: statistically significant vs Alpha-MSH group.

3.1.5.2.4 Effect of *Rhinacanthus nasutus* on cellular melanin content

Antimelanogenic effect of ethanol extract from *Rhinacanthus nasutus* leaves was determined by the absorbance at 470 nm using ELISA reader. The results showed a concentration-dependent decrease in the melanin content of *Rhinacanthus nasutus*-treated B16F10 cells (Figure 63) *Rhinacanthus nasutus* at 6.25 and 12.5 µg/ml significantly decreased melanin production by 43.92% and 144.21%, respectively. Whereas, there was no significant difference after treatment with *Rhinacanthus nasutus* at 1.5625 and 3.125 µg/ml. So, we used two high concentrations for next experiment.

Figure 63. Effect of *Rhinacanthus nasutus* on cellular melanin content. B16F10 cells were treated with *Rhinacanthus nasutus* in the presence of alpha-MSH (1 µM) for 48 h. Each percentage values for treated cells is reported relative to that of control group. Data are the mean ± SEM from three independent experiments. [###]P<0.001: statistically significant vs Control group. *P<0.05, ***P<0.001: statistically significant vs Alpha-MSH group.

3.1.5.2 Effect of alpha-MSH and plant extracts on cellular tyrosinase activity

We investigated the inhibitory effect of plant extracts on cellular tyrosinase activity. Tyrosinase activity was determined by measuring the rate of L-DOPA oxidation by using a previously described method (248). L-DOPA as a substrate is oxidized to DOPAquinone by tyrosinase. DOPAquinone is further converted to DOPAchrome which is a substrate for eumelanin (7). Kojic served as tyrosinase inhibitor. In our study, we used the highest concentration of each plant extract which was not toxic in B16F10 cells. The cells were stimulated with alpha-MSH (1 µM) in the presence of each plant extracts for 48 h. As Figure 18 indicates, the alpha-MSH treated cells had tyrosinase activity more than control cells about 2.65 fold. Kojic acid significantly reduced cellular tyrosinase activity by 106.71%. Like melanin content assay, four plant extracts including *Croton roxburghii*, *Croton sublyratus*, *Phylllanthus acidus* and *Rhinacanthus nasutus*, significantly suppress cellular tyrosinase activity by 134.38%, 159.33%, 150.35% and 171.84%, respectively (Figure 64) when compared with control cells. In addition, *Hibiscus mutabilis, Ipomoea pes-caprae* and *Streblus asper* also significantly inhibited alpha-MSH-stimulated melanin content. Whereas, *Ardisia elliptica, Senna alata* and *Streblus asper* increased the enzyme activity. Moreover, *Gynura pseudochina* and *Stemona curtisii* did not inhibit tyrosinase activity. All of these results, we diluted the concentrations of *Croton roxburghii*, *Croton sublyratus*, *Phylllanthus acidus* and *Rhinacanthus nasutus* for tyrosinase activity assay. After treatment, we chose two concentration of these plants for mRNA and protein expression of melanogenic genes.
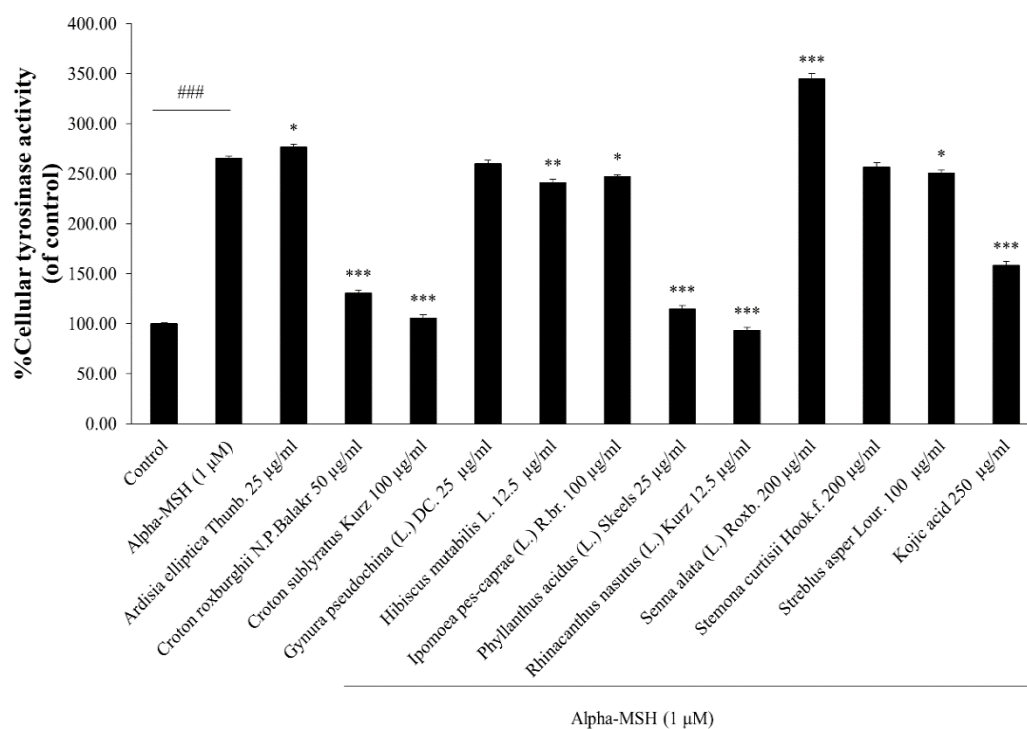
Figure 64. Effect of plant extracts on cellular tyrosinase activity. B16F10 cells were treated with plant extracts in the presence of alpha-MSH (1 µM) for 48 h. Each percentage values for treated cells is reported relative to that of control group. Data are the mean ± SEM from three independent experiments. [###]P<0.001: statistically significant vs Control group. *P<0.05, **P<0.01, ***P<0.001: statistically significant vs Alpha-MSH group.

3.1.5.2.1 Effect of *Croton roxburghii* on cellular tyrosinase activity

To evaluate the anti-tyrosinase activity, B16F10 cells were incubated with ethanol extract of *Croton roxburghii* at 6.25, 12.5, 50 and 100 µg/ml in the presence of alpha MSH (1 µM) for 48 h. As shown in Figure 65, ethanol extract from *Croton roxburghii* reduced cellular tyrosinase activity in a dose-dependent manner. The results indicated that the tyrosinase activity was suppressed by three concentrations of *Croton roxburghii.* The residual enzyme activity was 21.22%, 68.56% and 134.38% of control for 12.5, 25 and 50 µg/ml of *Phyllanthus acidus*. However, dose of 6.25 µg/ml did not have any effect on cellular tyrosinase activity. All of these results showed a dose-response effect similar to the effect of *Croton roxburghii* on melanin content. So, we used the two concentrations for next experiment.
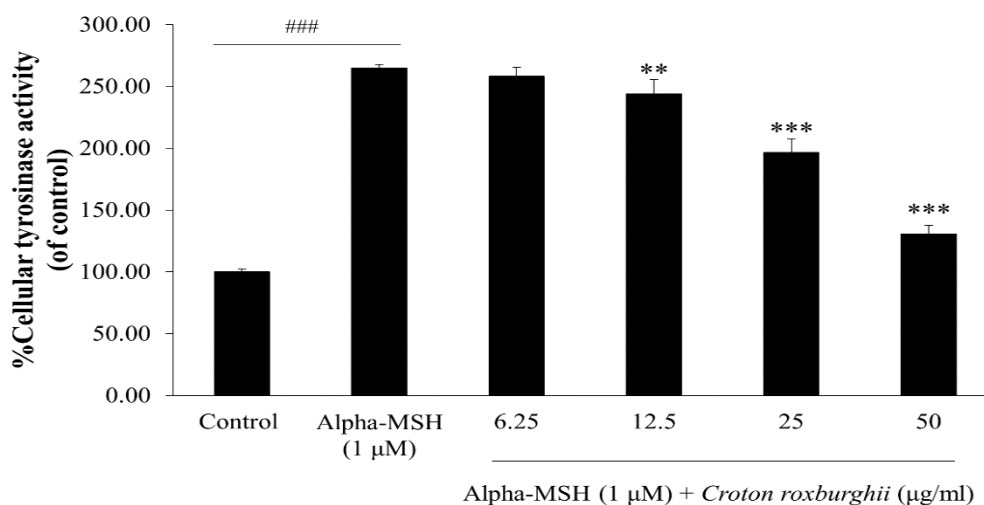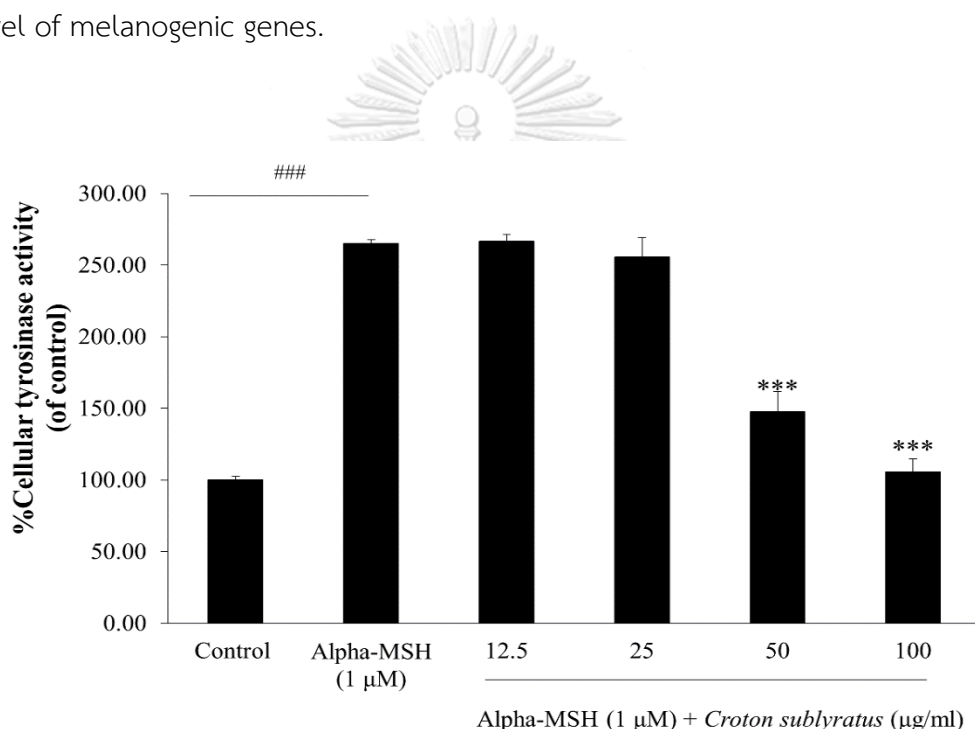

Figure 65. Effect of *Croton roxburghii* on cellular tyrosinase activity. B16F10 cells were treated with *Croton roxburghii* in the presence of alpha-MSH (1 µM) for 48 h. Each percentage values for treated cells is reported relative to that of control group. Data are the mean ± SEM from three independent experiments. [###]P<0.001: statistically significant vs Control group. *P<0.05, **P<0.01, ***P<0.001: statistically significant vs Alpha-MSH group.

3.1.5.2.2 Effect of *Croton sublyratus* on cellular tyrosinase activity

Effect of *Croton sublyratus* on cellular tyrosinase activity in alpha-MSH-stimulated B16F10 cells was investigated. Upon exposure to *Croton sublyratus*, tyrosinase activity of B16F10 cells was significantly reduced in a dose-dependent manner, with 117.16% inhibition at 50 µg/ml and 159.33% inhibition at 100 µg/ml (Figure 66). While, low concentrations (12.5 and 25 µg/ml) did not suppress tyrosinase activity. These results were similar to melanin content assay. So, we used two concentrations for determining the effect of *Croton sublyratus* on mRNA and protein level of melanogenic genes.

Figure 66. Effect of *Croton sublyratus* on cellular tyrosinase activity. B16F10 cells were treated with *Croton sublyratus* in the presence of alpha-MSH (1 µM) for 48 h. Each percentage values for treated cells is reported relative to that of control group. Data are the mean ± SEM from three independent experiments. [###]$P<0.001$: statistically significant vs Control group. ***$P<0.001$: statistically significant vs Alpha-MSH group.

3.1.5.2.3 Effect of *Phyllanthus acidus* on cellular tyrosinase activity

To determine the effect of *Phyllanthus acidus* on cellular tyrosinase activity, B16F10 were treated with four concentrations of *Phyllanthus acidus*. As shown in Figure 67, the ethanol extract of *Phyllantus acidus* significantly inhibited tyrosinase activity in a dose-dependent manner. *Phyllanthus acidus* at 12.5 and 25 µg/ml induced significant inhibition on tyrosinase activity by 57.25% and 150.35%, respectively. However, at dose 3.125 and 6.25 µg/ml did not exhibit anti-tyrosinase activity. So, we chose *Phyllanthus acidus* at the concentration at 12.5 and 25 µg/ml for estimating the effect of this extract on melanogenic gene expression.
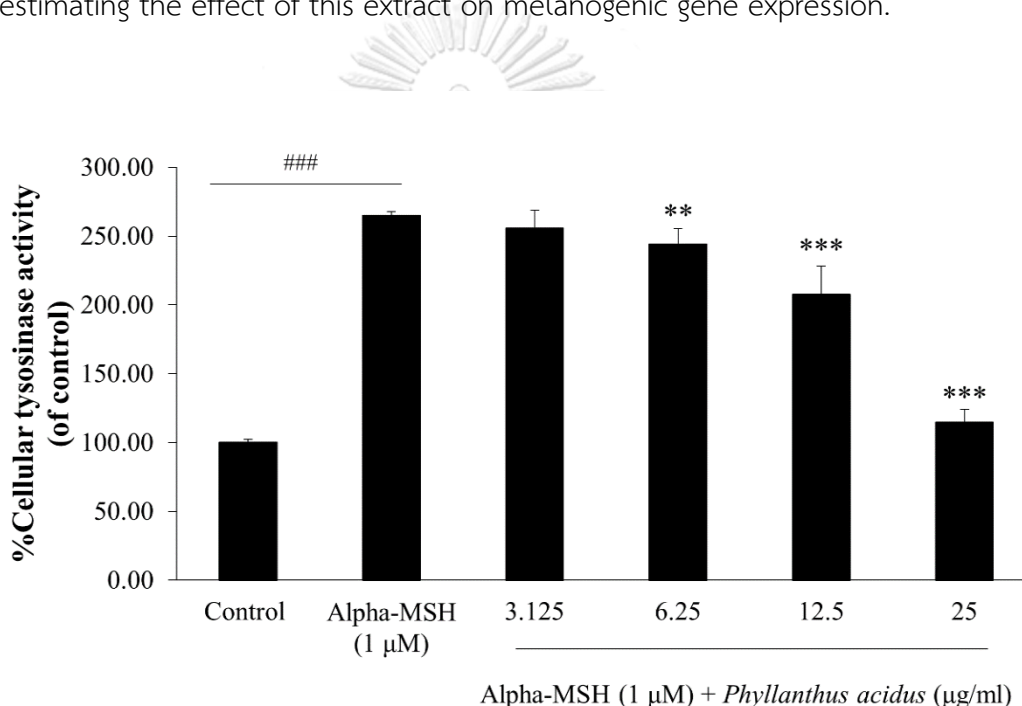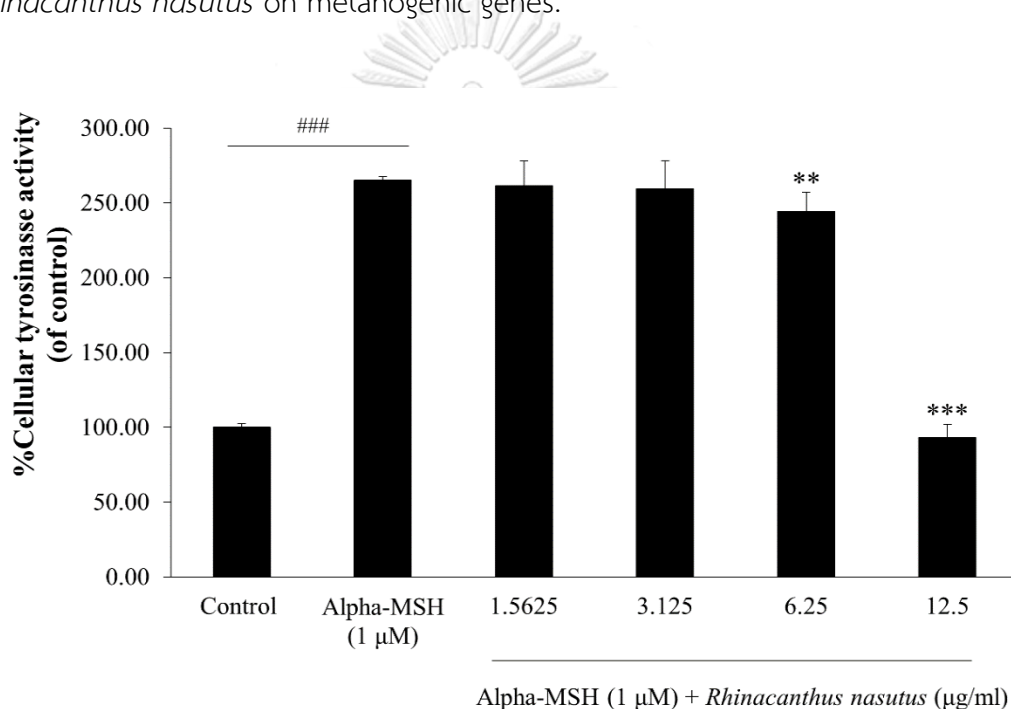

Figure 67. Effect of *Phyllanthus acidus* on cellular tyrosinase activity. B16F10 cells were treated with *Phyllanthus acidus* in the presence of alpha-MSH (1 µM) for 48 h. Each percentage values for treated cells is reported relative to that of control group. Data are the mean ± SEM from three independent experiments. [###]$P<0.001$: statistically significant vs Control group. **$P<0.01$, ***$P<0.001$: statistically significant vs Alpha-MSH group.

3.1.5.2.4 Effect of *Rhinacanthus nasutus* on cellular tyrosinase activity

B16F10 cells were stimulated with alpha-MSH (1 μM) in the presence of ethanol extract of *Rhinacanthus nasutus* at range of 1.5625-12.5 μg/ml. The results showed that *Rhinacanthus nasutus* induced a dose-dependent reduction in tyrosinase activity in B16F10 cells, which was significant at dose of 6.25 and 12.5 μg/ml (Figure 68). While, *Rhinacanthus nasutus* at 1.5625 and 3.25 μg/ml did not diminish tyrosinase activity in alpha-MSH stimulated B16F10 cells. Therefore, we selected at the concentration of 6.25 and 12.5 μg/ml for assessing the effect of *Rhinacanthus nasutus* on melanogenic genes.

Figure 68. Effect of *Rhinacanthus nasutus* on cellular tyrosinase activity. B16F10 cells were treated with *Rhinacanthus nasutus* in the presence of alpha-MSH (1 μM) for 48 h. Each percentage values for treated cells is reported relative to that of control group. Data are the mean ± SEM from three independent experiments. $^{###}$P<0.001: statistically significant vs Control group and **P<0.01, ***P<0.001: statistically significant vs Alpha-MSH group.

3.1.5.3 Effect of ethanol plant extracts on mRNA expression of proteins involved in melanogenesis

To determine the effect of selected plant extracts involved mRNA expression of melanogenic enzymes such as tyrosinase, tyrosinae-related protein 1 (TRP-1) and tyrosinase-related protein 2 (TRP-2) through MITF, we performed realtime PCR analysis. B16F10 cells were treated with alpha-MSH (1 μM) of selected plants. After treatment, RNA was isolated from cell lysates. RNA isolation from sample was reversed into cDNA using reverse transcriptase. The cDNA will be amplified with specific primers using qRT-PCR. Glyceraldehyde 3-phosphate dehydrogenase (GAPDH) served as an internal control.

3.1.5.3.1 Effect of selected ethanol extracts on mRNA level of MITF gene involved in melanogenesis

To access the effect of ethanol extracts from *Croton roxburghii* and *Croton sublyratus* on melanogenesis, we investigated the effect of these extracts on mRNA level of MITF in cells treated with alpha-MSH and these extracts. Figure 69 indicates, the alpha-MSH treated cells showed the increased level of MITF as expected (when compared with control cells). The increase of MITF leads to the up-regulation of melanogenic enzymes such as tyrosinase, tyrosinase-related protein 1 and tyrosinase-related protein 2 (6). Interestingly, *Croton sublyratus* and *Croton roxburghii* showed significantly reduction in the MITF mRNA level at P<0.01. Figure 70 showed MITF mRNA level along with an internal control (GAPDH) after treatment with alpha-MSH in the presence of *Phyllanthus acidus* and *Rhinacanthus nasutus.* MITF mRNA level was also decreased by treatment with *Phyllanthus acidus* and *Rhinacanthus nasutus* extracts. These results suggested that four ethanol extracts from *Croton sublyratus, Phyllanthus acidus, Phyllanthus acidus* and *Rhinacanthus acidus* inhibit alpha-MSH induced melanin synthesis with downregulation of MITF at transcription level.
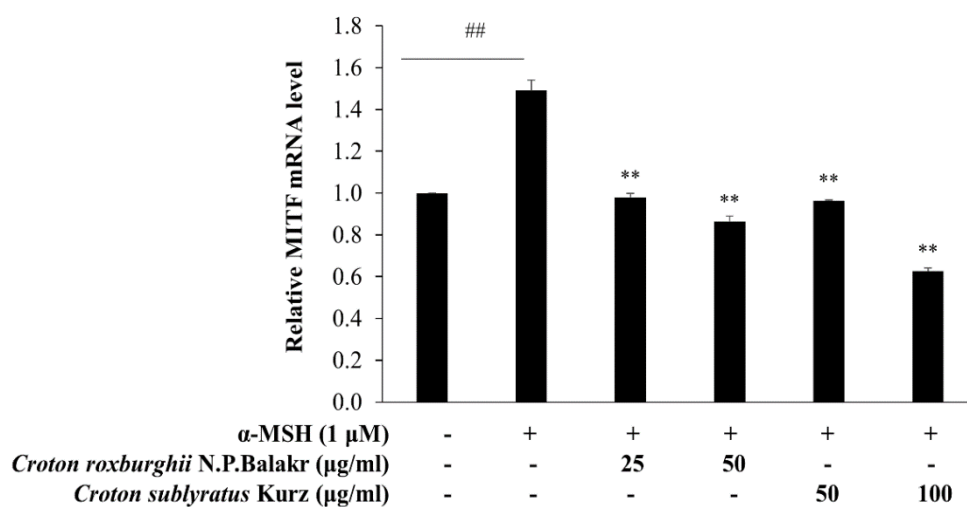
Figure 69. Effect of *Croton roxburghii* and *Croton sublyratus* extracts on mRNA level of MITF gene involved in melanogenesis. Total RNA from B16F10 cells treated with *Croton roxburghii* and *Croton sublyratus* extracts collected at 48 h. MITF mRNA level was examined by qPCR, using GAPDH as an internal control. [###]P<0.001: statistically significant vs Control group and **P<0.01, ***P<0.001 vs Alpha-MSH group.
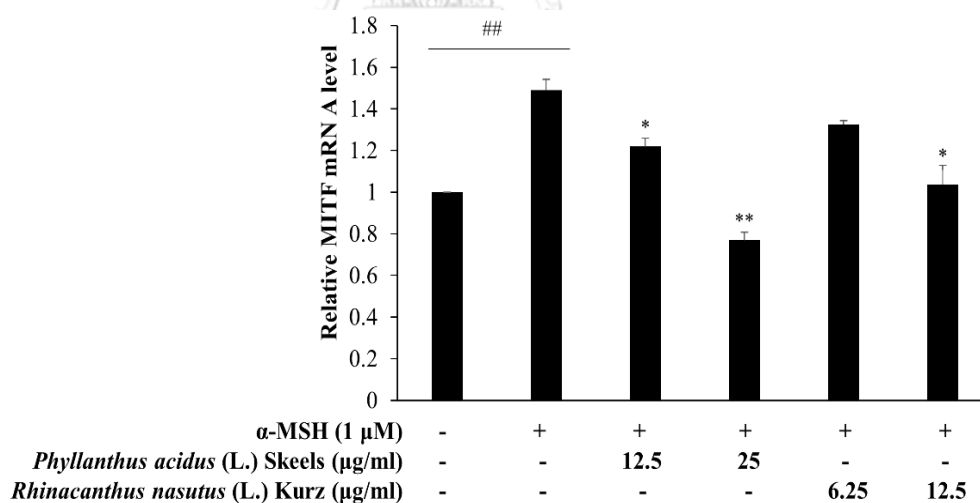

Figure 70. Effect of *Phyllanthus acidus* and *Rhinacanthus nasutus* extracts on mRNA level of MITF gene involved in melanogenesis. Total RNA from B16F10 cells treated with *Phyllanthus acidus* and *Rhinacanthus nasutus* extracts collected at 48 h. MITF mRNA level was examined by qPCR, using GAPDH as an internal control. [###]P<0.001: statistically significant vs Control group and *P<0.05, **P<0.01 vs Alpha-MSH group.

3.1.5.3.2 Effect of selected ethanol extracts on mRNA level of TYR involved in melanogenesis

Melanin biosynthesis requires tyrosinase. The first step of melanin formation is mediated by tyrosinase. This enzyme catalyzes the hydroxylation of L-tyrosine into 3,4-dihidroxyphenylalanine (L-DOPA). Inhibition of this reaction blocks melanin synthesis (9). Subsequently, L-DOPA is oxidized to DOPAquinone by tyrosinase (78). We next investigated whether selected ethanol extracts could reduce tyrosinase (TYR) gene transcription under alpha-MSH stimulation. B16F10 cells were exposed to 1 µM of alpha-MSH in the presence of each plant extract for 48 h. The changes in the level of tyrosinase expression were analyzed by qPCR. As shown in Figure 71, mRNA level of tyrosinase in alpha-MSH induced cells was increased about 1.73 fold. *Croton roxburghii* at 25 and 50 µg/ml effectively reduced alpha-MSH stimulated tyrosinase transcriptional level at $P<0.01$ and $P<0.001$, respectively. Similarly, *Croton sublyratus* at 50 and 100 µg/ml also decreased TYR mRNA level at $P<0.001$. As Figure 72 indicates, *Phyllanthus acidus* at 25 and 50 µg/ml significantly reduced tyrosinase at transcriptional level (at $P<0.01$ and $P<0.001$, orderly). *Rhinnacanthus acidus* at 6.25 and 12.5 µg/ml also suppressed tyrosinase at transcription level when compared with alpha-MSH treated cells. Interestingly, all of these results suggested that four ethanol extracts, including *Croton roxburghii, Croton sublyratus, Phyllanthus acidus Phyllanthus acidus* and *Rhinnacanthus acidus* have the inhibitory effect on tyrosinase at transcriptional level in alpha-MSH stimulated B16F10 cells.
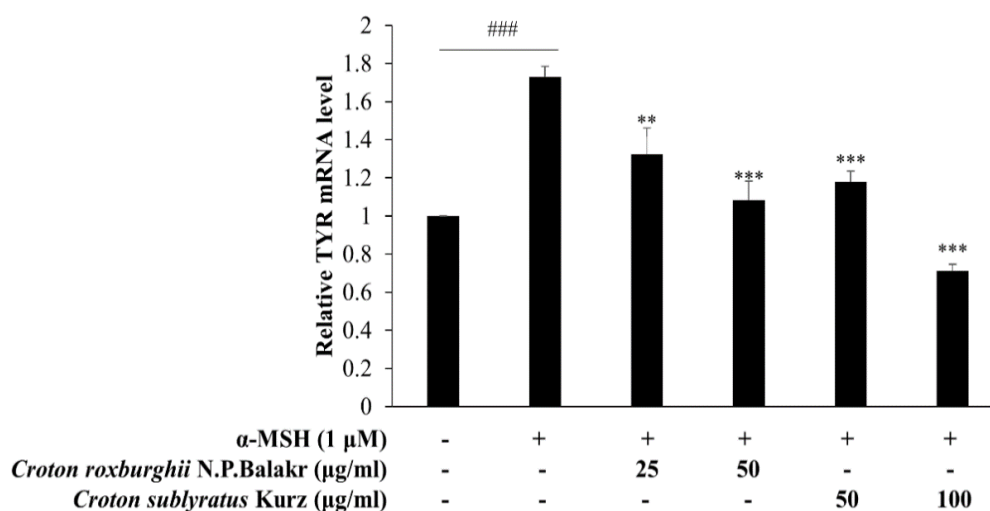
Figure 71. Effect of *Croton roxburghii* and *Croton sublyratus* on mRNA level of TYR gene involved in melanogenesis. Total RNA from B16F10 cells treated with *Croton roxburghii* and *Croton sublyratus* extracts collected at 48 h. TYR mRNA level was examined by qPCR, using GAPDH as an internal control. [###]$P<0.001$: statistically significant vs Control group and *$P<0.05$, **$P<0.01$, ***$P<0.001$ vs Alpha-MSH group.
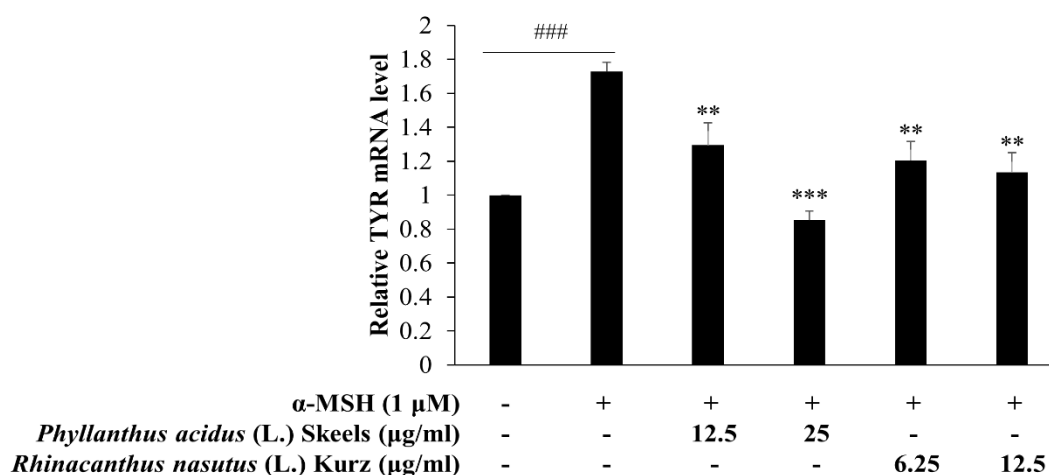

Figure 72. Effect of *Phyllanthus acidus* and *Rhinacanthus nasutus* extracts on mRNA level of TYR gene involved in melanogenesis. Total RNA from B16F10 cells treated with *Phyllanthus acidus* and *Rhinacanthus nasutus* extracts collected at 48 h. TYR mRNA level was examined by qPCR, using GAPDH as an internal control. [###]$P<0.001$: statistically significant vs Control group and *$P<0.05$, *$P<0.01$, ***$P<0.001$ vs Alpha-MSH group.

3.1.5.3.2 Effect of selected ethanol extracts on mRNA level of TRP-1 involved in melanogenesis

Melanin biosynthesis requires tyrosinase-related protein 1 (TRP-1) for eumelanin synthesis. Tyrosinase-realated protein 1 (TRP-1), also known as DHICAoxidase, catalyzes the oxidation of DHICA to indole-5,6-quinone carboxylic acid which can be formed to produce brown, poorly soluble and intermediate molecular weight melanin (7). Therefore, the effect of selected ethanol extracts on mRNA level of TRP-1 gene was investigated in alpha-MSH induced B16F10 cells. The cells were stimulated with alpha-MSH in the presence of selected ethanol extracts for 48 h. We performed qPCR analysis using specific primers for TRP-1. GAPDH served as an internal control. As shown in Figure 73, alpha-MSH group significantly increased mRNA level of TRP-1 when compared with control cells. *Croton roxburghii* at the concentration of 25 and 50 μg/ml significantly decreased TRP-1 mRNA level at $P<0.05$ and $P<0.001$, respectively. Similar to *Croton roxburghii*, there was a reduction of TRP-1 at transcription level by *Croton sublyratus* extracts in a dose dependent manner. Moreover, *Phyllanthus acidus* extract at the concentration of 12.5 and 25 μg/ml markly reduced TRP-1 mRNA level at $P<0.05$ and $P<0.001$. *Rhinacanthus nasutus* extracts at 6.25 and 12.5 μg/ml also suppressed mRNA level of TRP-1 at $P<0.05$ and $P<0.01$, orderly (Figure 74). Similarly, these results suggested that four selected plant extracts including *Croton roxburghii*, *Croton sublyratus*, *Phyllanthus acidus* and *Rhinnacanthus acidus*, down-regulate TRP-1 at transcription level which may lead to reduce melanin synthesis in alpha-MSH induced B16F10 cells.
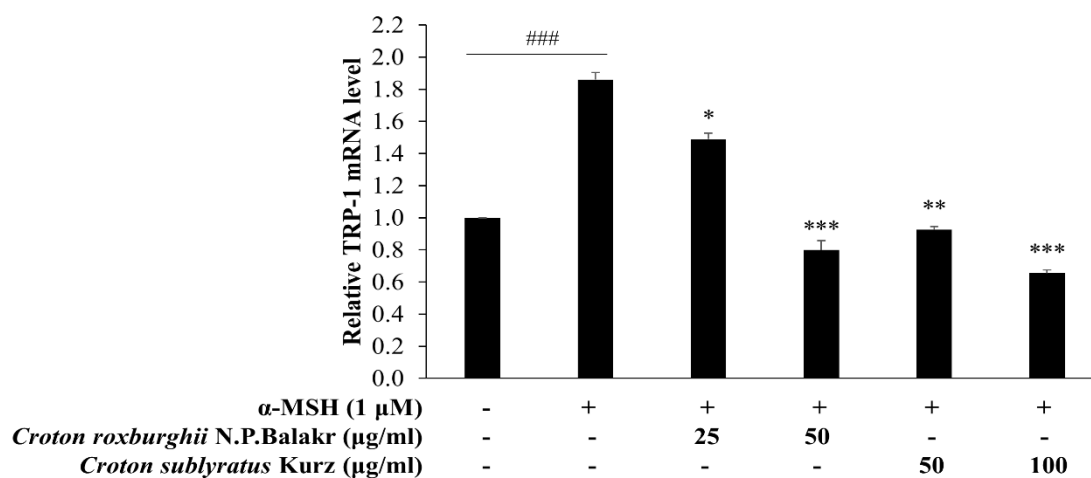
Figure 73. Effect of *Croton roxburghii* and *Croton sublyratus* on mRNA level of TRP-1 gene involved in melanogenesis. Total RNA from B16F10 cells treated with *Croton roxburghii* and *Croton sublyratus* extracts collected at 48 h. TRP-1 mRNA level was examined by qPCR, using GAPDH as an internal control. ###P<0.001: statistically significant vs Control group and **P<0.01, ***P<0.001 vs Alpha-MSH group.
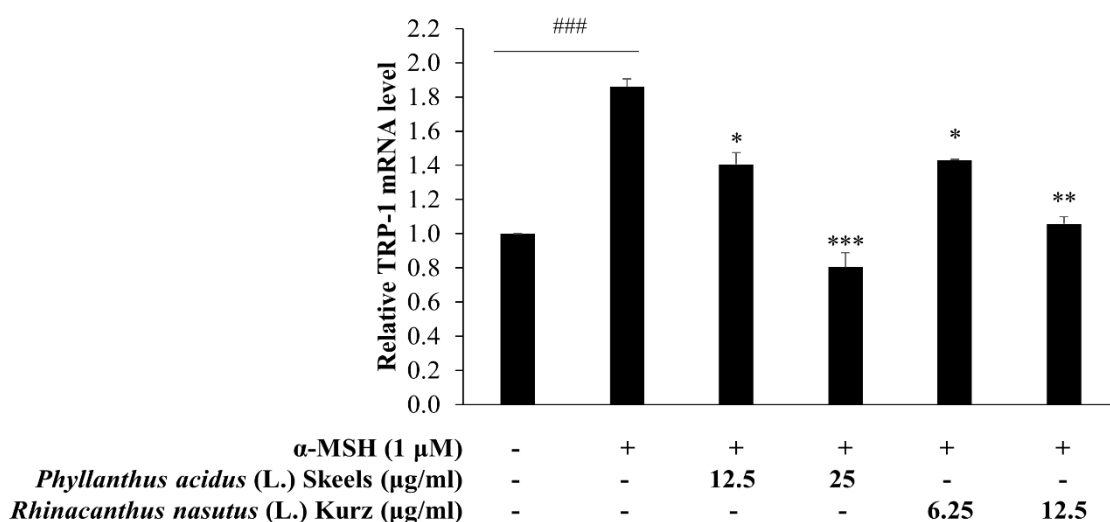

Figure 74. Effect of *Phyllanthus acidus* and *Rhinacanthus nasutus* extracts on mRNA level of TRP-1 gene involved in melanogenesis. Total RNA from B16F10 cells treated with *Phyllanthus acidus* and *Rhinacanthus nasutus* extracts collected at 48 h. TYR mRNA level was examined by qPCR, using GAPDH as an internal control. ###P<0.001: statistically significant vs Control group and *P<0.05, ***P<0.001 vs Alpha-MSH group.

3.1.5.3.2 Effect of selected ethanol extracts on mRNA level of TRP-2 involved in melanogenesis

Tyrosinase-related protein 2 (TRP-2), known as DOPAchrome tautomerase, involves melanin synthesis by tautomerizing DOPAchrome into 5,6-dihydroxyindole-2-carboxylic acid (DHICA). This enzymes is essential for eumelanin synthesis (79). B16F10 cells were stimulated with alpha-MSH (1 µM) in the presence of selected plant extracts for evaluating the effect of plant extract on TRP-2 at transcriptional level. GAPDH was used as internal control for qPCR analysis with specific primers. As shown in Figure 75, the results are expressed as fold change relative to control cells. When the cells were cultured in medium containing alpha-MSH at 48 h, TRP-2 mRNA level in alpha-MSH group were increased when compared with control cells (no treatment). *Croton roxburghii* extracts at the concentration of 25 and 50 µg/ml significantly suppressed TRP-2 mRNA level at P<0.01 and P<0.001. Moreover, two concentrations of *Croton sublyratus* extracts (50 and 100 µg/ml) also markly decreased mRNA level of TRP-2 at P<0.01 and P<0.001, respectively. Similarly, *Phyllanthus acidus* (at 12.5 and 25 µg/ml) and *Rhinacanthus nasutus* (at 6.25 and 12.5 µg/ml) extracts showed the inhibition effect on TRP-2 mRNA level when compared with alpha-MSH stimulated cells (Figure 76). Thus, four selected plant extracts including *Croton roxburghii, Croton sublyratus, Phyllanthus acidus* and *Rhinnacanthus acidus,* decreased TRP-2 at transcription level which may lead to reduce melanin production in alpha-MSH induced B16F10 cells.
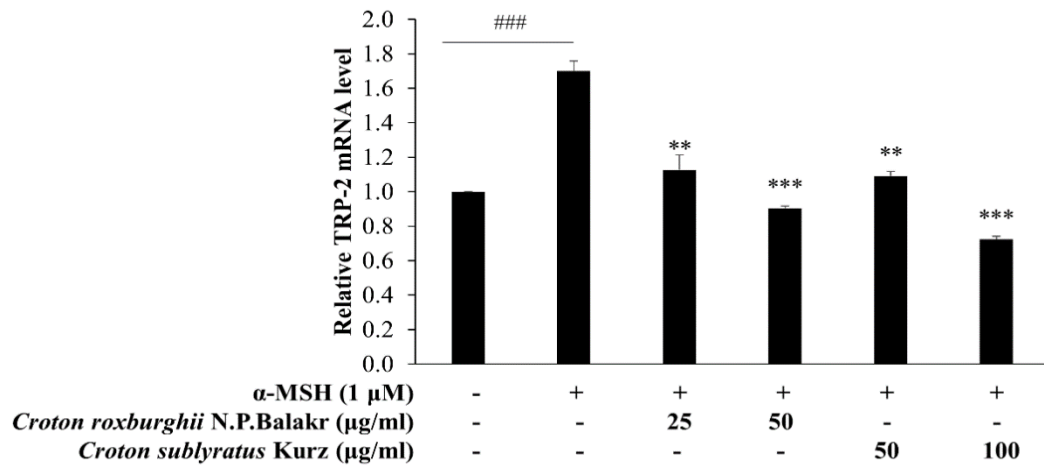
Figure 75. Effect of *Croton roxburghii* and *Croton sublyratus* on mRNA level of TRP-2 involved in melanogenesis. Total RNA from B16F10 cells treated with *Croton roxburghii* and *Croton sublyratus* extracts collected at 48 h. TRP-2 mRNA level was examined by qPCR, using GAPDH as an internal control. ###$P<0.001$: statistically significant vs Control group and **$P<0.01$, ***$P<0.001$ vs Alpha-MSH group.
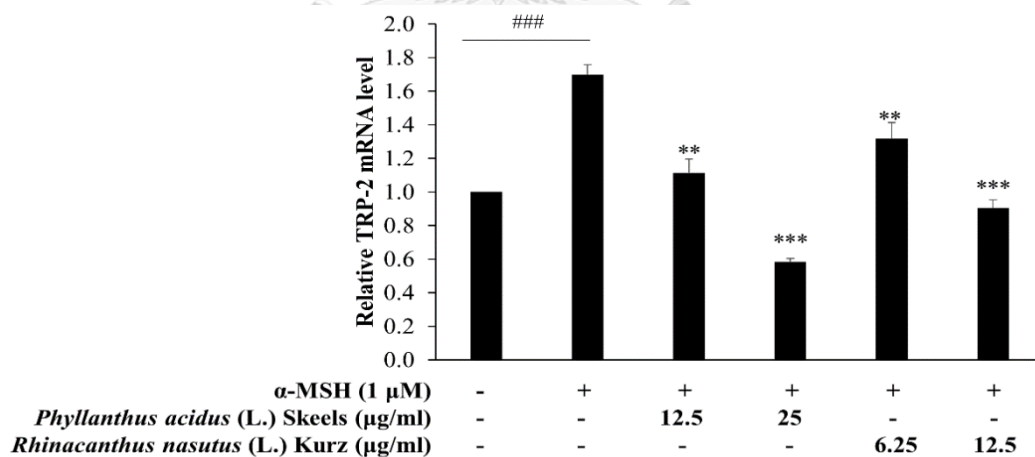

Figure 76. Effect of *Phyllanthus acidus* and *Rhinacanthus nasutus* extracts on mRNA level of TRP-2 gene involved in melanogenesis. Total RNA from B16F10 cells treated with *Phyllanthus acidus* and *Rhinacanthus nasutus* extracts collected at 48 h. TRP-2

mRNA level was examined by qPCR, using GAPDH as an internal control. [###]P<0.001: statistically significant vs Control group and *P<0.05, ***P<0.001 vs Alpha-MSH group.

3.1.5.3 Effect of ethanol plant extracts on expression of melanogenic proteins involved in melanogenesis

Melanin biosynthesis is regulated by tyrosinase gene family, these genes are activated by MITF gene (77). The increase of MITF may lead to the up-regulation of melanogenic enzymes such as tyrosinase, tyrosinase-related protein 1 (TRP-1) and tyrosinase-related protein 2 (TRP-2) (6). To determine the effect of ethanol plant extracts on melanogenic-related proteins, we performed MITF, TYR, TRP-1, and TRP-2 at protein level by Westernblot analysis. B16F10 cells were stimulated with alpha-MSH (1 µM) in the presence of selected four plant extract including *Croton roxburghii*, *Croton sublyratus*, *Phyllanthus acidus* and *Rhinacanthus nasutus* for 48 h. Total proteins were extracted from cell lysate by lysis buffer with protease inhibitor. Target proteins on the membrane were detected by chemiluminescent. GAPDH served as internal control for this method.

3.1.5.3.1 Effect of selected plant extracts on MITF in alpha-MSH induced B16F10 cells

On binding to MC1R, α-MSH from kertinocytes activates adenylate cyclase which upregulates the cAMP level, leading to CREB activation and binding to CRE in Mitf promoter to induce MITF transcription. The increased MITF may lead to up-regulate of pigment enzymes for melanin synthesis (100). We investigated the inhibitory effect of selected plant extracts on MITF which is a transcription factor for melanin synthesis in alpha-MSH induced B16F10 cells. The cells were stimulated with alpha-MSH (1 µM) and treated with selected plant extracts for 48 h. After treatment, cellular proteins were extracted from the cells by lysis buffer. MITF proteins were detected by primary antibodies (1:1000) and then further incubated with anti-rabbit horseradish peroxidase antibody (1:2000). Bound antibodies were detected using an enhanced chemiluminescence kit. Loading control was assessed using anti-GAPDH antibody. As shown in Figure 77, alpha-MSH induced cells increased MITF

overexpression when compare with control cells. We also treated the cells with *Croton roxburghii* at 25 and 50 µg/ml. Figure 77 indicates that two concentrations of *Croton roxburghii* significantly reduced MITF protein when compared with alpha-MSH group. Similarly, *Croton sublyratus* also effectively decreased MITF protein in alpha-MSH induced B16F10 cells. Moreover, ethanol extract of *Rhinacanthus nasutus* at dose of 6.25 and 12.5 µg/ml markly inhibited MITF at protein level (Figure 78). *Phyllanthus acidus* also decreased MITF protein at P<0.05. All of these results, *Croton roxburghii, Croton sublyratus, Phyllanthus acidus* and *Rhinacanthus nasutus* effectively decreased MITF protein which lead to diminish melanin content in alpha-MSH stimulated B16F10 cells
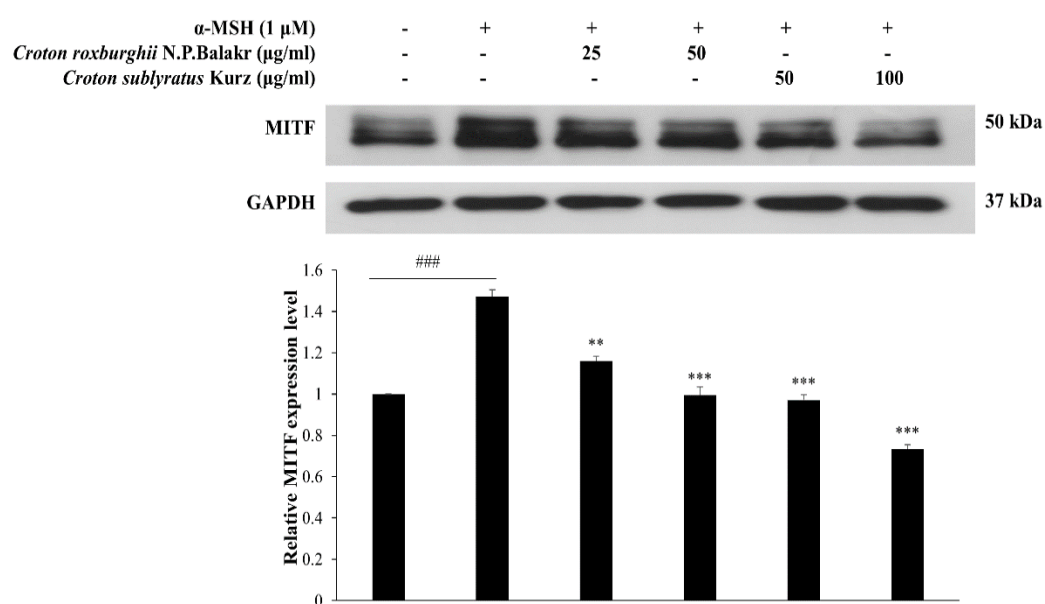

Figure 77. Effect of *Croton roxburghii* and *Croton sublyratus* extracts on protein level of MITF involved in melanogenesis. Total protein from B16F10 cells treated with *Croton roxburghii* and *Croton sublyratus* extracts was collected at 48 h. MITF at protein level was examined by Western Blot analysis, using GAPDH as a loading control. Results are expressed as mean ±SEM from three independent experiments. [###]P<0.001 vs Control cells and **P<0.01, ***P<0.001 vs Alpha-MSH group.
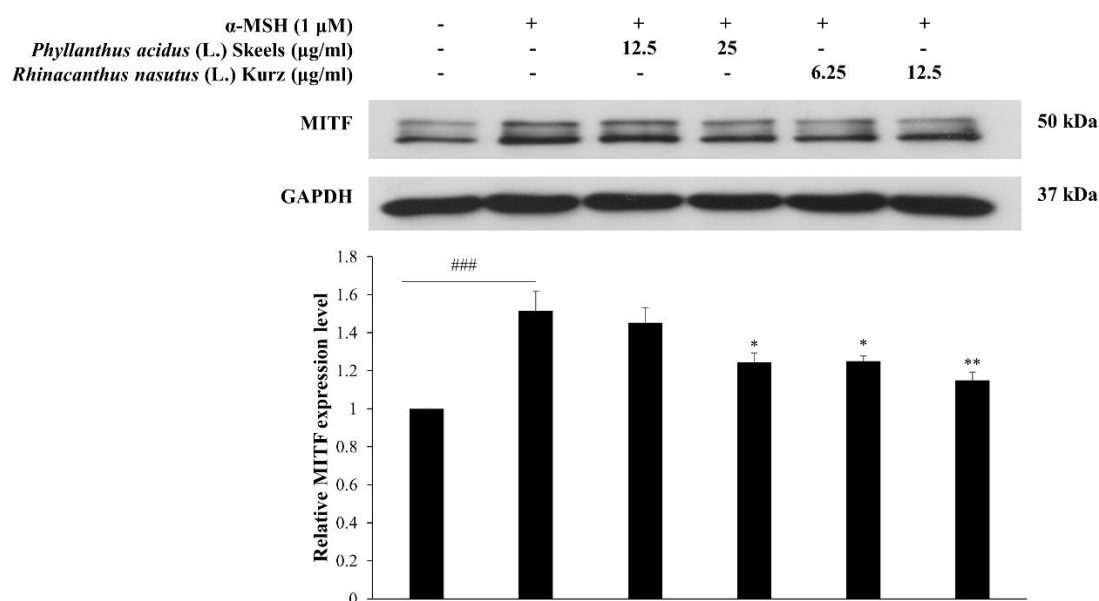
Figure 78. Effect of *Phyllanthus acidus* and *Rhinacanthus nasutus* extracts on protein level of MITF involved in melanogenesis. Total protein from B16F10 cells treated with *Phyllanthus acidus* and *Rhinacanthus nasutus* extracts was collected at 48 h. MITF at protein level was examined by Western Blot analysis, using GAPDH as a loading control. Results are expressed as mean ±SEM from three independent experiments. [###]P<0.001 vs Control cells and *P<0.05, **P<0.01, ***P<0.001 vs Alpha-MSH group.

3.1.5.3.2 Effect of selected plant extracts on TYR in alpha-MSH induced B16F10 cells

We determined the effect of selected plant extracts (ethanol extracts) on TYR at protein level. Tyrosinase is an enzyme which catalyzes the hydroxylation of L-tyrosine into 3,4-dihidroxyphenylalanine (L-DOPA) (7). L-DOPA is further oxidized to DOPAquinone by tyrosinase. After oxidation, DOPAquinone is further converted to DOPAchrome which is a substrate for eumelanin synthesis (78). B16F10 cells were induced with alpha-MSH (1 μM) and then treated with selected plant extracts for 48 h. We extracted total proteins from cell lysate. TYR protein expression were detected by primary antibody (1:2000) and anti-rabbit horseradish peroxidase antibody (1:5000). Bound antibodies were detemined using an enhanced chemiluminescence kit. GAPDH served as a loading control for normalization with TYR. As shown in Figure 79, alpha MSH increased TYR protein expression when compared with control cells which were not treated any agents. We found that *Croton roxburghii* at 25 and 50 μg/ml effectively decreased TYR protein levels in alpha-MSH induced B16F10 cells (Figure 79). Like *Croton roxburghii* extract, *Croton sublyratus* at dose of 50 and 100 μg/ml significantly decreased alpha-MSH induced tyrosinase. Moreover, *Phyllanthus acidus* at 12.5 and 25 μg/ml clearly dimished TYR protein levels when compared with alpha-MSH treated cells (Figure 80). *Rhinacanthus nasutus* extracts also reduced the alpha-MSH induced tyrosinase protein. These results suggest that the inhibitory effect of four ethanol extracts is not directly due to inhibition of melanin content, but rather is mediated by down-regulation of tyrosinase expression at protein levels.
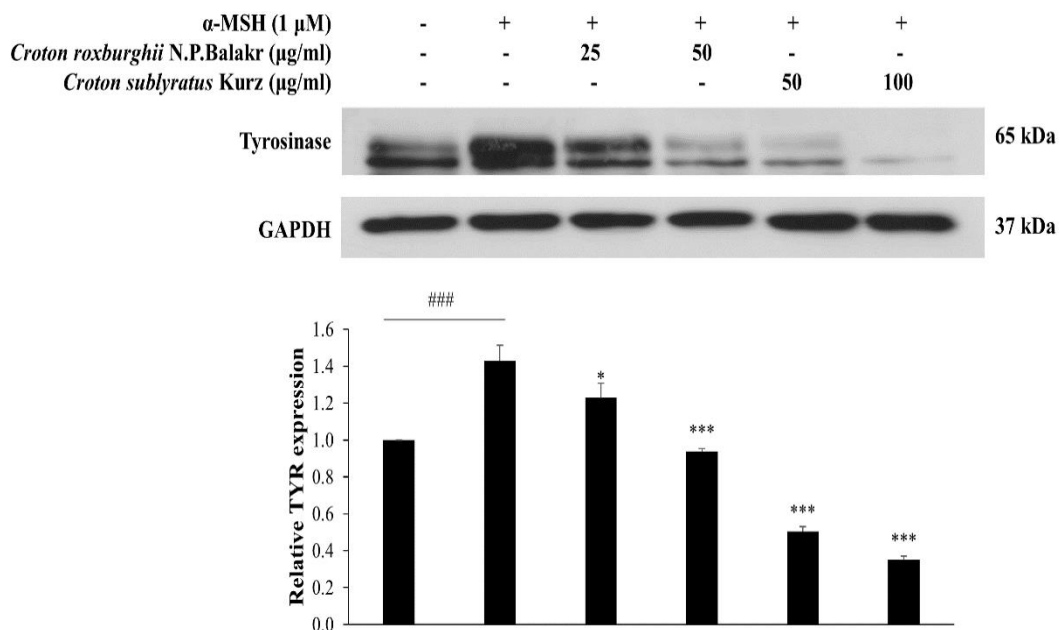
Figure 79. Effect of *Croton roxburghii* and *Croton sublyratus* extracts on protein level of TYR involved in melanogenesis. Total protein from B16F10 cells treated with *Croton roxburghii* and *Croton sublyratus* extracts was collected at 48 h. TYR at protein level was examined by Western Blot analysis, using GAPDH as a loading control. Results are expressed as mean ±SEM from three independent experiments. . [###]P<0.001 vs Control cells and *P<0.05 and ***P<0.001 vs Alpha-MSH group.

Figure 80. Effect of *Phyllanthus acidus* and *Rhinacanthus nasutus* extracts on protein level of TYR involved in melanogenesis. Total protein from B16F10 cells treated with *Phyllanthus acidus* and *Rhinacanthus nasutus* extracts was collected at 48 h. TYR at protein level was examined by Western Blot analysis, using GAPDH as a loading control. Results are expressed as mean ±SEM from three independent experiments. [###]P<0.001 vs Control cells and [***]P<0.001 vs Alpha-MSH group.
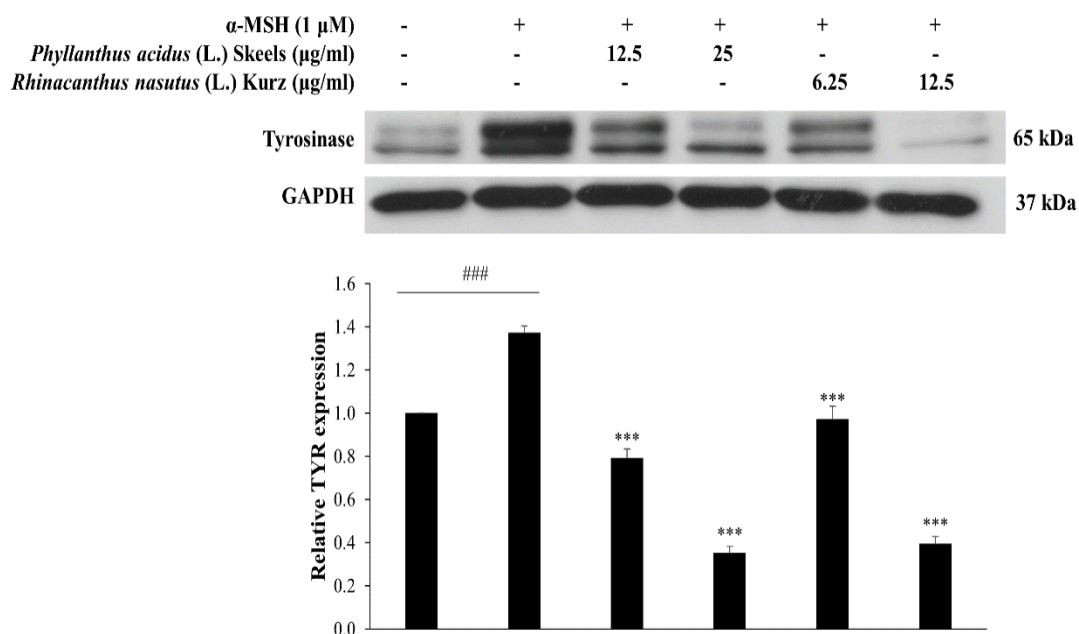
3.1.5.3.3 Effect of selected plant extracts on TRP-1 in alpha-MSH induced B16F10 cells

Tyrosinase-related protein 1 is involved in the regulation of melanognesis through stimulation of MITF (6). TRP-1, also known as DHICAoxidase, catalyzes the oxidation of DHICA to indole-5,6-quinone carboxylic acid which can be formed to produce brown, poorly soluble and intermediate molecular weight melanin (79). To analyze the effect of four plant extracts on TRP-1 expression, B16F10 cells were treated with alpha-MSH (1 µM) in the presence of selected extracts for 48 h. Total protein was extracted from cell lysate. TRP-1 protein expression were detected by primary antibody (1:1000) and anti-mouse horseradish peroxidase antibody (1:2000). GAPDH was used as loading control for normalization to TRP-1. Treatment with alpha-MSH, alpha-MSH group increased TRP-1 proteins when compared with control cells. Upon exposure to *Croton roxburghii*, TRP-1 protein levels were significantly decreased when compared with alpha-MSH cells (Figure 81). Similarly, *Croton sublyratus* at dose of 50 and 100 µg/ml effectively reduced TRP-1 expression at protein level in a dose-dependent manner. The inhibition was dose dependent: *Phyllanthus acidus* at 12.5 and 25 µg/ml induced significantly inhibition on TRP-1 protein expression at $P<0.01$ (Figure 82). *Rhinacanthus nasutus* also reduced TRP-1 protein levels in a dose-dependent manner when compared with alpha-MSH stimulated cells (Figure 82). These results suggest that four selected ethanol extracts, including *Croton roxburghii*, *Croton sublyratus*, *Phyllanthus acidus* and *Rhinacanthus nasutus*, inhibit melanin content that the results may be related to downregulation of alpha-MSH induced TRP-1 protein expression.
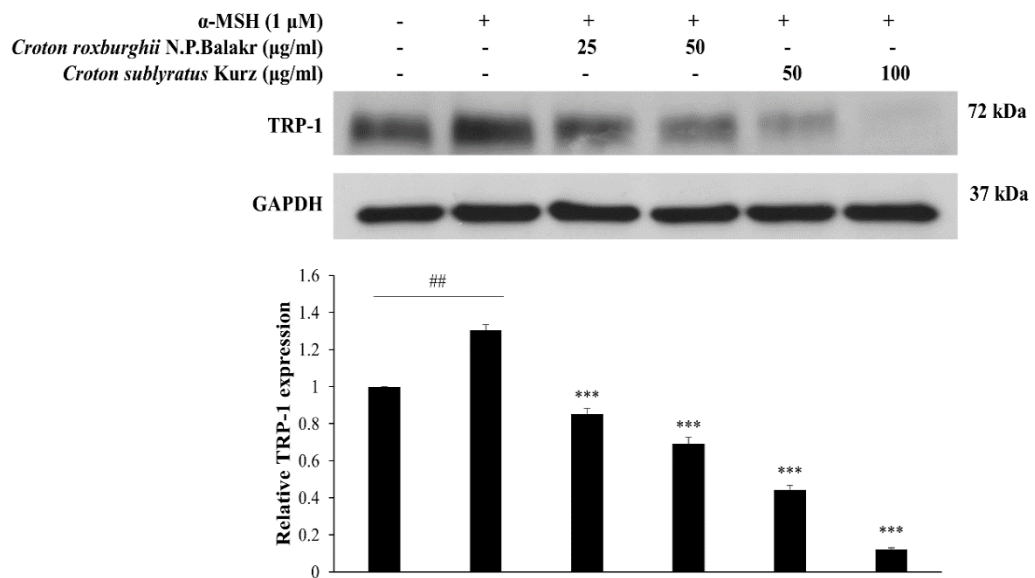
Figure 81. Effect of *Croton roxburghii* and *Croton sublyratus* extracts on protein level of TRP-1 involved in melanogenesis. Total protein from B16F10 cells treated with *Croton roxburghii* and *Croton sublyratus* extracts was collected at 48 h. TRP-1 at protein level was examined by Western Blot analysis, using GAPDH as a loading control. Results are expressed as mean ±SEM from three independent experiments. ##P<0.01 vs Control cells and *P<0.01 and ***P<0.001 vs Alpha-MSH group.

Figure 82. Effect of *Phyllanthus acidus* and *Rhinacanthus nasutus* extracts on protein level of TRP-1 involved in melanogenesis. Total protein from B16F10 cells treated with *Phyllanthus acidus* and *Rhinacanthus nasutus* extracts was collected at 48 h. TRP-1 at protein level was examined by Western Blot analysis, using GAPDH as a loading control. Results are expressed as mean ±SEM from three independent experiments. [##]P<0.01 vs Control cells and **P<0.01, ***P<0.001 vs Alpha-MSH group.
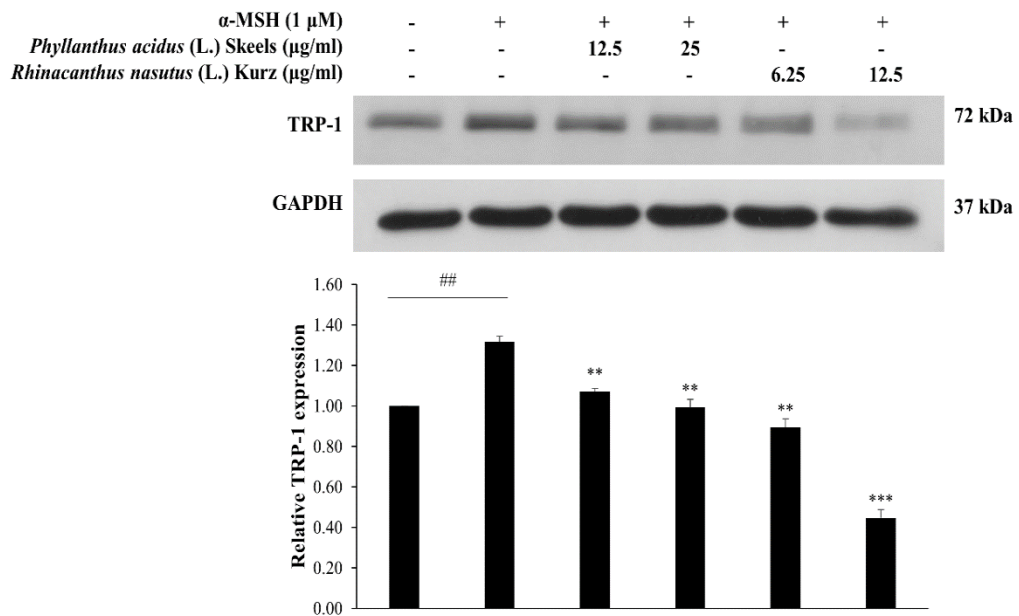
3.1.5.3.4 Effect of selected plant extracts on TRP-2 in alpha-MSH induced B16F10 cells

Melanin synthesis requires tyrosinase, tyrosinase-related protein 1 and 2 (7). In the presence of tyrosinase-realated protein 2 (TRP-2), known as DOPAchrome tautomerase, DOPAchrome is tautomerized to 5,6-dihydroxyindole-2-carboxylic acid (DHICA) which is a substrate for brown eumelanin (79). We examined the effect of selected ethanol extracts on TRP-2 expression in alpha-MSH induced B16F10 cells for 48 h. Proteins were extracted by cell lysis buffer with protease inhibitor. TRP-2 protein was detected with primary antibody (1:2000) and anti-rabbit horseradish peroxidase antibody (1:5000). GAPDH was used as normalization to TRP-2 protein expression. As shown in Figure 83, alpha-MSH stimulated cells had TRP-2 protein levels more than control cells which were not treated with alpha-MSH and plant extracts. We found that *Croton roxburghii* at 50 µg/ml decreased alpha-MSH induced TRP-2 expression when compared with alpha-MSH group. Like *Croton roxburghii*, *Croton sublyratus* also reduced TRP-2 expression. Moreover, there was a reduction of TRP-2 protein levels in the cells treated with *Phyllanthus acidus* at the concentration of 6.25 and 12.5 µg/ml (Figure 84). Similarly, *Rhinacanthus nasutus* significantly suppress TRP-2 expression at protein level. These results suggest that four ethanol extracts, including *Croton roxburghii*, *Croton sublyratus*, *Phyllanthus acidus* and *Rhinacanthus nasutus*, decrease TRP-2 protein expression and appear to inhibit melanin content.
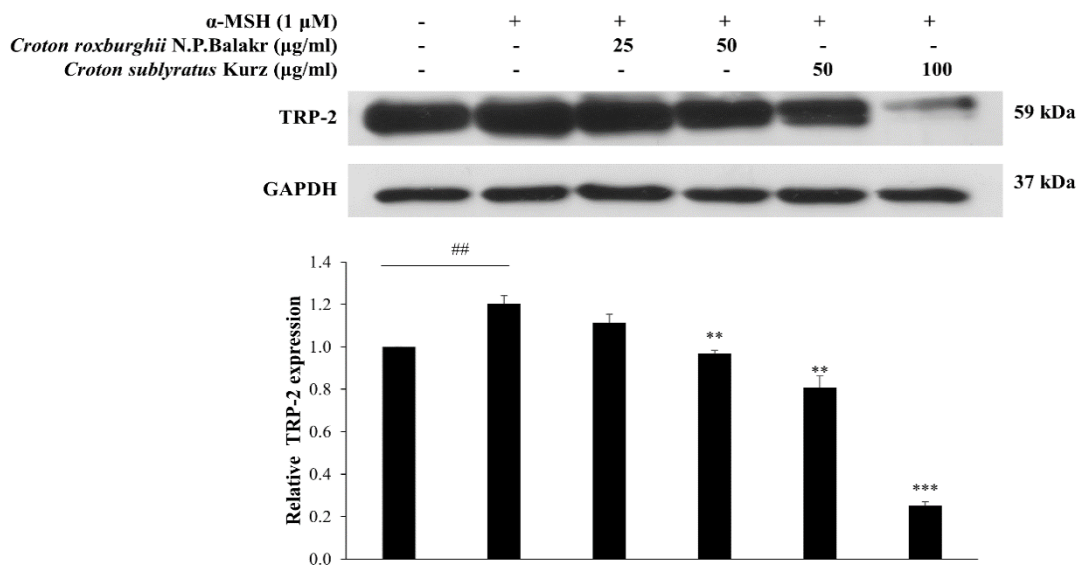
Figure 83. Effect of *Croton roxburghii* and *Croton sublyratus* extracts on protein level of TRP-2 involved in melanogenesis. Total protein from B16F10 cells treated with *Croton roxburghii* and *Croton sublyratus* extracts was collected at 48 h. TRP-2 at protein level was examined by Western Blot analysis, using GAPDH as a loading control. Results are expressed as mean ±SEM from three independent experiments. [##]P<0.01 vs Control cells and **P<0.01, ***P<0.001 vs Alpha-MSH group.

Figure 84. Effect of *Phyllanthus acidus* and *Rhinacanthus nasutus* extracts on protein level of TRP-2 involved in melanogenesis. Total protein from B16F10 cells treated with *Phyllanthus acidus* and *Rhinacanthus nasutus* extracts was collected at 48 h. TRP-2 at protein level was examined by Western Blot analysis, using GAPDH as a loading control. Results are expressed as mean ±SEM from three independent experiments. [##]P<0.01 vs Control cells and ***P<0.001 vs Alpha-MSH group.

3.1.5.4 Effect of four ethanol plant extracts on CREB phosphorylation

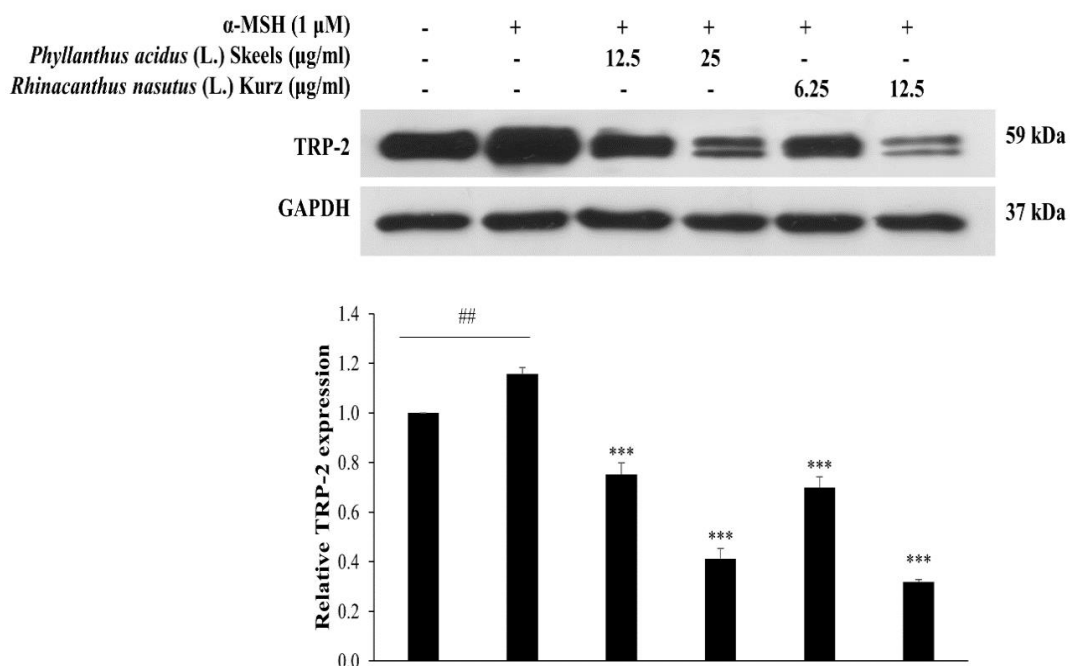On binding to the melanocortin receptor (MC1R) on melanocytes in the epidermis layer of the skin, alpha-MSH from keratinocytes activates intracellular adenyl cyclase followed by increased intracellular cyclic AMP (cAMP) level from adenosine triphosphate (ATP) (5). Cyclic AMP further activates protein kinase A (PKA). The PKA phosphorylates and activates cAMP-response element binding protein (CREB) that binds to cAMP response element (CRE) presenting in the M promoter of the microphthalmia-associated transcription factor (MITF) gene. The increase of phosphorylated CREB lead to the up-regulation of MITF and melanogenic enzymes such as tyrosinase, tyrosinase-related protein 1 and tyrosinase-related protein 2 (6). To determine the effect of four ethanol plant extract on CREB phosphorylation, B16F10 cells were treated with 1 μM of alpha-MSH in the presence of four plant extracts for 0, 15, 30, 60 and 120 min. Proteins were extract with 1X RIPA buffer and 1X phosphatase inhibitor. Phosphorylated CREB was detected with anti-phospho-CREB antibody (1:1000) and anti-rabbit horseradish peroxidase antibody (1:2000). GAPDH was used as internal control. In the same membrane, total CREB was also determined by anti-total CREB antibody (1:1000) and anti-rabbit horseradish peroxidase antibody (1:2000). Ratio of phosphorylated CREB to total CREB was calculated in band intensity. All ratios were normalized to starting time point (0 min) of alpha-MSH group.

As shown in Figure 85, alpha-MSH significantly increased phospho-CREB level at 15-60 min. The alpha-MSH stimulated the hightest level of phospho-protein at 60 min. The phospho-CREB were decreased at 120 min. So, we tested the effect of four extracts on CREB phosphorylation between 0-120 min. Our results showed that ethanol extract of four plant extracts significantly increased phospho-CREB at 0 min. However, *Croton roxburghii* extract significantly decreased at 15-60 min (Figure 86, 90). While, *Croton sublyratus* extract markly inhibited phospho-CREB level at 30-60 min (Figure 87, 90). *Phyllanthus acidus* showed the inhibition of phospho-CREB at 30-60 min (Figure 88, 90). *Rhinacanthus nasutus* extract reduced alpha-MSH induced phospho-CREB protein at 120 min (Figure 89, 90). These results suggest that four

plant extracts can decrease melanin synthesis through downregulation of phospho-CREB level.
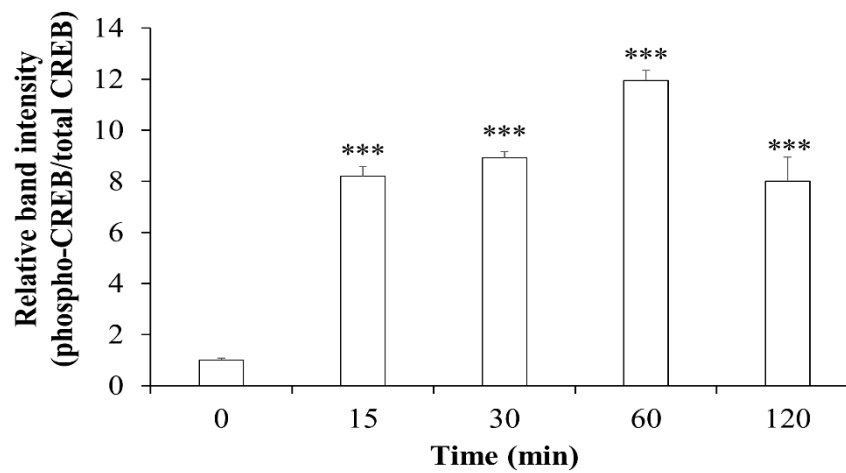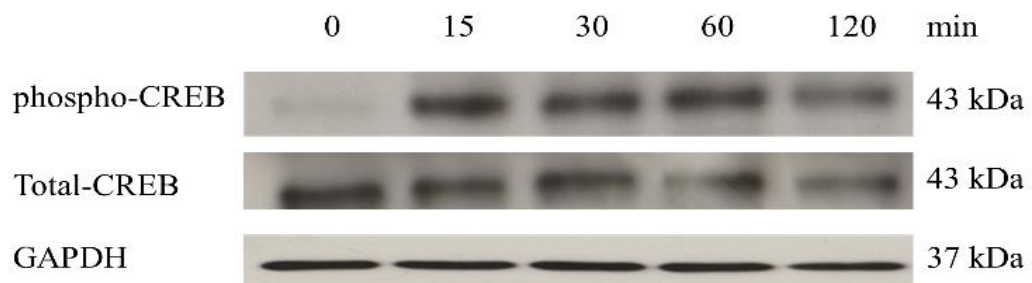
Figure 85. Effect of alpha-MSH on CREB phosphorylation. B16F10 cells were incubated with 1 µM of alpha-MSH at 0, 15, 30, 60 and 120 min. Total protein was extracted and examined by Western blot assay. Results are expressed as mean ±SEM from three independent experiments. ***$P<0.001$ vs Alpha-MSH group at 0 min.
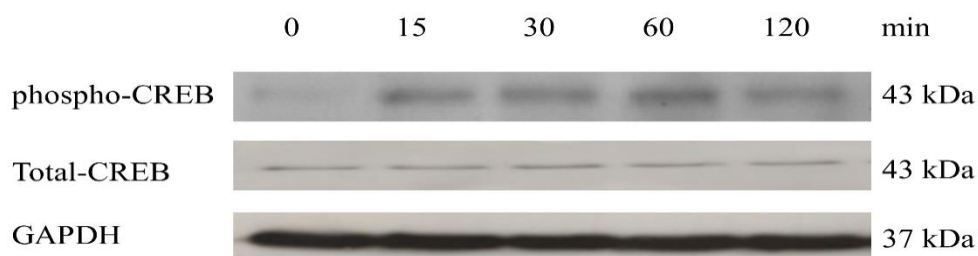
Figure 86. Effect of *Croton roxburghii* extract on CREB phosphorylation. B16F10 cells were incubated with 1 µM of alpha-MSH and *Croton roxburghii* extract at 0, 15, 30, 60 and 120 min. Total protein was extracted and examined by Western blot assay.
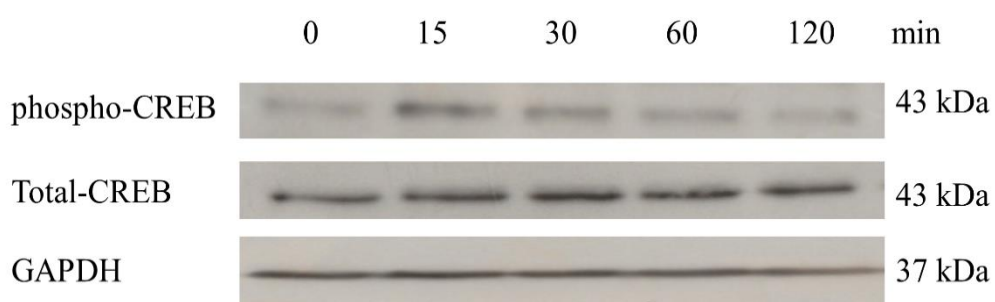
Figure 87. Effect of *Croton sublyratus* extract on CREB phosphorylation. B16F10 cells were incubated with 1 µM of alpha-MSH and *Croton sublyratus* extract at 0, 15, 30, 60 and 120 min. Total protein was extracted and examined by Western blot assay.
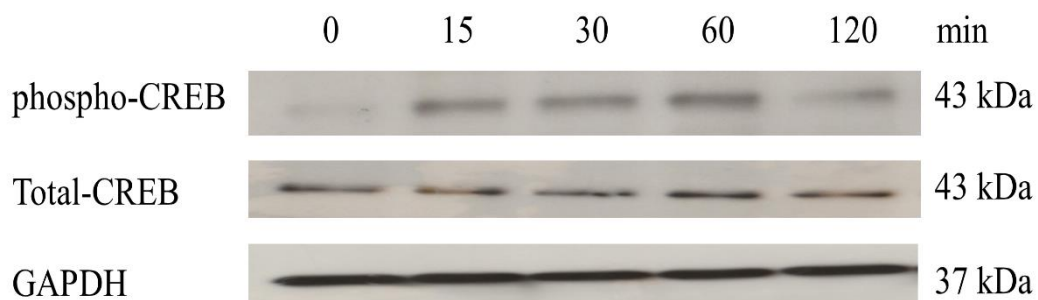
Figure 88. Effect of *Phyllanthus acidus* extract on CREB phosphorylation. B16F10 cells were incubated with 1 μM of alpha-MSH and *Phyllanthus acidus* extract at 0, 15, 30, 60 and 120 min. Total protein was extracted and examined by Western blot assay.
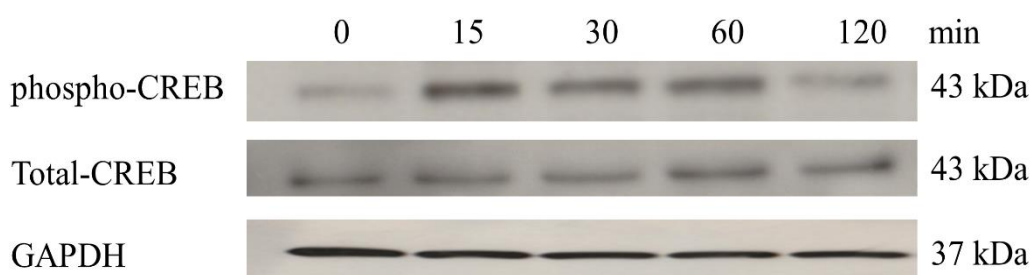
Figure 89. Effect of *Rhinacanthus nasutus* extract on CREB phosphorylation. B16F10 cells were incubated with 1 μM of alpha-MSH and *Rhinacanthus nasutus* extract at 0, 15, 30, 60 and 120 min. Total protein was extracted and examined by Western blot assay.

Figure 90. Effect of alpha-MSH and four extracts on CREB phosphorylation. B16F10 cells were incubated with 1 µM of alpha-MSH in the presence of each extract at 0, 15, 30, 60 and 120 min. Total protein was extracted and examined by Western blot assay. Results are expressed as mean ±SEM from three independent experiments. *P<0.05,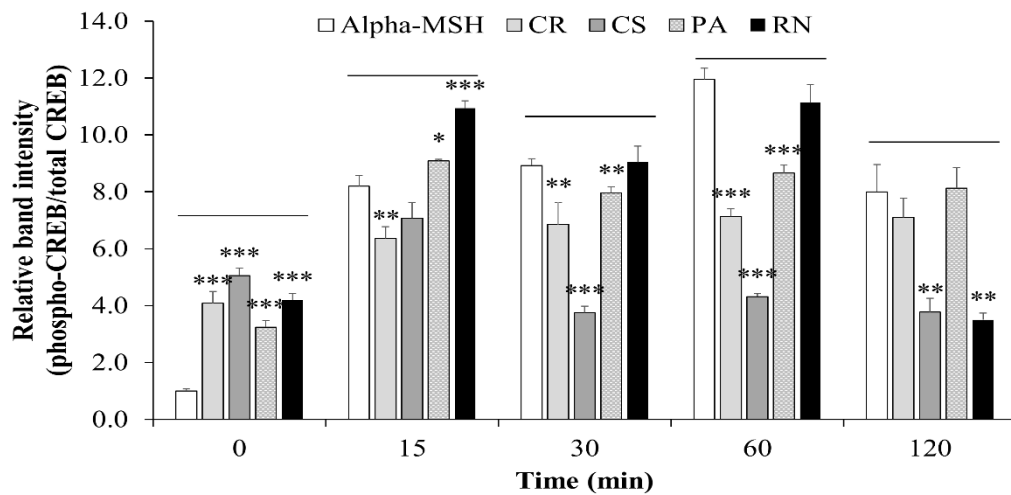 **P<0.01, ***P<0.001 vs Alpha-MSH group in each time. CR: *Croton roxburghii*; CS: *Croton sublyratus*; PA: *Phyllanthus acidus*; RN: *Rhinnacanthus nasutus*

CHAPTER IV

DISCUSSION

Melasma is a chronic acquired hypermelanosis which occurs systematically on sun-exposed area of the skin. Genetic background, sun exposure, age (elderly) and female sex hormones are classical involving factors (2). Pathogenesis of the melasma contains the overexpression of alpha-MSH, the increase in size of melanosomes in keratinocytes and melanocytes, the high amount of melanin and the high level of tyrosinase activity (103). Melasma had an impact on individual emotional well-being and quality of life in women (261). Melasma treatment depend on whether the pigmentation is on epidermal or dermal. Only epidermal pigmentation responds well to treatment (10). Hydroquinone is the most popular depigmenting agent for melasma. It can inhibit tyrosinase activity. However, the hydroquinone is oxidized semi-quinone-like as free radical. This radical can damage protein and lipid (126). Adverse effects of hydroquinone include erythema, stinging, colloid milium, irritant and allergic contact dermatitis, nail discoloration, transient hypochromia, and paradoxical postinflammatory hypermelanosis (11). In addition, the prolonged usage of hydroquinone leads to ochronosis (127). Recently, many researchers seek new agents for melasma treatment. The new agents from natural products should be safety and efficacy without side effects. Naturally occurring herbal extracts, active compounds such as phenol, flavonoid, gallic acid, epigallocatechin, aloesin, hydroxystillbene and ellagic acid (12). In this study, we the inhibitory effect of selected Thai plant extracts against melanin synthesis and their molecular mechanism in alpha-MSH induced B16F10 cells.

First, the dried powder of leaves and pericarps from 13 plants was extracted in petroleum ether, dichloromethane and ethanol, respectively. After extraction, the solvents were removed by vacuum rotary evaporator under reduced pressure.

Concentrated samples were dissolved in dimethyl sulfoxide (DMSO). After that, we determined total phenolic content of 13 plant extracts by Follin Ciocalteu method. This method is based on a phenolic or polyphenolic compound which reduces phosphomolybdic /phosphotungstic acid complexes (yellowish color) to a blue-colored complex in alkaline condition. The results showed that phenolic content of 13 plant extracts varied from 2.51 ± 0.22 to 84.00 ± 6.23 mg GAE/g dry plant material. The ethanol fractions had the richest phenolic content, followed by dichloromethane and petroleum ether fractions. The phenolic content depends on the polarity of active compounds in each fractions. High polarity of active compounds dissolves in ethanol, dichloromethane and ethanol fractions, orderly. In the previous study, there was a significance different among solvent fractions. Polar fractions have the high phenolic content (262). Moreover, many plants materials, such as pomegranate peel, ginger, oriental cherry leaves, green tea leaves, grape seeds, aloe vera leaves, and orchid leaves have been investigated for their tyrosinase inhibitory activity (263-269). This inhibition effect occurs from phenolic compounds in these plants.

Flavonoids are pigments in flowers, leaves, fruits and seeds. These compounds are secondary metabolites of plants and widely distributed among plant species (251). Total flavonoid content was determined using aluminium chloride colorimetric method. Normally, dichloromethane fractions had the highest flavonoid when compared with other fractions. All of the extracts, the ethanol extract from *Senna alata* (L.) Roxb leaves had the highest flavonoid content. While, *Ardisia elliptica* Thunb. had the richest flavonoid content in dichloromethane fractions. In addition, *Ipomoea pes-caprae* (L.) R.br. had the highest flavonoid content among petroleum extracts. We found that total phenolic content did not correlate with total flavonoid content in all plant extracts. Flavonoid contains two benzene rings which are separated by oxygen containing a pyrane ring. Flavonoids act as a scavenger (270). Flavonoids are classified into flavones, flavonols, isoflavones, and

flavones. Isoflavones, including glycitein, daidzein, and genistein, had a little tyrosinase inhibition. However, 6,7,4′-trihydroxyisoflavone showed as a potent tyrosinase inhibitor stronger than kojic acid. Flavanones, including hesperidin, eriodictyol, and naringenin, have a structure as well as hydroquinone (260). So, flavonoid compounds can inhibit tyrosinase activity.

Free radical scavenging activity was examined using DPPH and ABTS assay. In DPPH assay, DPPH receives a hydrogen atom from an antioxidant, and ascorbic acid was used as a standard antioxidant (271). Antioxidant activity of aqueous and lipid phases in the plants was evaluated by a decolorization assay using ABTS (272). ABTS is converted to its radical cation by adding of potassium persulfate. In the presence of an antioxidant, the reactive ABTS cation or $ABTS^{•+}$ is converted to its colorless natural form (243). Ascorbic acid also served as standard. We found that ethanol fraction showed the high levels of scavenging activity compared with other fractions by DPPH and ABTS assay. In DPPH and ABTS assay, four ethanol extracts, including *Ardisia elliptica*, *Garcinia mangostana*, *Phyllanthus acidus*, and *Stemona curtisii* had scavenging activity more than 90%. Moreover, *Senna alata* ethanol extract also showed the high scavenging activity at 99% by ABTS assay. The results suggest that ABTS assay reflect the antioxidant contents in plant extracts better than DPPH assay. In the previous study, ABTS assay is more useful than ABTS assay in reflecting of antioxidant levels of food containing hydrophilic and lipophilic (273). High correlation was observed between DPPH scavenging activity and total phenolic content (R^2 = 0.8948). ABTS was strongly correlated with total phenolic content (R^2 = 0.7393). DPPH radical scavenging activity of plant extracts highly correlated with ABTS radical scavenging activity. While, there was no significant relationship between DPPH or ABTS radical scavenging activity and total flavonoid content. These results suggested that the phenolic content in plant extracts is the major active compound for free radical scavenging activities.

Next, we investigated the effect of plant extracts to inhibit tyrosinase activity in alpha-MSH stimulated B16F10 cells. In the melanogenesis, tyrosinase is the key enzyme in the rate-limiting step in which L-tyrosine is hydroxylated to L-DOPA, which is further oxidized into DOPAquinone. After that, DOPAquinone is converted into DOPAchrome that is a substrate for eumelanin synthesis (70). We used mushroom tyrosinase activity for screening the inhibition effect of plant extracts. We found that ethanol extracts of *Ardisia elliptica*, *Datura metel*, *Ipomoea pes-caprae*, *Phyllanthus acidus*, *Rhinacanthus nasutus*, and *Senna alata* leaves significantly decreased mushroom tyrosinase activity. Moreover, petroleum ether and dichloromethane fractions of *Ardisia elliptica* leaves also showed anti-mushroom tyrosinase activity. In the previous study, three fractions of D. *metel* contains acetone, dichloromethane, and methanol which exhibited inhibitory effect on tyrosinase activity in a dose dependent manner. Methanol fraction of D. *metel* leaves had the highest inhibition of tyrosinase activity when compared with other fractions (181). Similarly, Toshiya et al. reported that methanol extract of *I. pes-caprae* extracts at 500 µg/ml demonstrated the inhibitory activity of tyrosinase about 34.6% (274). Ultraviolet radiation from sunlight induces reactive oxygen species (ROS) in the skin. Skin immediately responds to ROS by detoxifying enzymes, including superoxide dismutase, catalase, thioredoxin reductase, and low-molecular mass antioxidant molecules such as glutathione, α-tocopherol and ascorbic acid. But these responses are not enough to prevent skin damage (275). Plants have their own protection against the damage of the sun. Plants have rich sources of natural products which can decrease skin damage from the sun (276). In this study, we investigated the effect of plant extracts on cellular tyrosinase activity in α-MSH-induced B16F10 mouse melanoma cells. We chose the ethanol extracts of 13 plants because only ethanol plant extracts significantly decreased mushroom tyrosinase activity. Moreover, the ethanol extracts of 13 plants have more antioxidant content and antioxidant activity than petroleum ether and dichloromethane extracts. We varied

the concentrations of each ethanol extract and tested the cell viability. We selected two concentrations which were not toxic in α-MSH-induced B16F10 mouse melanoma cells. We found that ethanol extracts of four plants including *Croton roxburghii, Croton sublyratus, Phylllanthus acidus,* and *Rhinacanthus nasutus,* significantly reduced cellular tyrosinase activity when compared with alpha-MSH group (stimulated by α-MSH). These results suggest that ethanol extracts of *Croton roxburghii, Croton sublyratus, Phylllanthus acidus*, and *Rhinacanthus nasutus* markly inhibited tyrosinase activity which converses L-DOPA to dopachrome.

Melanin, the endproduct of melanogenesis, is responsible for determining the color of human skin, hair and eyes. Melanin biosynthesis requires tyrosinase, tyrosinase-related protein 1 and 2. Tyrosinase catalyzes the hydroxylation of L-tyrosine into 3,4-dihydroxyphenylalanine (L-DOPA) (7). Then, L-DOPA is oxidized to DOPAquinone by tyrosinase. DOPAquinone is further converted to DOPAchrome which can be converted to 5,6-dihydroxyindole (DHI) or 5,6-dihydroxyindole-2-carboxylic acid (DHICA). DHI can be formed into produce black eumelanin. While, DHICA can be changed into brown eumelanin by TRP-1 and TRP-2 (79). We measured melanin content in the cells which were treated with each plant extract. We found that four plant extracts including *Croton roxburghii, Croton sublyratus, Phylllanthus acidus*, and *Rhinacanthus nasutus*, significantly reduced melanin production at $P < 0.001$. So, we selected four ethanol extracts for examining the effect of plant extracts on gene expression of melanogenetic proteins in α-MSH-induced B16F10 mouse melanoma cells. Moreover, we tested the effect of selected extracts on cellular tyrosinase activity in α-MSH-induced B16F10. Similar with melanin content assay, the results showed that *Croton roxburghii, Croton sublyratus, Phylllanthus acidus*, and *Rhinacanthus nasutus*, significantly decreased cellular tyrosinase activity at $P < 0.001$. *Phyllanthus acidus* and *Rhinacanthus acidus* also inhibited mushroom tyrosinase activity. This result indicates *Phyllanthus acidus* and *Rhinacanthus acidus* can suppress tyrosinase activity which is a target for skin whitenting agents. In this study,

we used L-DOPA as a substrate for cellular tyrosinase activity. Structure of tyrosinase contains two copper ions which are surrounded by three histidines residues for catalytic activity of tyrosinase. There are three states of active site; oxy, met and deoxy forms in the formation of pigment. At the active site, copper ions react with dioxygen to produce a highly reactive chemical intermediate which directly participate in the hydroxylation of monophenols to diphenols and in the oxidation of *o*-diphenols to *o*-quinones (277). Thus, the regulation of melanin synthesis by inhibiting tyrosinase activity is a major target of whitening agents. This study suggests that selected plant extracts inhibited melanin content through inhibiting tyrosinase activity (figure 91).

Croton roxburghii (CR)
Croton sublyratus (CS)
Phylllanthus acidus (PA)
Rhinacanthus nasutus (RN)
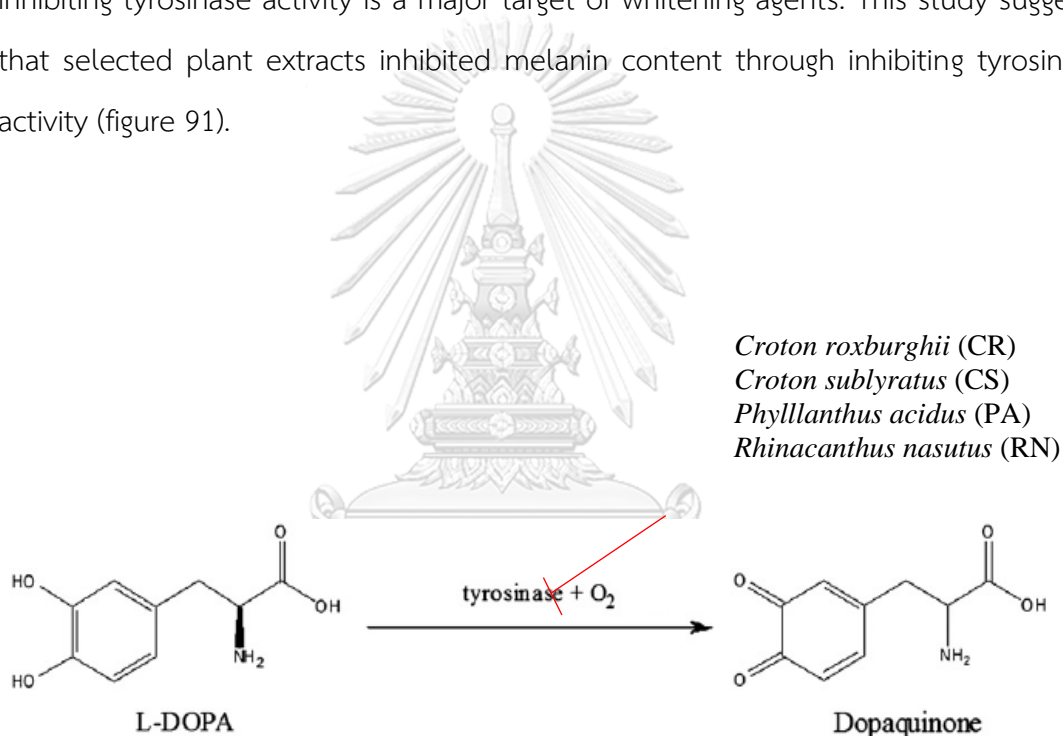
Figure 91. Oxidation of L-DOPA to DOPA-quinone by tyrosinase (278).

To determine the effect of selected plant extracts, involved mRNA expression of melanogenic enzymes such as tyrosinase, tyrosinae-related protein 1 (TRP-1) and tyrosinase-related protein 2 (TRP-2) through MITF, we performed realtime PCR analysis. B16F10 cells were treated with 1 µM of alpha-MSH and selected plant extracts. UV is a major factor of melasma by stimulating the secretion of alpha-MSH

from proopiomelanocortin (POMC) in keratinocytes (121). Alpha-MSH increases the upregulation of tyrosinase, TRP-1 and TRP-2 through the increase of MITF. This reaction leads to increase melanin synthesis (278). Thus, MITF also is major target for developing new whitening agents. Our results showed that *Croton roxburghii, Croton sublyratus, Phyllanthus acidus* and *Rhinnacanthus acidus* decreased tyrosinase, TRP-1 and TRP-2 through downregulation of MITF at transcription level which can lead to reduce melanin production in alpha-MSH induced B16F10 cells. Moreover, we examined the effect of selected plant extracts involved gene expression of melanogenic enzymes at protein level in alpha-MSH stimulated B16F10 cells. Similar with transcriptional level, *Croton roxburghii, Croton sublyratus, Phyllanthus acidus* and *Rhinnacanthus acidus* also inhibited tyrosinase, TRP-1 and TRP-2 via downregulation of MITF at post-translation level in a dose-dependent manner when compared with alpha-MSH group. These extracts contain phenolics and flavonoids with high antioxidant activity. These results suggest that anti melanogenic effects of *Croton roxburghii, Croton sublyratus, Phyllanthus acidus* and *Rhinnacanthus acidus* are associated with their antioxidant properties.

UV stimulated the secretion of alpha-MSH from keratinocytes. The alpha-MSH activates intracellular adenyl cyclase followed by increased intracellular cyclic AMP (cAMP) level from adenosine triphosphate (ATP) (5). Cyclic AMP further activates protein kinase A (PKA). The PKA phosphorylates and activates cAMP-response element binding protein (CREB) that binds to cAMP response element (CRE) presenting in the M promoter of the microphthalmia-associated transcription factor (MITF) gene. The increase of phosphorylated CREB lead to the up-regulation of MITF (6). This reaction increased melanin synthesis in the skin, resulting in melasma. To study the effect of four plant extract on CREB phosphorylation, we analyzed phospho-CREB level by Western Blot assay. B16F10 cells were treated with 1 µM of alpha-MSH in the presence of each extract at time point (0, 15, 30, 60, 120 min). Our results showed that *Croton roxburghii* extract significantly decreased at 15-60 min. While, *Croton sublyratus* extract markly inhibited phospho-CREB level at 30-60 min. *Phyllanthus acidus* also showed the inhibition of phospho-CREB at 30-60 min. *Rhinacanthus nasutus* extract reduced alpha-MSH induced phospho-CREB protein at

120 min. These results suggest that four plant extracts can decrease melanin content through downregulation of phospho-CREB level.

The present study determined that ethanol extracts of *Croton roxburghii*, *Croton sublyratus*, *Phyllanthus acidus* and *Rhinnacanthus acidus* leaf significantly decrease melanin synthesis. Furthermore, four ethanol extracts was found to reduce MITF, tyrosinase, TRP-1 and TRP-2 through downregulation of phospho-CREB. Our results suggest that four extracts have a potential for anti-melanogenic activity and may be useful for treating melasma.

Four ethanol eaxtracts of this study, including *Croton roxburghii*, *Croton sublyratus*, *Phyllanthus acidus* and *Rhinnacanthus acidus* leaf, are crude extracts. Further study, we will separate the active compounds from these crude extracts by High Performance Liquid Chromatography (HPLC). These active compound will be tested for anti-melanogenic activity. We tested the anti-melanogenic activity in cell model only. This study is limited to use in human skin. Four plant extracts should be tested in animal model for determining toxicity, efficiency and absorption of four plant extracts. After that, four plant extracts should be tested in human skin for skin irritation, absorption test and anti-melanogenic activity.

จุฬาลงกรณ์มหาวิทยาลัย
CHULALONGKORN UNIVERSITY

CHAPTER V

CONCLUSION

Natural products have recently become popular to treat melasma and hyperpigmentation. Because hydroquinone have many side effects such as dermatitis, erytherm, leukoderma, burning and ochronosis. Active compounds of natural products have a potential to decrease melanin synthesis in melasma lesion. UVB induces reactive oxygen species (ROS) in skin damage. ROS can destroy lipid, protein and nucleic acids in the skin. It can induce skin inflammation, cell damage and skin cancer. So, plant extracts have antioxidant activities, phenolics and flavonoids which can reduce ROS. Our results show that 13 plant extracts had varied values of total phenolic and flavonoid contents as well as DPPH and ABTS scavenging activities which is based on polarities of the extract. We also found that the six ethanol extracts, including *Rhinnacanthus nasutus* (65%), *Ardisia elliptica* (50%), *Phyllanthus acidus* (43%), *Senna alata* (24%), *Ipomoea pes-caprae* (23%) *and Datura metel* (20%), have a potential to decrease mushroom tyrosinase activity. In cell model, ethanol extracts of *Croton roxburghii* (CR), *Croton sublyratus* (CS), *Phyllanthus acidus* (PA) and *Rhinnacanthus nasutus* (RN) leaves significantly decreased melanin content and cellular tyrosinase activity in alpha-MSH stimulated B16F10 mouse melanoma cells by suppressing MITF, tyrosinase, TRP-1 and TRP-2 at transcription and translation level through downregulating of CREB phosphorylation in a dose dependent manner as shown in figure 92. Tyrosinase activity is the target for melasma treatment. As same as in a result of anti-mushroom tyrosinase activity, *Rhinnacanthus nasutus* leaves also had the highest inhibition of the cellular tyrosinase activity. *Phyllanthus acidus* also decreased both mushroom tyrosinase activity and cellular tyrosinase activity. Our results indicate that these four extracts have phenolics and flavonoids with high antioxidant activity. Therefore the four ethanolic extracts may provide a potential to be ingredients for an alternative

therapy of melasma treatment. However, we tested anti-melanogenic effect of four plant extracts *in vitro*. These extracts should be determined a toxic effect in mouse model and human skin before use. Further studies are important to find the active components and investigate safety of these extracts in human skin.
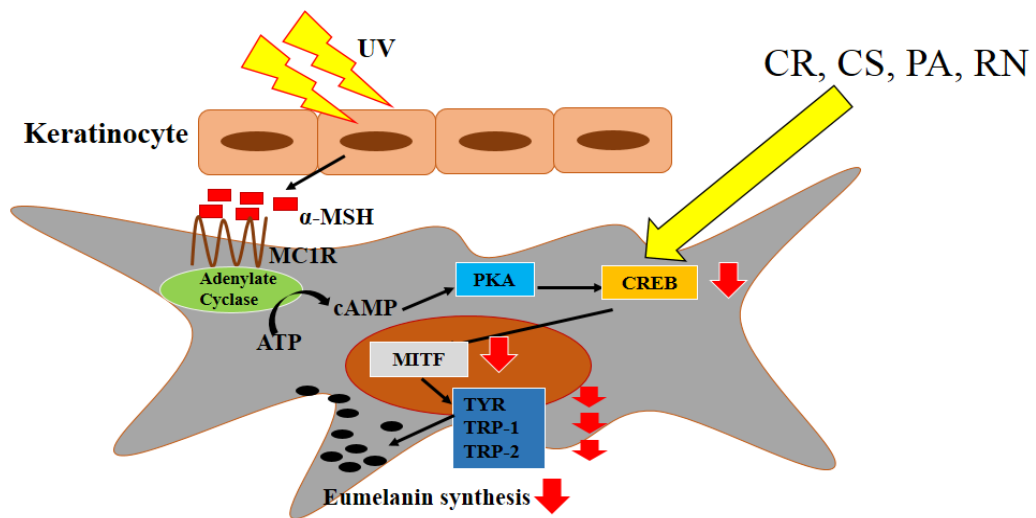
Figure 92. Effect of four ethanol extracts in alpha-MSH induced B16F10 cells. *Croton roxburghii* (CR)*, Croton sublyratus* (CS)*, Phyllanthus acidus* (PA) and *Rhinnacanthus nasutus* (RN) leaves significantly decreased melanin content and cellular tyrosinase activity in alpha-MSH stimulated B16F10 mouse melanoma cells by suppressing MITF, tyrosinase, TRP-1 and TRP-2 at transcription and translation level through downregulating of CREB phosphorylation in a dose dependent manner.

REFERENCES

1.   Dell'Angelica EC. Melanosome biogenesis: shedding light on the origin of an obscure organelle. Trends in Cell Biology. 2003;13(10):503-6.

2.   Passeron T. Melasma pathogenesis and influencing factors - an overview of the latest research. Journal of the European Academy of Dermatology Venereology. 2013;27 Suppl 1:5-6.

3.   Choi W, Miyamura Y, Wolber R, Smuda C, Reinhold W, Liu H, et al. Regulation of human skin pigmentation in situ by repetitive UV exposure: molecular characterization of responses to UVA and/or UVB. Journal of Investigative Dermatology. 2010;130(6):1685-96.

4.   Hirobe T. Role of keratinocyte-derived factors involved in regulating the proliferation and differentiation of mammalian epidermal melanocytes. Pigment Cell Research. 2005;18(1):2-12.

5.   Im S, Moro O, Peng F, Medrano EE, Cornelius J, Babcock G, et al. Activation of the cyclic AMP pathway by alpha-melanotropin mediates the response of human melanocytes to ultraviolet B radiation. Cancer Research. 1998;58(1):47-54.

6.   Tachibana M. MITF: a stream flowing for pigment cells. Pigment Cell Research. 2000;13(4):230-40.

7.   Riley PA. The great DOPA mystery: the source and significance of DOPA in phase I melanogenesis. Cellular and Molecular Biology (Noisy-le-grand). 1999;45(7):951-60.

8.   Ito S, Wakamatsu K. Chemistry of mixed melanogenesis--pivotal roles of dopaquinone. Photochemistry and Photobiology. 2008;84(3):582-92.

9.   Sarangarajan R, Apte SP. The polymerization of melanin: a poorly understood phenomenon with egregious biological implications. Melanoma Research. 2006;16(1):3-10.

10.   Bandyopadhyay D. Topical treatment of melasma. Indian Journal of Dermatology. 2009;54(4):303-9.

11.	Picardo M, Carrera M. New and experimental treatments of cloasma and other hypermelanoses. Dermatologic Clinics. 2007;25(3):353-62, ix.

12.	Ebanks JP, Wickett RR, Boissy RE. Mechanisms Regulating Skin Pigmentation: The Rise and Fall of Complexion Coloration. International Journal of Molecular Sciences. 2009;10(9):4066-87.

13.	Kim D, Park J, Kim J, Han C, Yoon J, Kim N, et al. Flavonoids as mushroom tyrosinase inhibitors: a fluorescence quenching study. Journal of Agricultural and Food Chemistry. 2006;54(3):935-41.

14.	No JK, Soung DY, Kim YJ, Shim KH, Jun YS, Rhee SH, et al. Inhibition of tyrosinase by green tea components. Life Sciences. 1999;65(21):PL241-6.

15.	Elias PM, Choi EH. Interactions among stratum corneum defensive functions. Experimental dermatology. 2005;14(10):719-26.

16.	Casey G. Physiology of the skin. Nursing Standard. 2002;16(34):47-51; quiz 3, 5.

17.	Gaur M, Dobke M, Lunyak V. Mesenchymal Stem Cells from Adipose Tissue in Clinical Applications for Dermatological Indications and Skin Aging. International Journal of Molecular Sciences. 2017;18(1):208.

18.	Muroyama A, Lechler T. Polarity and Stratification of the Epidermis. Seminars in cell & developmental biology. 2012;23(8):890-6.

19.	Eckert RL, Rorke EA. Molecular biology of keratinocyte differentiation. Environmental Health Perspectives. 1989;80:109-16.

20.	Potten CS, Booth C. Keratinocyte stem cells: a commentary. Journal of Investigative Dermatology. 2002;119(4):888-99.

21.	Fuchs E, Raghavan S. Getting under the skin of epidermal morphogenesis. Nature reviews Genetics. 2002;3(3):199-209.

22.	Ishida-Yamamoto A, Igawa S, Kishibe M. Order and disorder in corneocyte adhesion. The Journal of dermatology. 2011;38(7):645-54.

23.	Delva E, Tucker DK, Kowalczyk AP. The Desmosome. Cold Spring Harbor Perspectives in Biology. 2009;1(2):a002543.

24.	Mort RL, Jackson IJ, Patton EE. The melanocyte lineage in development and disease. Development (Cambridge, England). 2015;142(4):620-32.

25.   Boot PM, Rowden G, Walsh N. The distribution of Merkel cells in human fetal and adult skin. The American Journal of dermatopathology. 1992;14(5):391-6.

26.   Tachibana T. The Merkel cell: recent findings and unresolved problems. Archives of histology and cytology. 1995;58(4):379-96.

27.   Lucarz A, Brand G. Current considerations about Merkel cells. European journal of cell biology. 2007;86(5):243-51.

28.   Proksch E, Brandner JM, Jensen JM. The skin: an indispensable barrier. Experimental dermatology. 2008;17(12):1063-72.

29.   Chomiczewska D, Trznadel-Budzko E, Kaczorowska A, Rotsztejn H. [The role of Langerhans cells in the skin immune system]. Polski merkuriusz lekarski : organ Polskiego Towarzystwa Lekarskiego. 2009;26(153):173-7.

30.   Manabe M, O'Guin WM. Keratohyalin, trichohyalin and keratohyalin-trichohyalin hybrid granules: an overview. The Journal of dermatology. 1992;19(11):749-55.

31.   Madison KC, Swartzendruber DC, Wertz PW, Downing DT. Lamellar granule extrusion and stratum corneum intercellular lamellae in murine keratinocyte cultures. Journal of Investigative Dermatology. 1988;90(2):110-6.

32.   Menon GK, Cleary GW, Lane ME. The structure and function of the stratum corneum. International Journal of Pharmaceutics. 2012;435(1):3-9.

33.   Ramos AP, Lafleur M. Chain Length of Free Fatty Acids Influences the Phase Behavior of Stratum Corneum Model Membranes. Langmuir : the ACS journal of surfaces and colloids. 2015;31(42):11621-9.

34.   Wilhelm KP, Cua AB, Maibach HI. Skin aging. Effect on transepidermal water loss, stratum corneum hydration, skin surface pH, and casual sebum content. Archives of dermatology. 1991;127(12):1806-9.

35.   Grice EA, Segre JA. The skin microbiome. Nature reviews Microbiology. 2011;9(4):244-53.

36.   Holbrook KA, Byers PH, Pinnell SR. The structure and function of dermal connective tissue in normal individuals and patients with inherited connective tissue disorders. Scanning electron microscopy. 1982(Pt 4):1731-44.

37.	Prost-Squarcioni C, Fraitag S, Heller M, Boehm N. [Functional histology of dermis]. Annales de dermatologie et de venereologie. 2008;135(1 Pt 2):1s5-20.

38.	Venus M, Waterman J, McNab I. Basic physiology of the skin. Surgery (Oxford). 2011;29(10):471-4.

39.	Shoulders MD, Raines RT. Collagen structure and stability. Annual Review of Biochemistry. 2009;78:929-58.

40.	Cua AB, Wilhelm KP, Maibach HI. Elastic properties of human skin: relation to age, sex, and anatomical region. Archieves of Dermatology Research. 1990;282(5):283-8.

41.	Benyon RC. The human skin mast cell. Clinical and experimental allergy : journal of the British Society for Allergy and Clinical Immunology. 1989;19(4):375-87.

42.	Wysocki AB. Skin anatomy, physiology, and pathophysiology. Nursing Clinics of North America. 1999;34(4):777-97, v.

43.	Smahel J. Adipose tissue in plastic surgery. Annals of plastic surgery. 1986;16(5):444-53.

44.	Lee SH, Jeong SK, Ahn SK. An Update of the Defensive Barrier Function of Skin. Yonsei Medical Journal. 2006;47(3):293-306.

45.	Landmann L. The epidermal permeability barrier. Anatomy and embryology. 1988;178(1):1-13.

46.	Luther U, Dichmann S, Schlobe A, Czech W, Norgauer J. UV light and skin cancer. Medizinische Monatsschrift für Pharmazeuten. 2000;23(8):261-6.

47.	Brodell LA, Rosenthal KS. Skin Structure and Function: The Body's Primary Defense Against Infection. Infectious Diseases in Clinical Practice. 2008;16(2):113-7.

48.	Shibasaki M, Crandall CG. Mechanisms and controllers of eccrine sweating in humans. Frontiers in bioscience (Scholar edition). 2010;2:685-96.

49.	Charkoudian N. Skin blood flow in adult human thermoregulation: how it works, when it does not, and why. Mayo Clinic proceedings. 2003;78(5):603-12.

50.	Charkoudian N. Mechanisms and modifiers of reflex induced cutaneous vasodilation and vasoconstriction in humans. Journal of Applied Physiology. 2010;109(4):1221-8.

51.   Hayward MG, Keatinge WR. Roles of subcutaneous fat and thermoregulatory reflexes in determining ability to stabilize body temperature in water. The Journal of Physiology. 1981;320:229-51.

52.   Blais M, Parenteau-Bareil R, Cadau S, Berthod F. Concise Review: Tissue-Engineered Skin and Nerve Regeneration in Burn Treatment. Stem Cells Translational Medicine. 2013;2(7):545-51.

53.   Fleming MS, Luo W. The anatomy, function, and development of mammalian Aβ low-threshold mechanoreceptors. Frontiers in biology. 2013;8(4):10.1007/s11515-013-1271-1.

54.   Holick MF, Smith E, Pincus S. Skin as the site of vitamin d synthesis and target tissue for 1,25-dihydroxyvitamin d3: Use of calcitriol (1,25-dihydroxyvitamin d3) for treatment of psoriasis. Archives of dermatology. 1987;123(12):1677-83a.

55.   Nair R, Maseeh A. Vitamin D: The "sunshine" vitamin. Journal of Pharmacology & Pharmacotherapeutics. 2012;3(2):118-26.

56.   Joy W. Vitamin D in Children's Health. Children. 2014;1(2):208.

57.   Larue L, de Vuyst F, Delmas V. Modeling melanoblast development. Cellular and Molecular Life Sciences. 2013;70(6):1067-79.

58.   Plonka PM, Passeron T, Brenner M, Tobin DJ, Shibahara S, Thomas A, et al. What are melanocytes really doing all day long...? Experimenatal Dermatology. 2009;18(9):799-819.

59.   Seiberg M. Keratinocyte-melanocyte interactions during melanosome transfer. Pigment Cell Research. 2001;14(4):236-42.

60.   Tsatmali M, Ancans J, Thody AJ. Melanocyte function and its control by melanocortin peptides. The Journal of Histochemistry & Cytochemistry. 2002;50(2):125-33.

61.   Imokawa G. Autocrine and paracrine regulation of melanocytes in human skin and in pigmentary disorders. Pigment Cell Research. 2004;17(2):96-110.

62.   Brenner M, Hearing VJ. The Protective Role of Melanin Against UV Damage in Human Skin†. Photochemistry and Photobiology. 2008;84(3):539-49.

63.   Cichorek M, Wachulska M, Stasiewicz A, Tymińska A. Skin melanocytes: biology and development. Advances in Dermatology and Allergology/Postępy Dermatologii I Alergologii. 2013;30(1):30-41.

64.   Watabe H, Valencia JC, Le Pape E, Yamaguchi Y, Nakamura M, Rouzaud F, et al. Involvement of Dynein and Spectrin with Early Melanosome Transport and Melanosomal Protein Trafficking. Journal of Investigative Dermatology. 2007;128(1):162-74.

65.   Kushimoto T, Basrur V, Valencia J, Matsunaga J, Vieira WD, Ferrans VJ, et al. A model for melanosome biogenesis based on the purification and analysis of early melanosomes. Proceedings of the National Academy of Sciences of the United States of America. 2001;98(19):10698-703.

66.   Berson JF, Harper DC, Tenza D, Raposo G, Marks MS. Pmel17 initiates premelanosome morphogenesis within multivesicular bodies. Molecular Biology of the Cell. 2001;12(11):3451-64.

67.   Venkatesha Basrur, Feng Yang, Tsuneto Kushimoto, Youichiro Higashimoto, Ken-ichi Yasumoto, Julio Valencia, et al. Proteomic analysis of early melanosomes: identification of novel melanosomal proteins. Journal of Proteome Research. 2003;2(1):69-79.

68.   Liu Y, Hong L, Wakamatsu K, Ito S, Adhyaru B, Cheng CY, et al. Comparison of structural and chemical properties of black and red human hair melanosomes. Photochemistry and Photobiology. 2005;81(1):135-44.

69.   Winder A, Kobayashi T, Tsukamoto K, Urabe K, Aroca P, Kameyama K, et al. The tyrosinase gene family--interactions of melanogenic proteins to regulate melanogenesis. Cellular & Molecular Biology Research. 1994;40(7-8):613-26.

70.   Iwata M, Corn T, Iwata S, Everett MA, Fuller BB. The relationship between tyrosinase activity and skin color in human foreskins. Journal of Investigative Dermatology. 1990;95(1):9-15.

71.   Park H-Y, Pongpudpunth M, Lee J, Yaar M. Chapter 72 Biology of Melanocytes. Fitzpatrick's Dermatology in General Medicine.Eighth edition.

72.   Kobayashi T, Urabe K, Winder A, Jimenez-Cervantes C, Imokawa G, Brewington T, et al. Tyrosinase related protein 1 (TRP1) functions as a DHICA oxidase in melanin biosynthesis. The EMBO Journal. 1994;13(24):5818-25.

73.   Solano F, Martinez-Liarte JH, Jimenez-Cervantes C, Garcia-Borron JC, Lozano JA. Dopachrome tautomerase is a zinc-containing enzyme. Biochemical and Biophysical Research Communications. 1994;204(3):1243-50.

74.   Berson JF, Harper DC, Tenza D, Raposo G, Marks MS. Pmel17 initiates premelanosome morphogenesis within multivesicular bodies. Mol Biol Cell. 2001;12(11):3451-64.

75.   Theos AC, Truschel ST, Raposo G, Marks MS. The Silver locus product Pmel17/gp100/Silv/ME20: controversial in name and in function. Pigment Cell Research. 2005;18(5):322-36.

76.   Hoashi T, Watabe H, Muller J, Yamaguchi Y, Vieira WD, Hearing VJ. MART-1 is required for the function of the melanosomal matrix protein PMEL17/GP100 and the maturation of melanosomes. Journal of Biological Chemistry. 2005;280(14):14006-16.

77.   Thody AJ, Higgins EM, Wakamatsu K, Ito S, Burchill SA, Marks JM. Pheomelanin as well as eumelanin is present in human epidermis. Journal of Investigative Dermatology. 1991;97(2):340-4.

78.   Tomita Y, Hariu A, Kato C, Seiji M. Radical production during tyrosinase reaction, dopa-melanin formation, and photoirradiation of dopa-melanin. Journal of Investigative Dermatology. 1984;82(6):573-6.

79.   Nappi AJ, Vass E. Hydrogen peroxide generation associated with the oxidations of the eumelanin precursors 5,6-dihydroxyindole and 5,6-dihydroxyindole-2-carboxylic acid. Melanoma Research. 1996;6(5):341-9.

80.   Munoz-Munoz JL, García-Molina F, Varón R, Tudela J, García-Cánovas F, Rodríguez-López JN. Generation of hydrogen peroxide in the melanin biosynthesis pathway. Biochimica et Biophysica Acta (BBA) - Proteins and Proteomics. 2009;1794(7):1017-29.

81.   Seiberg M, Paine C, Sharlow E, Andrade-Gordon P, Costanzo M, Eisinger M, et al. The protease-activated receptor 2 regulates pigmentation via keratinocyte-melanocyte interactions. Experimental Cell Research. 2000;254(1):25-32.

82.   Gilchrest BA, Park HY, Eller MS, Yaar M. Mechanisms of ultraviolet light-induced pigmentation. Photochemistry and Photobiololgy. 1996;63(1):1-10.

83.   Mahmoud BH, Ruvolo E, Hexsel CL, Liu Y, Owen MR, Kollias N, et al. Impact of long-wavelength UVA and visible light on melanocompetent skin. Journal of Investigative Dermatology. 2010;130(8):2092-7.

84.   Denat L, Kadekaro AL, Marrot L, Leachman SA, Abdel-Malek ZA. Melanocytes as instigators and victims of oxidative stress. Journal of Investigative Dermatology. 2014;134(6):1512-8.

85.   Panich U. Antioxidant Defense and UV-Induced Melanogenesis: Implications for Melanoma Prevention. Current Management of Malignant Melanoma. 2011.

86.   Barsh GS. What Controls Variation in Human Skin Color? PLoS Biology. 2003;1(1):e27.

87.   Sachdeva S. Fitzpatrick skin typing: applications in dermatology. Indian journal of dermatology, venereology and leprology. 2009;75(1):93-6.

88.   de Laat A, van Tilburg M, van der Leun JC, van Vloten WA, de Gruijl FR. Cell cycle kinetics following UVA irradiation in comparison to UVB and UVC irradiation. Photochemistry and Photobiology. 1996;63(4):492-7.

89.   Freeman SE, Hacham H, Gange RW, Maytum DJ, Sutherland JC, Sutherland BM. Wavelength dependence of pyrimidine dimer formation in DNA of human skin irradiated in situ with ultraviolet light. Proceedings of the National Academy of Sciences of the United States of America. 1989;86(14):5605-9.

90.   Hussein MR. Ultraviolet radiation and skin cancer: molecular mechanisms. Journal of Cutaneous Pathology. 2005;32(3):191-205.

91.   Date A, Hakozaki T. In vitro Method to Visualize UV-induced Reactive Oxygen Species in a Skin Equivalent Model. In: Farage M, Miller K, Maibach H, editors. Textbook of Aging Skin: Springer Berlin Heidelberg; 2010. p. 477-85.

92.   Drouin R, Therrien JP. UVB-induced cyclobutane pyrimidine dimer frequency correlates with skin cancer mutational hotspots in p53. Photochemistry and Photobiology. 1997;66(5):719-26.

93. Sklar LR, Almutawa F, Lim HW, Hamzavi I. Effects of ultraviolet radiation, visible light, and infrared radiation on erythema and pigmentation: a review. Photochemical & Photobioliology Sciences. 2013;12(1):54-64.

94. Svobodova A, Walterova D, Vostalova J. Ultraviolet light induced alteration to the skin. Biomedical Paper of the Medical Facaulty University Palacky, Olomouc, Czech Repubublic. 2006;150(1):25-38.

95. Miller R, Aaron W, Toneff T, Vishnuvardhan D, Beinfeld MC, Hook VY. Obliteration of alpha-melanocyte-stimulating hormone derived from POMC in pituitary and brains of PC2-deficient mice. Journal of Neurochemistry. 2003;86(3):556-63.

96. Rees JL. Genetics of hair and skin color. Annual Review of Genetics. 2003;37:67-90.

97. Gantz I, Miwa H, Konda Y, Shimoto Y, Tashiro T, Watson SJ, et al. Molecular cloning, expression, and gene localization of a fourth melanocortin receptor. Journal of Biological Chemistry. 1993;268(20):15174-9.

98. Coelho SG, Choi W, Brenner M, Miyamura Y, Yamaguchi Y, Wolber R, et al. Short- and long-term effects of UV radiation on the pigmentation of human skin. Journal of Investigative Dermatology Symposium Proceedings. 2009;14(1):32-5.

99. Rana BK. New insights into G-protein-coupled receptor signaling from the melanocortin receptor system. Molecular Pharmacology. 2003;64(1):1-4.

100. D'Orazio J, Jarrett S, Amaro-Ortiz A, Scott T. UV Radiation and the Skin. International Journal of Molecular Sciences. 2013;14(6):12222-48.

101. Pasricha JS, Khaitan BK, Dash S. Pigmentary disorders in India. Dermatologic Clinics. 2007;25(3):343-52, viii.

102. Handel AC, Lima PB, Tonolli VM, Miot LDB, Miot HA. Risk factors for facial melasma in women: a case–control study. British Journal of Dermatology. 2014;171(3):588-94.

103. Kang HY, Suzuki I, Lee DJ, Ha J, Reiniche P, Aubert J, et al. Transcriptional profiling shows altered expression of wnt pathway- and lipid metabolism-related genes as well as melanogenesis-related genes in melasma. Journal of Investigative Dermatology. 2011;131(8):1692-700.

104.   Kang WH, Yoon KH, Lee ES, Kim J, Lee KB, Yim H, et al. Melasma: histopathological characteristics in 56 Korean patients. British Journal of Dermatology 2002;146(2):228-37.

105.   Mandry Pagan R, Sanchez JL. Mandibular melasma. Puerto Rico health sciences journal. 2000;19(3):231-4.

106.   Ponka D, Baddar F. Wood lamp examination. Canadian Family Physician. 2012;58(9):976-.

107.   Gupta L, Singhi M. Wood's lamp. Indian Journal of Dermatology, Venereology, and Leprology. 2004;70(2):131-5.

108.   Achar A, Rathi SK. MELASMA: A CLINICO-EPIDEMIOLOGICAL STUDY OF 312 CASES. Indian Journal of Dermatology. 2011;56(4):380-2.

109.   Tamler C, Fonseca RMR, Pereira FBC, Barcauí CB. Classifi cation of melasma by dermoscopy: comparative study with Wood's lamp. Surgical & Cosmetic Dermatology. 2009;1(3):115-9.

110.   Hann SK, Im S, Chung WS, Kim do Y. Pigmentary disorders in the South East. Dermatologic Clinics. 2007;25(3):431-8, x.

111.   Sonthalia S, Sarkar R. Etiopathogenesis of melasma. Pigment International. 2015;2(1):21-7.

112.   Lee A-Y. An updated review of melasma pathogenesis. Dermatologica Sinica. 2014;32(4):233-9.

113.   Ortonne JP, Arellano I, Berneburg M, Cestari T, Chan H, Grimes P, et al. A global survey of the role of ultraviolet radiation and hormonal influences in the development of melasma. Journal of the European Academy of Dermatology and Venereology : JEADV. 2009;23(11):1254-62.

114.   Zainuddin F, Anwar AI, Djawad K, Seweng A, Sjahril R, Adriani A. The Correlation Between Malondialdehyde Serum Levels and the Duration of Sun Exposure; and Melasma Area and Severity Index in Patients with Melasma in Makassar. American Journal of Clinical and Experimental Medicine. 2016;3(4):68-75.

115.   Im S, Kim J, On WY, Kang WH. Increased expression of alpha-melanocyte-stimulating hormone in the lesional skin of melasma. British Journal of Dermatology 2002;146(1):165-7.

116.   Tada A, Pereira E, Beitner-Johnson D, Kavanagh R, Abdel-Malek ZA. Mitogen- and Ultraviolet-B-Induced Signaling Pathways in Normal Human Melanocytes. Journal of Investigative Dermatology. 2002;118(2):316-22.

117.   Videira IFdS, Moura DFL, Magina S. Mechanisms regulating melanogenesis. Anais brasileiros de dermatologia. 2013;88(1):76-83.

118.   Brenner M, Hearing VJ. Modifying skin pigmentation – approaches through intrinsic biochemistry and exogenous agents. Drug discovery today Disease mechanisms. 2008;5(2):e189-e99.

119.   Kadekaro AL, Kavanagh R, Kanto H, Terzieva S, Hauser J, Kobayashi N, et al. α-Melanocortin and Endothelin-1 Activate Antiapoptotic Pathways and Reduce DNA Damage in Human Melanocytes. Cancer Research. 2005;65(10):4292-9.

120.   Kadekaro AL, Kavanagh RJ, Wakamatsu K, Ito S, Pipitone MA, Abdel-Malek ZA. Cutaneous photobiology. The melanocyte vs. the sun: who will win the final round? Pigment Cell Research. 2003;16(5):434-47.

121.   Kang HY, Ortonne J-P. What Should Be Considered in Treatment of Melasma. Annals of Dermatology. 2010;22(4):373-8.

122.   Thornton MJ. The biological actions of estrogens on skin. Experimental dermatology. 2002;11(6):487-502.

123.   Kim NH, Cheong KA, Lee TR, Lee AY. PDZK1 upregulation in estrogen-related hyperpigmentation in melasma. Journal of Investigative Dermatology. 2012;132(11):2622-31.

124.   Cestari TF, Dantas LP, Boza JC. Acquired hyperpigmentations. Anais Brasileiros de Dermatologia. 2014;89(1):11-25.

125.   Prabha N, Mahajan VK, Mehta KS, Chauhan PS, Gupta M. Cosmetic Contact Sensitivity in Patients with Melasma: Results of a Pilot Study. Dermatology Research and Practice. 2014;2014:9.

126.   Palumbo A, d'Ischia M, Misuraca G, Prota G. Mechanism of inhibition of melanogenesis by hydroquinone. Biochim Biophys Acta. 1991;1073(1):85-90.

127.   Levin CY, Maibach H. Exogenous ochronosis. An update on clinical features, causative agents and treatment options. American Journal of Clinical Dermatology 2001;2(4):213-7.

128. Katsambas A, Antoniou C. Melasma. Classification and treatment. Journal of the European Academy of Dermatology and Venereology : JEADV. 1995;4(3):217-23.

129. Burdock GA, Soni MG, Carabin IG. Evaluation of Health Aspects of Kojic Acid in Food. Regulatory Toxicology and Pharmacology. 2001;33(1):80-101.

130. Cabanes J, Chazarra S, Garcia-Carmona F. Kojic acid, a cosmetic skin whitening agent, is a slow-binding inhibitor of catecholase activity of tyrosinase. Journal of Pharmacy and Pharmacology. 1994;46(12):982-5.

131. Lim JT. Treatment of melasma using kojic acid in a gel containing hydroquinone and glycolic acid. Dermatologic Surgery. 1999;25(4):282-4.

132. Parejo I, Viladomat F, Bastida J, Codina C. A single extraction step in the quantitative analysis of arbutin in bearberry (Arctostaphylos uva-ursi) leaves by high-performance liquid chromatography. Phytochemical Analysis. 2001;12(5):336-9.

133. Maeda K, Fukuda M. Arbutin: mechanism of its depigmenting action in human melanocyte culture. Journal of Pharmacology and Experimental Therapeutics. 1996;276(2):765-9.

134. Matsuo Y, Ito A, Masui Y, Ito M. A case of allergic contact dermatitis caused by arbutin. Contact Dermatitis. 2015;72(6):404-5.

135. Kligman AM, Willis I. A new formula for depigmenting human skin. Archives of dermatology. 1975;111(1):40-8.

136. Talwar HS, Griffiths CE, Fisher GJ, Russman A, Krach K, Benrazavi S, et al. Differential regulation of tyrosinase activity in skin of white and black individuals in vivo by topical retinoic acid. Journal of Investigative Dermatology. 1993;100(6):800-5.

137. Romero C, Aberdam E, Larnier C, Ortonne JP. Retinoic acid as modulator of UVB-induced melanocyte differentiation. Involvement of the melanogenic enzymes expression. Journal of cell science. 1994;107 (Pt 4):1095-103.

138. Thomas JR, 3rd, Doyle JA. The therapeutic uses of topical vitamin A acid. Journal of the American Academy of Dermatology. 1981;4(5):505-13.

139. Fitton A, Goa KL. Azelaic acid. A review of its pharmacological properties and therapeutic efficacy in acne and hyperpigmentary skin disorders. Drugs. 1991;41(5):780-98.

140.   Sarkar R, Bhalla M, Kanwar AJ. A comparative study of 20% azelaic acid cream monotherapy versus a sequential therapy in the treatment of melasma in dark-skinned patients. Dermatology (Basel, Switzerland). 2002;205(3):249-54.

141.   Menter A. Rationale for the use of topical corticosteroids in melasma. Journal of drugs in dermatology : JDD. 2004;3(2):169-74.

142.   Kim H, Choi H-R, Kim D-S, Park K-C. Topical Hypopigmenting Agents for Pigmentary Disorders and Their Mechanisms of Action. Annals of Dermatology. 2012;24(1):1-6.

143.   Mimesh S, Pratt M. Allergic contact dermatitis from corticosteroids: reproducibility of patch testing and correlation with intradermal testing. Dermatitis : contact, atopic, occupational, drug. 2006;17(3):137-42.

144.   Rendon MI, Berson DS, Cohen JL, Roberts WE, Starker I, Wang B. Evidence and Considerations in the Application of Chemical Peels in Skin Disorders and Aesthetic Resurfacing. The Journal of clinical and aesthetic dermatology. 2010;3(7):32-43.

145.   Tung RC, Bergfeld WF, Vidimos AT, Remzi BK. alpha-Hydroxy acid-based cosmetic procedures. Guidelines for patient management. American Journal of Clinical Dermatology 2000;1(2):81-8.

146.   Rendon M, Berneburg M, Arellano I, Picardo M. Treatment of melasma. Journal of the American Academy of Dermatology. 2006;54(5 Suppl 2):S272-81.

147.   Fabbrocini G, Annunziata MC, D'Arco V, De Vita V, Lodi G, Mauriello MC, et al. Acne Scars: Pathogenesis, Classification and Treatment. Dermatology Research and Practice. 2010;2010:893080.

148.   Gold MH. Dermabrasion in dermatology. American Journal of Clinical Dermatology. 2003;4(7):467-71.

149.   Kim EK, Hovsepian RV, Mathew P, Paul MD. Dermabrasion. Clinics in plastic surgery. 2011;38(3):391-5, v-vi.

150.   Pei S, Inamadar AC, Adya KA, Tsoukas MM. Light-based therapies in acne treatment. Indian Dermatology Online Journal. 2015;6(3):145-57.

151.   Babilas P, Schreml S, Szeimies RM, Landthaler M. Intense pulsed light (IPL): a review. Lasers in surgery and medicine. 2010;42(2):93-104.

152.   Moreno Arias GA, Ferrando J. Intense pulsed light for melanocytic lesions. Dermatologic surgery : official publication for American Society for Dermatologic Surgery [et al]. 2001;27(4):397-400.

153.   Husain Z, Alster TS. The role of lasers and intense pulsed light technology in dermatology. Clinical, Cosmetic and Investigational Dermatology. 2016;9:29-40.

154.   Arora P, Sarkar R, Garg VK, Arya L. Lasers for Treatment of Melasma and Post-Inflammatory Hyperpigmentation. Journal of Cutaneous and Aesthetic Surgery. 2012;5(2):93-103.

155.   Stratigos AJ, Dover JS, Arndt KA. Laser treatment of pigmented lesions--2000: how far have we gone? Archives of dermatology. 2000;136(7):915-21.

156.   Mittal R, Sriram S, Sandhu K. Evaluation of Long-pulsed 1064 nm Nd:YAG Laser-assisted Hair Removal vs Multiple Treatment Sessions and Different Hair Types in Indian Patients. Journal of Cutaneous and Aesthetic Surgery. 2008;1(2):75-9.

157.   Nakagawa M, Kawai K, Kawai K. Contact allergy to kojic acid in skin care products. Contact Dermatitis. 1995;32(1):9-13.

158.   Jones K, Hughes J, Hong M, Jia Q, Orndorff S. Modulation of Melanogenesis by Aloesin: A Competitive Inhibitor of Tyrosinase. Pigment Cell Research. 2002;15(5):335-40.

159.   Kim YM, Yun J, Lee CK, Lee H, Min KR, Kim Y. Oxyresveratrol and hydroxystilbene compounds. Inhibitory effect on tyrosinase and mechanism of action. Journal of Biological Chemistry. 2002;277(18):16340-4.

160.   Lin CB, Babiarz L, Liebel F, Roydon Price E, Kizoulis M, Gendimenico GJ, et al. Modulation of microphthalmia-associated transcription factor gene expression alters skin pigmentation. Journal of Investigative Dermatology. 2002;119(6):1330-40.

161.   Yoshimura M, Watanabe Y, Kasai K, Yamakoshi J, Koga T. Inhibitory effect of an ellagic acid-rich pomegranate extract on tyrosinase activity and ultraviolet-induced pigmentation. Bioscience, Biotechnology and Biochemistry. 2005;69(12):2368-73.

162.   Cho YH, Kim JH, Park SM, Lee BC, Pyo HB, Park HD. New cosmetic agents for skin whitening from Angelica dahurica. Journal of Cosmetic Sciences. 2006;57(1):11-21.

163.   Lee TH, Seo JO, Baek S-H, Kim SY. Inhibitory Effects of Resveratrol on Melanin Synthesis in Ultraviolet B-Induced Pigmentation in Guinea Pig Skin. Biomolecules & Therapeutics. 2014;22(1):35-40.

164.   Hu S, Zheng Z, Zhang X, Chen F, Wang M. Oxyresveratrol and trans-dihydromorin from the twigs of Cudrania tricuspidata as hypopigmenting agents against melanogenesis. Journal of Functional Foods. 2015;13(Complete):375-83.

165.   Ching J, Chua T-K, Chin L-C, Lau A-J, Pang Y-K, Jaya JM. β-Amyrin from Ardisia elliptica Thunb. is more potent than aspirin in inhibiting collagen-induced platelet aggregation. Indian Jounal of Experimental Biology. 2010;48:275-9.

166.   Ching J, Chua TK, Chin LC, Lau AJ, Pang YK, Jaya JM, et al. Beta-amyrin from Ardisia elliptica Thunb. is more potent than aspirin in inhibiting collagen-induced platelet aggregation. Indian journal of experimental biology. 2010;48(3):275-9.

167.   Khatun A, Rahman M, Kabir S, Akter MN, Chowhury SA. Phytochemical and pharmacological properties of methanolic extract of Ardisia humilis VAHL. (MYRSINACEAE). International Journal of Research in Ayurveda and Pharmacy. 2013;4(1):38-41.

168.   Phadungkit M, Luanratana O. Anti-Salmonella activity of constituents of Ardisia elliptica Thunb. Natural product research. 2006;20(7):693-6.

169.   Alias NZ, Ishak NKM. Chemical Constituents and Bioactivity Studies of Ardisia Elliptica The Open Conference Proceedings Journal. 2014;5(2):1-4.

170.   Al-Abd NM, Nor ZM, Mansor M, Zajmi A, Hasan MS, Azhar F, et al. Phytochemical constituents, antioxidant and antibacterial activities of methanolic extract of Ardisia elliptica. Asian Pacific Journal of Tropical Biomedicine. 2017;7(6):569-76.

171.   Raga DD, Herrera AA, Alimboyoguen AB, Shen C-C, Ragasa CY. Effects of triterpenes from Ardisia cf. elliptica (subgenus Tinus) and sterols from Ardisia pyramidalis Cav Pers on Artemia salina and Danio rerio toxicity and caudal fin regeneration. Journal of Chemical and Pharmaceutical Research. 2014;6(3):1014-22.

172.   Patel E, Padiya R, Acharya R, Shukla V. Preliminary Phytochemical evaluation of stem bark, root, leaf of Croton roxburghii Balak. (Euphorbiaceae) Pharmaceutical and Biological Evaluations. 2014;1:29-34.

173.   Panda SK, Dutta SK, Bastia AK. Antibacterial activity of Croton roxburghii Balak. against the enteric pathogens. Journal of Advanced Pharmaceutical Technology & Research. 2010;1(4):419-22.

174.   Panda SK, Bastia AK, Dutta SK. Anticandidal activity of *Croton roxburghii* Balak. International Journal of Current Pharmaceutical Research. 2010;2(4):55-9.

175.   Sivakumar T, Rajavel R, Karthikeyan D, Duraisamy R, Srinivasan K, kumar SS, et al. Anti-pyretic and anti-inflammatory activity of chloroform extract of Croton roxburghii in standard animal models. Oriental Pharmacy and Experimental Medicine. 2008;8(3):252-9.

176.   Esser H-J, Chayamarit K. Two new species and a new name in Thai Croton (Euphorbicaceae). Thai Forest Bulletin (Botany). 2001;29:51-7.

177.   Kawai K, Tsuno NH, Kitayama J, Okaji Y, Yazawa K, Asakage M, et al. Anti-angiogenic properties of plaunotol. Anti-cancer drugs. 2005;16(4):401-7.

178.   Matsumoto Y, Hamashima H, Masuda K, Shiojima K, Sasatsu M, Arai T. The antibacterial activity of plaunotol against Staphylococcus aureus isolated from the skin of patients with atopic dermatitis. Microbios. 1998;96(385):149-55.

179.   Chaotham C, Chivapat S, Chaikitwattana A, De-Eknamkul W. Acute and Chronic Oral Toxicity of a Partially Purified Plaunotol Extract from Croton stellatopilosus Ohba. BioMed Research International. 2013;2013:12.

180.   Monira KM, Munan SM. Review on Datura metel L.: A Potential Medicinal Plant Global Journal of Research on Medicinal Plants & Indigenous Medicine 2012;1(4):123-32.

181.   Sanni DM, Omotoyinbo OV. Inhibitory Effect of Extracts from Datura metel Leaf on Mushroom Tyrosinase. American Journal of Life Sciences. 2016;4(2):47-50.

182.   Dhawan D, Gupta J. Comparison of Different Solvents for Phytochemical Extraction Potential from Datura metel Plant Leaves. International Journal of Biological Chemistry. 2017;11:17-22.

183.   Sangeetha S, Deepa M, Sugitha N, Mythili S, Sathiavelu A. Antioxidant activity and Phytochemical Analysis of Datura metel. International Journal of Drug Development and Research. 2014;6(4):280-5.

184.   Maheshwari NO, Khan A, Chopade BA. Rediscovering the medicinal properties of Datura sp.: A review. Journal of Medicinal Plants Research. 2013;7(39):2885-97.

185.   Pedraza-Chaverri J, Cárdenas-Rodríguez N, Orozco-Ibarra M, Pérez-Rojas JM. Medicinal properties of mangosteen (Garcinia mangostana). Food and Chemical Toxicology. 2008;46(10):3227-39.

186.   Arif NJ, Yahya A, Hamid MA, Yaakob H, Mohamed R, Zulkifli. Development of Lightening Cream from Mangosteen Pericarp Extract with Olivoil Emulsifier International Conference on Education, Research and Innovation. 2014;68:58-65.

187.   Chomnawang MT, Surassmo S, Nukoolkarn VS, Gritsanapan W. Effect of Garcinia mangostana on inflammation caused by Propionibacterium acnes. Fitoterapia. 2007;78(6):401-8.

188.   Chomnawang MT, Surassmo S, Nukoolkarn VS, Gritsanapan W. Effect of Garcinia mangostana on inflammation caused by Propionibacterium acnes. Fitoterapia. 2007;78:401-8.

189.   Li G, Thomas S, Johnson JJ. Polyphenols from the mangosteen (Garcinia mangostana) fruit for breast and prostate cancer. Frontiers in Pharmacology. 2013;4:80.

190.   Shan T, Ma Q, Guo K, Liu J, Li W, Wang F, et al. Xanthones from Mangosteen Extracts as Natural Chemopreventive Agents: Potential Anticancer Drugs. Current molecular medicine. 2011;11(8):666-77.

191.   Kosem N, Ichikawa K, Utsumi H, Moongkarndi P. In vivo toxicity and antitumor activity of mangosteen extract. Journal of Natural Medicines. 2013;67(2):255-63.

192.   Nakbanpote W, Paitlertumpai N, Sukadeetad K, Meesungeon O, Noisa-nguan W. Advances in Phytoremediation Research: A Case Study of Gynura Pseudochina (L.) DC. Advanced Knowledge Application in Practice. 2010:353-78.

193.   Siriwatanametanon N, Prieto J, Heinrich M. Chemical and biological studies on the methanol extract of Gynura pseudochina var. hispida. Planta Medica. 2010;76(12):P286.

194.   Rerknimitr P. Gynura pseudochina downregulates nuclear factor-kB leading to an improvement of chronic plaque psoriasis. Journal of the American Academy of Dermatology. 2016;74(5):AB252.

195.   Windono T, Jenie UA, Kardono LBS. Isolation and Elucidation of Pyrrolizidine alkaloids from tuber of Gynura pseudo-china (L.) DC. Journal of Applied Pharmaceutical Science. 2012;2(5):5-9.

196.   Shanker R, Vankar PS. Dyeing cotton, wool and silk with Hibiscus mutabilis (Gulzuba). Dyes and Pigments. 2007;74(2):464-9.

197.   Das S, Lariya S, Gautam GK. Antidiabetic Activity of Methanolic Extract of Hibiscus Mutabilis Leaves Against Alloxan Induced Diabetes in Rats. International Journal of Pharmaceutical and Chemical Sciences. 2013;2(3):1204-7.

198.   Kumar D, Kumar H, Vedasiromoni JR, C.Pal B. Bio-assay Guided Isolation of a-GlucosidaseInhibitory Constituents from HibiscusMutabilis Leaves. Phytochemical analysis. 2012;23:421-5.

199.   Liu D, Mei Q, Wan X, Que H, Li L, Wan D. Determination of Rutin and Isoquercetin Contents in Hibisci mutabilis Folium in Different Collection Periods by HPLC. Journal of Chromatographic Science. 2015;53(10):1680-4.

200.   Wong S, Lim Y, Chan E. Evaluation of Antioxidant, Anti-tyrosinase and Antibacterial Activities of Selected Hibiscus Species2010. 781 p.

201.   Wang J, Li X, Gao L, Wang X. In Vitro Anti-Inflammatory Mechanism of Folium Hibisci Mutabilis Leaves Ethanol Extracts. African Journal of Traditional, Complementary, and Alternative Medicines. 2014;11(1):127-30.

202.   Manigaunha A, Ganesh N, Kharya MD. Morning glory: A new thirst in-search of de-novo therapeutic approach. International Journal of Phytomedicine 2010;2:18-21.

203.   U P, L B, S S, S W. Antiinflammatory activity of Ipomoea pes-caprae (L.) R. Br. Phytotherapy Research. 1991;5(2):63-6.

204.   Pongprayoon U, Bohlin L, Wasuwat S. Neutralization of toxic effects of different crude jellyfish venoms by an extract of Ipomoea pes-caprae (L.) R. Br. Journal of Ethnopharmacology. 1991;35(1):65-9.

205.   Ganjir M, Behera DR, Bhatnagar S. Phytochemical Analysis, Cytotoxic And Antioxidant Potential Of Ipomoea Pes Caprae(L)R.Br And Merremia Umbellata(L.)H. Hallier. International Journal of Scientific & Technology Research. 2013;2(5):80-3.

206. S S, C E, A B. Hepatoprotective effect of *Ipomoea pes-caprae* leaves extract in streptozotocin induced diabetic rats. International Journal of Pharmacy and Pharmaceutical Science Research. 2014;4(2):27-30.

207. Pongprayoon U, Bohlin L, Soonthornsaratune P, Wasuwat S. Antiinflammatory activity of Ipomoea pes‑caprae (L.) R. Br1991. 63-6 p.

208. Venkataraman ND, Atleeb WC, Prabhuc TP, Kannana R. Anti-inflammatory potential of ethanolic extracts from aerial parts of Ipomoea pes-caprae (L.) R.Br using cotton pellet induced granuloma model2013. 61-3 p.

209. P N, V UR. Pharmacological potential of Ipomea pes-caprae (L.) R. Br. whole plant extracts Pelagia Research Library 2015;6(2):52-60.

210. Devi SS, Paul SB. AN OVERVIEW ON Cicca acida (Phyllanthus acidus). Assam University Journal of Science & Technology: Biological and Environmental Sciences. 2011;7(1):156-60.

211. Jain NK, Singhai AK. Protective effects of Phyllanthus acidus (L.) Skeels leaf extracts on acetaminophen and thioacetamide induced hepatic injuries in Wistar rats. Asian Pacific Journal of Tropical Medicine. 2011;4(6):470-4.

212. Talubmook C, Buddhakala N. Hypoglycemic and Hypolipidemic Properties of Leaf Extracts from Phyllanthus acidus (L.) Skeels., Leucaena leucocephala (Lam.) de Wit. and Psidium guajava (L.) in StreptozotocinInduced Diabetic Rats GSTF International Journal of BioSciences. 2013;2(2):30-4.

213. Singh J, Kaur S. Phyllanthus embilica Leaves Extract: A Potential Amylase enzyme Inhibitor with antioxidant and antimicrobial activity. International Journal of Pharmacological Research. 2015;5(9):200-6.

214. Kumari OS, Rao NB, Chawhan3 LP, Rachel B. Phyto-chemical analysis of *Phyllanthus amarus* (NELA USIRI), *Phyllanthus embilica* and *Phyllanthus acidus*. World Journal of Pharmaceutical Research. 2014;4(1):1457-62.

215. Das N. Propagation prospects of dye yielding plant *Rhinnacanthus nasutus* (Linn.) Kurz. Natural Product Raddiance 2006;5(1):42-3.

216. Visweswara Rao P, Madhavi K, Dhananjaya Naidu M, Gan SH. Rhinacanthus nasutus Ameliorates Cytosolic and Mitochondrial Enzyme Levels in Streptozotocin-

Induced Diabetic Rats. Evidence-Based Complementary and Alternative Medicine. 2013;2013:6.

217.   Bhusal N, Panichayupakaranant P, Reanmongkol W. In vivo analgesic and anti-inflammatory activities of a standardized Rhinacanthus nasutus leaf extract in comparison with its major active constituent rhinacanthin-C. Songklanakarin Journal of Science and Technology. 2014;36(3):325-31.

218.   Tomomura M, Suzuki R, Shirataki Y, Sakagami H, Tamura N, Tomomura A. Rhinacanthin C Inhibits Osteoclast Differentiation and Bone Resorption: Roles of TRAF6/TAK1/MAPKs/NF-KB/NFATc1 Signaling. PLOS ONE. 2015;10(6):e0130174.

219.   G J, F GS. Phytochemical analysis and antimicrobial efficacy of Rhinacanthus nasutus (l) Linn. Journal of Pharmacognosy and Phytochemistry. 2015;3(6):83-6.

220.   Visweswara Rao P, Dhananjaya Naidu M. Anti Diabetic Effect of Rhinacanthus nasutus Leaf Extract in Streptozotocin Induced Diabetic Rats2010.

221.   Visweswara Rao P, Madhavi K, Dhananjaya Naidu M, Gan SH. Rhinacanthus nasutus Improves the Levels of Liver Carbohydrate, Protein, Glycogen, and Liver Markers in Streptozotocin-Induced Diabetic Rats. Evidence-based Complementary and Alternative Medicine : eCAM. 2013;2013:102901.

222.   Dave H, Ledwani L. A review on anthraquinones isolated from *Cassia* species and their applications. Indian Jounal of Natural Products and Resources. 2012;3(3):291-319.

223.   Gritsanapan W, Mangmeesri P. Standardized *Senna alata* leaf extract. Journal of Health Research. 2009;23(2):59-64.

224.   Esimone C, Nworu C, Ekong U, Okereke B. Evaluation of the antiseptic properties of Cassia alata-based herbal soap. The Internet Journal of Alternative Medicine. 2007;6(1):1-5.

225.   Saito ST, Trentin DdS, Macedo AJ, Pungartnik C, Gosmann G, Silveira JdD, et al. Bioguided Fractionation Shows Cassia alata Extract to Inhibit Staphylococcus epidermidis and Pseudomonas aeruginosa Growth and Biofilm Formation. Evidence-based Complementary and Alternative Medicine : eCAM. 2012;2012:867103.

226.   Yakubu MT, Musa IF. Effects of Post-coital Administration of Alkaloids from Senna alata (Linn. Roxb) Leaves on some Fetal and Maternal Outcomes of Pregnant Rats. Journal of Reproduction & Infertility. 2012;13(4):211-7.

227.   Roy S, Ukil B, Lyndem LM. Acute and sub-acute toxicity studies on the effect of Senna alata in Swiss Albino mice. Cogent Biology. 2016;2(1).

228.   Kongkiatpaiboon S, Mikulicic S, Keeratinijakal V, Greger H, Gritsanapan W. HPLC simultaneous analysis for quality assessment of Stemona curtisii roots and determination of their insecticidal activities. Industrial Crops and Products. 2013;43:648-53.

229.   Chaiyong S, Jatisatienr A, Mungkornasawakul P, Sastraruji T, Pyne SG, Ung AT, et al. Phytochemical Investigations of Stemona curtisii and Synthetic Studies on Stemocurtisine Alkaloids. Journal of Natural Products. 2010;73(11):1833-8.

230.   Ghosh A, Chowdhury N, Chandra G. Plant extracts as potential mosquito larvicides. Indian Journal of Medical Research. 2012;135(581-598).

231.   Chiranthanut N, Khonsung P, Jatisatienr A, Dheeranupatana S, Panthong A. Acute Dermal Toxicity and Repeated Dose 90-Day Oral Toxicity Studies of the Bioinsecticide from Stemona curtisii Hook. F. CMU Journal of Natural of Sciences. 2011;10(1):15-26.

232.   Rastogi S, Kulshreshtha DK, Rawat AKS. Streblus asper Lour. (Shakhotaka): A Review of its Chemical, Pharmacological and Ethnomedicinal Properties. Evidence-based Complementary and Alternative Medicine. 2006;3(2):217-22.

233.   Wongkham S, Laupattarakasaem P, Pienthaweechai K, Areejitranusorn P, Wongkham C, Techanitiswad T. Antimicrobial Activity of Streblus asper Leaf Extract. Phytotherapy Research. 2001;15:199-21.

234.   Taweechaisupapong S, Choopan T, Singhara S, Chatrchaiwiwatana S, Wongkham S. In vitro inhibitory effect of Streblus asper leaf-extract on adhesion of Candida albicans to human buccal epithelial cells. Journal of Ethnopharmacology. 2005;96(1-2):221-6.

235.   Sripanidkulchai B, Junlatat J, Wara-aswapati N, Hormdee D. Anti-inflammatory effect of Streblus asper leaf extract in rats and its modulation on inflammation-

associated genes expression in RAW 264.7 macrophage cells. Journal of Ethnopharmacology. 2009;124(3):566-70.

236. Rastogi S, Kulshreshtha DK, Rawat AKS. Streblus asper Lour. (Shakhotaka): A Review of its Chemical, Pharmacological and Ethnomedicinal Properties. Journal and Oxford University Press. 2006;3(2):217-22.

237. Kumar RBS, Puratchikodi A, Prasanna A, Dolai N, Majumder P, Mazumder UK, et al. Pre clinical studies of Streblus asper Lour in terms of behavioural safety and toxicity. Oriental Pharmacy and Experimental Medicine. 2011;11(4):243-9.

238. Jensen WB. The Origin of the Soxhlet Extractor. Journal of Chemical Education. 2007;84(12):1913.

239. Chang L-W, Yen W-J, Huang SC, Duh P-D. Antioxidant activity of sesame coat. Food Chemistry. 2002;78(3):347-54.

240. C. Zongo, A. Savadogo, L. Ouattara, I.H.N. Bassole, C.A.T. Ouattara, A.S. Ouattara, et al. Polyphenols Content, Antioxidant and Antimicrobial Activities of Ampelocissus grantii (Baker) Planch. (Vitaceae): A Medicinal Plant from Burkina Faso. International Journal of Pharmacology. 2010;6:880-7.

241. Kalita P, Tapan BK, Pal TK, Kalita R. Estimation of total flavonoids content (TFC) and antiocidant activities of methnolic whole plants extract of *Biophytum Sensitivum* Linn. Journal of Drug Delivery and Therapeutics. 2013;3(4):33-7.

242. Yamasaki K, Hashimoto A, Kokusenya Y, Miyamoto T, Sato T. Electrochemical method for estimating the antioxidative effects of methanol extracts of crude drugs. Chemical & Pharmaceutical Bulletin (Tokyo). 1994;42(8):1663-5.

243. Re R, Pellegrini N, Proteggente A, Pannala A, Yang M, Rice-Evans C. Antioxidant activity applying an improved ABTS radical cation decolorization assay. Free Radical Biology & Medicine. 1999;26(9-10):1231-7.

244. Nithitanakool S, Pithayanukul P, Bavovada R, Saparpakorn P. Molecular docking studies and anti-tyrosinase activity of Thai mango seed kernel extract. Molecules. 2009;14(1):257-65.

245. van Meerloo J, Kaspers GJ, Cloos J. Cell sensitivity assays: the MTT assay. Methods in Molecular Biology. 2011;731:237-45.

246. Su TR, Lin JJ, Tsai CC, Huang TK, Yang ZY, Wu MO, et al. Inhibition of melanogenesis by gallic acid: possible involvement of the PI3K/Akt, MEK/ERK and Wnt/beta-catenin signaling pathways in B16F10 cells. International Journal of Molecular Sciences. 2013;14(10):20443-58.

247. Ernst O, Zor T. Linearization of the Bradford Protein Assay. Journal of Visualized Experiments : JoVE. 2010(38):1918.

248. Seon Kyu Han, Wook Hee Choi, Hyoung Soo Ann, Ryoung Me Ahn, Yi SY. Effects of EGb 761 and Korean Red Ginseng on Melanogenesis in B16F10 Melanoma Cells and Protection Against UVB Irradiation in Murine Skin. Molecular & cellular toxicology. 2008;4(1):85-91.

249. Kim HE, Ishihara A, Lee SG. The effects of Caffeoylserotonin on inhibition of melanogenesis through the downregulation of MITF via the reduction of intracellular cAMP and acceleration of ERK activation in B16 murine melanoma cells. BMB Reports. 2012;45(12):724-9.

250. Sulaiman CT, Balachandran I. Total phenolics and total flavonoids in selected Indian medicinal plants. Indian Journal of Pharmaceutical Sciences. 2012;74(3):258-60.

251. Falcone Ferreyra ML, Rius SP, Casati P. Flavonoids: biosynthesis, biological functions, and biotechnological applications. Frontiers in Plant Science. 2012;3:222.

252. Norlida Mamat, Jamia Azdina Jamal, Ibrahim Jantan , Khairana Husain. Xanthine Oxidase Inhibitory and DPPH Radical Scavenging Activities of Some Primulaceae Species. Sains Malaysiana. 2014;43(12):1827-33.

253. Penpun Wetwitayaklung, Juree Charoenteeraboon, Chutima Limmatvapirat, Phaechamud T. Antioxidant Activities of Some Thai and Exotic Fruits Cultivated in Thailand. Research Journal of Pharmaceutical, Biological and Chemical Sciences. 2012;3(1):12-21.

254. Kumar Devendra, Dhurandhar Kiran, Verma Ritesh, Barman Satyendra, Abhishek K. To Evaluation of Total Phenolics and Flavonoids in Different Plant of Chhattisgarh. Journal of Pharmacognosy and Phytochemistry. 2013;2(4):116-8.

255. A.M. Siti-Azima, Noriham A, Nurhuda M. Antioxidant Activities of Syzygium Cumini and ArdisiaElliptica in Relation to Their Estimated Phenolic Compositions and

Chromatic Properties. International Journal of Bioscience, Biochemistry and Bioinformatics. 2013;3(4):314-7.

256.   Solovchenko A, Schmitz-Eiberger M. Significance of skin flavonoids for UV-B-protection in apple fruits. Journal of Experimental Botany. 2003;54(389):1977-84.

257.   Gonzalez-Gallego J, Sanchez-Campos S, Tunon MJ. Anti-inflammatory properties of dietary flavonoids. Nutrición Hospitalaria. 2007;22(3):287-93.

258.   A. Sudha, K. Sumathi, S. Manikandaselvi, N.M. Prabhu, Srinivasan P. Anti-hepatotoxic Activity of Crude Flavonoid Fraction of Lippia nodiflora L. on Ethanol Induced Liver Injury in Rats. Asian Journal of Animal Sciences. 2013;7(1):1-13.

259.   Sak K. Cytotoxicity of dietary flavonoids on different human cancer types. Pharmacognosy Reviews. 2014;8(16):122-46.

260.   Zhu W, Gao J. The Use of Botanical Extracts as Topical Skin-Lightening Agents for the Improvement of Skin Pigmentation Disorders. Journal of Investigative Dermatology Symposium Proceedings. 2008;13(1):20-4.

261.   Freitag FM, Cestari TF, Leopoldo LR, Paludo P, Boza JC. Effect of melasma on quality of life in a sample of women living in southern Brazil. Journal of the European Academy of Dermatology and Venereology : JEADV. 2008;22(6):655-62.

262.   Augustus OK, Janet JO, Ebenezer TB, Ogboma UJ. Antioxidant Activities, Total Flavonoid and Total Phenolic Contents of Whole Plant of Kyllinga Erecta Shumach. Journal of Food and Nutrition Research. 2015;3(8):489-94.

263.   Fawole OA, Makunga NP, Opara UL. Antibacterial, antioxidant and tyrosinase-inhibition activities of pomegranate fruit peel methanolic extract. BMC Complementary and Alternative Medicine. 2012;12(1):200.

264.   Chan EWC, Lim YY, Wong LF, Lianto FS, Wong SK, Lim KK, et al. Antioxidant and tyrosinase inhibition properties of leaves and rhizomes of ginger species. Food Chemistry. 2008;109(3):477-83.

265.   Park JW, Yuk HG, Lee SC. Antioxidant and tyrosinase inhibitory activities of different parts of oriental cherry (Prunus serrulata var. spontanea). Food Science and Biotechnology. 2012;21(2):339-43.

266. Liu Q, Zhang YJ, Yang CR, Xu M. Phenolic antioxidants from green tea produced from Camellia crassicolumna Var. multiplex. Journal of Agricultural and Food Chemistry. 2009;57(2):586-90.

267. Yamakoshi J, Sano A, Tokutake S, Saito M, Kikuchi M, Kubota Y, et al. Oral intake of proanthocyanidin-rich extract from grape seeds improves chloasma. Phytotherapy research : PTR. 2004;18(11):895-9.

268. Ali SA, Galgut JM, Choudhary RK. On the novel action of melanolysis by a leaf extract of Aloe vera and its active ingredient aloin, potent skin depigmenting agents. Planta Med. 2012;78(8):767-71.

269. Tadokoro T, Bonte F, Archambault JC, Cauchard JH, Neveu M, Ozawa K, et al. Whitening efficacy of plant extracts including orchid extracts on Japanese female skin with melasma and lentigo senilis. Journal of Dermatology. 2010;37(6):522-30.

270. Evans JA, Johnson EJ. The Role of Phytonutrients in Skin Health. Nutrients. 2010;2(8):903-28.

271. Kedare SB, Singh RP. Genesis and development of DPPH method of antioxidant assay. Journal of Food Science and Technology. 2011;48(4):412-22.

272. Lesley K MacDonald-Wicks, Lisa G Wood, Garg ML. Methodology for the determination of biological antioxidant capacity in vitro: a review. Journal of the Science of Food and Agriculture. 2006;86(13):2046-56.

273. Floegel A, Kim D-O, Chung S-J, Chun OK. Comparison of ABTS/DPPH assays for the detection of antioxidant capacity in foods. The FASEB Journal. 2010;24(1 Supplement):535.9.

274. Masuda T, Yamashita D, Takeda Y, Yonemori S. Screening for Tyrosinase Inhibitors amnong Extracts of Seashore Plants and Identification of Potent Inhibitors from Garcinia subelliptica. Bioscience, Biotechnology and Biochemistry. 2005;69(1):197-201.

275. F'Guyer S, Afaq F, Mukhtar H. Photochemoprevention of skin cancer by botanical agents. Photodermatology, photoimmunology & photomedicine. 2003;19(2):56-72.

276. Narendhirakannan RT, Hannah MAC. Oxidative Stress and Skin Cancer: An Overview. Indian Journal of Clinical Biochemistry. 2013;28(2):110-5.

277.   Pillaiyar T, Manickam M, Namasivayam V. Skin whitening agents: medicinal chemistry perspective of tyrosinase inhibitors. Journal of Enzyme Inhibition and Medicinal Chemistry. 2017;32(1):403-25.

278.   Moonrungsee N, Shimamura T, Kashiwagi T, Jakmunee J, Higuchi K, Ukeda H. Sequential injection spectrophotometric system for evaluation of mushroom tyrosinase-inhibitory activity. Talanta. 2012;101:233-9.

APPENDIX

Appendix A

Calibration curve

1. Calibration curve of standard gallic acid for determining total phenolic content by using Folin-Ciocalteu method.
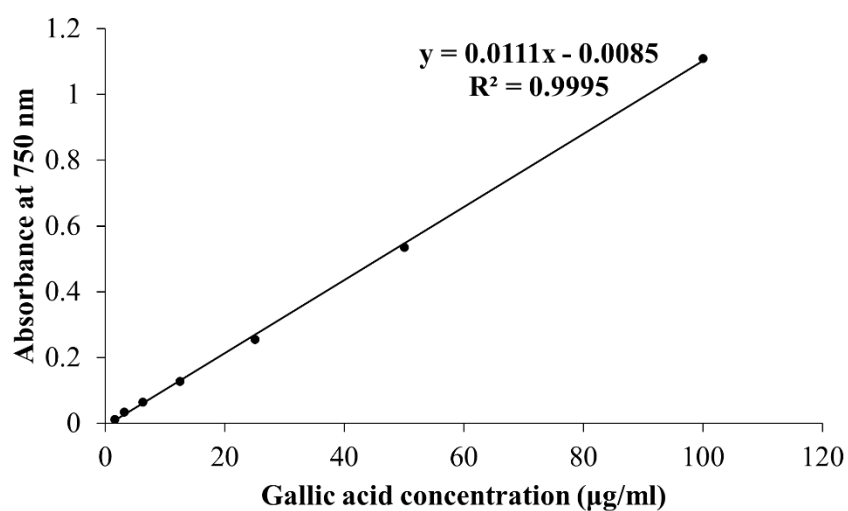
Figure 93. Calibrate curve of gallic acid.

2. Calibration curve of standard quercetin for estimating total flavonoid content by using Aluminium Chloride Colorimetric assay.
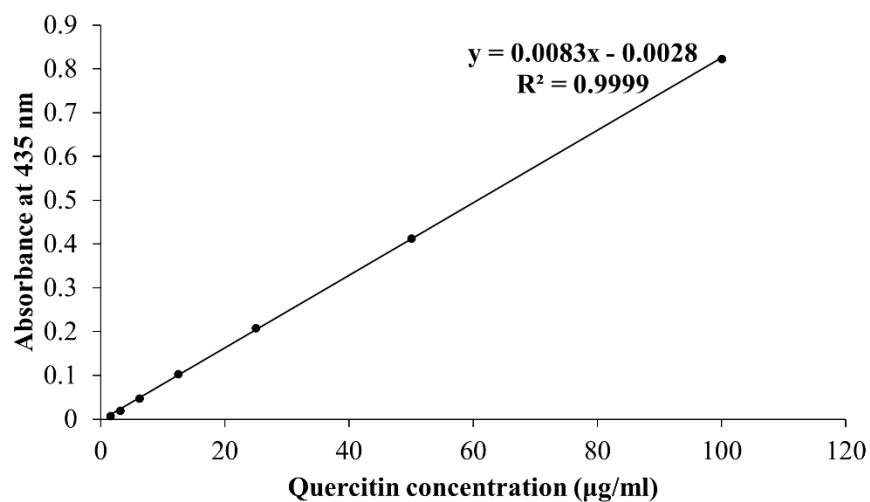
Figure 94. Calibrate curve of quercetin.

3. Calibration curve of standard ascorbic acid for investigating DPPH radical scavenging activity by DPPH assay.
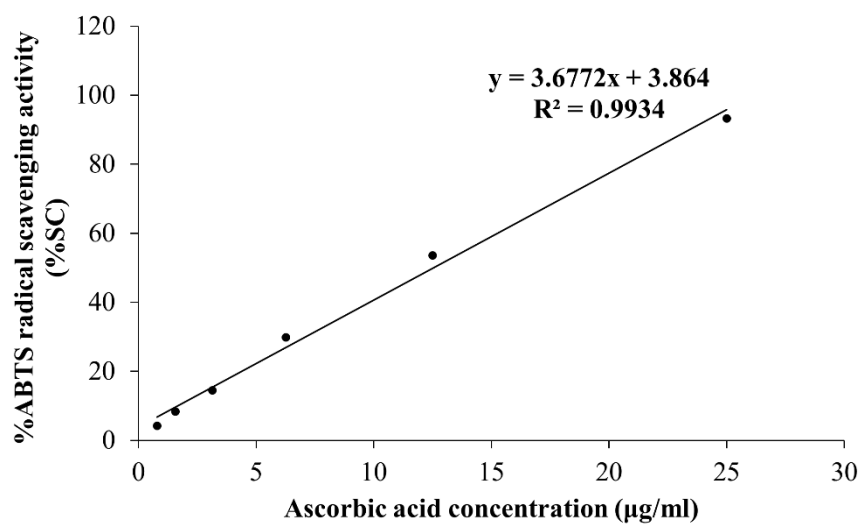
Figure 95. Calibrate curve of ascorbic acid.

4. Calibration curve of standard ascorbic acid for estimating ABTS radical scavenging activity by ABTS assay.

Figure 96. Calibration curve of ascorbic acid.

5. Calibration curve of standard synthetic melanin for determining melanin content.

Figure 97. Calibration curve of synthetic melanin.

6. Calibration curve of bovine serum albumin (BSA) for investigating protein concentration by using Bradford assay.
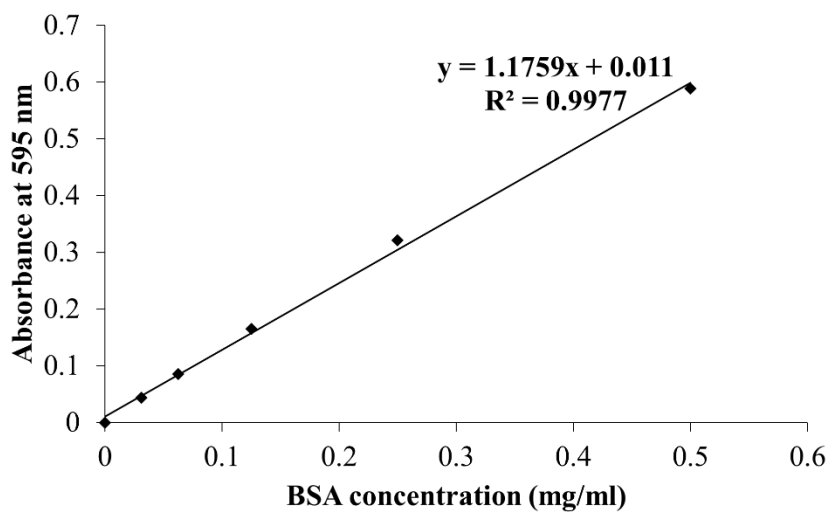
Figure 98. Calibration curve of synthetic melanin.

Appendix B

Reagents and Chemicals

1. Folin-Ciocalteu method

    1.1 10% Folin-Ciocalteu reagent

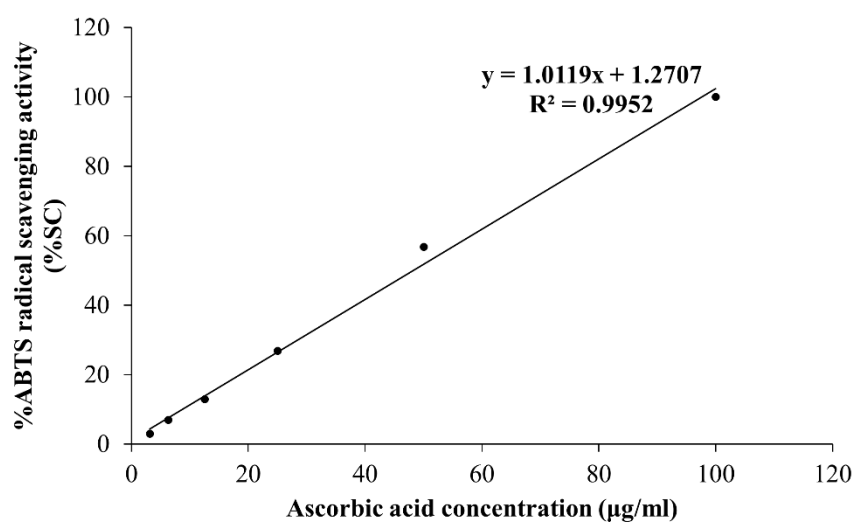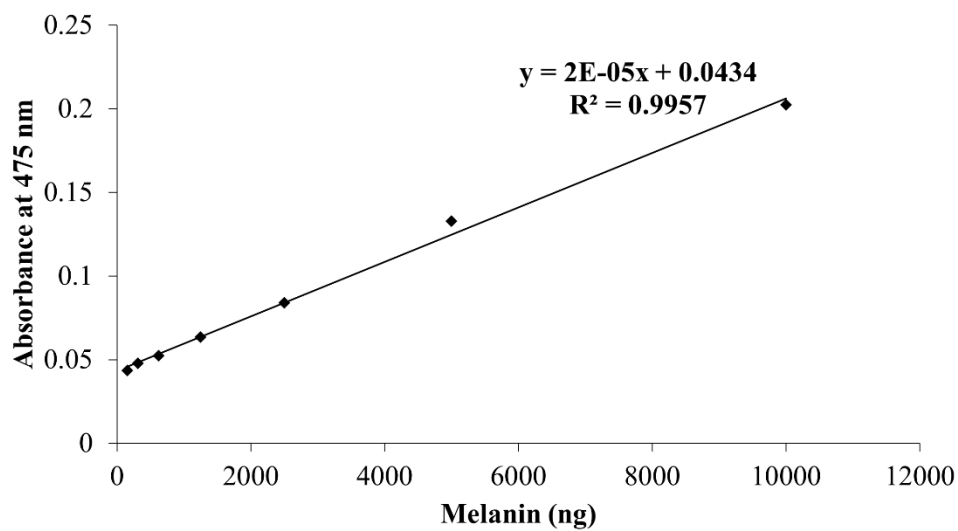   10% Folin-Ciocalteu reagent was prepared from 2 ml of 100% Folin-Ciocalteu reagent dissolved in 18 ml of distilled water and kept at 4°C.

    1.2 0.1 M Sodium carbonate (Na_2CO_3)

    0.1M Na_2CO_3 was prepared by dissolving 10.60 g of Na_2CO_3 in 100 ml of distilled water and kept at 4°C.

    1.3 1 mg/ml of Gallic acid

    1 mg of gallic acid was dissolved in 1 ml of distilled water and kept at -20°C.

2. Aluminium chloride ($AlCl_3$) colorimetric assay

    2.1 2% $AlCl_3$

    2% $AlCl_3$ was prepared from 1 g of $AlCl_3$ dissolved in 50 ml of distilled water and kept at 4°C.

    2.2 80% Ethanol solution

    40 ml of absolute ethanol was dissolved in 10 ml of distilled water and kept at 4°C.

    2.3 1 mg/ml of Quercetin

    Quercetin (1 mg) was prepared in 80% ethanol solution and kept at -20°C.

3. DPPH assay

    3.1 2.5 mM DPPH solution (prepare freshly before use)

    2.5 mM DPPH solution was prepared from 4.95 g of DPPH dissolved in 50 ml of absolute methanol and adjusted the absorbance about 0.7 ± 0.02 at 514 nm.

3.2 1 mg/ml of Ascorbic acid

        1 mg of ascorbic acid was dissolved in 1 ml of absolute methanol and kept at -20°C.

4. ABTS assay

    4.1 7 mM ABTS solution

        144 mg of ABTS was dissolved in 40 ml of distilled water and kept at -20°C.

    4.2 2.45 mM Potassium permanganate ($KMnO_4$)

        3.31 mg of $KMnO_4$ was dissolved in 50 ml of distilled water and kept at -20°C.

    4.3 ABTS$^{\bullet+}$ solution (prepare freshly)

- 8 ml of 7 mM ABTS solution was mixed with 12 ml of 2.45 mM $KMnO_4$ and stand in a dark condition at 4°C for 16-18 h.

- Absorbance of ABTS$^{\bullet+}$ solution was adjusted with absolute ethanol about 0.7 ± 0.02 at 734 nm.

    4.4 1 mg/ml of Ascorbic acid

        Ascorbic acid at 1 mg/ml was prepared from 1 mg dissolved in 1 ml of absolute ethanol and kept at -20 $^{\circ}$C.

5. Anti-mushroom tyrosinase activity

    5.1 20 mM Sodium phosphate buffer

        312 mg of NaH_2PO_4 and 284 mg of Na_2HPO_4 were dissolved in 100 ml of distilled water.

    5.2 2.5 mM L-DOPA

        L-DOPA (2.465 mg) was dissolved in 5 ml of distilled water.

    5.3 Kojic acid at 1 mg/ml

        1 mg of kojic acid was dissolve in 1 mg of 20 mM sodium phosphate buffer.

6. Culture medium for B16F10 cells

    6.1 DMEM/High glucose with 10% fetal bovine serum albumin (FBS)

        45 ml of DMEM/High glucose medium was mixed with 5 ml of FBS and supplemented with 100 U/mL penicillin and 100 µg/mL streptomycin.

    6.2 1X Phosphate Buffer Saline (PBS), pH 7.4

        100 ml of Phosphate buffer saline was diluted in 900 ml of milliQ water and kept at 4°C.

7. MTT assay

    7.1 MTT at 5 mg/ml

        MTT (50 mg) was dissolved in 10 ml of phosphate buffer saline at pH and then filter with 0.22 µm (kept at -20°C.)

    7.2 Stock solution of 6×10^{-4} M Alpha-MSH solution

        5 mg of alpha-MSH was diluted in 5 ml of autoclaved milliQ water and kept at -20°C.

8. Melanin content assay

    8.1 Stock of synthetic melanin at 10 mg/ml

        Synthetic melanin (10 mg) was dissolved in 1 ml of 1 N NaOH and kept at -20°C.

    8.2 1 Sodium hydroxide (NaOH)

        4 g of NaOH was dissolved in 40 ml of distilled water and kept at 4°C.

9. Bradford assay

    9.1 1X Bradford reagent

        10 ml of 5X Bradford reagent was diluted in 40 ml of distilled water and filtered through Whatman No.1.

    9.2 Bovine serum albumin (BSA) at 1 mg/ml

        Bovine serum albumin (1 mg) was dissolve in 1 ml of distilled water and kept at 4°C.

10. Cellular tyrosinase activity

    10.1 11% Triton X-100

        5 ml of Triton X-100 was diluted in 45 ml of phosphate buffer saline (PBS) and kept at 4°C.

    10.2 0.1 M Sodium phosphate buffer, pH 7.0

        0.7098 of Na_2HPO_4 and 0.5999 g of Na_2HPO_4 were dissolved in 50 ml of distilled water and adjusted at pH 7.0.

    10.3 5 mM 3, 4-Dihydroxyl-L-phenylalanine (L-DOPA)

        L-DOPA (0.986 mg) was dissolved in 1 ml of 0.1 M sodium phosphate buffer.

11. RNA extraction

    11.1 75% Ethanol solution

        37.5 ml of Absolute ethanol was diluted in 12.5 ml of distilled water.

12. Western blot assay

    12.1 1X RIPA buffer

        5 ml of 10X RIPA buffer was dissolved in 45 ml of distilled water.

    12.2 Lysis buffer with 1X protease/phosphatase inhibitor (prepare freshly)

        990 µl of 1X RIPA buffer was mixed with 10 µl of 100X/phosphatase inhibitor.

    12.3 4X Laemmli buffer with 10% β-mercaptoethnaol

        4X Laemmli buffer was prepared from 2g of SDS, 5 mg of bromphenol blue, 12.5 ml of 0.5 M Tris (pH 6.8), 10 ml of glycerol and 5 ml of β-mercaptoethnaol (kept at 4°C).

12.4 20% Sodium dodecyl sulfate (SDS)

10 g of Sodium dodecyl sulfate was dissolved in 100 ml of distilled water and kept at room temperature.

12.5 10% Ammonium persulfate (APS) (Prepare freshly)

50 mg of Ammonium persulfate was dissolved in distilled water 50 µl.

12.6 10X Running buffer

30 g of Tris-base and 144 g of glycine was dissolved in 1000 ml of distilled water and kept at room temperature.

12.7 5 M Sodium chloride (NaCl)

14.61 g of NaCl was dissolved in 50 ml of distilled water and kept at room temperature.

12.8 0.5 M Tris pH 6.8

30.29 g of Tris base was dissolved in 500 ml of distilled water and adjusted pH 6.8 (kept at room temperature).

12.9 1 M Tris pH 7.4

60.57 g of Tris base was dissolved in distilled water and adjusted pH 7.4 (kept at room temperature).

12.10 1.5 M Tris pH 8.8

90.86 g of Tris base was dissolved in 500 ml of distilled water and adjusted pH 8.8 (kept at room temperature).

12.11 6% Stacking gel

6% Stacking gel was prepared as following:

- Distilled water	4.8	ml
- 30% Acrylamide gel	4.0	ml
- 1.5 Tris at pH 8.8	3.0	ml
- 20% SDS	60	µl
- Distilled water	60	µl
- 10% Ammonium persulfate	120	µl
- Trimethylethylenediamine	12	µl

12.12 10% Seperating gel

10% Seperation gel was prepared as following:

- Distilled water	2.6	ml
- 30% Acrylamide gel	1.0	ml
- 0.5 M Tris at pH 6.8	1.25	ml
- 20% SDS	25	μl
- Distilled water	25	μl
- 10% Ammonium persulfate	50	μl
- TEMED	5	μl

12.13 1X Running buffer

10X Running (100 ml) was mixed with 900 ml of distilled water and 5 ml of 20% SDS (kept at room temperature).

12.13 Transfer buffer

100 ml of 10X Running buffer was mixed with 100 ml of absolute methanol and 500 μl of 20%SDS in 800 ml of distilled water (kept at 4°C).

12.14 TBST buffer

20 ml of 1 M Tris pH 7.4 was mixed with 30 ml of 5 M NaCl, 500 μl of Tween 20 and adjusted total volume into 1000 ml (kept at room temperature).

12.15 5% Non-fat dry milk

Non-fat dry milk (0.5 g) was dissolved in 10 ml of TBST buffer and kept at 4°C.

12.16 5% Bovine serum albumin (BSA)

BSA (5 g) was dissolved in 10 ml of TBST buffer and kept at 4°C.

\

Appendix C

Abbreviations

ΔΔCt	Delta-delta-Ct
$^{\circ}$C	Degree Celsius
μg	Microgram
mg	Milligram
ml	Millilitre
μM	Micromolar
w/w	Weight/weight
GAE	Gallic acid equivalent
SEM	Standard error of the mean
QE	Quercitin equivalent
VCEAC	Vitamin C Equivalent Antioxidant Capacity
NA	Not available
DPPH	2, 2-Diphenyl-1-picrylhydrazyl
ABTS	2, 2'-azinobis (3-ethylbenzothiazoline-6-sulfonic acid) radical
SC	Scavenging activity
MTT	3-(4, 5-dimethylthiazol-2-yl)-2,5-diphenyl tetrazolium bromide

L-DOPA	L-3,4-dihydroxyphenylalanine
NADH	Nicotinamide adenine dinucleotide hydrogenase
NADPH	Nicotinamide adenine dinucleotide phosphate hydrogenase
alpha-MSH (α-MSH)	Alpha-melanocyte stimulating hormone
%	Percentage
β	Beta
/	Per
Ab	Antibody
TYR	Tyrosinase
TRP-1	Tyrosinase-related protein 1
TRP-2	Tyrosinase-related protein 2
DCT	Dopachrome tautomerase
MITF	Microphthalmia-associated transcription Factor
APS	Ammonium persulfate
bp	Base pair
BME	β-mercaptoethanol
BSA	Bovine serum albumin
O_2	Oxygen

O_2^-	Superoxide anion
ROS	Reactive oxygen species
cm^3	Cubic centimeter
DNA	Deoxyribonucleic acid
DMEM	Dulbecco's modified Eagle's medium
FBS	Fetal bovine serum albumin
DMSO	Dimethyl sulfoxide
DW	Distilled water
EDTA	Ethylenediaminetetraacetic acid
B16F10	B16F10 melanoma cell line
kDa	Kilo Dalton
M	Molar
mRNA	messenger ribonucleic acid
NaCl	Sodium chloride
Na_2HPO_4	Sodium phosphate dibasic
NaH_2PO_4	Sodium phosphate monobasic
P	P value
pH	Potential of hydrogen ion
rpm	Revolution per minute
SDS	Sodium dodecyl sulfate
SDS-PAGE	Sodium dodecyl sulfate polyacrylamide gel

electrophoresis

TBST   Tetramethylethylenediamine

TBST   Tris-buffered saline and Tween 20

cDNA   Complementary Deoxy ribonucleic acid

α Alpha

nm   Nanometre

h   Hour

CO_2 Carbon dioxide

Min   Minute

VITA

My name is Moragot Chatatikun. I was born on March 28, 1988 in Bangkok, Thailand. I graduated with a Bachelor's degree (Major: Medical technology, Minor: Molecular Biology, second class honors) from faculty of Allied Health Sciences, Chulalongkorn University. After that, I was a sale representative in Clinical Diagnostics Ltd. Part (Oxoid Microbiology product) in 2010-2011. I got a Master's degree in Clinical Biochemistry and Molecular Medicine from faculty of Allied Health Sciences, Chulalongkorn University in 2012. I further studied in Doctoral degree program in Clinical Biochemistry and Molecular Medicine at faculty of Allied Health Sciences, Chulalongkorn University. My research focused on the effects of plant extracts for melasma treatment. By 2016-2017, I was an exchange student at Department of Dermatology, Tohoku University, in Professor Setsuya Aiba's laboratory.

จุฬาลงกรณ์มหาวิทยาลัย
CHULALONGKORN UNIVERSITY